26 October 2012 | $10

# Science

AAAS

Inside:
The 2012
US Election

## EDITORIAL

443 Thriving on Common Ground
*Bruce Alberts*
*>> News Focus section p. 456; Policy Forum p. 472*

## NEWS OF THE WEEK

448 A roundup of the week's top stories

## NEWS & ANALYSIS

451 Prison Terms for L'Aquila Experts Shock Scientists
452 Questions About Japanese Researcher Go Back Years
455 When a Brain Scan Bears Bad News

## NEWS FOCUS

456 2012 ELECTION
Congratulations! Now Get to Work
For Once, Science Is an Issue in Race for a Seat in Congress
Food Labeling Issue Tops State Ballot Questions
Want to Tear Down Your Rival? Here's What Might Work Best
*>> Editorial p. 443; Policy Forum p. 472;* Science *Podcast*

## LETTERS

467 A Curiosity Moment for Tropical Biology?
*C. H. Cannon*
The Real Costs of Research
*H. R. Rawlings III* et al.
Duty of Care: Protecting Researchers Abroad
*B. Pafford and R. Macpherson*
469 CORRECTIONS AND CLARIFICATIONS
469 TECHNICAL COMMENT ABSTRACTS

## BOOKS *ET AL.*

470 Transhumanist Dreams and Dystopian Nightmares
*M. J. Mehlman, reviewed by M. A. Goldman*
471 Darwin's Ghosts
*R. Stott, reviewed by S. Firestein*

## POLICY FORUM

472 Social Media and the Elections
*P. T. Metaxas and E. Mustafaraj*
*>> Editorial p. 443; News Focus section p. 456;* Science *Podcast*

## PERSPECTIVES

474 The Risks of Overfishing
*E. K. Pikitch*
*>> Report p. 517*
475 The Mood of a Worm
*S. W. Emmons*
*>> Reports pp. 540 and 543*
476 Measuring Solar Magnetism
*A. G. de Wijn*
478 Did Australopiths Climb Trees?
*S. Larson*
*>> Report p. 514*
479 Lending Handedness to the Cyclopentadienyl Ligand
*H. Wang and F. Glorius*
*>> Reports pp. 500 and 504*
480 Fishing for Answers off Fukushima
*K. O. Buesseler*
482 Decoding the Neuronal Tower of Babel
*C. J. McBain*
*>> Report p. 536*
483 Can Intellectual Property Save Drug Development?
*G. A. FitzGerald*

## *SCIENCE* PRIZE ESSAYS

485 Student-Directed Discovery of the Plant Microbiome and Its Products
*C. A. Bascom-Slack* et al.
487 A Mutant Search—*Caenorhabditis elegans* and Gene Discovery
*C. C. LaRue and P. A. Padilla*

CONTENTS continued >>


page 456

page 470


## COVER

Skull and shoulders of "Selam"—a 3.3-million-year-old female child *Australopithecus afarensis* from Dikika, Ethiopia. The upside-down view reveals her palate, vertebral column, and both shoulder blades (in this orientation, the scapula on the right measures 60 millimeters across). The scapulae were recently freed from their sandstone matrix and are described in the Report on page 514. The scapulae display several apelike characteristics, implying that *A. afarensis* was still a capable climber.

***Image: Zeresenay Alemseged/Dikika Research Project***

## DEPARTMENTS

439 This Week in *Science*
444 Editors' Choice
446 *Science* Staff
489 AAAS News & Notes
549 New Products
550 *Science* Careers

## REVIEW

491 Glial Progenitor Cell–Based Treatment and Modeling of Neurological Disease
*S. A. Goldman* et al.

## RESEARCH ARTICLE

496 Detecting Causality in Complex Ecosystems
*G. Sugihara* et al.
A new method, based on nonlinear state space reconstruction, can distinguish causality from correlation.

## REPORTS

500 Biotinylated Rh(III) Complexes in Engineered Streptavidin for Accelerated Asymmetric C–H Activation
*T. K. Hyster* et al.
Modifying an achiral ligand to dock in a protein renders catalysis by its rhodium complex asymmetric.

504 Chiral Cyclopentadienyl Ligands as Stereocontrolling Element in Asymmetric C–H Functionalization
*B. Ye and N. Cramer*
A ligand rarely applied to asymmetric catalysis has been chirally modified to furnish a highly selective rhodium catalyst.
>> *Perspective p. 479*

506 Fluorescence Enhancement at Docking Sites of DNA-Directed Self-Assembled Nanoantennas
*G. P. Acuna* et al.
A DNA origami structure enhances the emission of a dye molecule by directing the proximate binding of gold nanoparticles.

510 Feathered Non-Avian Dinosaurs from North America Provide Insight into Wing Origins
*D. K. Zelenitsky* et al.
Analysis of feathered theropod fossils from North America suggests that feathers may have first evolved for display.

514 *Australopithecus afarensis* Scapular Ontogeny, Function, and the Role of Climbing in Human Evolution
*D. J. Green and Z. Alemseged*
The shoulder of *Australopithecus afarensis* implies that, although bipedal, this early human was an active climber.
>> *Perspective p. 478;* Science *Podcast*

517 Status and Solutions for the World's Unassessed Fisheries
*C. Costello* et al.
Poorly monitored, small-size fisheries are in decline, but few of them are near collapse.
>> *Perspective p. 474*

520 The APC/C Inhibitor XErp1/Emi2 Is Essential for *Xenopus* Early Embryonic Divisions
*T. Tischer* et al.
The protein XErp1 regulates cell cycle progression in frog embryos by inhibiting the anaphase-promoting complex/cyclosome.

524 Maturation-Dependent HIV-1 Surface Protein Redistribution Revealed by Fluorescence Nanoscopy
*J. Chojnacki* et al.
Rearrangements of the interior structural lattice cluster a surface glycoprotein as the virus preps for cell entry.

528 In Vivo Architecture and Action of Bacterial Structural Maintenance of Chromosome Proteins
*A. Badrinarayanan* et al.
SMC proteins form a dimer of adenosine triphosphate (ATP)–bound dimers, which translate ATP hydrolysis into mechanical DNA remodeling.

532 Regulatory T Cells Increase the Avidity of Primary CD8$^+$ T Cell Responses and Promote Memory
*L. Pace* et al.
Regulatory T cells enhance the avidity of T cells, thereby promoting responses to foreign antigens instead of self-antigens.

536 Elfn1 Regulates Target-Specific Release Probability at CA1-Interneuron Synapses
*E. L. Sylwestrak and A. Ghosh*
A protein in a hippocampal postsynaptic neuron templates transmitter release kinetics in its presynaptic neuron.
>> *Perspective p. 482*

540 Oxytocin/Vasopressin-Related Peptides Have an Ancient Role in Reproductive Behavior
*J. L. Garrison* et al.
Oxytocin/vasopressin-related peptides and their receptors coordinate male mating programs in *Caenorhabditis elegans*.

543 Vasopressin/Oxytocin-Related Signaling Regulates Gustatory Associative Learning in *C. elegans*
*I. Beets* et al.
Nematode neuropeptides and their G protein–coupled receptors support behavioral responses to salt.
>> *Perspective p. 475*

**CONTENTS** continued >>

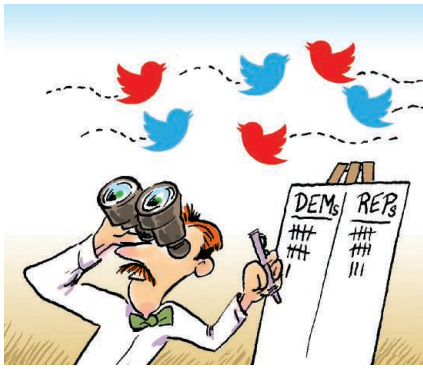


page 472

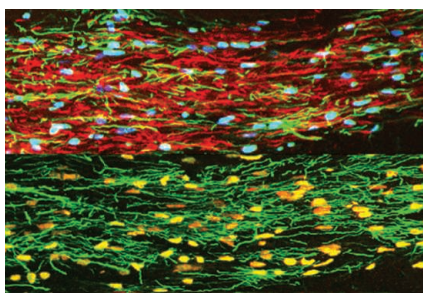

page 491

page 510

CREDIT: (BOTTOM) JULIUS CSOTONYI

# ONLINE**HIGHLIGHTS**

## *SCIENCE*XPRESS

www.sciencexpress.org

Publication Ahead of Print

A Global Pattern of Thermal Adaptation in Marine Phytoplankton
*M. K. Thomas* et al.
10.1126/science.1224836

Akt-Mediated Regulation of Autophagy and Tumorigenesis Through Beclin 1 Phosphorylation
*R. C. Wang* et al.
10.1126/science.1225967

The *Legionella* Effector RavZ Inhibits Host Autophagy Through Irreversible Atg8 Deconjugation
*A. Choy* et al.
10.1126/science.1227026

A Bipolar Spindle of Antiparallel ParM Filaments Drives Bacterial Plasmid Segregation
*P. Gayathri* et al.
10.1126/science.1229091

Binary Millisecond Pulsar Discovery via Gamma-Ray Pulsations
*H. J. Pletsch* et al.
10.1126/science.1229054

## TECHNICAL**COMMENTS**

Comment and Response on "Conspecific Negative Density Dependence and Forest Diversity"
*Comment: I. A. Dickie* et al.
http://dx.doi.org/10.1126/science.1225520
*Response: D. J. Johnson* et al.
http://dx.doi.org/10.1126/science.1225996

## *SCIENCE*NOW

www.sciencenow.org

Highlights From Our Daily News Coverage

Raw Food Not Enough to Feed Big Brains
A new study supports the idea that cooking helped human ancestors expand their minds.
http://scim.ag/Big_Brains

Caesar, the Orchid Chief
A temple erected by a Roman emperor is among the earliest evidence of orchids in Western art.
http://scim.ag/Evidence_Orchids

Antibiotic-Resistant Bugs Go Wild
Researchers find deadly hospital bacterium in rabbits and a migratory shorebird.
http://scim.ag/Hospital-Bacterium

## *SCIENCE*SIGNALING

www.sciencesignaling.org

The Signal Transduction Knowledge Environment

**23 October issue: http://scim.ag/ss102312**

RESEARCH ARTICLE: Akt Phosphorylates the Transcriptional Repressor Bmi1 to Block Its Effects on the Tumor Suppressing *Ink4a-Arf* Locus
*Y. Liu* et al.

PODCAST
*S. D. Nimer and A. M. VanHook*
Akt counteracts growth-promoting signals by stimulating the transcription of tumor suppressor genes.

PERSPECTIVE: PKR-Dependent Inflammatory Signals
*R. Kang and D. Tang*
The RNA-dependent protein kinase activates the inflammasome to promote inflammation.

PRESENTATION: The Effect of Acute and Chronic Stress on Growth
*L. Sävendahl*
The glucocorticoids and inflammatory cytokines induced by stress can impair bone growth.

PRESENTATION: The Effects of Acute and Chronic Stress on Diabetes Control
*M. L. Marcovecchio and F. Chiarelli*
Stress-induced hormonal changes alter glucose homeostasis in both diabetic and healthy patients.

PRESENTATION: P450 Oxidoreductase Deficiency—A Disorder of Steroidogenesis with Multiple Clinical Manifestations
*W. L. Miller* et al.
Mutations in a steroid biosynthetic enzyme cause a range of clinical symptoms.

## *SCIENCE*TRANSLATIONAL MEDICINE

www.sciencetranslationalmedicine.org

Integrating Medicine and Science

**24 October issue: http://scim.ag/ss102412**

RESEARCH ARTICLE: NADPH Oxidase Inhibits the Pathogenesis of Systemic Lupus Erythematosus
*A. M. Campbell* et al.
Neutrophil NETs are not required for SLE development in a mouse model.

RESEARCH ARTICLE: Targeting Cancer with a Lupus Autoantibody
*J. E. Hansen* et al.

FOCUS: Lupus Antibody Tops Cancer Cells
*J. M. Ford*
A cell-penetrating lupus anti-DNA antibody inhibits DNA repair and is toxic to cancer cells.

RESEARCH ARTICLE: Quantitative Image Analysis of Cellular Heterogeneity in Breast Tumors Complements Genomic Profiling
*Y. Yuan* et al.
Quantitative image analysis of breast tumors contributes to a predictor of survival.

FOCUS: Building a Life Sciences Innovation Ecosystem
*K. D. Harrison* et al.
Universities should support research with commercial potential.

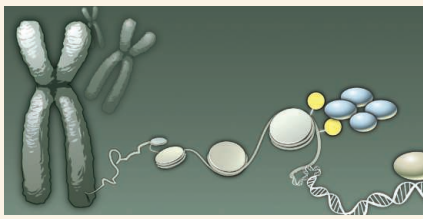

SCIENCE**SIGNALING**
Silencing a transcriptional silencer.

## *SCIENCE*CAREERS

www.sciencecareers.org/career_magazine

Free Career Resources for Scientists

**http://scim.ag/SciCareers26October2012**

Experimental Error: A Cure for Listlessness
*A. Ruben*
Our columnist lists the top N of everything in science careers, where N = fun.

Teaching Postdocs to Be Professors
*M. Price*
An NIH program readies teaching-focused postdocs—especially minorities—for lab-and-classroom jobs.

Life at the Bottleneck
*R. Müller*
A social scientist discusses how career pressures affect how postdocs work and relate in the lab.

## *SCIENCE*PODCAST

www.sciencemag.org/multimedia/podcast

Free Weekly Show for 26 October 2012

Listen to stories on the Twitter vote, our climbing ancestors, science and the next U.S. president, and more.

**SCIENCE (ISSN 0036-8075) is published weekly on Friday, except the last week in December, by the American Association for the Advancement of Science, 1200 New York Avenue, NW, Washington, DC 20005.** Periodicals Mail postage (publication No. 484460) paid at Washington, DC, and additional mailing offices.  The title SCIENCE is a registered trademark of the AAAS. Domestic individual membership and subscription (51 issues): $149 ($74 allocated to subscription). Domestic institutional subscription (51 issues): $990; Foreign postage extra: Mexico, Caribbean (surface mail) $55; other countries (air assist delivery) $85. First class, airmail, student, and emeritus rates on request. Canadian rates with GST available upon request, GST #1254 88122. Publications Mail Agreement Number 1069624. **Printed in the U.S.A.**

**Change of address:** Allow 4 weeks, giving old and new addresses and 8-digit account number. **Postmaster:** Send change of address to AAAS, P.O. Box 96178, Washington, DC 20090–6178. **Single-copy sales:** $10.00 current issue, $15.00 back issue prepaid includes surface postage; bulk rates on request. 

AAAS
ADVANCING SCIENCE, SERVING SOCIETY

CREDIT: Y. HAMMOND/AAAS

## First, Find Fish>>

While salmon, cod, and tuna fisheries are regularly monitored and assessed, this is not the case for about 80% of the fish species harvested throughout the world. **Costello *et al.*** (p. 517 published online 27 September; see the Perspective by **Pikitch**) used a model that integrates harvest, population, and ecological data to estimate the status of unassessed fisheries, based on ecologically analogous, regularly assessed fisheries. Generally, unassessed fisheries are in worse condition with declining fish stocks compared with regularly assessed fisheries.

## Myelination Redux

Failures in myelination result from accident, disease, or normal aging, and can severely debilitate those affected. **Goldman *et al.*** (p. 491) review knowledge about oligodendrocytes, the cells that myelinate axons, and describe possibilities for replacing them after damage or decline.

## Building a Fluorescent Hotspot

When two gold nanoparticles come close together, their overlapping plasmonic fields can create a region that acts as a nanoantenna that can enhance the fluorescent emission of a molecule. **Acuna *et al.*** (p. 506) used a surface-anchored DNA origami structure to assemble one or two gold nanoparticles next to a dye trapped within the structure. A > 100-fold enhancement in fluorescent emission was observed when the dye molecules were located in a 23-nm gap between two 100-nm gold nanoparticles.

## Fancy Feathers

In the past few decades, an increasing number of dinosaurs have been shown to have possessed feathers. While it seems likely that feathers themselves may have evolved for thermoregulation, the original function of wings has been less clear and remained a matter of debate. Based on examination of three Theropod specimens from the genus *Ornothomimus*, **Zelenitsky *et al.*** (p. 510) conclude that the feathered wing may have evolved not for locomotion or prey capture (the animals were herbivores), but rather as a courtship display. All of the individuals examined had a covering consisting of short filamentous feathers, but the adult specimens, which would have reached sexual maturity, also had long shafted feathers on their forelimbs.

## Cause or Correlation?

Three centuries ago, Bishop Berkeley's 1710 classic "A treatise on the nature of human knowledge," first spelled out the "correlation vs. causation" dilemma. **Sugihara *et al.*** (p. 496, published online 20 September) present an approach to this conundrum, and extend current discussions about causation to dynamic systems with weak to moderate coupling (such as ecosystems). The resulting method, convergent cross mapping can detect causal linkages between time series.

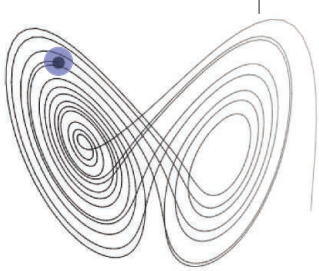

## Climbing Like an Ape

Recently, studies of several early human leg and foot fossils have implied that in some early species—even after humans became bipedal—climbing may have still been important. Shoulder bones, which would provide important complementary information, are scarce, however. One of the few examples is from *Australopithecus afarensis* skeleton (DIK-1-1), which includes both scapula. **Green and Alemseged** (p. 514; see the Perspective of **Larson**) provide an analysis of the fossil's shoulders and show that, unlike modern humans, they retain several traits that are common in climbing apes, which may indicate that *A. afarensis* was an active climber.

## Mastering Early Divisions

The regulation of canonical mitotic cell cycles is well understood, but the basic principles of the rapid, synchronized early mitotic divisions in embryos remains a mystery. Early embryos lack key mitotic regulators such as checkpoints, the anaphase-promoting complex/cyclosome (APC/C)–inhibitory protein Emi1, and the inhibitory phosphorylations of cyclin-dependent kinase 1 (Cdk1). Working in *Xenopus* embryos, **Tischer *et al.*** (p. 520, published online 27 September) identified XErp1/Emi2 as a mitotic APC/C-inhibitor essential for early mitotic divisions. The mitotic APC/C-inhibitory activity of XErp1 is positively regulated by protein kinase A (PKA) and protein phosphatase IIA (PP2A), which antagonizes Cdk1's inhibitory effect on XErp1. Thus, Cdk1 and PP2A/PKA appear to act antagonistically to control XErp1 activity, which results in the oscillatory activation and inactivation of the APC/C required for fast and synchronous mitotic divisions.

## Switching on HIV

Newly assembled human immunodeficiency virus (HIV) virions bud from the host cell as immature particles. Proteolysis of the Gag protein, which forms a structural lattice below the viral membrane, leads to the formation of mature infectious HIV. Fusion of mature HIV virions with a target cell is mediated by viral envelope (Env) proteins that occur in trimeric "spikes" on the surface of the virion. **Chojnacki *et al.*** (p. 524) used subdiffraction microscopy to show that the spikes were dispersed on the immature virion but clustered into a single focus on the mature virion. The clustering was important for infectivity. Coupling Gag proteolysis with clustering may ensure that only particles whose interior has switched to the entry mode are competent for membrane fusion.

## Making a Move

Structural Maintenance of Chromosome (SMC) complexes act ubiquitously in chromosome processing in all domains of life, but their mode of action in living cells has remained an enigma.

*Continued on page 441*

CREDITS: (TOP TO BOTTOM): STEVE GAINES; SUGIHARA *ET AL.*

*Continued from page 439*

**Badrinarayanan *et al.*** (p. 528) used noninvasive millisecond single-molecule imaging to understand SMC complex molecular biochemistry in living bacterial cells with super-resolution spatial precision. *Escherichia coli* SMC complexes, which are important for chromosome segregation, formed dimers that bound to DNA in an adenosine triphosphate (ATP)–dependent manner and that could be released upon ATP-hydrolysis. By functioning in pairs, the complexes are likely to be able to undergo multiple cycles of ATP-hydrolysis without being released from DNA.

## Treg-ulating Immune Responses

There are many checks and balances to keep the immune system from running amok. One of the most critical is a specialized population of T cells, called regulatory T cells ($T_{regs}$). In their absence, a lethal autoimmune disease develops in both humans and mice. Although $T_{regs}$ are well known for their suppression of autoimmune responses, how they modulate responses to infectious agents is less well understood. Using inducible deletion of $T_{regs}$ in mice, **Pace *et al.*** (p. 532) showed that $T_{regs}$ are important for shaping the avidity of $CD8^+$ T cell responses. In the absence of $T_{regs}$, $CD8^+$ T cell responses were of lower avidity, and the $CD8^+$ T cells were more responsive to lower-affinity antigens. When $T_{regs}$ were absent, stable interactions between T cell and antigen-presenting cells were increased as a result of higher amounts of chemokine expression in the lymph nodes. $T_{reg}$ depletion also resulted in a lower-avidity $CD8^+$ T cell response to infection with the bacterial pathogen *Listeria monocytogenes*.

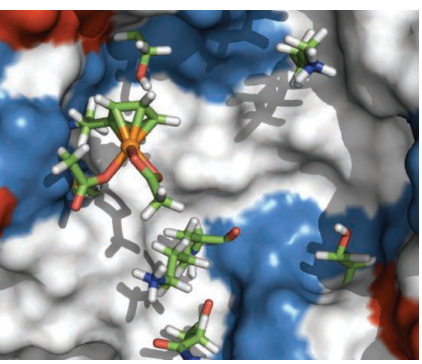

## Forced Asymmetry in Cp

The cyclopentadienyl (Cp) ligand—a pentagon of carbons—is a common feature in transition metal catalysts, but chiral variants of the structure have rarely been applied to asymmetric reactions. Two studies now demonstrate distinct approaches to rendering a Cp-derived rhodium catalyst enantioselective in a tandem carbon-hydrogen activation-ring closure reaction that couples olefins with benzamides (see the Perspective by **Wang and Glorius**). **Hyster *et al.*** (p. 500) tethered a biotin derivative to the Cp ligand to enable docking in a chiral streptavidin protein cavity, which in turn was engineered to further optimize catalytic performance. **Ye and Cramer** (p. 504) appended chiral substituents on the Cp framework to bias the rest of the coordination environment around the metal center.

## On the Receiving End

One type of neuron, the hippocampal pyramidal neuron, forms two different types of synapses with two different downstream partners. When the partner is an oriens-lacunosum moleculare (O-LM) interneuron, the pyramidal neuron only releases its synaptic vesicles with a low probability. When the cell on the receiving end is a parvalbumin (PV)-positive interneuron, the likelihood of synaptic vesicle release is high. How can the postsynaptic cell change the release characteristics of the presynaptic cell? **Sylwestrak and Ghosh** (p. 536, published online 4 October; see the Perspective by **McBain**) describe how the extracellular leucine-rich repeat fibronectin containing 1 (Elfn1) protein in the postsynaptic OLM interneurons affects vesicle release probability in the presynaptic pyramidal neuron. Misexpression of Elfn1 in PV interneurons converted vesicle release to the OLM pattern. Thus, a regulator located in the postsynaptic cell can modulate the function of the synapse.

## Social Neuropeptides in Nematodes

The neuropeptides oxytocin and vasopressin stimulate maternal, reproductive, aggressive, and affiliative behaviors in mammals. They are implicated in behaviors ranging from ewe-lamb bonding in sheep to pair bonding in voles (see the Perspective by **Emmons**). Now, **Garrison *et al.*** (p. 540) and **Beets *et al.*** (p. 543) extend the evolutionary reach of these social neuropeptides to the invertebrate nematode worm, *Caenorhabditis elegans.* A similar neuropeptide was found to function in mating and also to modulate salt-taste preference, based on prior experience, suggesting an ancient role in associative learning.

CREDIT: HYSTER *ET AL.*

Bruce Alberts is Editor-in-Chief of *Science*.

# Thriving on Common Ground

A MAJOR U.S. ELECTION IS IMMINENT, WITH VOTING ON 6 NOVEMBER (SEE THE SPECIAL NEWS section on p. 456). A central issue dividing the two major political parties is how best to allocate scarce resources, as the country attempts to reduce its budget deficit without jeopardizing national prosperity. In last week's Editorial, John Hamre, a former U.S. Deputy Secretary of Defense, described how this challenge, coupled with the polarization of U.S. politics and a dogmatic refusal to compromise, has created "one of the most perilous conditions that I can remember in my professional life."* To move forward, it is important to identify general principles for a successful future on which essentially all Americans can agree—principles that are also relevant for other nations.

Why are some nations much more successful than others? In my second year in college, I had a "eureka" moment when, struggling to come to grips with the forces that shape human societies, I suddenly became aware of the vital role of "institutions": organizations such as universities, corporations, or governments, in which people cooperate to produce results that individuals could never accomplish alone. Although I had previously interacted with many such organizations, until that moment I had totally ignored their fundamental importance to society.

I have since learned that it is primarily through their roles in institutions that talented and well-motivated individuals can make enormous contributions to a nation. And it is the sum of many thousands of institutions, and millions of such people, that makes a nation thrive. Any successful nation must therefore support a system of education and training that casts a very wide net for talent, thereby enabling as many of its people as possible to acquire the abilities, motivation, and skills essential for maintaining and continually improving its important institutions. The United States is fortunate to have a strong and respected higher education system, with major public universities as well as over 1000 local community colleges that provide low-cost, multiple entry points to a higher education. But these critical institutions have been suffering from decades of decreasing resources, and they urgently need more support.


Can Americans agree that our political leaders should pay much more attention to improving and nurturing the public education system at all levels?

Developing talent is fundamental, but it is not enough. Each nation must also support a legal system that forces its institutions to behave in appropriate ways, as well as systems of ethical standards that promote prosocial behavior.† Less obvious is the need for merit-based systems that allow only the most capable people to advance to the many positions of responsibility and authority in a nation's institutions. Rules that support automatic tenure and promotion, so as to "protect individual rights," may seem well-meaning, but such rules have calamitous results. Each nation will thrive only to the extent that its institutions promote and maintain individuals in positions of responsibility based on their demonstrated performance, irrespective of seniority, family connections, or national origins. Can Americans agree that it is crucial to constantly enhance policies that build and encourage such a merit-based society?

Finally, institutions thrive when they are rooted in scientific principles—in rational thought, scientific knowledge, and the innovations derived from scientific understanding to benefit humanity. No matter how contentious the topic, whether climate change, the immunization of children, or the benefits of genetically modified crops, scientists and politicians must work together much more effectively to ensure that the scientific research needed for wise decision-making by vital institutions is both supported and never ignored. I am certain that millions of U.S. scientists are ready to contribute. Can all Americans agree? **– Bruce Alberts**

10.1126/science.1231652

*J. J. Hamre, *Science* **338**, 304 (2012). †D. Acemoglu, J. Robinson, *Why Nations Fail: The Origins of Power, Prosperity, and Poverty* (Crown Publishers, New York, 2012).







Published by AAAS

EDITED BY KRISTEN MUELLER AND MARIA CRUZ

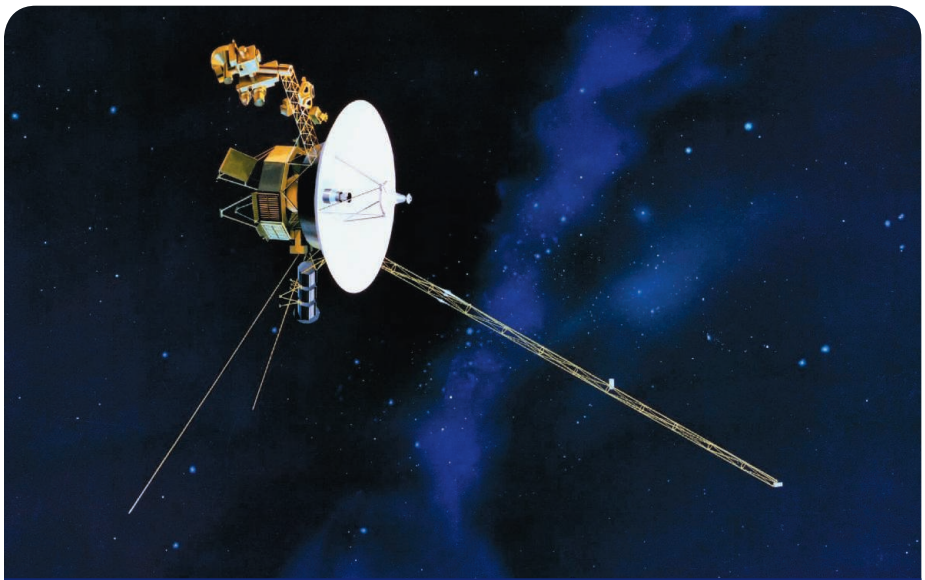

ASTRONOMY

## Blowing in the Solar Wind

Launched in 1977, the two Voyager spacecraft have traveled deep into space, but they are still transmitting data back to Earth. Having crossed the termination shock, the point where the solar wind is abruptly slowed down by the interstellar medium surrounding the solar system, both spacecraft are currently in the outermost layer of the heliosphere—the heliosheath. Richardson and Wang report recent data from the plasma instrument on Voyager 2, which crossed the termination shock in 2007 as solar activity was approaching its minimum. Previous data had shown a decrease in the solar wind density at the position of Voyager 2 6 months after it crossed the termination shock; now data from 2011 and 2012 reveal an increase in the plasma density back to the levels observed just after termination shock crossing, before the decrease was observed. These results may signal the end of solar minimum conditions in the heliosheath. — MJC

*Astrophys. J.* **759**, L19 (2012).

EDUCATION

## Pay for Percentile

What gets measured gets done. So claim advocates of high-stakes academic testing, arguing that paying teachers on the basis of student performance can improve education. Opponents of "pay for performance" argue that such a system pressures those being measured to game the system, which distorts the process being monitored. High-stakes assessments commonly use similar test topics, items, and formats to maintain consistency of the rating scale over time. This provides opportunity and incentive to "teach to the test," rather than improving student understanding and achievement. Barlevy and Neal detail an approach to motivate teachers on the basis of student test performance, while limiting the opportunity to teach to the test by using completely new tests each time. With each new test, a student's achievement is reported as an ordinal ranking among a cohort of similarly achieving, similarly tested peers in the school system. A teacher's performance is measured as the sum of her/his students' individual percentile ranks among their respective peer comparison groups. The authors show how "contests" among teachers based on this summed ranking can elicit efficient teacher effort in every classroom. — BW

*Am. Econ. Rev.* **102**, 1805 (2012).

NEUROSCIENCE

## Countering Impaired Cognition

Cognitive impairment is a cardinal feature of many psychiatric disorders, including schizophrenia. Blockade of 5-$HT_6$ receptors is a potential strategy for correcting the cognitive deficits of schizophrenia and other central nervous system disorders. However, the molecular mechanisms underlying the deleterious impact of 5-$HT_6$ receptors on cognitive function are still unknown. Using an unbiased proteomic approach to find protein partners and signaling mechanisms engaged by 5-$HT_6$ receptors, Meffre *et al*. identified several members of the mammalian target of rapamycin (mTOR) signaling complex. mTOR has been implicated in the cognitive impairment associated with a number of genetic disorders. 5-$HT_6$ receptor stimulation activated mTOR-dependent signaling, and the mTOR inhibitor rapamycin reversed some of the disruptive effects induced by a 5-$HT_6$ receptor agonist in a recognition memory paradigm and in a social interaction test. In two developmental rodent models of schizophrenia, 5-$HT_6$ receptor–elicited activation of the mTOR pathway was detected in the prefrontal cortex of adult rats, and rapamycin mimicked 5-$HT_6$ antagonists in reversing the accompanying cognitive deficits. These results provide new insights into the molecular substrates mediating the negative impact of 5-$HT_6$ receptors on cognition and into cellular events underlying cognitive deficits in schizophrenia. — PRS

*EMBO Mol. Med.* **4**, 1043 (2012).

GEOPHYSICS

## The Core from Above

Earth's core is split into a solid inner core and a fluid outer core. The convection and rotation of the outer core produce Earth's magnetic field and redistribute mass within the planet. Measured from orbiting satellites, variations in the magnetic field over time indicate changing outer core dynamics. Mass redistribution from fluid motion in the outer core should be detectable by gravity-sensing satellites, but surface processes such as the movement of water in the oceans and within river basins tend to dominate local gravity measurements. Mandea *et al.* reexamined global magnetic data to determine how the outer core changed over 8 years and correlated them with variations in gravitational data over the same time frame. Both sets of data show a distinct spatial feature centered under Africa, suggesting that core contributions to the gravity field are indeed measurable. A physical explanation for this feature may be related to density heterogeneity or interactions between the core and overlying mantle; however, more data collected from ongoing and future high-resolution satellites are needed to better understand the short-term dynamics of the outer core. — NW

*Proc. Natl. Acad. Sci. U.S.A.* **109**, 10.1073/pnas.1207346109 (2012).

BIOCHEMISTRY

## A Viral Turn-Off

Chronic hepatitis C virus (HCV) infection is a major cause of liver failure. The NS3 protein of HCV has been aggressively pursued as a drug target because it is involved in viral polyprotein processing, through a serine protease domain,

CREDIT: NASA





Published by AAAS

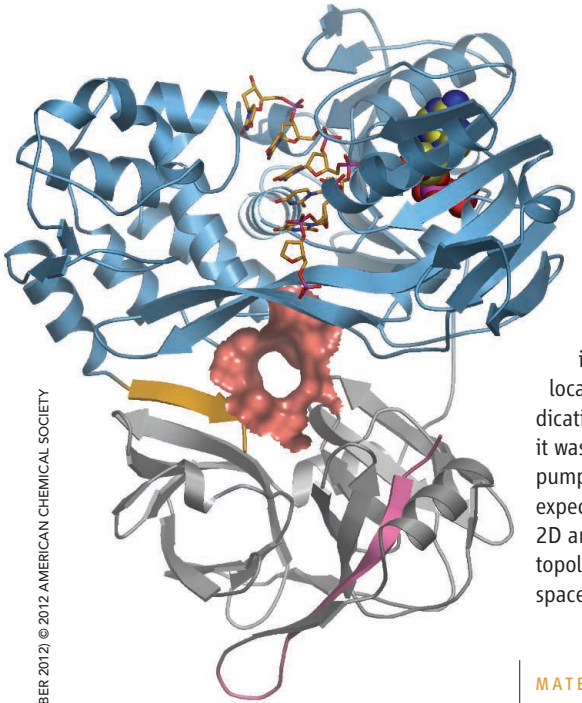

CREDITS (TOP TO BOTTOM): S. M. SAALAU-BATHELL *ET AL.*, *NAT. CHEM. BIOL.* (30 SEPTEMBER 2012) © 2012 NPG/ASTEX PHARMACEUTICALS; M. HEMPEL *ET AL.*, *NANO LETT.* (1 OCTOBER 2012) © 2012 AMERICAN CHEMICAL SOCIETY

and in viral replication, through a helicase domain. Moreover, two drugs targeting the protease domain were approved in 2011, but more are needed. To identify new inhibitors, Saalau-Bethell *et al.* performed a fragment-based screen using crystals of the NS3 protein bound to NS4a (a peptide cofactor). Binding was detected at the interface of the protease and helicase domains, and the low-affinity fragments were elaborated into tight binding leads. The tightest binder had $K_d = 0.02$ μM, exhibited antiviral activity, and inhibited protease activity of the full-length protein, but not the isolated protease domain. Part of the NS3 helicase domain has been shown to bind the active site of the protease domain, and two species consistent with closed and open conformations have been suggested. The authors propose that inhibitors that bind at the NS3 domain interface shift the equilibrium toward the closed state, thereby inhibiting protease activity through a noncompetitive mechanism and probably helicase activity, too. — VV

*Nat. Chem. Biol.* 10.1038/NCHEMBIO.1081 (2012).

PHYSICS

## Topological Quasicrystals

The discovery of topological order has changed the traditional view of phase transitions in condensed-matter physics. Topological phases are characterized by boundary states that are immune to certain types of perturbation and appear, for example, as edge states or surface states in two-dimensional (2D) and 3D systems, but are absent in 1D systems under most circumstances. Kraus *et al.* found evidence for topological boundary states in 1D quasicrystals—materials that can be viewed as a "projection" of periodic systems onto a lower-dimensional physical space. The experimental system consisted of parallel photonic waveguides engineered to realize a quasiperiodic Hamiltonian; when light was injected into a middle waveguide, it spilled over to its neighbors and beyond, whereas it stayed localized if injected into the leftmost guide, indicating a boundary state. In a modified setup, it was also possible to observe the adiabatic pumping of light between the boundaries. It is expected that the results can be generalized to 2D and 3D quasicrystals, which would have the topological properties of the higher dimensional spaces they are projected from. — JS

*Phys. Rev. Lett.* **109,** 106402 (2012).

MATERIALS SCIENCE

## Feeling the Strain

Traditional strain gauges use a patterned metallic foil, in which the change in shape on deformation translates into a change in electrical conductivity. These devices typically have a gauge factor of 2 to 5; thus, for measuring smaller deformations, silicon gauges are used, which have a gauge factor closer to 100 but are more sensitive to temperature changes and mechanical deformation. Hempel *et al.* have developed a scalable deposition method for making strain gauges based on graphene, in which the sensitivity of the device can be tuned by varying the deposition conditions. Solutions containing graphene flakes were spray-coated onto a substrate to make a percolating network as the active part of the sensor. Thicker films had less electrical resistance but lower transparency, and it was shown that the gauge factor could be correlated to the initial resistance of the films. Unlike metal gauges, in which the metal itself deforms during strain, in these sensors the graphene flakes don't deform. Rather, the layers slide past each other, and it is the reduction in flake overlap that changes the electrical conductivity. Gauge factors between 10 and 150 were demonstrated, but in theory much higher values could be obtained. In addition, the sensors can be deposited onto existing surfaces, including curved ones such as light bulbs. — MSL

*Nano Lett.* 10.1021/nl302959a (2012).



Published by AAAS

## AROUND THE WORLD

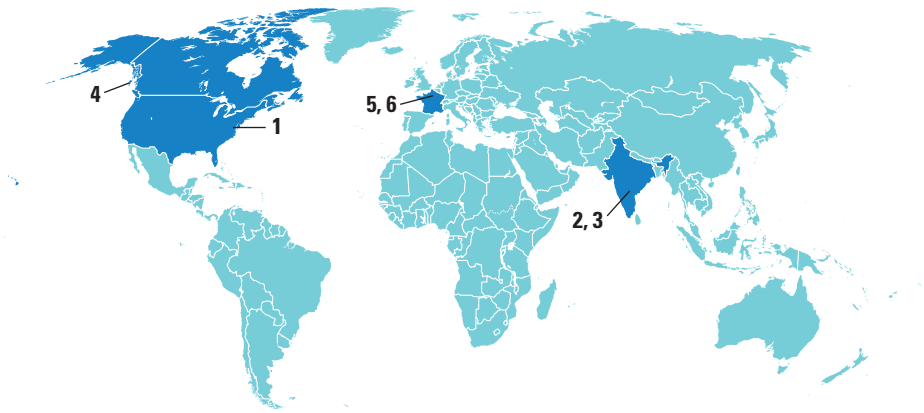


Washington, D.C. **1**

### Fisheries Data Restricted to Protect Trade Secrets

The National Oceanic and Atmospheric Administration (NOAA) spends about $40 million annually to put independent observers on fishing vessels, where they collect data on what's caught in U.S. waters. The information is crucial for evaluating how well fishery management plans are working. Now, NOAA wants to limit public access to these data to protect confidential business information.

The agency's proposed changes include withholding information about where and when a vessel caught fish, which kinds and how many it caught, and what kind of gear it used. The public would have to request such information directly from fishing permit holders. NOAA says it can still give out "detailed and useful information" by aggregating fisheries data to keep it anonymous, but it doesn't say how it would do that.

Fisheries data are far less useful when aggregated, says marine ecologist Larry Crowder of Stanford University in Palo Alto, California, who is trying to devise new approaches to management. "In most cases, our only reliable peek at what's going on in fisheries is the observer data," he says.
**http://scim.ag/NOAArule**

Hyderabad, India **2**

### Doubling Biodiversity Aid

Two years after setting targets for saving global biodiversity, the U.N. Convention on Biological Diversity has struck its first deal on how to pay for those goals. Developed nations agreed to double their aid to developing nations by 2015, a move welcomed by conservation organizations. The new amount—$10 billion a year—covers half of what scientists estimate is needed for those parts of the world (http://scim.ag/costbiod). Several developing nations pledged to boost their own biodiversity spending, including $50 million from India. "The fact that India made a financial commitment at national and international levels sets a precedent for other emerging economies to offer more support to global biodiversity conservation," said Lasse Gustavsson, WWF International's executive director of conservation in a statement.
**http://scim.ag/BiodivPledge**

Hyderabad, India **3**

### A 10-Year Ban for GM Field Trials?

On 17 October, a scientific panel appointed by India's Supreme Court called for a 10-year moratorium on field trials of genetically modified (GM) food crops, as well as nonfood crops such as cotton that have insect-resistant *Bacillus thuringiensis* genes. A decade, the panel said, "is a reasonable length of time" to strengthen India's regulatory regime and develop "a cadre of experts in areas of relevance to food safety evaluation, environmental impact assessment etc."

The recommendations are not binding, and the court has not yet scheduled a hearing on the report, after which it could issue a directive compelling the government to implement a ban.

This call clashes with a report released on 9 October by Indian Prime Minister Manmohan Singh's scientific advisory council, which hailed genetic modification as a transformational technology that has paid dividends for agriculture and health.

Maharaj Kishan Bhan, a vaccine specialist and secretary of the Department of Biotechnology in New Delhi, argues that GM research should be stepped up to meet challenges to food productivity posed by climate change and a rising population.
**http://scim.ag/_moratorium**

Haida Gwaii, Canada **4**

### Rogue Geoengineering Experiment

Questions continue to swirl around what critics call a rogue geoengineering experiment in international waters off the coast of British Columbia. Last week, *The Guardian* newspaper first reported that in July, a retrofitted fishing trawler dispersed 100 tons of iron dust in an ocean eddy about 321 kilometers west of the island of Haida Gwaii. The iron was intended to foster phytoplankton growth, boosting the entire marine food chain.

Satellite images taken before and after fertilization indicate a marked increase in

### NOTED

**>Life may lurk in Antarctica's subglacial Lake Vostok,** but it's still elusive. The Russian scientists who drilled through 4000 meters of ice to reach the lake in February are going back this winter to sample it. First, though, **they tested the ice clinging to the drill bit,** which may be old, refrozen lake water. It had few microbes, the team reported last week at an astrobiology conference in Stockholm.







Published by AAAS

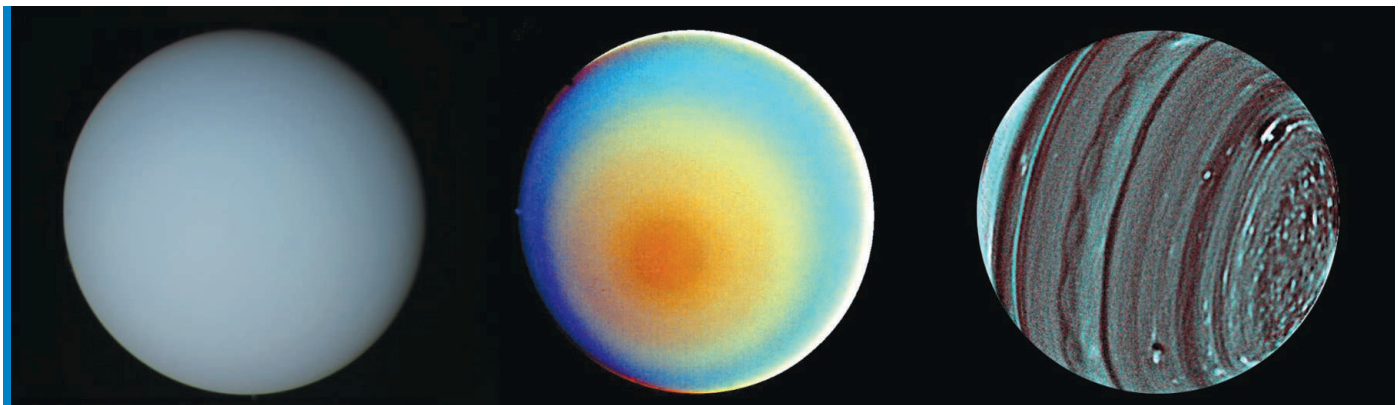

## Sharper, Sharper, and Sharper Still

**Uranus has never looked better. The Voyager 2 spacecraft took the gas-enshrouded ice giant's first and only close-up in 1986 (left), but even tweaking the contrast (middle pole, in false color) could not reveal much character to the sun's seventh most distant planet.**

**Now, new technology and exceptionally good observing conditions one night last July have yielded the sharpest views yet of Uranus. Astronomers used the 10-meter Keck II telescope on Hawaii's Mauna Kea—equipped with a near-infrared camera to up the clouds' contrast and adaptive optics to reduce earthly atmospheric blurring.**

**As planetary astronomer Lawrence Sromovsky of the University of Wisconsin, Madison, and colleagues reported at last week's meeting of the Division for Planetary Sciences in Reno, Nevada, Uranus has cloud bands reminiscent of Saturn and Jupiter and, surprisingly, "popcorn" clouds in its north polar region (right side). Although such convective clouds typify summer thunderstorms on Earth, the team will be watching to see whether this oddball convection shuts down as uranian summer comes on.**



phytoplankton. But oceanographer Kenneth Denman of the University of Victoria in Canada says there's no way to know whether the added iron caused it. In the area where the iron was released, ocean eddies carry iron-rich coastal waters as far as 1000 kilometers off shore, triggering natural phytoplankton blooms each summer; those blooms could be most or all of what the satellite images show, Denman says. He adds that because it appears no one performed careful control studies comparing fertilized and unfertilized regions, researchers are unlikely to produce useful science from the test. **http://scim.ag/Geoeng**

Paris **5**

### Small Satellite, Big Mission

The European Space Agency has signed off on a new mission to study extrasolar planets orbiting nearby bright stars. The Characterizing Exoplanets Satellite (Cheops), expected to launch in 2017, will focus on studying known exoplanets rather than finding new ones.

The green light for Cheops, approved last week, is good news for European astronomers whose earlier proposals for an exoplanet mission never got funded. A proposed exoplanet-detecting spacecraft known as Eddington was left stranded on paper in the early 2000s. There was no reason to revive it after NASA's 2009 launch of Kepler, which does the job Eddington was supposed to do. A more ambitious, next-generation exoplanet finder called Darwin didn't get funded either.

Estimated to cost the agency no more than €50 million, Cheops will monitor stars to measure the dip in their brightness as orbiting planets pass in front of them. That's what Kepler does, too, but Cheops will take detailed observations of known exoplanets, helping researchers accurately characterize them.

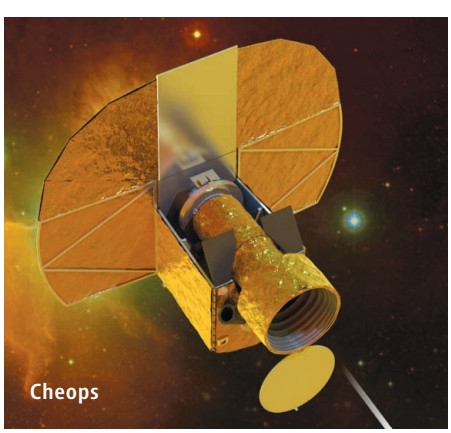


Paris **6**

### French Opinion on GM Study

The French High Council of Biotechnology and the Agency for Food, Environmental and Occupational Health & Safety (ANSES) have each concluded that a controversial rodent study linking ingestion of genetically modified (GM) corn to tumors is inconclusive due to methodological, statistical, and interpretative limitations. The study, which had led the French government to consider asking the European Union to stop importing the GM crop, has drawn fierce criticism. The government now says it will push for a revision of European procedures for evaluation, approval, and control of GM organisms, although it insists the rodent study didn't influence this decision. Study author Gilles-Eric Séralini says he accepts the criticisms but demands that the Monsanto studies leading to the GM corn approval undergo the same scrutiny as his research did. ANSES did commend Séralini for examining GM plants and pesticide toxicity over long time periods. **http://scim.ag/FranceGM**





Published by AAAS

FINDINGS

## Using Gut Bacteria To Fight Diarrhea

Researchers have pinpointed the exact mix of microbes needed to rid mice of a hard-to-treat bacterial pathogen whose spores lead to chronic diarrhea. Antibiotics backfire because they kill the gut's normal microbial community, clearing the way for the pathogen, *Clostridium difficile*, to resettle. Physicians have restored normal gut microbiota by giving patients fecal material from a healthy person, but the treatment can introduce other undesirable pathogens. Microbiologist Trevor Lawley from the Wellcome Trust Sanger Institute in Hinxton, U.K., and colleagues developed a similar treatment that cured mice. Then they cultured bacteria from the fecal material used in the cure, trying to narrow down the number of potential bacteria responsible. Researchers tried different combinations of the 18 types of bacteria they isolated. Only one particular mix of six bacteria cured the mice, the team reports this week in *PLoS Pathogens*. Now, the researchers are culturing the human fecal material used to eradicate this infection in people. If they succeed, someday "a simple suppository of the bacteria could prevent *C. difficile* reinfection and obviate the need for antibiotics, which may exacerbate the problem," says Brendan Wren, a microbiologist at the London School of Hygiene & Tropical Medicine who was not involved with the mouse study. **http://scim.ag/GutBacteria**

## Butterfly Mystery Solved

Monarchs aren't the only continent-hopping butterflies. A new study finds that painted ladies (*Vanessa cardui*), common in Europe and the United Kingdom, are also long-distance commuters, traveling back and forth to North Africa. Although the insect's northward trip to Britain has been well-documented by citizen scientists, few saw them heading south again across the English Channel—suggesting the commute might be one-way. But in the spring of 2009, millions of painted ladies hit the shores of the United Kingdom, enabling researchers to correlate some 60,000 sightings with data from radars monitoring insect movements above 150 meters.

Painted lady butterfly

The radar revealed a high-altitude southward migration route: Most painted ladies ascended to 500 meters or so to hitch rides on fast-moving winds, ecologists reported last week in *Ecography*.

The southbound insects—offspring of the northward-traveling migrants—left for North Africa in two waves, one in August and one in October, sometimes traveling more than 50 kilometers an hour—twice as fast as they can fly on their own, the researchers say. Radar sightings suggest that in 2009 11 million painted ladies landed in the United Kingdom and 26 million left—evidence that, far from being a dead end, the British Isles gave the species a boost. **http://scim.ag/PaintedLady**

### Random Sample

## Fright Night

In 2004, when cognitive scientist Lisa Feldman Barrett was looking for ways to raise money for a local food bank charity, her 6-year-old daughter Sophia had an idea. "She loves candy, loves Halloween, and she knew her mom was an 'emotion scientist,' " says Barrett of Northeastern University in Boston. So why not use her research on fear to design the ultimate haunted house?

Their spooky-looking Victorian house was perfect for the job. To maximize its scariness, Barrett and her lab focused on stimulating the amygdala, the ancient, almond-shaped structure deep inside the brain that regulates the arousal crucial for fear. "It is easy to increase amygdala activation by showing people blood and guts," Barrett says, but it can also traumatize, so they focused on subtler triggers: uncertainty, ambiguity, and novelty. If you can't be sure what is inanimate or alive—such as Barrett's graduate students disguised as ghouls and skeletons—then "the amygdala activates the sympathetic nervous system to increase heart rate, sweating, and breathing rate," Barrett says. The amygdala is also wired to detect how much of the whites of other people's eyes are showing. So they filled the haunted house with actors in costumes with their eyes showing, creepily tracking visitors as they passed through.

Doors open on 27 October, if you're brave enough to be a research subject in this scary experiment. More details at www.newtonhauntedhouse.org.

### BY THE NUMBERS

**500,000** Number of children who developed tuberculosis in 2011, according to the World Health Organization's first analysis of this disease burden in children, published on 17 October in its *Global Tuberculosis Report 2012*.

**17.6** Percentage of journal articles published in 2011 available as open access either immediately or within 12 months of publication, according to a *BMC Medicine* analysis of the Directory of Open Access Journals.

**Science LIVE**

Join us on Thursday, 1 November, at 3 p.m. EDT for a live chat on a hot topic in science. **http://scim.ag/science-live**

CREDITS (TOP TO BOTTOM): DENIS KHVESHCHENIK/ISTOCKPHOTO.COM; JANICE CARR/CDC; DANIEL J. BARRETT





Published by AAAS

CREDIT: RANIERO PIZZI/AP

**Moment of truth.** Defendants Claudio Eva (*center*) and Bernardo De Bernardinis (*center right*) await the verdict this week.

SCIENCE AND THE LAW

# Prison Terms for L'Aquila Experts Shock Scientists

**L'AQUILA, ITALY**—In a decision that has sent shock waves through the scientific community, a judge in this central Italian town has handed down manslaughter sentences of 6 years to each of seven experts who gave advice ahead of the deadly earthquake that struck here in 2009. The four scientists, two engineers, and a government official were accused of having carried out only a superficial analysis of seismic risk and providing false reassurances to the public ahead of the quake, which killed 309 people. The lawyers for those convicted say they will appeal the verdict.

Alfredo Biondi, the defense lawyer for one of the seven, Claudio Eva, a seismologist at the University of Genova, says the verdict was "extremely mistaken." He added: "When someone says how things are, they shouldn't end up in jail for 6 years."

Following a yearlong, highly emotional trial (*Science*, 12 October, p. 184), local residents welcomed the verdict. "I think it is truth and justice," says Vincenzo Vittorini, who lost his wife and daughter in the quake. "It wasn't a trial against science; it was a trial against those who didn't know how to evaluate the risk, who didn't know to mitigate the risk."

But scientists, thousands of whom signed petitions or sent letters protesting the pretrial investigation, are mostly appalled by Judge Marco Billi's decision. "It's incredible that scientists trying to do their job under the direction of a government agency have been convicted for criminal manslaughter," says earth scientist Thomas Jordan of the University of Southern California in Los Angeles. "We know that the system for communicating risk before the L'Aquila earthquake was flawed, but this verdict will cast a pall over any attempt to improve it. I'm afraid that many scientists are learning to keep their mouths shut. This won't help those of us who are trying to improve risk communication between scientists and the public."

"If it stands, this verdict will have a chilling effect on earthquake science in Italy and throughout Europe," said Sandy Steacy of the University of Ulster, Coleraine, in the United Kingdom, in a statement. "For instance, who would now be willing to serve on an earthquake hazard evaluation panel when getting it wrong could mean a conviction for manslaughter?"

> ***"Who would now be willing to serve on an earthquake hazard evaluation panel when getting it wrong could mean a conviction for manslaughter?"***
>
> **—SANDY STEACY, UNIVERSITY OF ULSTER**

All seven defendants took part in a meeting of Italy's National Commission for the Forecast and Prevention of Major Risks that was held in L'Aquila on 31 March 2009, 6 days before the quake struck. They are: Franco Barberi, a volcanologist at the University of Rome (Roma Tre); Enzo Boschi, a geophysicist at the University of Bologna; Gian Michele Calvi, a seismic engineer at the University of Pavia; Eva; Mauro Dolce, a seismic engineer at Italy's Civil Protection Department (DPC); Giulio Selvaggi, a seismologist at Italy's National Institute of Geophysics and Volcanology (INGV); and Bernardo De Bernardinis, a hydraulic engineer who in 2009 was deputy head of DPC.

The prosecution alleged that the information provided by the experts led many people to stay indoors in the early hours of 6 April 2009 rather than seek safety outside. The men were not being charged with having failed to predict the exact time, place, and magnitude of the deadly quake but with having made a series of "banal and self-contradictory" statements during their 2009 meeting, many of which were "at best scientifically useless" or, worse, "misleading," said public prosecutor Fabio Picuti.

Among the most controversial statements were those made by De Bernardinis in a television interview ahead of the meeting. The DPC deputy head said that the ongoing tremors posed "no danger" and that "the scientific community continues to confirm to me that in fact it is a favorable situation," because the ongoing tremors helped discharge energy.

In response to the prosecution's charges, Boschi's lawyer, Marcello Melandri, was keen to distance the statements of De Bernardinis from those of the rest of the commission, telling the court that, according to Picuti, "De Bernardinis suddenly becomes a prophet" insofar as he made his infamous comments before and not after the meeting. Barberi's lawyer, Francesco Petrelli,





Published by AAAS

meanwhile, said in a press interview after the meeting, it was "impossible" to regard as reassuring comments on the unpredictability of earthquakes made by his client, De Bernardinis's advocate, Filippo Dinacci, also emphasized the impossibility of predicting earthquakes. "We are asking the conviction of seven Christians just because an event happened," he told the court.

Responding to this point shortly before the verdict, prosecutor Picuti argued that the defense failed to distinguish between a natural disaster and the risk of such a disaster. While an earthquake is not possible to predict, he said, its risk can be predicted. That logic, he maintained, is borne out in the very name of the commission.

The conviction has stunned many Italian scientists. "I am upset and really shocked" was the reaction of Warner Marzocchi, chief scientist at INGV. "I want to understand why we have arrived at this verdict," he says. "It is hard to know what to do in similar situations in the future." Paolo Scandone, a geologist at the University of Pisa and a member of the Major Risks Commission in the 1980s, says that he feels "deep sadness" at the verdict. But he is nevertheless critical of modern risk assessment in Italy. He argues that in decades past, scientists were "aware of their role" in such assessments and that there was what he calls "a moral tension" among scientists. That tension, he maintains, no longer exists.

Following this week's verdict—during which Billi also awarded victims €7.8 million in compensation—the judge has up to 90 days to deposit a document explaining his reasoning, and the defense will then have 45 days to lodge an appeal. But with two or even three stages, says civil party lawyer Fabio Alessandroni, the appeals process could last up to 6 years. After the verdict, De Bernardinis said in a statement: "I consider myself innocent before God and men. My life will change from tomorrow onwards, but if my responsibilities are demonstrated in all the levels of appeal I will accept them completely."

Willy Aspinall, a risk expert at the University of Bristol in the United Kingdom, describes the prison terms as "distressing and alarming" but nevertheless believes the trial points to a number of "salutary lessons." He says that analysis of natural hazards needs to be "much more formalized and structured," with advice contained in a written document and "off-the-cuff remarks" avoided. He also warns that scientists will "need to become much more litigation aware." **–EDWIN CARTLIDGE**

Edwin Cartlidge is a science writer in Rome.

CREDIT: KYODO/AP

SCIENTIFIC INTEGRITY

# Questions About Japanese Researcher Go Back Years

A startling case involving a groundbreaking stem cell experiment by an unknown researcher, a bogus Harvard affiliation, and multiple collaborators who appear to have signed their names to papers they knew little about is raising questions about the research enterprise and just how easy it can be to pretend you're someone you're not in the world of science.

At the center of the storm is Hisashi Moriguchi of the University of Tokyo Hospital, whose career today stands in tatters. Earlier this month, he admitted to lying about a series of stem cell-based transplants in humans. At least three journals are investigating his papers on stem cells, hepatitis C, and other topics. On many publications, he falsely claimed affiliations with Harvard Medical School and Massachusetts General Hospital (MGH) in Boston as far back as 2002. Two major Japanese institutions that supported Moriguchi's work have launched inquiries. And Moriguchi has been fired.

In a 2-hour interview with *Science* in a Tokyo hotel last weekend, Moriguchi admitted he had made mistakes but insisted he has had a long-standing affiliation with Harvard, despite strenuous denials from that institution. He also said he participated in the stem cell transplants thrown into question, although on only one patient as opposed to the six originally claimed.

Moriguchi perpetuated his alleged fraud for at least a decade, but it grew more elaborate in recent years. He persuaded many others to sign on to his papers and allegedly convinced a Harvard gastroenterologist to file a patent on his behalf. In Japan, there are questions about Moriguchi's possible misuse of research funds. He was brazen: On seven papers co-authored with the gastroenterologist, Raymond Chung, he claimed that he was a member of Chung's own department at MGH.

At least a couple of Moriguchi's co-authors say they often did not read the publications on which their names appeared or did not see them in their final form, thereby never catching the false Harvard affiliation. Some co-authors say they were unaware that Moriguchi was using their names. His supervisor at the University of Tokyo Hospital, surgeon Makoto Mihara, thought his claimed stem cell work occurred in the States, according to the hospital's public relations center. In his interview with *Science*, Moriguchi said he was flying solo, performing stem cell research—but no clinical work—on his own in a rented facility in the Boston area and financing the work out of his own pocket.

The story broke on 11 October, thanks largely to Moriguchi himself. He was attending the annual translational research conference of The New York Stem Cell Foundation in New York City, where a poster of his was

**Hot seat.** Investigations are under way into Hisashi Moriguchi's iPS cell treatment claims.

on display. It contained a bombshell: results from the first-ever human transplants of cells derived from induced pluripotent stem (iPS) cells, which are mature cells reprogrammed to behave like those from an early embryo. Based on an abstract obtained by *Science*, Moriguchi and co-author Chifumi Sato claimed to have generated iPS cells and then derived cardiac muscle cells that were transplanted into six cardiac patients. Japanese reporters were well-represented at the conference because Kazutoshi Takahashi of Kyoto University was being awarded the foundation's Robertson Prize. On the first day of the meeting, 10 October, Moriguchi "just went straight to the press" to speak with them, says Kevin Eggan, chief scientific officer of The New York Stem Cell Foundation and a stem cell biologist at Harvard University. Eggan was familiar with Moriguchi's abstract, having reviewed it along with all the others months in advance of the meeting. But he says he was unsuspecting.

Moriguchi's secondary Harvard affiliation, listed on the abstract, didn't raise red flags because many researchers have ties to multiple institutions, says Eggan, who wondered what this unknown researcher from Japan might have to say about his transplants. Meanwhile, Moriguchi was chatting up his home-country press. "None of us have any idea of what they're saying in Japanese," Eggan says.

He found out soon enough. The next day, a Thursday, the well-respected Japanese daily *Yomiuri Shimbun* described Moriguchi's remarkable work on its front page: He said he was part of a team that had performed the stem cell transplants at Harvard. Eggan, plugged into the Harvard stem cell scene, couldn't imagine this to be true. Harvard checked its records and quickly issued a denial that the transplants had been carried out there. The university stated that Moriguchi had no current connection to the institution. The poster was taken down. "We don't have a way of knowing … everything that is happening at other institutions," Eggan says.

In Japan, Moriguchi's story was collapsing just as quickly. In Friday morning editions, Japanese wire service reports questioned Moriguchi's claims. By midmorning, all related articles had disappeared from both the Japanese and English sites of the *Yomiuri*. (*Yomiuri* apologized to its readers for the erroneous stories the following day.) The University of Tokyo Hospital confirms that Moriguchi had a post there but states that the hospital was not supporting any iPS research. It turned out that Moriguchi's undergraduate training was in nursing and his master's degree in health promotion. The university confirms that under a system common in Japan, he later earned a Ph.D. from the University of Tokyo for a dissertation related to hepatitis C without going through a formal doctoral course.

By Friday evening, Moriguchi's master's adviser and frequent co-author, Sato, who specializes in liver disease and health promotion at Tokyo Medical and Dental University (TMDU), appeared at a hastily called press conference and apologized for his role in the commotion. Ikuo Morita, a TMDU trustee in charge of research, promised an investigation into the validity of all of Moriguchi papers bearing a connection to the university.

Sato writes in an e-mail to *Science* that in his student days, Moriguchi "was an excellent researcher." But he says Moriguchi deceived him about his postgraduation career, explaining that he was working on iPS cells in the United States. Sato writes that Moriguchi sent him many papers that he looked over, only to learn later that the full papers had been rejected. Moriguchi had then shortened them and published them as correspondence. At the 12 October press conference in Tokyo, Sato said he would reflect upon his responsibilities as a co-author.

As more details emerged, it became clearer how Moriguchi had managed to keep his story alive. Chung's relationship with Moriguchi began in 1999, when the two met at an event at the Harvard School of Public Health and Chung agreed to let Moriguchi work in his MGH lab for a month late that year, according to Susan McGreevey, a spokesperson for MGH. In the 13 years since, the two were in periodic contact, and Chung was a co-author on nine of Moriguchi's papers, seven of which carried the Harvard/MGH affiliation. Chung declined to speak to *Science*, but McGreevey writes in an e-mail that Chung did not read the final manuscripts of those articles. Six of the papers were correspondence published in the journal *Hepatology*. Chung primarily provided "editorial assistance," for example, making sure the English was correct, McGreevey says.

Chung "was not sent any of the proofs for review," McGreevey writes to *Science*. "Dr. Moriguchi was the corresponding author, and Dr. Chung had no notification of changes Dr. Moriguchi may have made to the original manuscripts or proofs." In a follow-up note several days later, McGreevey writes that "the fact that Sato was senior author on all the papers co-authored by Ray [Chung] led Ray to give Moriguchi the benefit of any doubt as to the accuracy of the final versions of the reports." On seven papers dating back to 2002, Moriguchi claimed to be a member of the gastrointestinal unit of MGH, Chung's own department there, where he is medical director of the liver transplant program.

In 2011, Chung's connection with Moriguchi took a new turn. "Moriguchi started very persistently asking Dr. Chung for Mass General to file a patent application," McGreevey says in an interview with *Science*. "He told the people in our intellectual property office that he had informed people in the University of Tokyo of this so-called discovery of his and that they were not interested in patenting it," and over the course of "many, many e-mails" sought help from Chung. On 7 July 2011, Chung and Moriguchi filed a U.S. patent application, titled

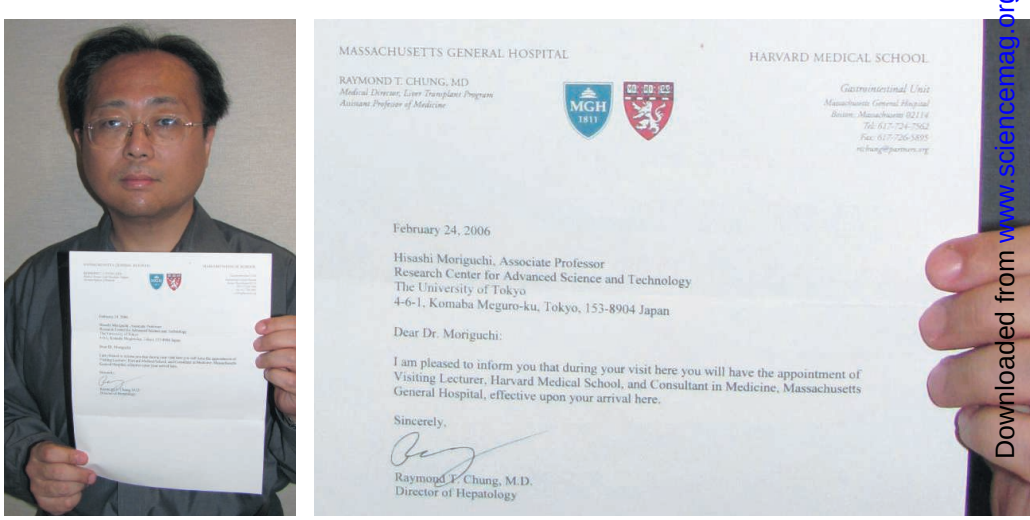


**Open invitation.** Hisashi Moriguchi says a letter giving him privileges "during your visit" confirms a long-term affiliation with Harvard Medical School and Massachusetts General Hospital.

CREDITS: D. NORMILE (2)





Published by AAAS

"Methods and Compositions for Reprogramming Cells." McGreevey says this was based on the papers on which Chung was a co-author. The owner, or assignee, of the patent was The General Hospital Corporation, the legal entity that runs MGH. The inventors listed were Moriguchi and Chung. "We have asked the patent office to abandon the application," McGreevey says.

Both Sato and the University of Tokyo Hospital write in e-mails to *Science* that the fact that MGH had submitted a patent application bolstered Moriguchi's claims to be conducting iPS research in the United States.

Asked whether Chung had violated any Harvard or MGH policies or would be sanctioned in any way, McGreevey says not as far as she knew. Chung "feels betrayed," she says, but "he is hanging in there."

As it happened, several subway stops away, at a different Harvard teaching hospital, a second researcher had developed ties with


死の間際 iPSしかなかった

心筋移植 森口講師

日本なら無理だった

事故で研究止まっては…

臨床応用 慎重な日本側

FRIDAY, OCTOBER 12, 2012

Patients treated with iPS cells

Harvard University team injects cardiac muscle cells into 6 people

**Lost in translation.** *Yomiuri Shimbun* got the Moriguchi story wrong in both its Japanese and English editions.

Moriguchi. Yue Zhang, who was a postdoctoral fellow at Beth Israel Deaconess Medical Center in Boston, writes in an e-mail to *Science* that he first met Moriguchi in June 2011 at the annual Harvard Stem Cell Institute retreat. There, Zhang writes, Moriguchi presented a poster listing his "affiliation with MGH/HMS [Harvard Medical School] before all HMS colleagues." The retreat is intended for Harvard affiliates.

Zhang's former adviser is a soft-spoken molecular biologist, Stuart Calderwood, who works in the radiation oncology department at Beth Israel. As Calderwood recalls, Moriguchi told Zhang that "he was very interested in his work." Zhang "was flattered."

At the time, Zhang was a promising young scientist, having joined Calderwood's lab in the summer of 2008 from the University of Pittsburgh. He was studying autophagy, a process of cellular degradation. In that same e-mail to *Science*, Zhang writes that he checked out Moriguchi's credentials and saw numerous publications in respected journals, a previous news article in *Yomiuri Shimbun* that included his Harvard/MGH title, and business cards listing him as a visiting lecturer at Harvard Medical School and MGH. "He looks like a serious scientist, collaborative, good-willing," Zhang writes.

Less than 5 months after meeting Moriguchi, in October 2011, Zhang abruptly left the lab. In an e-mail, he tells *Science* that he ran into visa problems and moved to Canada with his wife and young sons. Calderwood says he learned about his departure the day he left. Zhang corresponded with *Science* from a Yahoo e-mail account and wrote he has a "temporary position" but declined to be more specific.

In November 2011, Zhang's name began appearing on papers alongside Moriguchi's. Two papers appear in *Scientific Reports*, a *Nature* journal. One describes a simple method of reprogramming liver cancer cells; the other, a new cryopreservation approach for ovarian tissue. In both, Moriguchi included a Harvard affiliation (as did Zhang, who no longer worked there). The four authors, including Mihara and Sato, claimed both studies had been green-lighted by institutional review boards (IRBs) at Harvard Medical School and the University of Tokyo. Both Harvard and the University of Tokyo Hospital say they have no record of IRB approvals. (The University of Tokyo is still checking the records of its various other boards.)

Moriguchi told *Science* that it was unclear whether the planned experiments needed IRB approval, which he never sought. Including the statements in the papers "was a procedural miss," he said. He added that he has informed *Scientific Reports* he would like to retract the papers.

Zhang says he performed "data analysis, assessment, and interpretation of manuscripts." He says he has requested that the *Scientific Reports* papers be withdrawn, if appropriate. "It turns out my mistake [was] to put trust in him," Zhang wrote to *Science.*

The publications in *Scientific Reports* were peer-reviewed. Still, journals vary widely in what they expect of authors. Like most, *Nature* journals do not verify author affiliations. They also don't require that all the authors see a final version of the manuscript. "Submission to a *Nature* journal is taken by the journal to mean that all the listed authors have agreed to all the contents," writes Ruth Francis, head of press for Nature Publishing Group, in an e-mail. "The corresponding (submitting) author is responsible for having ensured that this agreement has been reached."

Other journals have more stringent rules. *Hepatology*, where Chung's name appears alongside Moriguchi's, expects all authors to look over the final manuscript.

But counting on authors to do this isn't always sufficient, as the Moriguchi case makes clear. "We don't expect anyone to read our instructions for authors," admits Drummond Rennie, an editor at the *Journal of the American Medical Association*. *JAMA* requires that all authors sign off on a copy of the manuscript before it goes to press. *Science* has a similar policy. Still, Rennie thinks it's unreasonable to expect journals to double-check affiliations. "Every year there are more things we would check and ideally should check, but we can't" do it all, Rennie says. "Where do you stop?"

*Scientific Reports*, *Protocol Exchange*, and *Hepatology* are investigating. The University of Tokyo has two committees looking into the matter and has acknowledged that the Japan Society for the Promotion of Science, a government-affiliated funding organization, has asked for information on the use of public monies. TMDU's investigation is continuing.

Moriguchi, meanwhile, is sticking to his claim that he supplied cardiac muscle cells derived from a patient's own iPS cells for transplantation, although he's downgraded the number of patients from six to one. When speaking with *Science,* Moriguchi was polite, gracious, and relaxed. He would say only that the surgery was performed at a hospital in Boston and declined to identify the hospital or his collaborators. But for that one case, "I'm very confident" in its veracity, he said.

**–JENNIFER COUZIN-FRANKEL AND DENNIS NORMILE**





*Published by AAAS*

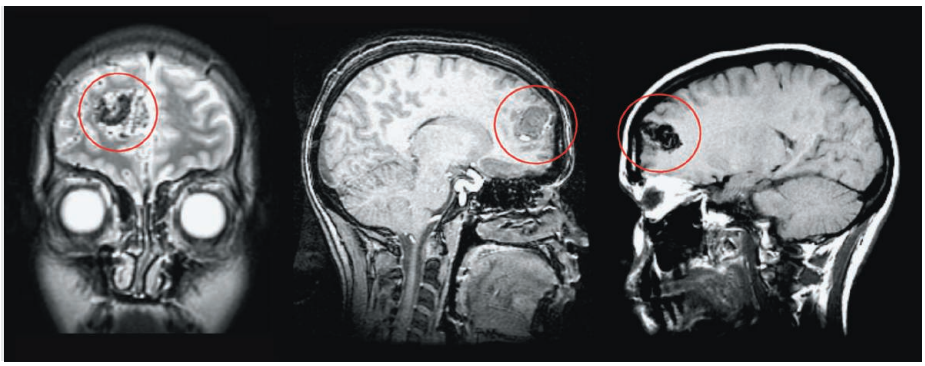

**Not subtle.** A cluster of malformed veins and arteries in Sarah Hilgenberg's brain, discovered by her classmate in 2002.

NEUROETHICS

# When a Brain Scan Bears Bad News

In 2002, Sarah Hilgenberg was in her first quarter at Stanford University School of Medicine in Palo Alto, California, when a classmate, Matthew Kirschen, asked if she'd be interested in getting her brain scanned for his memory study. She agreed immediately, glad for the $40 and the chance to help. A healthy college athlete, she had no reason to suspect that anything was amiss.

"You have a beautiful brain," she heard Kirschen say over the speaker as she lay in the MRI chamber. As he looked at the images, however, Kirschen says a knot formed in his stomach. When she asked to see her scans, he made excuses for not showing them and asked a barrage of questions: Had she been having headaches? Vision problems? When she left, he rushed the scans to Gary Glover, the lab director, and the on-call radiologist. Together, they decided that Hilgenberg needed to go to the emergency room. Further MRI scans revealed that Hilgenberg had a web of malformed arteries and veins in her brain that could kill her if it ruptured.

Various studies have shown that as many as 20% of MRI scans performed for research turn up things that seem abnormal but have nothing to do with the study, says Judy Illes, a neuroethicist at the University of British Columbia, Vancouver, in Canada. Called incidental findings (IFs), roughly 2% of these abnormalities require urgent medical attention, she says. Since the scare with Hilgenberg, Illes has worked extensively with Glover and Kirschen, who is now at the Children's Hospital of Philadelphia, publishing numerous papers and convening working groups to develop clearer protocols for researchers dealing with IFs. On 18 October, she gathered 28 prominent neuroscientists, clinicians, ethicists, and lawyers in Washington, D.C., to hash out new guidance as part of a working group sponsored by the National Institutes of Health (NIH) and other U.S. and Canadian agencies. Amid intense debate, the group wrote guidelines that they hope granting agencies such as NIH and local institutional review boards (IRBs) will adopt.

Illes's earlier attempt to produce such guidelines at a meeting in a 2005 didn't go smoothly, she laughs: "Blood was spilt." The group deemed it "ethically desirable" to design research protocols for IFs, but they heatedly debated what the protocols should be and whether researchers should examine and disclose such findings in the first place. Although clinicians have a legal "duty to care" for their patients, scientific researchers are not legally bound or professionally trained to interpret brain scans diagnostically, says Susan Wolf, a professor of law and medicine at the University of Minnesota, Twin Cities. Aside from rare anecdotes like Hilgenberg's, some researchers argue, no data support the idea that looking at brain scans of apparently healthy people is a useful way to screen for disease. In addition, they say, the low resolution and contrast of typical research MRIs could increase the potential for emotionally and economically costly false positives.

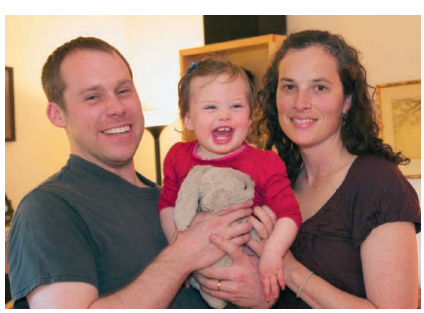

**Ten years later.** Sarah Hilgenberg with her husband and 19 month-old daughter.

Others argue that the chance, however slim, of saving lives like Hilgenberg's is worth delving into that gray area and is practically feasible for researchers. Since the Stanford Radiological Sciences Laboratory opened in 1990, they've kept a radiologist on call, Glover says. Although not every scan is read by a radiologist, students and researchers are trained to report anything odd. Hilgenberg, now an instructor of pediatrics at Lucile Packard Children's Hospital at Stanford and mother of a 19-month-old daughter, credits this protocol with saving her life. A few months after Kirschen found the web of arteries, she had it removed by a top neurosurgeon. "I feel lucky to have fallen into the hands of these folks," she says. "They provided me with a second go at life, and they weren't obligated to do that at all."

The government guidance that grew out of the 2005 meeting was loose, Illes says (*Science*, 10 February 2006, p. 783). For example, it suggests that researchers "anticipate potential for IFs in experimental design," but leave particulars up to individual funding agencies, research labs, and IRBs. The resulting noise creates inefficiency, with different procedures from lab to lab and funding agency to funding agency, she says: "We thought we were being appropriately flexible, but in fact we created Pandora's box."

Based on her surveys of neuroimagers in the United States and Canada since 2005, Illes says many researchers in the field are asking for more direction: "They don't want to be ethicists."

At the 18 October meeting, Illes hoped to persuade her colleagues to sign on to a recommendation that all research scans be read by a physician—a central point of contention from the 2005 meeting. The group stopped just short of Illes's goal, suggesting instead that the principal investigators of all brain-imaging studies establish access to a radiologist, neurosurgeon, or other physician qualified to read brain scans; the voluntary guidelines leave open the question of whether all scans get read or only those that appear suspect.

The working group plans to publish its recommendations through a notice in the *NIH Guide for Grants and Contracts*. The consolidated document is "a huge step forward" in providing clearer guidance to funding agencies, researchers, and IRBs, Illes says. The fact that the group was able to reach consensus, she adds, shows "how far we've come in solidifying partnerships between neuroscientists and ethicists."

–EMILY UNDERWOOD

CREDITS: COURTESY SARAH HILGENBERG (2)





Published by AAAS

# Congratulations! Now Get to Work

## Regardless of his margin of victory, the president will need all the help he can get in dealing with several intractable problems

**PROMISES DOMINATE POLITICAL CAMPAIGNS.** But once the election is over, either Mitt Romney or Barack Obama will have to govern.

This package examines the science-related issues facing the next occupant of the Oval Office and, for the few that have been featured in the campaign, the positions the candidates have taken on them. At the top of the president's "to-do" list will be trying to resolve the current budget deadlock; legislators will have another chance to address that next month during a lame-duck session of Congress. And while science needs funding to thrive, there are a host of other areas, including energy, education, the environment, space, and biomedicine, in which direction may be just as important as dollars.

Of course, not all wisdom resides in the White House. Next month's election will also determine the makeup of Congress for the next 2 years. So we bring you one House of Representatives race in which federal science policy is receiving an unusual amount of attention (p. 463). Another story explores new research on negative advertising, a reviled but increasingly popular mode of trying to influence voters (p. 465). And we also look at a passel of state initiatives appearing on the ballot that affect the scientific community, including a hotly contested proposal in California to label genetically modified foods (p. 464).

**–JEFFREY MERVIS AND DAVID MALAKOFF**

### Online

**sciencemag.org**

Podcast interview with David Malakoff (http://scim.ag/pod_6106).

### THE PRESIDENT'S TO-DO LIST

- FUNDING
- DEFENSE RESEARCH
- ENERGY RESEARCH
- CLIMATE + ENVIRONMENT
- EDUCATION
- SPACE SCIENCE
- BIODEFENSE
- IMMIGRATION
- BIOMEDICAL RESEARCH

CREDITS (TOP TO BOTTOM): BROOKS KRAFT/CORBIS; ISTOCKPHOTO.COM; WIKIMEDIA COMMONS





Published by AAAS

**BARACK OBAMA AND MITT ROMNEY** have promised, as president, to maintain U.S. scientific excellence while paring down a $1.4-trillion-a-year budget deficit. And it's the second half of the sentence that really worries the U.S. academic community. Although each man has said he believes basic research is essential for economic development, it's not at all clear how much is enough, and which areas should be emphasized.

President Obama has been proud to run on his record of support for science. He has repeatedly honored a pledge, first sounded by President George W. Bush, to boost the nation's investment in the physical sciences and engineering through a 10-year doubling of the budgets of the National Science Foundation, the Department of Energy's Office of Science, and the National Institute of Standards and Technology, although Congress has typically trimmed his annual requests for those agencies. The president has also set a goal of boosting the nation's overall spending on research to 3% of the country's gross domestic product, using federal dollars to spur private-sector R&D investment. In addition, the massive 2009 stimulus package included an unprecedented, one-time, $20 billion boost for basic research (*Science*, 27 November 2009, p. 1176).

As a former Massachusetts governor who has never served in Congress, Romney has no track record on federal funding for science. In speeches, he has affirmed the value of university-based research. But Romney has declined to provide any details. When he does mention basic research, it's most often in the context of energy policy, specifically, to contrast what he labels the Obama administration's misguided attempts to "pick winners" in promoting renewable energy technologies with his commitment "to spend the money more wisely."


That ambiguity has put the U.S. academic community on high alert. Their response has been a steady stream of reports and white papers documenting how research has contributed to the nation's prosperity, and petitions urging that it not be cut. Staying the course is even more critical now that other countries have learned from the United States and have begun making similarly large investments in research, they add.

The argument that research should be buffered, if not exempt, from the overall federal belt-tightening is not a new one, of course. But the current effort to trim the massive federal deficit adds urgency.

The immediate threat to U.S. science is $110 billion in across-the-board cuts to this year's budget, divided evenly between defense and domestic discretionary spending. Under those automatic cuts, which are scheduled to take effect on 2 January, most science agencies would see their 2013 budgets shrink by 8.2% from current levels. For the $31 billion National Institutes of Health, for example, that translates into a $2.5 billion reduction. The $7 billion National Science Foundation would lose $580 million, and the Department of Energy's $4.9 billion Office of Science programs would drop by $423 million.

Those cuts, called sequestration, were intended to be a last resort under a two-step agreement struck in August 2011 between the White House and Congress to begin reducing what is now a $1.4 trillion annual deficit. The two sides shook hands on more than $900 billion in projected cuts through 2021, starting with $21 billion in the 2012 fiscal year that ended on 30 September. The law created a committee to find an additional $1.2 trillion in some combination of spending cuts and increased revenues, but last December, Congress failed to adopt the committee's recommendations. That inaction started the clock running on sequestration.

So far this year, Congress has made no headway on resolving the deadlock. In fact, it's gone in the opposite direction, extending current spending levels for another 6 months in lieu of passing a spending bill for the 2013 fiscal year that began on 1 October.

A lame-duck session after the election will give it one more chance. Although most observers aren't optimistic, scenarios include a postelection détente that starts down a path toward shaving $4 trillion off the deficit over 10 years or a 6-month delay in the effective date of sequestration.

The election results will certainly influence any decision. A status-quo outcome—a Democratic president and a divided Congress—could nudge all sides toward a compromise, while a Republican sweep is likely to mean no movement until after the winners take office in January. And if sequestration is imposed, those cuts will seriously hamper the plans of whoever is elected.

Lurking in the shadows, however, is an ugly but unspoken truth: The era of American dominance in science is over. By any reasonable yardstick—spending, Ph.D. production, publications, patents, sales of high-tech manufactured goods, or something else—the rest of the world is narrowing the extraordinary lead in science that the United States has maintained for the past half-century. And although cutting back on research might accelerate that process, no foreseeable increase in federal spending will allow the United States to recapture that large advantage.

So be wary of any candidate who says his policies will guarantee U.S. preeminence in science. That ship has sailed. In the new era of constrained choices, investing more in one area usually requires spending less in another field. All-of-the-above may work as an energy strategy. But it's no longer a reasonable expectation for federal spending on research. **–JEFFREY MERVIS**


**WILL THE 2% SOLUTION SURVIVE?** The next president will need to decide whether to honor a long-standing commitment to grow the Department of Defense's (DOD's) relatively small basic research budget by 2% annually over the next 4 years despite overall cuts in military spending.

Although basic science accounts for less than 0.5% of the Pentagon's annual budget, the $2.1 billion is a lifeline for many academic researchers. Roughly half goes to universities, and DOD is the single largest government funder in many fields of engineering, mathematics, and computer science.

Military planners say research is essential for a modern fighting force. And former defense secretary Robert Gates—who served under both Obama and his Republican predecessor, George W. Bush—promised to prevent basic science spending from stagnating. Gates is gone, however, and his successors confront the tumultuous task of figuring out how to "rightsize" the Pentagon.

The Obama administration has said cuts must be made but it will try to limit the damage to DOD's basic research programs. Romney has promised to increase overall defense spending but hasn't said whether basic science would also grow. **–DAVID MALAKOFF**





Published by AAAS


**WHAT TO KEEP AND WHAT** to trim from the Department of Energy's (DOE's) sprawling $11 billion research portfolio is the big question facing the winner of next month's election. Neither candidate has said much during the campaign about how tightening budgets (see p. 457) would affect the department's research priorities, but they have offered divergent views on the government's role in commercializing technologies.

Scientists involved in physics and fusion studies that require big, expensive machines are particularly anxious about where fundamental studies that offer little promise of immediate practical payoffs will rank among the priorities in an Obama or Romney administration. Particle physicists, for instance, are wondering if the White House will back a nearly $800 million plan to build a scaled-down version of the Long-Baseline Neutrino Experiment (LBNE). In addition to documenting the behavior of these subatomic particles, the LBNE is the best hope for the survival of the last U.S. bastion of particle physics, the Fermi National Accelerator Laboratory in Batavia, Illinois (*Science*, 7 September, p. 1157).

The next president may also have to sacrifice one of three major projects in nuclear physics so that the others might survive. The Relativistic Heavy Ion Collider, an atom smasher at Brookhaven National Laboratory in Upton, New York, is considered the more vulnerable of two existing facilities because DOE recently upgraded the Continuous Electron Beam Accelerator Facility at the Thomas Jefferson National Accelerator Facility in Newport News, Virginia. The third, the Facility for Rare Isotope Beams, is under development at Michigan State University in East Lansing.

There is trouble brewing on two fronts for U.S. fusion researchers, who seek to reproduce on Earth the process that powers the sun. One formidable challenge comes from the ITER international fusion project under construction in France. The United States is expected to put about $2.2 billion into the $23 billion project over the next 8 years—meaning its annual contribution will ultimately match everything DOE now spends on fusion reactor research. So the next administration has three options: Increase the overall fusion budget, close several U.S.-based fusion laboratories, or reevaluate its support for ITER.

Fusion researchers may also be squeezed out of working on the National Ignition Facility (NIF) at the Lawrence Livermore National Laboratory in California, a $3.5 billion laser facility built for both fusion research and nuclear weapons studies. Last month, NIF scientists missed a DOE deadline for igniting a fusion reaction inside a tiny capsule filled with hydrogen fuel (*Science*, 21 September, p. 1444). As a result, NIF's focus is now shifting to weapons research.

It is unlikely that either Obama or Romney has strong views on these in-the-trenches science decisions, so the person serving as energy secretary could play an influential role. Nobel laureate Steven Chu hasn't said whether he expects to serve in a second Obama administration, but many Washington insiders will be surprised if he stays. Romney has made it clear that his energy team will focus primarily on ramping up domestic coal, oil, and gas production—a traditional stance for Republican administrations.

No matter who is elected, DOE's spending on efforts to commercialize new energy technologies is likely to be reshuffled. Romney has promised to eliminate loan-guarantee, tax-credit, and other programs aimed at accelerating the commercial development of nonfossil energy sources, such as solar and wind power, saying the market should decide "winners and losers." Obama has said he'll stand by those programs—some of which were created by Republicans—despite the high-profile bankruptcies of several government-backed companies. Any decisions will require buy-in from Congress, which has its own ideas.

One thing the two candidates agree on is continued funding for DOE's 3-year-old Advanced Research Projects Agency–Energy, which last year spent $275 million on research into emerging technologies that need a nudge to attract private investment. They are especially fond of the agency's administrative nimbleness, including its commitment to kill off projects that aren't meeting milestones.

**–DAVID MALAKOFF**


**IT IS HARD TO FIND TWO** issues that more starkly highlight the differences between Barack Obama and Mitt Romney than climate change and environmental regulation. At the same time, whoever wins the election will have to cope with sharp constraints on his ability to implement those policies.

Obama agrees that humans are causing climate change and says the federal government should take action to curb the emission of greenhouse gases that are contributing to global warming; Romney says the causes need more study, and that it's not clear that the government should do anything about greenhouse gases. Obama has adopted or set in motion a panoply of new rules aimed at reducing pollution and protecting habitat from development; Romney has vowed to roll back most if not all of them, arguing they harm the economy.

Neither candidate, however, has acknowledged the dirty little secret of environmental politics: Few presidents are able to move as far or as fast on environmental issues as they claim they'd like to. Just as Obama has been stymied on a number of fronts by Congress, the courts, and political opposition from both the left and the right, Romney would face a host of obstacles to undoing present policies.

Still, there are several areas where the winner can act unilaterally. For instance, Romney could rescind with a stroke of a pen several Obama-era executive orders that require government agencies to reduce greenhouse gas emissions and make "green" purchases. He could also slow the implementation of recent rules aimed at cutting carbon emissions from existing coal-fired power plants and essentially block efforts to extend those rules to new plants.

It's less clear, however, that he could undo court rulings that have upheld the Environmental Protection Agency's finding that those emissions "endanger" public health under the Clean Air Act and, therefore, require regulatory action. And Romney could also face legal tangles if he attempts to roll back other regulations targeting mercury pollution and ground-level ozone. In contrast, reelection would give Obama a chance to consolidate and entrench these regulatory approaches, but he could also face new legal challenges.




Published by AAAS

**FOR BETTER OR WORSE, TEACHERS** have captured the lion's share of the meager attention given to education during this year's presidential election. Their political activism infuriates Mitt Romney, who would like to ban teachers' unions from making campaign contributions. In addition, his support for vouchers—channeling federal funding for low-income and disabled students to parents rather than to local and state agencies—is designed in part to blunt the influence of teachers' unions in making policy. In contrast, President Barack Obama has relied on these unions to help get out the vote, and he frequently mentions that funds from his massive 2009 federal stimulus package have kept hundreds of thousands of classroom teachers on the payroll.


But what do the two candidates think about the job that those teachers are paid to do? Both men have said that teachers are the essential ingredient in a good school. And although it may be easy to dismiss their comments as an applause line, their position also squares with a growing body of research on the powerful influence of good teachers on student learning.

Those findings could play a role in several pieces of legislation coming up for review as soon as next year. Two key reauthorizations are the Elementary and Secondary Education Act, which former President George W. Bush branded "No Child Left Behind," and the Higher Education Act, which governs student lending and teacher training. Also on the table are special education and technical education programs, as well as the Department of Education's research arm, the Institute of Education Sciences. Scientists hope that research on teacher quality will get a boost regardless of which man is elected.

The federal government provides less than 10% of all funding for elementary and secondary education in the United States, and STEM (science, technology, engineering, and mathematics) education receives a tiny fraction of that federal investment. Even so, Obama has probably spent more time talking about STEM education than any president in recent memory. His stump speech invariably includes his promise to train 100,000 more science and math teachers over the next decade as part of a broader effort to build a more technology-savvy workforce. Obama has also run on his record of fostering state-based educational innovations through a $4 billion Race to the Top competition for schools, as well as a public-private partnership, called Educate to Innovate, created to attract more students, in particular women and minorities, into STEM fields.

Romney hasn't ignored the subject, although he has much less to say about science and math education. He believes that Washington has no business financing implementation of the so-called Common Core, a voluntary effort by 45 states and the District of Columbia to adopt a similar curriculum in math and language arts, and a companion common assessment of student performance. That stance presumably would also apply to the pending next-generation science standards that have yet to be embraced by the states. At the same time, however, he backs efforts by states to hold teachers accountable for how much students learn, including losing their jobs if test scores stagnate.

The importance of science education to the Obama administration is no coincidence. Physics Nobelist Carl Wieman was the driving force for STEM education policies during most of Obama's first term before leaving the White House Office of Science and Technology Policy in June for treatment of a serious medical condition. Wieman has spent more than a decade conducting research on two related issues: how to improve undergraduate science courses, and the training of future STEM teachers. He believes that both areas would benefit from an approach he calls "deliberate practice," that is, treating the brain as a muscle that acquires skills through extended and strenuous learning activities. Two recent reports, one by a presidential advisory body on improving STEM education and another by the U.S. National Academies on discipline-based science education, strike similar themes on what needs to be done.

In short, a second Obama administration will likely continue its push to beef up federal STEM education efforts. Romney, on the other hand, would probably be content to see local authorities take the initiative.

**–JEFFREY MERVIS**

The two candidates also differ on how to protect habitat on federal land. Obama has taken a two-pronged approach: Honor existing moratoria on oil and gas drilling in federal waters off the coasts of California and Florida and oppose drilling in Alaska's Arctic National Wildlife Refuge (ANWR), but move cautiously to allow exploratory wells in Arctic seas off Alaska. He also has stiffened regulatory requirements for companies wanting to drill, mine, or log on public lands.

Romney, in contrast, has said he would push to open for drilling ANWR and other coastal areas, as well as offering greater incentives to quickly develop areas that are already open to leasing. He has criticized Obama for crippling efforts to exploit public holdings and said he would give states a greater say in how to use federal lands within their boundaries.

The next administration will also need to decide how much political capital to invest on reaching an international deal to address climate change. Obama has said the U.S. will stay involved in desultory efforts to persuade other major greenhouse gas emitters—most notably China—to act in concert to curb their emissions. China has shown little appetite for the subject recently, however, and Congress fiercely opposes any deal that it believes puts the United States at an economic disadvantage. The Romney campaign, meanwhile, has said that it is skeptical of any global discussions, especially given the uncertainty surrounding the causes and impacts of climate change.

Although few are betting on any global agreement any time soon to curb emissions, the issue isn't going away. In September 2013, the U.N. Intergovernmental Panel on Climate Change will start releasing its next big report on the science, impacts, and potential mitigation of climate change. The new data are expected to rekindle debate on the topic.

Striking the right balance between protecting the environment and fostering economic development lies at the heart of another issue facing the next president, namely, how best to rewrite the Toxic Substances Control Act. It's the nation's flagship law regulating the use of new and existing chemicals. One especially thorny issue is how to regulate the minuscule products of nanotechnology without hobbling commercialization of that nascent field.

**–DAVID MALAKOFF**





Published by AAAS

**THE BUDGETS FOR SPACE SCIENCE** and space exploration at NASA may be comparable in size, but that's where their similarity ends. Human flight and the hardware needed to make it happen get most of the attention from Congress and the public, thanks in part to the clout of the aerospace industry and the popular appeal of astronauts. But scientific missions, such as Hubble and the Mars Curiosity rover, have racked up the biggest achievements in recent years.

The next president will be challenged to find a way to keep both sectors healthy, and it promises to be a tall order for either man. Critics of President Barack Obama say he lacks a comprehensive vision for human exploration and that NASA's pipeline of robotic missions is running dry. Meanwhile, Mitt Romney has settled for criticizing his opponent's record without offering any substantial plan of his own.

There is no shortage of scientific decisions facing the next administration. The agency's plans for exploring Mars in the next decade are only beginning to take shape, following the Obama administration's recent decision to cancel NASA's participation in the European-led ExoMars mission. NASA is under pressure to deliver the $8.8 billion James Webb Space Telescope by 2018, its new launch date, and the next president will have to ensure that the mission does not suffer any further cost increases.

The next administration will also have to wrestle with Congress over the way forward in promoting commercial spaceflight after Obama cancelled the Constellation program, whose goal was to return U.S. astronauts to the moon by 2020. That approach was replaced with a plan to commercialize human spaceflight, develop new technologies, and send humans to a nearby asteroid by 2025. The administration has had to overcome considerable resistance from Congress over the past 3 years to begin implementing Obama's vision.


If Republican nominee Romney has a position on these and other issues facing NASA, he's keeping it a secret. All he has said on the subject so far is that he doesn't like the direction in which NASA is headed. In a space policy white paper released by the Romney campaign last month, he attacked Obama for failing to "deliver a coherent policy for human space exploration and space security," which he said was eroding the nation's leadership in space. "The President's disjointed collection of scientific projects lack guiding principles, plausible objectives, or a roadmap for long-run success," Romney wrote in the white paper.

What would Romney do differently? His paper offers some rather broad hints. One would ensure that NASA has "practical and sustainable missions" that balance "pragmatic and top-priority science with inspirational and groundbreaking exploration programs." A second would improve the relationship between NASA and its international partners. A third calls for a clear road map for developing the commercial space industry. At the same time, some of his proposals sound like what NASA is already doing, such as developing "new generations of spacecraft for government missions" while transitioning out of "routine space operations in low Earth orbit as private sector capabilities mature."

If Obama wins a second term, he can expect to continue his tussle with Congress to secure funding for the programs NASA has embarked on at a time when the space agency's budget is only likely to flatten or decline. He's already compromised (supporters would say he's shown flexibility) by embracing two elements of the abandoned Constellation program—a stripped-down version of the Orion Crew Exploration Vehicle that is to serve as a lifeboat for the International Space Station and a heavy-lift rocket.

The fighting over the big redirection that Obama ordered may have finally subsided, but more recent changes are continuing to be met with resistance. Obama's decision to cancel NASA's participation in ExoMars has ignited protests from lawmakers on both sides of the aisle. NASA officials have responded by outlining a new Mars exploration program that would begin with an orbiter mission in 2018 followed by a sample return effort and culminating in a human mission to the Red Planet in the mid-2030s. But filling in the details of that plan will be just one of many challenges that await the next president.

**–YUDHIJIT BHATTACHARJEE**

**BIODEFENSE HAS BEEN WELL** below the radar in the election campaign, but the next administration will have to make an early decision on how much further to go in regulating basic research involving potentially risky pathogens. In March, the Obama administration expanded regulatory requirements for federally funded scientists working with 15 particularly dangerous agents after a global controversy over whether scientists should publish two studies showing how they made the H5N1 avian influenza virus potentially more dangerous to humans (*Science*, 6 April, p. 21).


The papers were ultimately published, but the episode is still reverberating through the bureaucracy. Government officials are working on plans that would ask universities to do more to help reduce the risks to society from biomedical research that might be used for good or evil. But any new system could take several years to implement, and academics are likely to push back against any rules that they see as adding to their workloads without truly reducing risks. The next administration will also have to help resolve the question of how—and when—to end a voluntary research moratorium that has stalled certain kinds of influenza studies.

The next president will also need to review a proposed $3.1 billion expansion of the controversial BioWatch early warning system designed to detect a bioweapons attack. The U.S. Department of Homeland Security (DHS) has so far spent about $1 billion to deploy BioWatch systems in 30 U.S. cities. But government auditors and independent analysts say the current technology—which involves air filters that are hand-checked daily for the presence of pathogens—is faulty and unreliable. BioWatch planners have proposed an upgrade, known as Generation 3, which would automate much of the system. But many members of Congress are skeptical of the cost and have called for a review before moving ahead. DHS officials have asked an outside group to take a look and report back sometime next year. **–DAVID MALAKOFF**




Published by AAAS


**ON THE CAMPAIGN TRAIL, PRESIDENT** Barack Obama and Mitt Romney differ sharply on what to do about illegal immigration, including the 12 million undocumented persons living in the United States.

But the candidates are not far apart on the issue of legal immigration, which gets much less attention. And they hold nearly identical positions on how to make it easier to retain the most talented foreign students after they graduate with advanced science and engineering degrees from U.S. universities. Their solution, often shortened to the sound bite "Staple a green card to their diplomas," is also a key objective for the U.S. high-tech community.

But the politics of immigration make achieving that goal difficult. Last month, for instance, the House of Representatives defeated a Republican-backed bill that included a "stapling-lite" provision because many Democrats objected to how it would be implemented. Conventional wisdom says that such changes will have to be part of comprehensive immigration reform, which so far has eluded Congress.

But next year could be different. "I can deliver, Governor, a whole bunch of Democrats to get comprehensive immigration reform done," Obama promised during last week's debate at Hofstra University in Hempstead, New York. Not to be outdone, Romney replied: "I'll get it done, first year." If the next president keeps his word, foreign-born scientists could find themselves with a much easier path toward permanent residency.

**–JEFFREY MERVIS**


**ALTHOUGH PRESIDENT BARACK OBAMA'S POLICY ON** stem cell research and his choices to lead the National Institutes of Health (NIH) and the National Cancer Institute have pleased the biomedical research community, his habit of singling out specific diseases for special attention in budget requests has ruffled some scientists' feathers.

Most scientists would prefer that a president rely on NIH's peer-review system to award money based on the strongest proposals. Mitt Romney, who has otherwise said little about biomedical research, has promised to do exactly that.

Obama administration officials have said that their emphasis on specific diseases is a response to public health needs and scientific opportunities. And the practice may be irresistible for politicians responding to key constituencies and their own health histories.

Obama, whose mother died of ovarian cancer, favored cancer research over the rest of NIH's portfolio in his 2010 and 2011 budget requests. His 2010 request also proposed doubling cancer research over 8 years. Congress, however, ignored those requests.

The Obama administration has enjoyed greater success in its bid to boost autism research, which grew by 28% over those 2 years. Research on Alzheimer's has also been favored in the past year. "We can't wait to act; reducing the burden of Alzheimer's disease on patients and their families is an urgent national priority," said Health and Human Services Secretary Kathleen Sebelius in February about the new Alzheimer's money.

The Romney campaign is not immune to such pleas, and Ann Romney, Mitt's wife, is a breast cancer survivor. The Republican platform says the party supports biomedical research, "especially … neuroscience research" on diseases such as autism, Alzheimer's, and Parkinson's. It also backs more research on cancer and other diseases among "formerly neglected groups."

At the same time, Romney's campaign Web site doesn't mention research on specific diseases. And he toed the biomedical community's line while campaigning in Iowa during the Republican primary. "Where I will spend money … will be determined not by the people who are the politicians but by the scientists and by people who measure where they think the impact will be the greatest," Romney told a boy with autism at a town hall meeting. "So I can tell you that I will do it in a fair and appropriate, nonpolitical way."

One of President Obama's most significant science policy changes was his 2009 executive order lifting limits on federal funding for research on human embryonic stem cells. Romney hasn't cleary indicated whether he would maintain or reverse that policy.

**–JOCELYN KAISER**

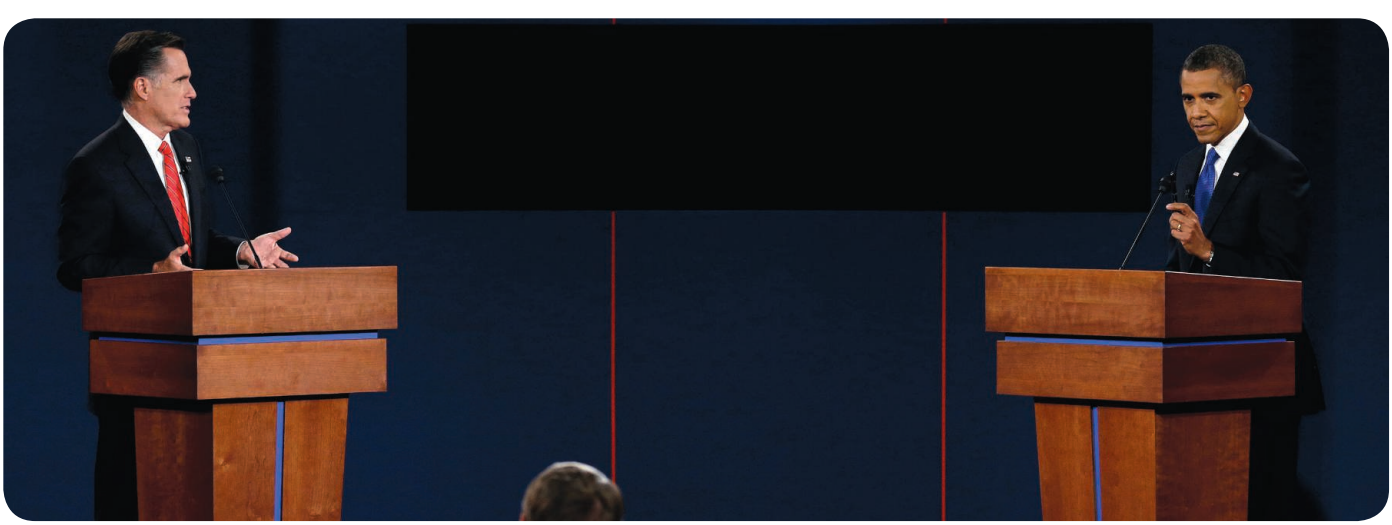

CREDIT: DARRIN HIGGINS; CHARLIE NEIBERGALL/AP/CORBIS





Published by AAAS


CREDIT: JOHN J. KIM/MCT/LANDOV

**Gloves off.** Biggert and Foster have sparred over science this fall in a campaign marked by attack ads.

# For Once, Science Is an Issue In Race for a Seat in Congress

**A physicist takes on a longtime friend of science in a tight Illinois race in which research matters**

Candidates for Congress rarely fight over how fervently they support science. But it's happening in Illinois's newly redrawn 11th district, a contorted swath of Chicago's southwestern suburbs. The election for a seat in the House of Representatives pits Democrat Bill Foster, a physicist who served in Congress from 2008 through the start of 2011, against Republican Judy Biggert, the seven-term incumbent who has served on the House science committee for her entire career.

Science features in the race because the district includes part of Argonne National Laboratory, a multipurpose lab owned by the Department of Energy (DOE). It also runs just south of DOE's Fermi National Accelerator Laboratory (Fermilab), the sole U.S. laboratory specializing in particle physics. Polls show Biggert, 75, and Foster, 57, in a dead heat, and the votes of scientists probably won't decide the contest. But the at-times-nasty campaign raises the question of whether it's better for researchers to have a longtime ally or one of their own on Capitol Hill.

The candidates are trading potshots over science. In a recent debate, Biggert, whose old district encompassed Argonne, all but accused Foster of abandoning his colleagues: "My opponent couldn't get on the science committee even though he's a scientist." After the debate, Foster told *Science* that if elected, he'd prefer a seat on the appropriations committee, where he could directly influence science funding.

But during the debate, Foster counterattacked on science. "You voted for the Ryan budget," he began, referring to the cost-cutting federal budget proposed by Republican vice-presidential nominee Paul Ryan, who chairs the House of Representatives Budget Committee. "You claim to be a supporter of science, and yet the Ryan budget has been analyzed and it provides for a 30% cut to federal research budgets." (An analysis by AAAS, the publisher of *Science*, estimates that nondefense research spending could drop by 27% under the Ryan budget.)

Scientists clearly prefer Foster. Records from the Federal Election Commission show that hundreds of researchers from all over the country have donated nearly $400,000 to his campaign. Only two donors who identify themselves as scientists show up on Biggert's tally. "If you think about the problems facing the country, most of the solutions involve science at some level," says Michael Turner, a Foster donor and a cosmologist at the University of Chicago, which manages Argonne for the DOE.

But Washington insiders say scientists often overestimate the influence that one of their own might exert in Congress, which is home to only a handful of scientists and engineers. "Personally, I would not vote for or against somebody because they were a scientist," says David Goldston, director of government affairs for the Natural Resources Defense Council. He served as chief of staff for the science committee under Republican leadership from 2001 through 2006.

Goldston and others say a nonscientist friend on the Hill may be more productive. And that's what Biggert has strived to be. A lawyer, she won election to the House in 1998 and says she immediately sought a spot on the science committee so she could advocate for Argonne. That decision paid off right away, she says. "President [Bill] Clinton cut $20 million from the electrometallurgical project at Argonne," she says, referring to work on a technology for reprocessing spent nuclear fuel, "but I got the money back."

By all accounts, Biggert played a leading role in drumming up Republican support for the 2007 America COMPETES Act, which authorized increases aimed at doubling the budgets for the National Science Foundation, the National Institute of Standards and Technology, and DOE's Office of Science over 10 years.

Biggert says she strongly favors basic research over applied efforts. For example, COMPETES also established the Advanced Research Projects Agency–Energy (ARPA-E), a program to quickly develop promising ideas from energy-related research. But Biggert worried that ARPA-E, which stresses more applied science, would take money away from DOE's fundamental research programs. So she lobbied successfully for language in COMPETES that said ARPA-E would receive money only after DOE's basic research efforts were fully funded. ARPA-E launched in 2009 with a one-time allocation of $400 million from the massive stimulus package. Its budget this year is $275 million, compared with $4.9 billion for the Office of Science.

Foster argues that his scientific expertise will make him a more effective advocate for the labs. He worked at Fermilab for 22 years before leaving in 2006. As a teenager, Foster and his younger brother started a theater lighting company that has made them wealthy. So Foster describes himself as "a scientist and a businessman."

In March 2008, Foster won a special midterm election to represent a district that was home to Fermilab and gained a full term 8 months later. But in November 2010 he lost his seat to Republican Randy Hultgren.

Foster takes an explicitly quantitative





Published by AAAS

approach to politics. "A scientist or an engineer has a natural instinct to attach a number to a problem," he says. "Very often, even having an approximate number gets you to the correct policy choice." Foster says his scientific bent served him well on the financial services committee when it took up reform of banking regulations. A numerical approach, he says, helped clarify which factors were of greatest importance in regulating complex financial instruments.

But some Washington insiders have doubts about such a science-as-policy approach. The few scientists who are in Congress don't always see eye to eye, Goldston says. On many issues there just isn't a "scientific position," he says.

Some observers say that Biggert's support for science has flagged since the conservative Tea Party gained influence within the Republican Party. The shift was evident when it came time to reauthorize COMPETES in 2010, says one congressional staffer. "She was a big champion of COMPETES in 2007," the staffer says. "2010 was a different story. … She was more cautious."

Biggert says she was unhappy that the reauthorization did not contain the clause ensuring full funding of basic research before funding of ARPA-E, but she eventually cast an "aye" vote. And the Ryan budget doesn't reflect her stance on science, she says: "I will fight as hard as I can so that there aren't cuts in basic research."

**On the job.** As a member of Congress, Bill Foster (*right*) went to Fermilab in 2009 to trumpet $60 million in new funding; Judy Biggert (*left*) helped break ground last year for a new facility at Argonne.

Fermilab's uncertain future has also become a campaign issue. Foster has blamed Biggert for the lab's inability over the past decade to snare a major new federally funded project, such as the proposed $800 million Long-Baseline Neutrino Experiment.

But the real hurdle has been DOE's Office of Science, which has held funding for particle physics flat while boosting spending on clean energy research, the Obama administration's priority. So if Foster wins and Obama remains in office, Foster would face an uphill battle to win new money for Fermilab. Still, Foster says that being a scientist makes him more credible in advocating for the value of such research: "There isn't a substitute for having people with real technical competence making those arguments all the way up the command chain."

The race to represent Illinois's 11th district will be decided on issues such as taxes and health care reform, not federal funding for research. But for the moment, the topic has become part of the public debate. And the discourse seems as rough as that on any other issue. **–ADRIAN CHO**

# Food Labeling Issue Tops State Ballot Questions

**Scientists say California's Proposition 37 would send misguided message to the public about genetically modified foods**

An attempt in California to require the labeling of food containing genetically modified (GM) material has rekindled a long-running debate about its safety. It has also angered many scientists, who say that such foods pose no danger to the public.

Proposition 37, one of 174 ballot issues facing voters next month in 37 states, would be the first such law in the United States. It would require labels on any food containing more than one part in 200 of GM material. That's an even lower threshold than the levels in existing labeling laws in Europe and Japan.

Those in favor of Prop 37, one of 11 issues being put to California voters on 6 November, say it's needed to educate consumers. But they also worry about the effects of GM food on health and the environment. In fact, many supporters hope that mandatory labeling will be the first step toward an outright ban of GM food products in the United States.

Most scientists argue that these concerns are unfounded. Genetic modification using recombinant DNA is a technique that does not alter food in any meaningful way, according to the U.S. Food and Drug Administration. Scientists worry that labeling will serve only to mark GM foods as "different," a designation that could discourage consumers from buying them. If that happens, scientists say, reduced demand could prevent advances in plant genetics from being commercialized.

"We have some very serious problems in agriculture, and we need to use all of the science that we can to solve these problems," says Robert Goldberg, a plant biologist at the University of California, Los Angeles. Goldberg calls the arguments for Proposition 37 "antiscience" and "ideological."

Although surveys earlier in the year found that two in three voters supported Prop 37, recent polls indicate that the race is tightening. Opponents have spent $35 million on a media blitz, funded in large part by contributions from agribusinesses such as Monsanto and DuPont. In contrast, supporters have raised only $5.4 million.

Several states are asking voters to support cash-starved higher education systems. By far the largest is California's Proposition 30, which would generate billions of dollars a year by hiking sales and income tax rates.

In South Dakota, Referred Law 14 would tap a portion of the taxes collected from contractors to provide grants for in-state projects costing more than $5 million, including research on alternative energy technologies and improving agricultural practices. New Jersey's Question 1 would authorize the state to issue $750 million in bonds to upgrade facilities at all manner of public colleges and universities. It includes $52.5 million for private institutions with small endowments. **–MEGHNA SACHDEV**

CREDITS (LEFT TO RIGHT): ARGONNE/FLICKR; FERMILAB





Published by AAAS

# Want to Tear Down Your Rival? Here's What Might Work Best

**A new study of negative political ads shows that timing and audience may be the keys to success**

If you want to attack your political opponent, do it *after* voters have made up their minds.

That's the conclusion of a new and controversial study on the impact of negative advertising in political campaigns. October is the critical month for election propaganda, says Yanna Krupnikov, a political scientist at Northwestern University in Evanston, Illinois. She finds that people are most susceptible to negative ads late in the campaign if they attack the candidate they have chosen. The ads can discourage people from voting, she reported last year in work funded by the National Science Foundation.

Negative ads are on the rise (see graph), and the idea that they discourage voting has been batted around for decades. Political scientists Stephen Ansolabehere and Shanto Iyengar reported in the mid-1990s that such ads significantly discourage voter turnout, and their work triggered scores of follow-up papers.

More recent analyses have been overwhelmingly skeptical of that conclusion, however. Some researchers have found the opposite effect: that negative ads actually boost participation. One prominent doubter, John Geer, a political scientist at Vanderbilt University in Nashville, assembled a database of 3 decades of ads created for presidential campaigns. His 2006 book, *In Defense of Negativity*, argues that such ads do not stifle voter turnout and are actually good for democracy because statements that challenge an opponent contain more factual information than feel-good image ads and, thus, promote a vigorous debate.

Northwestern's Krupnikov doesn't think it's that simple. She believes that other analysts may have missed the vote-suppressing effect of negative ads because they didn't look carefully at the timing and targeting of such ads. Had they done so, she argues, they might have found a similar effect.

Her work is based in part on how people make consumer and voting decisions. It's a two-step process, she says: People amass and evaluate information (including negative comments, which are helpful at this stage) before making a choice. Then they decide to act. A late blast of negative information may discourage voting without changing a person's choice, she says. If a voter thinks that a chosen candidate may not be any better than a disliked candidate, that voter "has no reason to turn out and vote."

Krupnikov used the 2004 presidential election to test her theory, examining the tone of advertising and surveys about voter turnout. She analyzed similar surveys from elections in 1976 through 2000 and melded those responses with ads in those seven earlier elections, cataloged in a database and evaluated by Geer and colleagues.

Krupnikov found that only late negative ads (those aired after 1 October) were linked to a significantly lower likelihood that people would turn out to vote. The data for the seven other elections are less precise, but in the October 2011 *American Journal of Political Science*, she writes that her analysis of the earlier years yielded "the same pattern" as for 2004.

This year, researchers are waiting to see what happens in a presidential election that appears headed for a record wave of negative ads. "Most of President Obama's advertising has been negative," says Kenneth Goldstein, a political scientist who last year became CEO of Kantar Media/Campaign Media Analysis Group, a Washington, D.C., consulting firm. "But so has Mitt Romney's advertising—and ads by all the allies and PACs [political action committees]."

Goldstein developed methods of tracking and analyzing political television ads as a professor at the University of Wisconsin, Madison, and at Wesleyan University in Middletown, Connecticut. The Wesleyan Media Project (WMP) reports that most ads being aired in the final stage of the 2012 presidential campaign are negative. September's TV ads fall into three "tone" categories, WMP says: 62.8% purely negative ("mentioning solely the opposition candidate"), 29.5% contrast ads ("those that mention both the favored candidate and the opposition"), and 7.8% positive ads ("mentioning solely the favored candidate"). The share of negative campaign ads in September has risen steadily throughout the decade, from 22.7% in 2000 to 30.5% in 2004 to 56.2% in 2008.

Goldstein isn't particularly concerned about the trend. "I've studied this every which way in many years and in many races. I don't always find positive effects [encouraging voter participation], … but I have never found negative effects."

What may be the most thorough scholarly rejection of the idea that negative ads suppress voting comes from a meta-analysis by Richard Lau, a political scientist at Rutgers University in New Brunswick, New Jersey, and colleagues. Their review of 111 papers in the November 2007 issue of *The Journal of Politics* found no significant vote-discouraging effect. "I spent 15 years of my life reading every damn paper that was written on this," Lau says.

His conclusion is that these ads, if they influence voters at all, actually stimulate participation in elections. Lau would be "a lot more concerned" about the ad blitz if one side heavily outspent the other. But in this year's presidential election, he says, "both Obama and Romney have more money than God."

**–ELIOT MARSHALL**

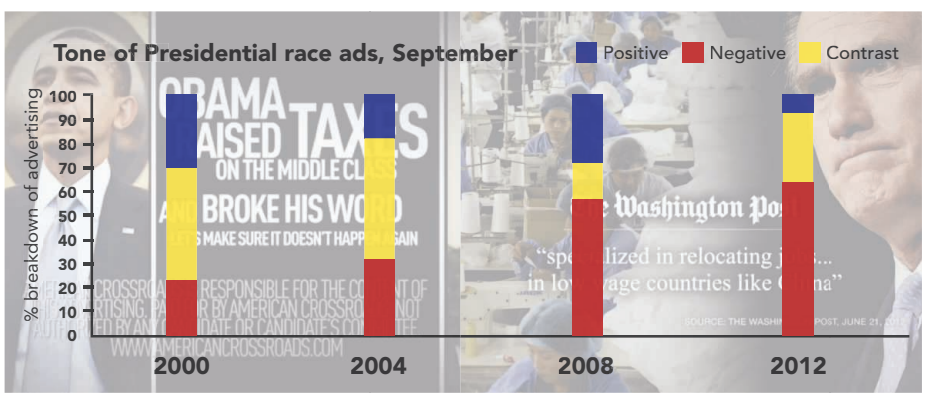


**Rising tide.** Purely negative TV campaign ads—those mentioning only a rival, like many now targeting Barack Obama and Mitt Romney—have risen sharply in the past decade just before the U.S. presidential election. This sample shows the breakdown of ad tone for September since 2000.

CREDIT: (DATA SOURCE) WESLEYAN MEDIA PROJECT-KANTAR MEDIA/CAMPAIGN MEDIA ANALYSIS GROUP





Published by AAAS

Social media and elections 472

Whither the world's fisheries? 474

LETTERS | BOOKS | POLICY FORUM | EDUCATION FORUM | PERSPECTIVES

# LETTERS

*edited by Jennifer Sills*

## A Curiosity Moment for Tropical Biology?

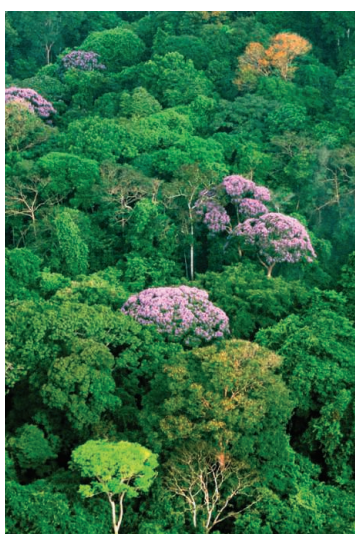

I WAS TRULY AMAZED BY THE REMARKABLE FEAT THAT NASA's Jet Propulsion Laboratory pulled off in landing the Curiosity rover on the surface of Mars. But it leaves me wondering whether we have ever spent a billion dollars examining any part of Earth's tropical rainforest.

We remain ignorant of even the most basic properties of Earth's equatorial forests, such as the number of large mammal species (or invertebrates, fungi, and microbes) in a forest, and their life cycles. The information that we do have is biased toward small intensively studied areas, whereas the vast intervening areas remain largely unexamined. The most extensive global network of observation plots, managed by the Center for Tropical Forest Science, encompasses a tiny fraction of total forest area. Acquiring a comprehensive knowledge of these forests seems impossible. Yet so did walking on the Moon 50 brief years ago.

There are tremendous technical challenges in navigating the canopy of the tropical rainforests. We need to view the study of rainforests as an engineering problem and develop the same kind of amazing technologies used to study the surface of Mars. I want to be able to hover in a little car above the trees. I want to release a small cat-like autonomous robot into the canopy and retrieve it a month later two kilometers away, all the while tracking its movements as it gathers samples and observations, downloading gigabytes of data each day. There would be tremendous opportunities to translate those technologies into useful applications on Earth. I am confident that the trickle down would be much more substantial than that from the space program.

Are we really going to have a colony on the Moon? Do we really plan on escaping to the stars? We have a few challenges here on Earth that we need to face before we can ever truly fulfill those dreams.

**CHARLES H. CANNON**

Department of Biological Sciences, Texas Tech University, Lubbock, TX 79409–3131, USA and Texas Tech University and Xishuangbanna Tropical Botanic Garden, Chinese Academy of Sciences, 666303, Yunnan, China. E-mail: chuck.cannon@ttu.edu

## The Real Costs of Research

IN THEIR 27 JULY EDITORIAL ("ICEBERG ALERT for NIH," p. 390), H. R. Bourne and M. O. Lively assert that "faculty, administrators, research institutions, and NIH must work together" to address the challenges of research funding during a time when the nation is struggling to regain its fiscal health. However, they mischaracterize the way institutions handle faculty salaries, indirect costs, and building of facilities.

Current data suggest that the National Institutes of Health (NIH) and other federal research agencies do provide critical support for salaries, but the majority of salary is still paid by the institutions. A recent survey of its members by the Association of American Medical Colleges showed that the percentage of full-time faculty salaries derived from sponsored-program funds was, on average, only 15.4% (*1*). When full-time faculty holding MD degrees are excluded, the figure rises to 32%. This is consistent with NIH's own data (*2*) and similar to the results of an annual salary survey conducted by the Association of Chairs of Departments of Physiology, which found that percentage of faculty salary support from federal research grants has declined in recent years (from 38.3% in 2003 to 37.3% in 2009) (*3*).

In addition, the assertion that indirect costs lead universities to speculatively build facilities, rather than invest in faculty, misconstrues the calculation of indirect costs and the motivations of universities. According to data from the National Science Foundation, the university share of support for research conducted by its faculty has grown faster than any other source of support over the past two decades, even as institutions are increasingly faced with state budget cuts and other financial pressures (*4*). Universities assume the upfront risks and costs of building new facilities, so it is not an activity they undertake lightly or without serious consideration of current and future needs. Although universities may recover some of the costs of the building, depending on how the building is used, surveys conducted of Association of American Universities institutions reveal that the primary motivation of institutions to construct new buildings is to replace aging, outdated facilities and equipment to meet current research needs, rather than in anticipation of growing research funding. Moreover, the cost of research and of regulatory compliance has increased, but there has not been a commensurate increase in the reimbursement of indirect costs (*5*), resulting in billions of dollars of additional funding from universities to cover the full costs of research.

Finally, universities invest substantially to "nourish their own faculty" beyond providing facilities and administrative support. A 7-year study of new faculty hires at the University of Rochester School of Medicine and Dentistry showed that the school had to

add about 40 cents on every grant dollar to cover all the costs of research, and recovered only 81% of its facilities and administration costs and none of its start-up costs during this time (*6*).

Research stakeholders—universities, scientists, trainees, and agencies—have much to gain by thinking creatively and collectively about improving regulations, reengineering the training and workforce pipeline, and communicating the positive benefits of research. But when considering how best to allocate limited resources, it is time to stop portraying institutions and investigators as being in competition with each other for research dollars and begin to talk about the full and real costs of research, as well as the need for sustained national investments in discovery to improve the nation's health. Otherwise, we are indeed only rearranging deck chairs on the Titanic.

**HUNTER R. RAWLINGS III,[1]* DARRELL G. KIRCH,[2] ANTHONY DECRAPPEO,[3] M. PETER MCPHERSON[4]**

[1]Association of American Universities, Washington, DC 20005, USA. [2]Association of American Medical Colleges, Washington, DC 20037, USA. [3]Council on Governmental Relations, Washington, DC 20005, USA. [4]Association of Public and Land-Grant Universities, Washington, DC 20005, USA.

*To whom correspondence should be addressed. E-mail: hunter.rawlings@aau.edu

**References**

1. M. Goodwin, A. Bonham, A. Mazzaschi, H. Alexander, J. Krakower, "Sponsored program salary support to medical school faculty in 2009" (Association of American Medical Colleges, Analysis in Brief, 2011), vol. 11; www.aamc.org/download/170836/data/aibvol11_no1.pdf.
2. NIH Office of Extramural Research, "Ways of managing NIF research" (2011); http://report.nih.gov/UploadDocs/Ways%20to%20Manage%20Final.pdf.
3. Association of Chairs of Departments of Physiology, ACDP Space and Budget Surveys (www.acdponline.org/Surveys.htm).
4. National Science Board, "Science and engineering indicators 2010" (National Science Foundation, NSB 10-01, Arlington, VA, 2010).
5. T. Smith, J. Trapani, A. DeCrappeo, D. Kennedy, "Reforming regulation of research universities" *Issues in Science and Technology* (Summer 2011); www.issues.org/27.4/smith.html.
6. E. R. Dorsey *et al.*, *Acad. Med.* **84**, 26 (2009).

## Duty of Care: Protecting Researchers Abroad

THE TRAGIC DEATH OF A UNIVERSITY OF California–Los Angeles research assistant in 2008, and the civil and criminal legal proceedings that followed (*1*), appropriately focused attention on the dangerous working conditions faced by junior lab researchers. However, there may be a greater danger facing international researchers: preventable accidents or illnesses when traveling outside their home country, especially to developing regions (for example, sustaining injuries while traveling on rugged roads or contracting malaria while conducting field work in Africa). This will likely be the next area where academic institutions and senior researchers find themselves held liable for injuries or death.

Historically, persevering over adversity was seen as a "rite of passage" for young researchers, and although most safety risks can now be easily mitigated or avoided, junior researchers rightly sense that voicing concerns about safety could harm their career prospects, and senior researchers often consider addressing safety issues as "inconvenient" or ignore them altogether. A recent policy paper details the concept of "duty of care," which establishes an academic organization's legal responsibility for staff and student safety (*2*). Under this doctrine, failure to provide necessary safety resources for staff working abroad may constitute actionable misconduct, exposing the university or research supervisor to legal or criminal lia-

bility in the event of injury or illness. Data on adverse events during research are rare, and determining the true scale of the problem would be an important initial step in improving safety. It is imperative that academic leadership at every level address the problem, providing adequate pre-deployment training, proper safety equipment, and a safe working environment abroad. A project's primary measure of success should not be publication or grant renewal, but that everyone returned safely. We must not wait for another bright, ambitious student to lose his or her life due to inattention to safety and security before making the necessary changes.

**BENNETT PAFFORD[1]* AND ROBERT MACPHERSON[2]**

[1]Department of Internal Medicine, George Washington University, Washington, DC 20037, USA. [2]Cosantóir Group, Charlotte, NC 28211, USA.

*To whom correspondence should be addressed. E-mail: bennettpafford@yahoo.com

**References**

1. K. Christensen, "Report faults professor, UCLA in death of lab assistant," *Los Angeles Times*, 21 January 2012 (http://articles.latimes.com/2012/jan/21/local/la-me-ucla-lab-20120121).
2. E. Kemp, M. Merkelbach, "Can you get sued? Legal liability of international humanitarian aid organizations towards their staff" (Geneva Center for Security Policy, Geneva, 2011).

## CORRECTIONS AND CLARIFICATIONS

**News Focus:** "Mountains of data" by R. Service (17 August, p. 793). Microsoft Research is located in Redmond, Washington, not Richmond, Washington.

**News & Analysis:** "Are world oil's prospects not declining all that fast?" by R. A. Kerr (10 August, p. 633). The credit line should have been "Credits: (graph) Adapted from S. Sorrell *et al*., *Energy* **37** (2012), with permission from Elsevier; (data source) M. Höök *et al*., *Natural Resources Research* **18** (2009); (photo) Shutterstock." The credit has been corrected in the HTML and PDF versions online.

**Reports:** "Divergent nematic susceptibility in an iron arsenide superconductor" by J.-H. Chu *et al*. (10 August, p. 710). References 12 and 13 should have been switched. Ref. 13 should be S. Kasahara *et al*., *Nature* **486**, 382 (2012), and Ref. 12 should have been "Materials and methods are available as supplementary materials on *Science* Online." The references have been corrected in the HTML version online.

## TECHNICAL COMMENT ABSTRACTS

### Comment on "Conspecific Negative Density Dependence and Forest Diversity"

**Ian A. Dickie, Jennifer M. Hurst, Peter J. Bellingham**

Johnson and colleagues (Reports, 18 May 2012, p. 904) claim that conspecific negative density dependence is a pervasive mechanism driving forest diversity, especially for rare tree species. We show that their results are due to a statistical bias in their analysis caused by the exclusion of joint absences.

Full text at http://dx.doi.org/10.1126/science.1225520

### Response to Comment on "Conspecific Negative Density Dependence and Forest Diversity"

**Daniel J. Johnson, Wesley T. Beaulieu, James D. Bever, Keith Clay**

Dickie, Hurst, and Bellingham question some of the methods of our recent study on conspecific density dependence in forests. Here, we reanalyze our data set with the inclusion of joint absence plots of each species. We find that our results are robust to further analyses and that patterns of abundance and richness correlate with our measure of density dependence, supporting our original conclusions.

Full text at http://dx.doi.org/10.1126/science.1225996

## Letters to the Editor

Letters (~300 words) discuss material published in *Science* in the past 3 months or matters of general interest. Letters are not acknowledged upon receipt. Whether published in full or in part, Letters are subject to editing for clarity and space. Letters submitted, published, or posted elsewhere, in print or online, will be disqualified. To submit a Letter, go to www.submit2science.org.

# Comment on "Conspecific Negative Density Dependence and Forest Diversity"

Ian A. Dickie,[1]* Jennifer M. Hurst,[1,2] Peter J. Bellingham[1]

Johnson and colleagues (Reports, 18 May 2012, p. 904) claim that conspecific negative density dependence is a pervasive mechanism driving forest diversity, especially for rare tree species. We show that their results are due to a statistical bias in their analysis caused by the exclusion of joint absences.

Johnson and colleagues (*1*) used the correlation of seedling density with conspecific tree density to show that there is a negative density dependence, which they argue is driven by host-specific enemies. However, their analysis is biased because they only included seedling abundances of zero in plots with conspecific trees, whereas they excluded zero seedling abundances in plots that lacked conspecific trees. Excluding these joint absences (of both seedlings and adults) may result in negative biases and cause apparent conspecific density dependence.

To test the implications of this bias, we randomly generated uncorrelated tree and seedling abundances as a null model and analyzed the simulated null model community twice, once without joint absences and once with. Excluding joint absences resulted in a negative conspecific density dependence (median −0.16, Wilcoxon test $P < 2.2 \times 10^{-16}$) and a highly significant correlation of abundance and conspecific density dependence ($P < 2.2 \times 10^{-16}$). These results are essentially indistinguishable from the findings of Johnson and colleagues (Fig. 1A). Analyzing the null-model data without excluding joint absences resulted in a median density dependence of near the true value of zero and no correlation of abundance and density dependence ($P = 0.25$) (Fig. 1B).

We applied the same procedures to 1144 20-m by 20-m forest plots on a systematic 8-km by 8-km grid spanning from 34°53'S to 47°13'S across all natural forests in New Zealand (*2*). We found overall positive conspecific density dependence regardless of statistical approach, but including joint absences resulted in density dependence 3.7 times more positive than when excluding joint absences (0.12 versus 0.032).

Therefore, Johnson and colleagues have not shown conspecific negative density dependence as a mechanism driving diversity. Their use of heterospecific density dependence as a null model is inappropriate, as few plots have no heterospecific trees and therefore few joint absences are excluded. The positive density dependence in the New Zealand data is most likely to result from local seed dispersal.

[1]Landcare Research, Lincoln, 7640 New Zealand. [2]New Zealand School of Forestry, University of Canterbury, Christchurch, 8140 New Zealand.

*To whom correspondence should be addressed. E-mail: dickiei@landcareresearch.co.nz

### References and Notes

1. D. J. Johnson, W. T. Beaulieu, J. D. Bever, K. Clay, *Science* **336**, 904 (2012).
2. S. K. Wiser, J. M. Hurst, E. F. Wright, R. B. Allen, *Appl. Veg. Sci.* **14**, 506 (2011).

**Acknowledgments:** I.A.D. was supported by funding from the Royal Society of New Zealand Marsden Fund and J.M.H. by the Ministry of Business, Innovation, and Employment (CO9X0802). We acknowledge the use of data from the Natural Forest plot data collected between January 2002 and March 2007 by the Land Use and Carbon Analysis System program for the Ministry for the Environment and Department of Conservation (available from nvs.landcareresearch.co.nz).

1 June 2012; accepted 17 August 2012
10.1126/science.1225520



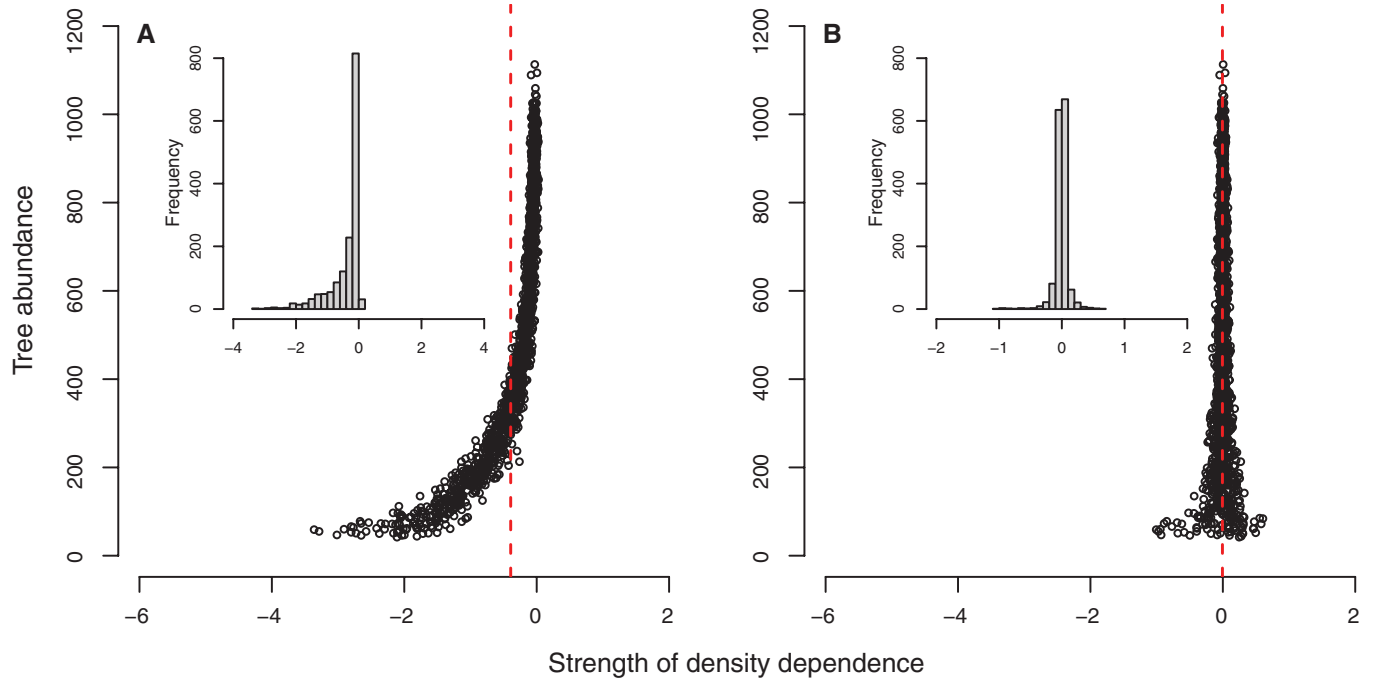


**Fig. 1.** Analysis of the null data set with the exclusion of joint absences results in a strong negative bias (**A**) and negative correlation of density dependence and abundance. The same null data set analyzed with joint absences included shows no density dependence (**B**). Null data set generated using random, uncorrelated negative binomial distributions for both trees and seedlings. Dashed line indicates the mean density dependence in each analysis.

# Response to Comment on "Conspecific Negative Density Dependence and Forest Diversity"

Daniel J. Johnson,* Wesley T. Beaulieu, James D. Bever, Keith Clay

Dickie, Hurst, and Bellingham question some of the methods of our recent study on conspecific density dependence in forests. Here, we reanalyze our data set with the inclusion of joint absence plots of each species. We find that our results are robust to further analyses and that patterns of abundance and richness correlate with our measure of density dependence, supporting our original conclusions.

Forest systems provide key tests for exploring hypotheses for the maintenance of diversity in ecological communities. One major hypothesis is conspecific negative density-dependent mortality, where seedling establishment is reduced with increasing density of conspecific neighbors. The goal of our study was to analyze patterns of seedling establishment in relation to tree density across eastern U.S. forests to determine the extent and influence of density dependence on forest communities (*1*).

Dickie, Hurst, and Bellingham (*2*) argue that our analyses of seedling establishment patterns are biased and spuriously correlate with species abundance because sample plots lacking both trees and seedlings of the focal species were excluded (*1*). In simulations using randomly generated independent and identically distributed tree and seedling abundances, they found that excluding joint absence plots resulted in $b$ values (the strength of density dependence estimated from the negative exponential function, $S = ae^{bT}$, where $a$ is the $y$ intercept, $S$ is the number of seedlings, and $T$ is the number of trees) that were significantly positively related to species abundance but not when joint absence plots were excluded (*2*).

Wholesale inclusion of joint absence data at the regional-cell level (2° latitude by longitude) numerically overwhelms presence data because most species do not occur everywhere (94.6% of species by cell samples are joint absences). Absence data often represent locations outside of species' physiological range and therefore are not biologically relevant to patterns of regeneration. Additionally, sample locations in which a species is not present provide no information about the interaction between conspecific individuals (*1*).

However, to address Dickie *et al.*'s Comment and explore whether excluding joint absences biased our results, we analyzed the data with a subset of joint absence plots included when the species were known to occur locally. Specifically, we included joint absences on plots where at least one of the four nearest neighbor plots (*1*) (fig. S1) contained the species of interest. This provides biologically meaningful absences by including joint absences when the species is known to occur in the vicinity and is therefore within geographical and physiological range of the species. Moreover, there is a high probability that the plot is within the dispersal distance of that species. The relation of the strength of conspecific density dependence to species abundance and richness remained significant and in the same respective directions as in our original study (Fig. 1).

Further, using a model-free approach, we found that the vast majority (96.7%) of seedling density is nonindependently associated with conspecific tree density with two-dimensional Kolmogorov Smirnov (2DKS) tests (*3*). These tests indicate that there are significant nonrandom negative relations in these bivariate data. Reanalyzing the strength of density dependence versus relative abundance with nonindependent species-cell combinations, determined by 2DKS tests, resulted in qualitatively identical results to those originally reported. Our results indicate that conspecific negative density dependence (CNDD) is widespread in forests, in support of the hypothesis that CNDD can maintain forest diversity.

Dickie *et al.* report an overall slight positive correlation between conspecific seedlings and trees in New Zealand (*2*). Local dispersal of seeds in the absence of ecological interactions will generate

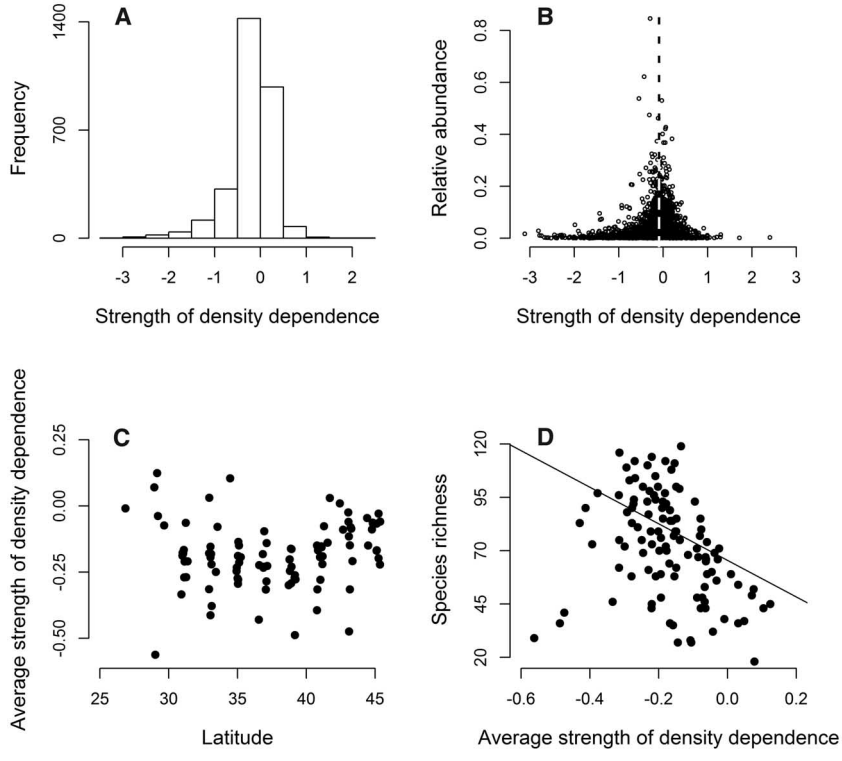


**Fig. 1.** Strength of density dependence when analyzed with joint absence U.S. Forest Service Forest Inventory and Analysis data shows the same pattern as originally reported. (**A**) Histogram of strength of density dependence by species-cell combination. (**B**) Relation between strength of density dependence and the relative abundance of the species in the regional cell (Spearman's rank correlation, $\rho = 0.138$, $P = 3.69 \times 10^{-14}$, $N = 2988$). (**C**) Latitude relation to average strength of density dependence per regional cell (Spearman's rank correlation, $\rho = 0.313$, $P = 0.00093$, $N = 110$). (**D**) Regression of the average strength of density dependence on species richness (correlation coefficient $r^2 = 0.1714$, $F_{1,108} = 22.35$, $P = 6.91 \times 10^{-6}$).

Department of Biology, Indiana University, Bloomington, IN 47405, USA.

*To whom correspondence should be addressed. E-mail: dj4@indiana.edu

positive correlations. Tests of whether the correlations observed in New Zealand are more positive than the null expectation of local dispersal would require detailed information on the dispersal kernels of the individual tree species in New Zealand forests. Therefore, although negative correlations, as we observed in North America, can be confidently interpreted as resulting from negative conspecific density dependence, positive correlations could be stronger or weaker than null expectations and are therefore ambiguous as tests of conspecific density dependence. In North America, we observed weaker CNDD in higher latitudes. The generality of this pattern across the globe in general and specifically whether the slight positive correlation of seedlings with conspecific adults observed in the climates of New Zealand is consistent with this pattern is an interesting possibility that will require further research. Our results indicate that positive conspecific density dependence is much less common than negative density dependence in forest systems and agree with empirical patterns reported from plant communities (*4*).

**References and Notes**

1. D. J. Johnson, W. T. Beaulieu, J. D. Bever, K. Clay, *Science* **336**, 904 (2012).
2. I. A. Dickie, J. M. Hurst, P. J. Bellingham, *Science* **338**, 469 (2012); www.sciencemag.org/cgi/content/full/338/6106/469-b.
3. J. E. Garvey, E. A. Marschall, R. A. Wright, *Ecology* **79**, 442 (1998).
4. A. Kulmatiski, K. H. Beard, J. R. Stevens, S. M. Cobbold, *Ecol. Lett.* **11**, 980 (2008).

**Acknowledgments:** The data used for these analyses are publicly available from http://fia.fs.fed.us.

4 July 2012; accepted 17 August 2012
10.1126/science.1225996

HUMAN GENETICS

# Worries of a Genomic Futurist

**Michael A. Goldman**

**Transhumanist Dreams and Dystopian Nightmares**
The Promise and Peril of Genetic Engineering
***by Maxwell J. Mehlman***
Johns Hopkins University Press, Baltimore, 2012. 286 pp. $29.95. ISBN 9781421406695.

"Some people look forward to the prospect of germ line genetic engineering as an opportunity to reengineer the human species. They call themselves 'transhumanists,' a term coined by Julian Huxley." Bioethicist Maxwell Mehlman thinks that we will inevitably reengineer the human species, and he writes about that and the mistakes we might make in the process.

*Transhumanist Dreams and Dystopian Nightmares* offers a deep and wide-ranging catalog of the implications of transhumanism as a philosophical doctrine and a careful analysis of potential pitfalls and concerns. Whereas many bioethicists today are concerned with immediate questions about whether or not innocent people should be able to get a confusing, probabilistic picture of their genetic fate direct from companies such as 23andMe, Mehlman (Case Western Reserve University School of Law) is looking at the bigger picture. Will our hubris lead to the transmutation of our species into the sublime, the grotesque, or both, or will we merely drive ourselves into extinction?

Clearly, a technology powerful enough to reengineer the species merits some form of regulation. Mehlman wrestles hard with the ability of our government to control technology properly. From this accomplished attorney, we get a superb view of interesting case law upon which government intervention in health derives. "The *Jacobson* case [in which an individual's refusal to be vaccinated against smallpox resulted in a jail sentence in Massachusetts] not only laid the foundation for all subsequent public health law but also was the only precedent that the Supreme Court cited nine years later in *Buck* v. *Bell*," which upheld the involuntary sterilization of the allegedly "feeble minded." Moving from infectious disease and the "barbaric Tuskegee experiment" to modern genetics, Mehlman comments that "the eugenics movement stands out as one of the most appalling examples of overreaching public health policy." He also discusses a simple screening for sickle cell disease that a number of states made mandatory in the mid-1970s (although often only for African Americans),which failed because "[f]ew people understood what it meant for a genetic disorder to be recessive." With its history of errors, one wonders whether the public health system has the sophistication to respond to long-term (on an evolutionary scale) rather than short-term problems.

Mehlman cites an AAAS report as giving us a legitimate reason to pursue genetic engineering as an obligation. The report itself states,

> The working group acknowledged that we have an intergenerational responsibility to guard the interests of future persons who are currently voiceless in this respect, but it took issue with those who claim that this obligation precludes IGM [inheritable genetic modification]. If we do have responsibilities to our descendants, our obligations undoubtedly encompass efforts to make life better for our children and subsequent descendants. This could include eliminating deleterious genes and thereby improving the health of future generations. (*1*)

The language is much more muted in the report than it seems from the account in the book, but it is a remarkable statement nonetheless.

Mehlman is clearly not trying to present a didactic view of the relevant science, but he seems to be largely up to date on topics such as our growing understanding of the role of "junk" DNA in gene regulation and the importance of epigenetics. He gives an occasional odd definition, for example: "The ability of the same gene to perform many functions as a result of being turned on or off is called pleiotropy." Nonetheless, he has a grasp on what pleiotropy implies about the complex nature of gene action: "Evolutionary biologists worry … that even a small number of changes in pleiotropic genes could have dramatic effects on the human species."

One of the strengths of Mehlman's approach is his keen attention to the evolutionary perspective. He offers a sweeping description of evolution as an inexact, still-developing science and of some of the personalities and controversies that have made it such an enticing field. This is to establish that we don't yet know enough about evolution to claim to control it. He writes,

> Scientifically, there is no question that natural evolution is real. Furthermore, we probably understand enough about it to be able to identify a number of potential threats to the continuation of our evolutionary lineage, such as a catastrophic loss of genetic diversity. But the lack of clarity about so much of the natural process of evolution complicates efforts to prevent evolutionary engineering from making harmful mistakes.

Although Mehlman understands and writes well about the role and value of genetic variation, he joins many other authors in failing to grasp just how little impact a few genetically engineered individuals will have on the gene (or is it genome) pool (ocean) of seven billion people on the planet. He fears

CREDIT: PHILIPP DAUB/THINKSTOCK.COM

The reviewer is at the Department of Biology, San Francisco State University, San Francisco, CA 94132–1722, USA. E-mail: goldman@sfsu.edu

rifts between the genetic haves and the have-nots reminiscent of the Eloi and the Morlocks as our divergent descendants in H. G. Wells's *The Time Machine* (*2*). Yet while Mehlman is certainly cautious—recognizing the importance of unanticipated genetic consequences, the risk of genetic engineering—not once do I get the feeling that I'm reading the words of a Luddite.

Mehlman has published extensively on the challenges and excitement of genomics and genetic enhancement. Accessible while having enough scientific substance to be taken seriously, *Transhumanist Dreams* provides a thought-provoking read for genetics professionals, ethicists, interested scientists, and concerned citizens. However, this dystopian nightmare isn't going to keep me up tonight.

**References**

1. M. S. Frankel, A. R. Chapman, *Human Inheritable Genetic Modifications: Assessing Scientific, Ethical, Religious, and Policy Issues* (AAAS Publications Services, Washington, DC, 2000); www.aaas.org/spp/sfrl/projects/germline/report.pdf.
2. H. G. Wells, *The Time Machine* (Heinemann, London, 1895).

10.1126/science.1229501

HISTORY OF SCIENCE

# Roots of *Origin*

**Stuart Firestein**

Arguments over attribution are among the most contentious in science. From authorship on papers, to correct citations of the preceding literature, to the choice of only three winners of a Nobel Prize, there is always disagreement about priority, contribution, and significance. Of course, attribution encompasses more than often seemingly petty arguments over order in the author list; it speaks to deeper issues in the history and philosophy of science—where do "new" ideas come from, and what constitutes a "new" idea.

Darwin's new idea (also Wallace's, of course) was arguably the most seminal, world-altering, paradigm-shifting conceptual leap in modern science, certainly in the life sciences. But did it spring de novo from Darwin's mind? Were there precedents? Was it "in the air"? How much of it was his and his alone? What, if anything, did he owe to predecessors?

**Darwin's Ghosts**
The Secret History of Evolution / In Search of the First Evolutionists
***by Rebecca Stott***
Spiegel and Grau, New York, 2012. 415 pp. $27. ISBN 9781400069378. Bloomsbury, London. £25. ISBN 9781408809082.

It is on this worry, one that plagued Darwin through continuously revised editions of the *Origin*, that Rebecca Stott masterfully hangs *Darwin's Ghosts*—a beautiful tapestry of the scientific and philosophical search for the answer to how life came to be the way it is on this planet. The book begins with Darwin constructing a list of possible sources that he had unwittingly failed to acknowledge (the ghosts of the title), at first wide ranging and then, as he crosses names off and adds new ones, more focused. Tracking them down, Stott weaves a story that proceeds through ancient Greece, the Middle East, medieval Europe, radical Enlightenment France, 19th-century Edinburgh, Malaysia (where Wallace caught a fever in the throes of which evolution by natural selection came to him), and of course Down House, Kent. Her account provides a view of Darwin and evolution quite different from the hero narratives we have become accustomed to and all the more fascinating for its sniffing out the bits and pieces of an idea so long on the verge of discovery.

The book offers a gripping narrative tension. One after another, great thinkers grapple with the notion that species cannot possibly be immutable, as the dominating biblical story says, but can't quite see through to the crucial idea of natural selection working its undirected way through multitudes of mutations. So many were so close for so long, you find yourself wanting to scream to Lamarck or Diderot or a host of others, "No, no, just look a little bit over here and all will be crystal clear." But of course hindsight is always easy, and the importance of appreciating the state of knowledge (or rather of ignorance) that prevailed prior to the moment of discovery is too often forgotten. All great leaps one day become common knowledge.

I was especially taken with a short digression on the young Darwin in the years he spent in Edinburgh, apparently failing at his medical studies. Have you ever wondered what motivated Darwin to go off on the *Beagle* voyage? I've always supposed it was for more or less superficial reasons: getting out of England and away from his father, travel is what other young men of means were doing at the time, the romance of voyaging, and other such simple youthful motives. And then, being a careful bookkeeper, the evidence just kind of piled up until, lo and behold, the idea of evolution by natural selection came to him. That is a story with more miraculous overtones than I think Darwin would have preferred.

**"The sponge philosopher."** Robert Edmond Grant.

Stott's discussion of Darwin's friendship with Edinburgh physician Robert Grant suggests alternatives. She tells us of Darwin's adventitious meeting with the radical Lamarckian, a seashore naturalist who, aided by a small club of boys, collected sponges and logged vast amounts of information about the marine animals that either washed up or were brought in by fishermen. This was after Grant had spent his inheritance on studies at the Museum of Natural History in Paris and travels in Europe to collect specimens and visit marine invertebrate specialists, libraries, and collections (another possible motive for Darwin's desire to travel). It was from Grant that Darwin picked up the habit of talking to locals, fishermen or their wives selling the creatures in the market, and extracting remarkable bits of intuitive knowledge from them. That investigative strategy appears in the *Origin* as his discussions with pigeon fanciers and domestic breeders of all sorts. It may have been Grant, through his amazingly detailed experiments and observations of sponges in search of an understanding of species mutability, who introduced Darwin to the method of using a detailed problem to ask and answer a big question (think barnacles, worms, and carnivorous plants)—to this day, the way much of biology progresses. Grant and Darwin fell out after a couple of years, and Grant died in obscurity. Stott brings deserved attention to this remarkable character and his influence on a young Darwin.

Grant's engaging story is one of many recounted in *Darwin's Ghosts*. Every chapter seems a travelogue in scientific history and culture, full of interesting material you didn't know or only thought you knew. Stott gives us a fascinating view of the evolution of one of the biggest ideas ever—evolution.

10.1126/science.1228701

The reviewer is at the Department of Biological Sciences, Columbia University, New York, NY 10027, USA. E-mail: sjf24@columbia.edu

SCIENCE AND SOCIETY

# Social Media and the Elections

Manipulation of social media affects perceptions of candidates and compromises decision-making.

**Panagiotis T. Metaxas and Eni Mustafaraj**

In the United States, social media sites—such as Facebook, Twitter, and YouTube—are currently being used by two out of three people (*1*), and search engines are used daily (*2*). Monitoring what users share or search for in social media and on the Web has led to greater insights into what people care about or pay attention to at any moment in time. Furthermore, it is also helping segments of the world population to be informed, to organize, and to react rapidly. However, social media and search results can be readily manipulated, which is something that has been underappreciated by the press and the general public.

In times of political elections, the stakes are high, and advocates may try to support their cause by active manipulation of social media. For example, altering the number of followers can affect a viewer's conclusion about candidate popularity. Recently, it was noted that the number of followers for a presidential candidate in the United States surged by over 110 thousand within one single day, and analysis showed that most of these followers are unlikely to be real people (*3*).

We can model propaganda efforts in graph-theoretic terms, as attempts to alter our "trust network": Each of us keeps a mental trust network that helps us decide what and what not to believe (*4*). The nodes in this weighted network are entities that we are already familiar with (people, institutions, and ideas), and the arcs are our perceived connections between these entities. The weights on the nodes are values of trust and distrust that we implicitly assign to every entity we know. A propagandist is trying to make us alter connections and values in our trust network, i.e., trying to influence our perception about the candidates for the coming elections, and thus "help us" decide on candidates of their choice.

The Web, as seen by search engines (*5*), is similarly a weighted network that is used to rank search results. The hyperlinks are considered "votes of support," and the weights are a computed measurement of importance assigned to Web pages (the nodes in the graph). It is also the target of propaganda attacks, known as "Web spam" (*6*). A Web spammer is trying to alter the weighted Web network by adding connections and values that support his or her cause, aimed at affecting the search engine's ranking decisions and thus the number of viewers who see the page and consider it important (*4*).

"Google bomb" is a type of Web spam that is widely known and applicable to all major search engines today. Exploiting the descriptive power of anchor text (the phrase directly associated with a hyperlink), Web spammers create associations between anchor words or phrases and linked Web pages. These associations force a search engine to give high relevancy to results that would otherwise be unrelated, sending them to the "top 10" search results. A well-known Google bomb was the association of the phrase "miserable failure" with the Web page of President G. W. Bush initially and later with those of Michael Moore, Hillary Clinton, and Jimmy Carter (*7*). Another Google bomb associated candidate John Kerry with the word "waffles" in 2004. A cluster of Google bombs was used in an effort to influence the 2006 congressional elections. Google has adjusted its ranking algorithm to defuse Google bombs on congressional candidates by restricting the selection of the top search results when querying their names (*8*). During the 2008 and 2010 elections, it proved impossible to launch any successful Google bombs on politicians, and it is hoped that the trend will continue.

During the 2010 Massachusetts Special Election (MASEN) to fill the seat vacated by the death of Senator Ted Kennedy, we saw attempts to influence voters just before the elections, launched by out-of-state political groups (*9*). Propagandists exploited a loophole introduced by the feature of including real-time information from social networks in the "top 10" results of Web searches. They ensured that their message was often visible by repeatedly posting the same tweet. A third of all election-related tweets sent during the week before the 2010 MASEN were tweet repeats (*9*). All search engines have since reacted by moving real-time results out of the organic results (results selected purely by information retrieval algorithms) and into a separate search category.

"Twitter bombs," however, are likely to be launched within days of the elections. A Twitter bomb is the act of sending unsolicited replies to specific users via Twitter in order to get them to pay attention to one's cause. Typically, it is done effectively by means of "bots," short-lived programs that can send a large quantity of tweets automatically. Twitter is good at shutting most of them down because of their activity patterns and/or users' complaints. However, bombers have used fake "replies" to spam real users who are not aware of their existence. For example, in the 2010 MASEN, political spammers created nine fake accounts that were used to send about 1000 tweets before being blocked by Twitter for spamming (*9*). Their messages were carefully focused, however, targeting users who in the previous hours were discussing the elections. With the retweeting help of similarly minded users, >60,000 Twitter accounts were reached within a day at essentially no cost. Twitter bombs, unfortunately, have become common practice.

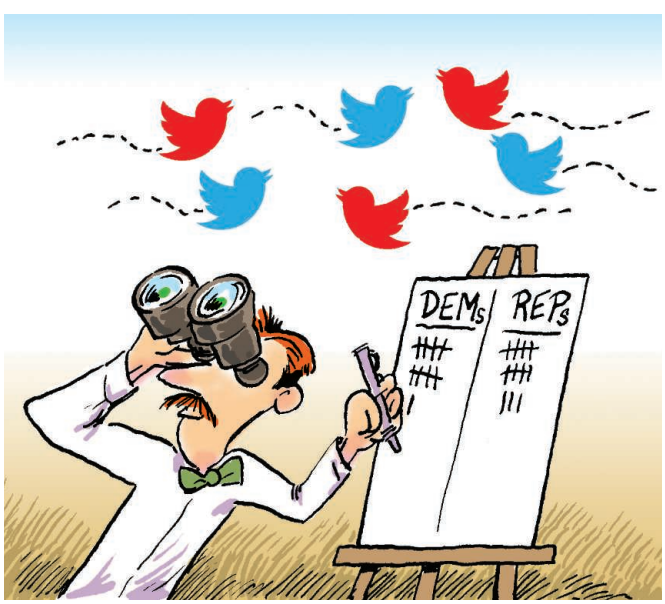


CREDIT: JOE SUTLIFF/JOESUTLIFF.COM

Department of Computer Science, Wellesley College, 106 Central Street, Wellesley, MA 02481, USA. E-mail: pmetaxas@wellesley.edu; emustafa@wellesley.edu





Published by AAAS

A more sophisticated effort to create a fake grassroots movement [often referred to as "astroturf" (*10*)] was the creation of a "prefab tweet factory" (*11*). Designed to evade Twitter's spam detection, a spammer created daily sets of tweets targeting journalists and urging other similarly minded users to tweet. The effect of this spam was to give the impression to the targeted journalists that their reporting was monitored and was not appreciated by "the public" and, thus, applied pressure to the reporters to modulate their views (*11*). We do expect to see such low-budget prefabricated tweets in the next elections and whenever opportunity for putting pressure on journalists arises (*12*).

One of the effective (but expensive) ways to spam is to buy online search ads (appearing at the top of the search results as "sponsored" search in search engines and as "promoted" tweets in Twitter) that appear in queries including names and characteristics of the political opponent. When a citizen searches for a candidate's name or other related terms, the prominently placed and aptly worded ad will encourage them to click on it, thus transporting them to a page designed and maintained by the opponent. An example in a limited form occurred in the 2008 elections, when a site unfavorable to a candidate (TheRealBobRoggio.com), appeared as an advertisement when searching for the name of the candidate (*13*). The contents of these ads can be adjusted rapidly, allowing experimentation with titles and contents that will draw maximal attention. The selection of the best ad can be further refined to match the profile of the specific user with the use of data collected and mined by a process often described as "microtargeting" (*14*). A newer advertising tool will be the use of "promoted trends" in Twitter (*15*) to attract the attention of a wider, yet focused, audience. These techniques may be effective and legal but they are expensive, compared with the spamming techniques we mentioned above.

Yet more ways to spread spam may be through the use of photographs and videos that ridicule the opponent. Search engines usually allocate a prominent place in their organic results for images and videos of well-known people, including political candidates. Their selection in the search results depends on the keywords associated with them (not with their visual contents) and with the popularity in clicks they achieve. Insulting-while-funny pictures typically attract the curiosity of the users and can go viral, allowing propagandists to pass their message, while avoiding any automatic filtering by the search engines (*16*). Although this was observed during the 2010 elections (*16*), there is some evidence that search engines are working to clean their organic results, by asking users to report images they find offensive.

Owing to their popularity and ease of access, social media data have been used to attempt to predict future events, such as movie box-office revenues (*17*, *18*), product sales (*19*), stock market fluctuations (*20*), and even electoral results. Predicting movie box-office revenues using Twitter (*17*) and Yahoo (*18*) search data can be extremely accurate if the predictions are based on unambiguous parameters and a careful consideration of potential confounders. Predicting election results via Twitter data (which are readily accessible) has been applied to reality TV competitions (*21*) and a few political elections (*22*–*24*). And it is easy to find Twitter polls promoted by newspapers for the current U.S. election (*25*). However, using social media for predicting political elections is highly controversial. There is no agreement among researchers yet on the measures responsible for any successful prediction (e.g., tweet volume or tweet content). The time period of data collection has also been variable, ranging from weeks to months before the elections and ending days to weeks before the elections. In most cases, researchers have filtered their data on the basis of decisions clearly made after the elections were over and the results were known (including which parties' tweets were included) (*23*). This has led to an inability to replicate reported success rates (*23*, *24*). Representativeness is currently the most important problem (*21*). Just having a large number of tweets does not mean that there has been representative sampling of the voting population [e.g., in political conversations, 1% of the Twitter accounts are often responsible for 30% of the tweet volume (*11*)].

Even more than in previous elections, we should expect that all candidates and political parties will use social media sites to create enthusiasm in their troops, raise funds, and influence our perception of candidates (or our perception of their popularity). We should be aware of how that works and be prepared to search for the truth behind the messages.

*"using social media for predicting political elections is highly controversial."*


**References and Notes**

1. Pew Foundation, 65% of online adults use social networking sites (2011); http://bit.ly/OWHYwA.
2. Pew Foundation, Search engine use 2012 (2012); http://bit.ly/T9t814.
3. M. C. Petermann, The Twitter underground economy: A blooming business (2012); http://bit.ly/W84BhK.
4. P. T. Metaxas, in *Lecture Notes in Business Information Processing* (Springer-Verlag, New York, 2010), vol. 45, pp. 170–182; http://bit.ly/ffYsuC.
5. A. Broder *et al.*, *Comput. Netw.* **33**, 309 (2000).
6. C. Castillo, B. D. Davison, *Found. Trends Inform. Retriev.* **4**, 377 (2010).
7. Google bomb, Wikipedia (2012); http://bit.ly/TjOeKa.
8. P. T. Metaxas, paper presented at Workshop on Information and Decision in Social Nets, MIT Media Lab, Cambridge, MA, 31 May to 1 June, 2011; http://bit.ly/NRmNox.
9. P. T. Metaxas, E. Mustafaraj, in *Proceedings of the WebSci10: Extending the Frontiers of Society On-Line*, Raleigh, NC, 26 to 27 April 2010; http://bit.ly/qInTmW.
10. The "Truthy" project, http://truthy.indiana.edu/.
11. E. Mustafaraj *et al.*, in *Proceedings of IEEE PASSAT/Conf. on Social Computing*, Minneapolis, MN, 9 to 11 October 2011 (IEEE, 2011), pp. 103–110; http://bit.ly/oZFqas.
12. Journalists and media outlets, who typically have large number of followers, should be careful when retweeting without comment. Even though some journalists declare in their Twitter profile that their "Retweet does not imply agreement," this distinction is missed by the vast majority of the user population who view retweet as endorsement.
13. E. Mustafaraj, P. T. Metaxas, in *Proceedings of ACM Information Retrieval and Advertising Workshop*, Boston, MA, 23 July 2009 (ACM, NY, 2009); http://bit.ly/RjcJYn.
14. T. Edsal, Let the nanotargeting begin, *New York Times Online* (2012); http://nyti.ms/QfX792.
15. See video clip of Z. Moffatt on *Wall Street Journal*, WorldStream Video; http://on.wsj.com/RjaxQH.
16. E. Mustafaraj, P. T. Metaxas, C. Grevet, *Proc. IEEE Comput. Sci. Eng.***4**, 320 (2009); http://bit.ly/RjAkLF.
17. S. Asur, B. A. Huberman, in *Proceedings of the IEEE/WIC/ACM International Conference on Web Intelligence and Intelligent Agent Technology* (IEEE Computer Society, Los Alamitos, CA, 2010), pp. 492–499.
18. S. Goel, J. M. Hofman, S. Lahaie, D. M. Pennock, D. J. Watts, Predicting consumer behavior with Web search. *Proc. Natl. Acad. Sci. U.S.A.* **107**, 17486 (2010).
19. H. Choi, H. Varian, Predicting the present with Google trends (Google, 2009); http://bit.ly/RdWiMB.
20. J. Bollen, H. Mao, X. J. Zeng, *J. Comput. Science* **2**, 1 (2011).
21. F. Ciulla *et al.*, *EPJ Data Science* **1**, 8 (2012).
22. D. Gayo-Avello, A meta-analysis of state-of-the-art electoral prediction from Twitter data, http://bit.ly/Pqwkd7 (2012).
23. A. Jungherr, P. Jürgens, H. Schoen, Why the Pirate Party won the German election of 2009 or the trouble with predictions: A response to Tumasjan, A., Sprenger, T. O., Sander, P. G., & Welpe, I. M. "Predicting elections with twitter: What 140 characters reveal about political sentiment," *Soc. Sci. Comput. Rev.* **30**, 229 (2012); http://bit.ly/OtbOqO.
24. P. T. Metaxas, E. Mustafaraj, D. Gayo-Avello, in *Proceedings of IEEE PASSAT/Conference on Social Computing* (IEEE, 2011), pp. 165–171; http://bit.ly/qUHJyv.
25. M. T. Moore, *USA Today*, 1 August 2012; http://usat.ly/Rjb1Gq.


**Acknowledgments:** The authors' work was supported by NSF grant CNS-1117693.

10.1126/science.1230456

OCEANS

# The Risks of Overfishing

Current global fisheries jeopardize not only individual species but also the overall integrity of marine ecosystems.

**Ellen K. Pikitch**

On page 517 of this issue, Costello *et al*. (*1*) paint a dismal picture of the state of the world's fisheries. The authors report that globally, the vast majority of exploited fish populations have been depleted to abundance levels well below those recommended by conventional management guidance. Of even greater concern, most species are on a continuing trajectory of decline. These insights were gleaned from analyses of data from previously unassessed fish populations. These poorly understood fisheries, which represent about 80% of the world's fish catch, are in much worse shape than the relatively well-studied fisheries on which previous global status reviews have relied (*2*, *3*).

The substandard and deteriorating condition of the preponderance of fisheries is ample cause for concern. However, Costello *et al*.'s findings are even more alarming in the context of the evolving understanding of fishing and its ecological effects.

First, the authors measured the status of fish stocks relative to conventional fishery management benchmarks. Traditionally, fishery assessments have focused on individual target fish species; many, including Costello *et al*., have concentrated on guidance aimed at obtaining maximum sustainable yield (MSY). However, MSY-based reference points are increasingly viewed as upper limits rather than goals. Modern fishery assessment and management advice increasingly sets target reference points far below MSY reference points, providing a buffer to guard against the ecological, economic and social risks of overfishing that can result from uncertainty (*3*, *4*).

Tiered management approaches, in which larger buffers are set in situations with less certain information, are increasingly recommended and applied (*3*, *5*). For example, Restrepo *et al*. have recommended that default fishing rates in the United States be set at no more than 75% of the level that would produce MSY yields, and that more risk-averse solutions be adopted in cases where data are poor (*3*). Australia, New Zealand, and other nations have adopted similar rules. Had Costello *et al*. considered such buffers in their analysis, the status of global fisheries would appear far worse than the already dismal picture portrayed.

Another important trend in fisheries management is the movement away from single-species management toward an ecosystem-based approach (*6*). The latter approach reverses the usual order of management priorities by making the goal of sustaining healthy ecosystems paramount. It takes into account the profound impacts that fishing can have on habitat, nontarget species caught as bycatch, genetic diversity and integrity, competition and predation, and other aspects of the structure and function of marine ecosystems. In this approach, it may be necessary to curtail fishing of a target species substantially below that indicated by an MSY approach to avoid unacceptable impacts to other species and the overall ecosystem (*6*).

Empirical and modeling evidence provides support for the view that fishery depletions often have cascading effects (see the figure). The loss of apex predators nearly always results in further marine ecosystem degradation (*7*). Empirical and modeling studies have shown that depletions of lower–trophic level species such as sardines, anchovies, herring, and krill can induce population declines in dependent predators such as seabirds (*8*) and larger fishes and marine mammals (*5*, *9*). For example, Pikitch *et al*. (*6*) found that the impact of forage fishing at MSY levels on their predators varied among species and across ecosystems, with median biomass declines of 54% for seabirds and 27% for all predators combined. On the basis of these and other observations, the Lenfest Forage Fish Task Force recommended that catches of many forage fish species be cut in half relative to conventional guidance, and that no new forage fish fisheries should be instituted in low-information circumstances (*5*).

Dayton (*10*) argued for a shift in the burden of proof for fisheries management decisions, in line with that applied in other natural resource and human health and safety policy arenas. This shift in the burden of proof would require demonstration of no serious impact before fishing could proceed. It is justified not least because the risks of continuing fishing when it results in serious negative consequences are generally much greater than the risks of curtailing fishing when it does not have a deleterious impact.

As Costello *et al*. show, the probability of making a mistake that leads to overfishing and depleted fish populations is higher in the information-poor circumstances that dominate contemporary global fisheries. At the same

**Cascading effects of overfishing.** Predators that feed on commercially exploited fishes have seen substantial declines. Costello *et al*. now report on the state of global fisheries. They show that poorly understood fisheries are in much worse shape than relatively well-studied fisheries, and that the vast majority of fisheries are deteriorating. These trends potentially have far-reaching effects on marine ecosystems.

CREDIT: BRANDON COLE/WWW.BRANDONCOLE.COM

Institute for Ocean Conservation Science, School of Marine and Atmospheric Sciences, Stony Brook University, Stony Brook, NY 11794, USA. E-mail: ellen.pikitch@stonybrook.edu





Published by AAAS

time, emerging research is highlighting the danger of irreversible effects of current fisheries on overall ecosystems. These insights provide forceful arguments for a more precautionary approach to fisheries management, in which fishing is restricted to those places and amounts where it can be conducted safely and with minimal risk of jeopardizing the integrity of marine ecosystems.


**References**

1. C. Costello *et al.*, *Science* **338**, 517 (2012); 10.1126/science.1223389.
2. B. Worm *et al.*, *Science* **325**, 578 (2009).
3. V. R. Restrepo, G. G. Thompson, P. M. Mace, W. L. Gabriel, L. L. Low, A. D. MacCall, R. D. Methot, J. E. Powers, B. L. Taylor, P. R. Wade, J. F. Witzig, *Technical Guidance on the Use of Precautionary Approaches to Implementing National Standard 1 of the Magnuson-Stevens Fishery Conservation and Management Act* (NOAA Technical Memorandum NMFS-F/SPO 31, 1998).
4. A. E. Punt *et al.*, *ICES J. Mar. Sci.* **69**, 624 (2012).
5. E. K. Pikitch *et al.*, *Little Fish, Big Impact: Managing a Crucial Link in Ocean Food Webs* (Lenfest Ocean Program, Washington, DC, 2012).
6. E. K. Pikitch *et al.*, *Science* **305**, 346 (2004).
7. J. A. Estes *et al.*, *Science* **333**, 301 (2011).
8. P. M. Cury *et al.*, *Science* **334**, 1703 (2011).
9. A. D. M. Smith *et al.*, *Science* **333**, 1147 (2011).
10. P. K. Dayton, *Science* **279**, 821 (1998).


10.1126/science.1229965

NEUROSCIENCE

# The Mood of a Worm

The behavioral effects of two hormones on the human brain are similar to those of a neuropeptide on sensory neurons in the worm.

**Scott W. Emmons**

The human nervous system is a vastly complex network of functionally interconnected cells whose detailed structure is at present beyond reach. All our actions, calculations, feelings, memories, dreams—consciousness itself—emerge from its workings. To understand this colossal, enigmatic structure, experimentally amenable model animals with tractable nervous systems many orders of magnitude smaller are studied. A popular choice has been the worm *Caenorhabditis elegans*, a nematode 1 mm long with a nervous system containing fewer than 400 neurons. On pages 540 and 543 in this issue, Garrison *et al*. (*1*) and Beets *et al*. (*2*), respectively, add to a growing body of evidence that even at the highest levels of coordinating fundamental and complex behaviors, the same neural mechanisms are at work in worms and humans.

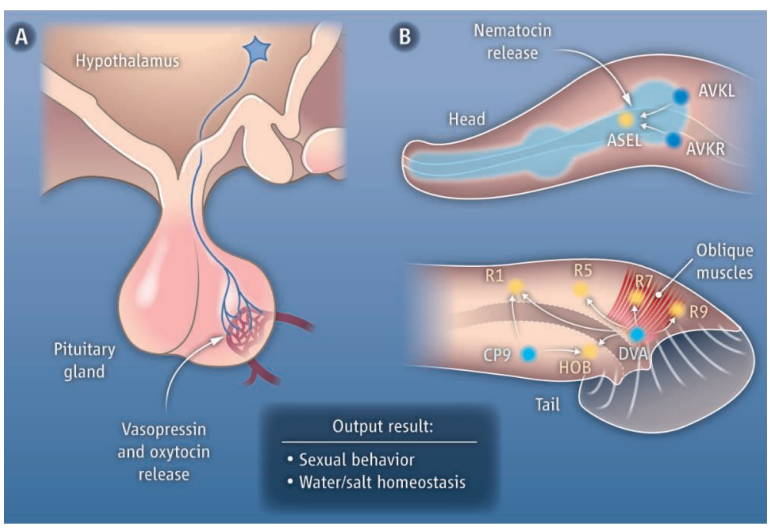


**Sex and salt.** (**A**) Neurons in the hypothalamus of the human brain secrete the hormones oxytocin to regulate sexual and reproductive behaviors, and vasopressin to control water balance. (**B**) Secretion of nematocin from neurons in the head and tail of the worm *C. elegans* regulates related behaviors—sexual behavior and salt chemotaxis. Names of neurons and muscles in the worm are indicated.

*C. elegans* neurons do not conform to a long-held principle of neuroscience that neurons are polar, with a clear input side consisting of the cell body with branching extensions called dendrites and a dedicated output process called an axon. Many *C. elegans* neurons are unbranched. Sites of input and output are often intermingled along processes, preventing a clear distinction between dendrite and axon. Moreover, some *C. elegans* neurons don't "fire" (discharge a short-lived electrical impulse, or action potential), but are analog devices with graded electrical responses. But the relevance of *C. elegans* was supported by genome sequencing. The *C. elegans* genome contains nearly the same suite of genes—encoding neurotransmitters, neurotransmitter receptors, ion channels, components of the synapse, transcription factors, and so forth—that underlie nervous systems of other animals, including humans (*3*). In addition, in some parts of the male nervous system, *C. elegans* neurons are highly branched and form a neural network with connectivity patterns also found in the human brain (*4*).

Garrison *et al*. and Beets *et al*. show that *C. elegans,* like other animals, expresses a neuropeptide related to oxytocin and vasopressin, key peptide hormones released by the neuroendocrine system of the human brain (see the figure). *C. elegans* uses this peptide to regulate behaviors similar to those modulated by oxytocin and vasopressin. Neuropeptides and other types of hormones are one of the three ways in which cells of the nervous system communicate with one another and with other tissues, the others being chemical synapses and gap junctions (electrical synapses). Oxytocin and vasopressin, similar short peptides of nine amino acids, are secreted by neurons in the hypothalamus and released into the blood stream and central nervous system. Although both have widespread effects, oxytocin regulates primarily sexual and reproductive behavior, whereas vasopressin is involved in homeostatic regulation of water balance, with effects on the kidneys, vascular system, feelings of thirst, and drinking behavior.

Garrison *et al*. demonstrate that similar to oxytocin, the *C. elegans* peptide, named nematocin, is required for normal sexual behaviors by the male. Mutant males lacking nematocin explored their environment in search of mates less frequently than wild-type males. When mutant males encountered a mating partner, they initiated copulation more slowly and executed poorly. This diffuse set of defects led the authors to speculate that nematocin primes a variety of neural circuits to stimulate an overall appetitive behavioral drive. Beets *et al*. show that nematocin allows worms to modify their behav-

Department of Genetics, Albert Einstein College of Medicine, 1300 Morris Park Avenue, Bronx, NY 10461, USA. E-mail: scott.emmons@einstein.yu.edu

CREDIT: C. BICKEL/*SCIENCE*





Published by AAAS

ior in light of recent experience. Normally, worms are attracted to salt. But if they experience salt in the absence of food, they quickly learn to avoid it. The authors observed that nematocin-deficient worms cannot do this. Function in salt attraction is reminiscent of vasopressin's role in water balance. A role for nematocin in memory of experience in the worm is similar to the roles of both oxytocin and vasopressin in establishing memory in parental, pair-bonding, and social settings in mammals (*5*, *6*).

An advantage of *C. elegans* is that every cell is known and the same in every animal. Garrison *et al*. and Beets *et al*. identify the relevant cells that secrete nematocin and the cells that bear nematocin receptors. In both studies, the receptors are in sensory neurons whereas secretion of the peptide is from a cell targeted by sensory neurons, suggesting a role in feedback. The sensory neurons expressing nematocin receptors were previously shown to act in the relevant pathways, male sexual behavior and salt chemotaxis. Expression of both peptide and receptor in additional cells indicates further functions yet to be identified.

Neuropeptides that function in other *C. elegans* circuits modify the responses of neurons such that functional circuitry is changed within fixed structural circuitry (*7*). The reason for multiple modes of communication within the nervous system may have to do with the time scales over which they operate. Gap junction– and chemical synapse–mediated communication occur over milliseconds to seconds, allowing for quick reactions. Neuropeptides and other types of hormones, by contrast, allow new points of communication between cells not in physical contact, and their effects can also persist over much longer periods. Thus, they establish behavioral states, enabling the nervous system to adjust its output to correspond to more slowly changing environmental and physiological circumstances, or intrinsic conditions such as sex or developmental time.

Nervous system function may be understood as the emergent collective property of a network rather than as the sum of individual circuits. This requires identifying all the interactions between the elements. Because gap junction communication and chemical synaptic communication occur at recognizable cellular sites, the potential functional network they create may be ascertained by describing the physical structure of the system. This has been done for *C. elegans* and is the goal of the field of connectomics (*4*, *8*–*10*). Interactions due to widely diffusing neuropeptides and other hormones can only be discovered by experimentation, which necessitates the use of tractable model systems. Just as today's major roads and highways may once have been ancient trails, biological systems can retain essential features derived from their origins. Although it is a mistake to consider small invertebrates as primitive, their systems may be closer to the ancestral condition than those of their larger cousins. Insights into what that ancestral condition was can help us understand function today.

**References**


1. J. L. Garrison *et al*., *Science* **338**, 540 (2012).
2. I. Beets *et al*., *Science* **338**, 543 (2012).
3. C. I. Bargmann, *Science* **282**, 2028 (1998).
4. T. A. Jarrell *et al*., *Science* **337**, 437 (2012).
5. A. Meyer-Lindenberg, G. Domes, P. Kirsch, M. Heinrichs, *Nat. Rev. Neurosci.* **12**, 524 (2011).
6. C. McCall, T. Singer, *Nat. Neurosci.* **15**, 681 (2012).
7. C. I. Bargmann, *Bioessays* **34**, 458 (2012).
8. O. Sporns *et al*., *PLOS Comput. Biol.* **1**, e42 (2005).
9. J. G. White *et al*., *Philos. Trans. R. Soc. B Biol. Sci.* **314**, 1 (1986).
10. L. R. Varshney, B. L. Chen, E. Paniagua, D. H. Hall, D. B. Chklovskii, *PLoS Comput. Biol.* **7**, e1001066 (2011).


10.1126/science.1230251

ASTRONOMY

# Measuring Solar Magnetism

How do you go about accurately measuring the magnetic field in the solar atmosphere?

**Alfred G. de Wijn**

The importance of magnetic fields in astrophysical processes has long been recognized. A thriving field of research is centered on the life cycle (the creation, evolution, and destruction) of magnetic fields in astrophysical plasmas, and prominently in solar physics. The discovery by Hale in 1908 that sunspots are associated with strong magnetic fields (*1*) spurred advances in spectroscopy, polarimetry, instrument development, and research into solar magnetism. Magnetism is now known to be the key to most unsolved problems in solar physics, including the 11-year activity cycle, chromospheric and coronal heating, flares, coronal mass ejections, and space weather. Even though more than a century has passed since the discovery of magnetism in the solar atmosphere, these measurements remain difficult.

High Altitude Observatory, National Center for Atmospheric Research, Boulder, CO 80307–3000, USA. E-mail: dwijn@ucar.edu

Magnetic field diagnostics are most mature for the solar photosphere, the deepest layer that can be directly observed with optical telescopes. During the past decade, measurements of the photospheric magnetic field have become routine with the development of the SpectroPolarimeter instrument of the Hinode Solar Optical Telescope (*2*, *3*) and the Helioseismic and Magnetic Imager (*4*) on the Solar Dynamics Observatory (*5*). Diagnostics of the magnetic field in the chromosphere and corona above the photosphere are in their infancy but are becoming more common.

There are, broadly speaking, two classes of magnetic field diagnostics: qualitative and quantitative. Of the former, the best known is proxy magnetometry, which involves the identification of locations of magnetic field through features associated with the field, such as sunspots (see the figure, panel A). Despite its limited diagnostic power, proxy magnetometry has contributed substantially to our understanding of solar magnetism; records of sunspot observations going back 300 years show the cyclical magnetic activity of the Sun (*6*).

Most quantitative measurements to date have relied on the Zeeman effect (*7*), whereby a magnetic field separates the single spectroscopic line of the degenerate atomic energy levels into three (or more) components. The separation of the components depends on the effective Landé factor of the line and the field strength. The former can be calculated from atomic models or measured by atomic spectroscopy, so that if the extent of the line separation can be measured, then the field strength can be determined. For regions of strong magnetic field in the photosphere, such as sunspots, the separation can be larger than the line width (see the figure, panel B). For weaker fields, the splitting is small and effectively only broadens the line. In this case, it is difficult or impossible to determine the separation from the intensity measurement alone. Fortunately, the two shifted components are circularly and oppositely polarized (see the

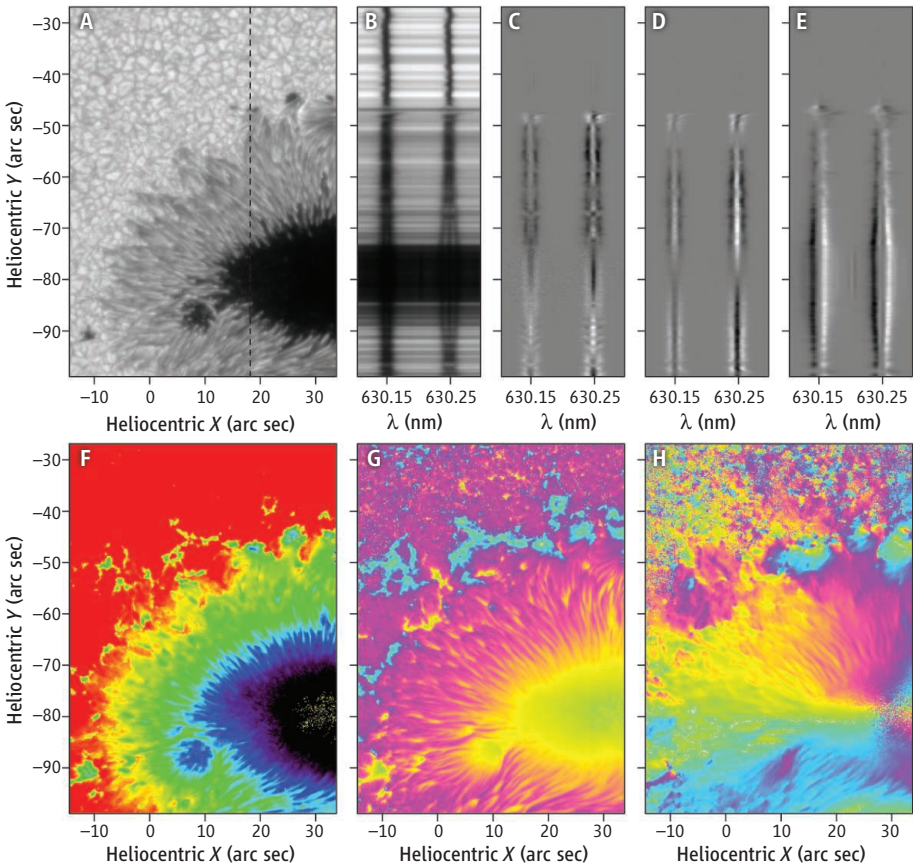


**A magnetic Sun.** (**A**) Continuum intensity image of a sunspot, made with the Hinode/SOT SpectroPolarimeter. (**B**) Intensity spectrum including two Fe I lines from the location indicated by the dashed vertical line in (A). (**C** and **D**) Linear polarization spectra. (**E**) Circular polarization spectrum. From these spectra the field strength (**F**), inclination (**G**), and azimuth (**H**) were determined by an inversion code. The inversion code fails to find the field strength accurately in some pixels in the dark umbra of the sunspot. The low intensity results in a low signal-to-noise ratio, and the cool temperature of the plasma allows for the existence of molecules that produce lines that are not modeled by code, further disrupting the fitting process. In the areas of quiet Sun (upper left corner of the field of view), the inclination and azimuth cannot be found because the polarization signal is very weak.

figure, panels C to E). Consequently, typical magnetographs are spectropolarimeters, recording both spectral and polarimetric information about the spectral lines.

To infer the magnetic field from such measurements is, however, not straigh forward. Only with the advent of charge-coupled device cameras that allowed direct digitization and subsequent analysis of the observations by computers did it become possible to derive the parameters of the plasma from which the spectral line originated. The most common method involves synthesizing observations based on an atmospheric model and external fields, and comparing the synthesis to the observations. The model and fields are adjusted until a match is found. This process is commonly referred to as an inversion (see the figure, panels F to H).

For many photospheric lines, the radiative transfer that governs the line formation is relatively benign. The simplest so-called Milne-Eddington atmospheric model was used as the basis for the first applications of spectropolarimetric inversions (*8*–*10*) and remains the workhorse for photospheric diagnostics (*11*). More sophisticated models assume that local thermal equilibrium (LTE) is a valid approximation. Atomic excitation must now be calculated, but in return one may derive more parameters, such as height-dependent information.

The approximation of LTE does not hold for lines formed in the chromosphere. The line synthesis calculation is considerably more difficult and requires that nonlocal effects be considered. The radiation field output feeds back into the calculation of the atomic excitation, which in turn influences the radiation. A time-consuming iteration is required to ensure consistency.

Inversion codes must find the global minimum in a multidimensional parameter space that typically has many local minima. For simpler atmospheric models, such as Milne-Eddington and LTE, the solution can often be found through general computer optimization methods. Non-LTE calculations are typically too costly for a brute-force approach. Recently, inversion codes that use pattern recognition techniques have been successfully applied to spectropolarimetric observations of chromospheric structures such as prominences (*12*) and filaments (*13*).

The difficulty of reconstructing the plasma parameters from the observation of line profiles is exacerbated by ambiguities in the data. For instance, the azimuth of the magnetic field can only be determined with an ambiguity of 180°. This problem is inherent to the nature of polarization and can only be resolved by making additional assumptions. Other ambiguities are more readily dealt with. Although the product of the fraction of the resolution element filled with magnetic field and the strength of the magnetic field is usually well determined from a line profile, often it is impossible to separate the two. This ambiguity can be resolved by simultaneously observing several spectral lines that are nearly identical in their formation but exhibit different effective Landé factors (*14*).

The structures of the solar chromosphere and corona are both dominated by magnetic fields. Many current problems in solar research cannot be resolved without knowledge of the magnetic field in those layers. Extrapolations from the photospheric magnetic field are generally inaccurate (*15*). Instruments are now being developed with the specific intent of measuring the magnetic field in the chromosphere and corona. As these instruments start to produce data, we will begin to understand the intricate nature of magnetism in the outer solar atmosphere and the heliosphere.

### References and Notes

1. G. E. Hale, *Astrophys. J.* **28**, 315 (1908).
2. T. Kosugi *et al.*, *Sol. Phys.* **243**, 3 (2007).
3. S. Tsuneta *et al.*, *Sol. Phys.* **249**, 167 (2008).
4. P. H. Scherrer *et al.*, *Sol. Phys.* **275**, 207 (2012).
5. W. D. Pesnell, B. J. Thompson, P. C. Chamberlin, *Sol. Phys.* **275**, 3 (2012).
6. D. H. Hathaway, *Living Rev. Sol. Phys.* **7**, 1 (2010).
7. P. Zeeman, *Verslagen van de Gewone Vergaderingen der Afdeeling Natuurkunde,* in *Koninklijke Akademie van Wetenschappen* (October 1896), pp. 181–248.
8. L. H. Auer *et al.*, *Sol. Phys.* **55**, 47 (1977).
9. B. W. Lites, A. Skumanich, *Astrophys. J. Suppl. Ser.* **49**, 293 (1982).
10. A. Skumanich, B. W. Lites, *Astrophys. J.* **322**, 473 (1987).
11. J. M. Borrero *et al.*, *Sol. Phys.* **273**, 267 (2011).
12. R. Casini *et al.*, *Astrophys. J.* **598**, L67 (2003).
13. C. Kuckein *et al.*, *Astron. Astrophys.* **501**, 1113 (2009).
14. J. O. Stenflo, *Sol. Phys.* **32**, 41 (1973).
15. M. L. DeRosa *et al.*, *Astrophys. J.* **696**, 1780 (2009).

**Acknowledgments:** The National Center for Atmospheric Research is sponsored by the NSF.

10.1126/science.1226336

ANTHROPOLOGY

# Did Australopiths Climb Trees?

The shoulder bones of a juvenile australopith resemble those of extant apes, suggesting that tree climbing continued to be important for these bipedal early human ancestors.

**Susan Larson**

What was the lifestyle of early members of the human lineage, such as *Australopithecus afarensis*? All fossil australopith skeletons display a mix of humanlike and apelike characteristics, but their lower limb features leave little doubt that these early members of our lineage walked on two legs. However, this mixture is more difficult to interpret for the upper limb. Some investigators see the apelike upper-limb characteristics as an indication that an ability to climb trees continued to have survival value (*1*–*4*). Others suggest that these features were simply retentions from an ancestral condition (*5*–*7*). On page 514 of this issue, Green and Alemseged (*8*) weigh in on this debate with an analysis of the shoulder bones of a juvenile australopith who lived around 3.3 million years ago.

The scapula, or shoulder blade, is key to the debate about australopith lifestyle. It is widely accepted that the characteristics of this bone are strongly influenced by how the shoulder is used. Most australopith scapular specimens are missing major portions, but it is apparent that they had an apelike upward-facing socket for the shoulder joint (glenoid fossa); in humans, the glenoid faces out to the side. Further, australopith scapulae have an apelike obliquely oriented scapular spine (the ridge of bone running across the shoulder blade); this ridge is more nearly horizontal in humans (see the figure).

For those investigators inclined to interpret anatomy in terms of function, these apelike features are evidence for the continued importance of tree climbing in *A. afarensis* (*1*, *2*). However, those who believe that the ability to climb trees no longer played a major role in australopith life argue that these characteristics are primitive retentions that offered no obvious disadvantage. In addition, it has been suggested that variation in these features is influenced by body size, implying that their appearance in *A. afarensis*—for example, an upward facing glenoid of the partial scapula from the famous "Lucy" skeleton (A.L. 288-1)—simply reflects small body size (*9*, *10*).

The discovery of a partial skeleton of a juvenile *A. afarensis* from Dikiki, Ethiopia (DIK-1-1), offered the first real glimpse at an intact australopith scapula (*11*). The initial analysis of the right scapula, still partially embedded in a sandstone matrix, revealed an overall similarity to juvenile gorillas, although the conclusions were equivocal regarding the implications of this result (*11*).

Green and Alemseged have now analyzed the left and right scapulae of this juvenile partial skeleton, freed from matrix. They show that the upward glenoid orientation characteristic of adult australopiths is also apparent in the DIK-1-1 scapulae. This feature suggests that australopiths, like apes, maintained a consistent upward glenoid orientation as they grew up. Humans, in contrast, start out with a somewhat downward-facing glenoid that gradually changes to face more directly outward as individuals mature (see the figure).

The fact that australopiths began life with a very different glenoid orientation than a modern human makes it clear that the upward facing glenoid in Lucy is not merely a reflection of small body size as has been argued (*9*, *10*). Occasionally, the scapula of a small human can have a glenoid angle comparable to that of Lucy, but that human would have started out life with a very different glenoid orientation than seen in DIK-1-1. Similarly, Green and Alemseged show that an oblique scapular spine (see the figure) was a characteristic of australopiths throughout their life span, as it is in apes. The human pattern of development is again different, with spine angle decreasing during growth.

The shoulder forms the foundation for the upper limb's range of motion. Contrasting patterns of scapula growth suggest differing functional demands on the shoulder as individuals matured. Overhead use of the upper limb while moving in trees begins early in the life of apes and continues to have survival value even among large-bodied adults. A similar growth pattern in australopiths, therefore, supports the view that some ability to climb trees continued to contribute to survival in our bipedal early ancestors. Humans do various things with their upper limbs, but without a major focus on overhead postures their scapulae follow a very different growth trajectory.

The DIK-1-1 scapulae resemble those of juvenile apes, particularly juvenile African apes, in other characteristics as well. For

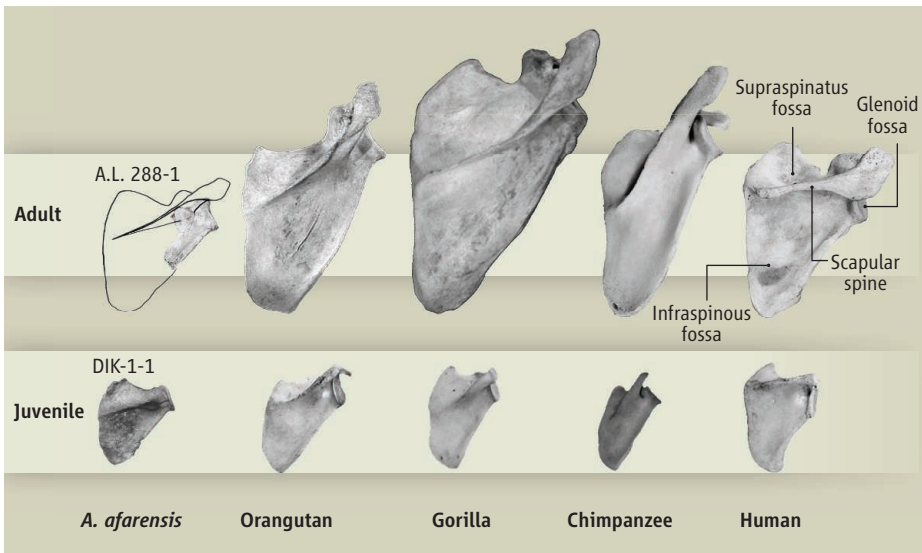


**Shoulder bone changes during growth in apes and humans.** The distinctive downward orientation of the juvenile human glenoid and its horizontal scapular spine is in contrast to the upward facing glenoids and oblique spines of the other species, including the juvenile australopith DIK-1-1 studied by Green and Alemseged. In adult apes and *A. afarensis*, the glenoid continues to face upward and the scapular spine remains oblique, whereas in adult humans, the glenoid faces out to the side and the scapular spine is more nearly horizontal. These differences provide clues to the lifestyle of australopiths. The reconstruction of the adult *A. afarensis* scapula is based on A.L. 288-1 and characteristics of DIK-1-1. The adult bones are only approximately to scale.

Anatomical Sciences, School of Medicine, Stony Brook University, Stony Brook, NY 11794, USA. E-mail: susan.larson@stonybrook.edu







Published by AAAS

example, they have a relatively broad supraspinous fossa and a relatively narrow infraspinous fossa (see the figure). Unfortunately, little is known about these characteristics in adult australopiths because most fossil scapulae are incomplete.

Comparison of the DIK-1-1 scapulae to those of adult australopiths confirms apelike shoulder characteristics in these early human ancestors. Their shoulder blades do not closely resemble those of any specific living ape, reflecting the fact that they were habitual bipeds on the ground. Nevertheless, the developmental stability in *A. afarensis* of an upward facing glenoid and oblique scapular spine indicate that overhead use of their upper limbs to climb and balance in trees remained part of their overall survival strategy.

The scapula of the early *Homo erectus (H. ergaster)* Turkana Boy (KNM-WT 15000) indicates that by about 1.8 million years ago, the shoulder of human ancestors had undergone a dramatic transformation. As in modern humans, the glenoid no longer faced upward, the scapular spine was transversely oriented, and the infraspinous fossa was broad (*8*). This reconfiguration was likely part of the emergence of our own genus *Homo* and a growing dependence on tools and culture for survival.


**Refereces**

1. J. T. Stern Jr., R. L. Susman, *Am. J. Phys. Anthropol.* **60**, 279 (1983).
2. R. L. Susman *et al.*, *Folia Primatol. (Basel)* **43**, 113 (1984).
3. R. L. Susman, J. T. Stern Jr., in *Origine(s) de la bipédie chez les hominidés,* Y. Coppens, B. Senut, Eds. (CNRS, Paris, 1991), pp. 121–131.
4. J. T. Stern, *Evol. Anthropol.* **9**, 113 (2000).
5. C. O. Lovejoy, *Sci. Am.* **259**, 118 (1988).
6. B. Latimer, in *Origine(s) de la Bipédie Chez les Hominidés,* Y. Coppens, B. Senut, Eds. (CNRS, Paris, 1991), pp. 169–176.
7. C. V. Ward, *Yearb. Phys. Anthropol.* **S35**, 185 (2002).
8. D. J. Green, Z. Alemseged, *Science* **338**, 514 (2012).
9. R. P. Mensforth, B. Latimer, S. Senturia, *Am. J. Phys. Anthropol.* **81**, 267 (1990).
10. S. E. Inouye, B. T. Shea, *Int. J. Primatol.* **18**, 629 (1997).
11. Z. Alemseged *et al.*, *Nature* **443**, 296 (2006).


10.1126/science.1230128

CHEMISTRY

# Lending Handedness to the Cyclopentadienyl Ligand

Chemical and biochemical modifications of the Cp ligand have allowed for the stereoselective formation of organic reaction products.

**Honggen Wang and Frank Glorius**

Chirality (handedness) represents an intrinsic property of many objects (such as hands and some molecules). The increasing demand for just one isomer of a compound, especially for pharmaceuticals, has been met largely by purifying racemic mixtures of chiral compounds. A powerful alternative to separation is to use chiral catalysts (*1*) to generate only the desired enantiomer; chiral metal complexes bearing specialized ligands based on heteroatoms such as phosphines and N-heterocyclic carbenes have been commonly used. In contrast, on pages 504 and 500 of this issue (*2*, *3*), the authors achieved highly asymmetric C–H functionalizations (*4*) (see the figure, panel A) by introducing chiral features to one of the most common ligands used in organometallic chemistry, cyclopentadienyl (Cp). Ye and Cramer (*2*) report a chemical route to create a chiral Cp derivative, and Hyster *et al*. (*3*) describe a biochemical approach that uses a modified Cp in a chiral protein environment.

The discovery of ferrocene ($FeCp_2$) and the identification of its sandwich structure by Woodward, Wilkinson, and Fischer in the 1950s triggered important developments in modern organometallic chemistry (*5*). The wide-scale use of Cp and its analogs stemmed from their inertness to both nucleophilic or electrophilic reagents, their strong binding to metal centers, and the easy modification of their steric and electronic properties by varying the substituents on the Cp ring (*6*). Nevertheless, in sharp contrast to other classes of ligands (e.g., phosphines), the application of chiral Cp derivatives in asymmetric catalysis has met with far less success, (*7*) likely because of the inherent difficulties of designing chiral versions of the Cp ligand. Despite this challenge, in

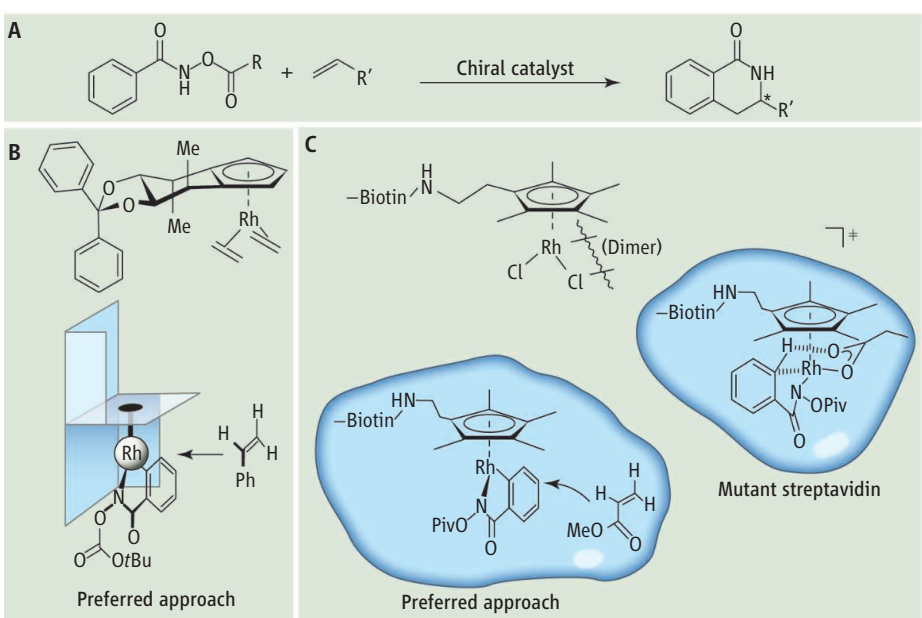


**Hand(ednes)s on an old ligand.** Two research groups report on different ways of modifying the Cp ligand so that Rh(III)-catalyzed C–H functionalization (**A**) would create preferred enantiomeric products (R and R′ are organic substituents; the star marks the product's chiral carbon). (**B**) Ye and Cramer chemically synthesized a chiral Cp ligand that determined the arrangement of substrate and reactant, resulting in high enantioselectivity (Me, methyl; Ph, phenyl; and *t*Bu, *tert*-butyl). (**C**) Hyster *et al*. biochemically modified Cp to create an artificial metalloenzyme. An appropriately positioned glutamate side chain within the host protein accelerated the C–H activation step, and the asymmetric environment around the metal led to stereoselective coupling (Piv, pivaloyloxy).

Organisch-Chemisches Institut, Westfälische Wilhelms-Universität Münster, Corrensstrasse 40, 48149 Münster, Germany. E-mail: glorius@uni-muenster.de; honggen.wang@uni-muenster.de.

many cases, the Cp moiety is an attractive candidate for chiral induction because it is often the only ligand that remains bound to the metal throughout the catalytic cycle.

Ye and Cramer synthesized an elegant chiral $C_2$-symmetric Cp ligand and then applied it in asymmetric catalysis with a rhodium catalyst system of the type [($\eta^5$-$C_5H_5$)$RhL^1L^2L^3$)] (see the figure, panel B), where the Cp ligand should selectively determine the spatial arrangement of the other three ligands—$L^1$, $L^2$, and $L^3$—around the metal. To achieve the required selectivity, three ligand features were critical. First, a $C_2$-symmetric ligand (one that is chiral and has only one 180° rotational symmetry axis) avoided the formation of two isomeric complexes derived from incomplete "facial selectivity" with respect to the coordination of ligand to the metal (that is, which side or "face" of the Cp-derived ligand binds). Second, steric bulk next to the Cp ring restricted rotation around the Cp moiety and allowed for a single preferential alignment of substrates. Third, shielding from a remote substituent on the ligand directed the approach of the incoming reactant to the opposite side.

The Cp*Rh(III)-catalyzed annulation of a benzohydroxamic acid derivative and alkenes, recently independently developed by Fagnou, Glorius, and their co-workers (*8*, *9*), offered an excellent opportunity to test the concept of chiral Cp ligands because of its mild and simple reaction conditions (*10*). Indeed, a rhodium precatalyst equipped with a carefully modified Cp ligand allowed Ye and Cramer to obtain dihydroisoquinolones in high yields and enantiomeric ratios (er's) up to 97:3. The Rh(III) catalyst generated in situ by oxidation was proposed to be the active catalyst. The reaction scope is quite general with high yields and er's, suggesting that the catalyst system is robust.

The biological approach taken by Hyster *et al*. functionalized Cp with biotin so that biotin-protein interactions would drive the incorporation of the Cp-metal complex (which continues to act as a catalyst) within a protein scaffold to form an artificial metalloenzyme (which creates a chiral environment) (*11*) (see the figure, panel C). The introduction of an appropriately positioned functional group within the protein should further facilitate the reaction. They also used the Cp*Rh(III)-catalyzed synthesis of dihydroisoquinolones as a test reaction (*8*, *9*). A biotinylated Rh(III) complex $[RhCp^{*biotin}Cl_2]_2$ was designed and incorporated within wild-type streptavidin.

Initially, the substrate conversion was disappointingly low. Noting that the presence of a basic residue in appropriate proximity to the metal center should help facilitate C–H activation (*12*), Hyster *et al*. created an artificial metallodyad by introducing a basic carboxylate residue within the protein through computational modeling and genetic engineering. An extensive survey of mutated streptavidin showed that a double mutant ($Ser^{112}$ to Tyr and $Lys^{121}$ to Glu) gave the desired product in excellent yield, with good regioselectivity and, most important, up to an enantiomeric ratio of 93:7. Only a few examples were demonstrated, indicating a limited substrate scope, but considering the high specificity of natural biocatalysis, this result is exciting and encouraging. It represents a rare case of an artificial metalloenzyme inducing high levels of both selectivity and reactivity.

Chiral Cp ligands bearing one or more additional coordination groups have already been successfully used together with early transition metals in asymmetric catalysis (*13*). In contrast, the application of these Cp derivatives to middle or late transition metal catalysis is intrinsically problematic because too many coordination sites of the metal are occupied. Considering that middle or late transition metal complexes are arguably more synthetically useful, and Cp is frequently responsible for their stability and reactivity, the successful design of chiral Cp derivatives will offer tremendous opportunities for late transition metal asymmetric catalysis.

**References**


1. E. N. Jacobsen, A. Pfaltz, H. Yamamoto, Eds., *Comprehensive Asymmetric Catalysis*, Vol. I-III, suppl. I-II (Springer, New York, 1999).
2. B. Ye, N. Cramer, *Science* **338**, 504 (2012).
3. T. K. Hyster, L. Knörr, T. R. Ward, T. Rovis, *Science* **338**, 500 (2012).
4. M. Wasa, K. M. Engle, D. W. Lin, E. J. Yoo, J. Q. Yu, *J. Am. Chem. Soc.* **133**, 19598 (2011).
5. H. Werner, *Angew. Chem. Int. Ed.* **51**, 6052 (2012).
6. J. Hartwig, *Organometallic Transition Metal Chemistry: From Bonding to Catalysis* (University Science Books, Sausalito, CA, 2010).
7. A. Gutnov *et al*., *Angew. Chem. Int. Ed.* **43**, 3795 (2004).
8. N. Guimond, S. I. Gorelsky, K. Fagnou, *J. Am. Chem. Soc.* **133**, 6449 (2011).
9. S. Rakshit, C. Grohmann, T. Besset, F. Glorius, *J. Am. Chem. Soc.* **133**, 2350 (2011).
10. J. Wencel-Delord, T. Dröge, F. Liu, F. Glorius, *Chem. Soc. Rev.* **40**, 4740 (2011).
11. T. R. Ward, *Acc. Chem. Res.* **44**, 47 (2011).
12. L. Ackermann, *Chem. Rev.* **111**, 1315 (2011).
13. A. H. Hoveyda, J. P. Morken, *Angew. Chem. Int. Ed. Engl.* **35**, 1262 (1996).


10.1126/science.1229830

ECOLOGY

# Fishing for Answers off Fukushima

**Ken O. Buesseler**

Radionuclide levels in fish off Fukushima are highly variable but remain elevated, indicating a continuing source of radiation.

The triple disaster of the 11 March 2011 earthquake, tsunami, and subsequent radiation releases at Fukushima Dai-ichi were, and continue to be, unprecedented events for the ocean and for society. More than 80% of the radioactivity from Fukushima was either blown offshore or directly discharged into the ocean from waters used to cool the nuclear power plants (*1*). Although offshore waters are safe with respect to international standards for radionuclides in the ocean (*2*), the nuclear power plants continue to leak radioactive contaminants into the ocean (*3*); many near-shore fisheries remain closed. What are the prospects for recovery?

Public anxieties in Japan about seafood safety remain high, in part because the Japanese are among the world's highest per capita consumers of seafood. On 1 April 2012, regulators tightened restrictions for cesium-134 and cesium-137 in seafood from 500 to 100 becquerels per kilogram wet weight (Bq/kg wet) in an effort to bolster confidence in the domestic supply. In fact, this measure may have had the opposite effect, as the public now sees more products considered unfit for human consumption.

The Japanese Ministry of Agriculture, Forestry and Fisheries (MAFF) has been monitoring radionuclides in fish and other seafood products since 23 March 2011. They have been releasing these data on a regular basis, most notably in a single annual compilation of more than 8500 samples of fish, shellfish, and seaweeds collected at major landing ports and inland freshwater sites, particularly in the most affected coastal areas near Fukushima (*4*).

Woods Hole Oceanographic Institution, Woods Hole, MA 02543, USA. E-mail: kbuesseler@whoi.edu

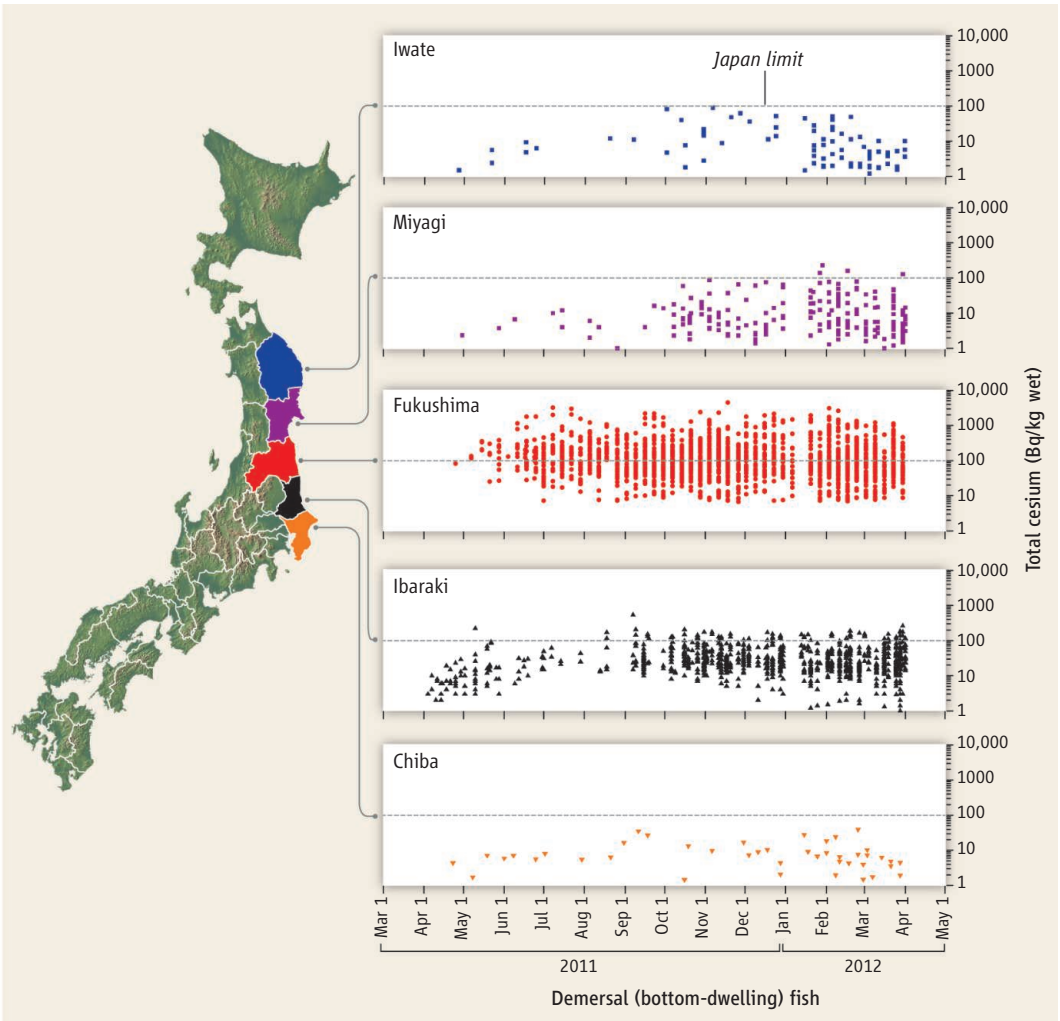


**Still radioactive.** Changes in total cesium ($^{137}$Cs + $^{134}$Cs in Bq/kg wet) over time in demersal (bottom-dwelling) fish for five prefectures in eastern Japan closest to Fukushima. Since the nuclear disaster, total cesium levels have been highest in fish caught off Fukushima prefecture.

The MAFF results show that total cesium levels in demersal (bottom-dwelling) fish, including many important commercial species, are highest off Fukushima and lower in four prefectures to the north and south (see the figure). Fishing for these species is currently banned off Fukushima, where 40% of fish are above the new regulatory limit of 100 Bq/kg wet (*4*).

Demersal fish have higher cesium levels than other marine fish types, grouped here as epipelagic (near-surface), pelagic (open ocean), and neuston (surface-dwelling) fish. Contamination levels of demersal fish are comparable only to those of freshwater fish (see fig. S1). Cesium levels have not decreased 1 year after the accident, except perhaps in neuston, and as of August 2012, fish are still being found with cesium levels above 100 Bq/kg wet (*5*). The highest total cesium levels found to date, more than 25,000 Bq/kg wet, are from two greenling caught in August 2012 closer to shore off Fukushima (*6*).

Cesium accumulates in fish muscle tissues with relatively modest concentration factors; the Cs concentration in fish is typically 100 times that in the surrounding seawater (*7*). The concentration factors increase only slightly as one moves up the food chain (*8*). Bioaccumulation is much higher in general in freshwater fish because of lower salinities (*9*) (see fig. S1). Uptake of cesium is balanced by loss back to the ocean, which increases with body size and metabolic rate (*8*). The loss rate is a few percent per day on average and has been shown to be faster if the cesium supply is pulsed rather than steady (*10*).

Given these high loss rates and the fact that cesium-134 and cesium-137 remain elevated in fish, particularly in bottom-dwelling species, there must be a continued source of cesium contamination associated with the seafloor. Reports of Fukushima cesium in marine sediments, although not extensive, support the assumption that the seafloor is a possible source of continued contamination (*11*). Given the 30-year half-life of $^{137}$Cs, this means that even if these sources were to be shut off completely, the sediments would remain contaminated for decades to come.

The variability in total cesium levels for any given date and fish type is extremely high, making management decisions of when to open or close a particular fishery more difficult. The wide range of observed cesium levels may be due to variability in the cesium loss rates from fish, the life stages of each species, and differences in habitat. Of course, many fish move over wide spatial scales, which will also affect cesium levels in fish caught at a particular location that may have been exposed elsewhere.

The MAFF data show that the vast majority of fish remain below even the new, stricter regulatory limit for seafood consumption. Many naturally occurring radionuclides appear in fish at similar or higher levels and are not considered a health threat. For example, in fish sampled in June 2011 off Japan, natural levels of potassium-40, a naturally occurring beta emitter like cesium, were more than 10 times those of Fukushima-derived cesium (*2*). Moreover, because cesium is rapidly lost from muscle after exposure stops, fish that migrate to less affected waters will gradually lose much of their Fukushima-derived cesium, as seen in a report of tuna caught off San Diego (*12*).

Nonetheless, the fact that many fish are just as contaminated today with $^{134}$Cs and $^{137}$Cs as they were more than 1 year ago implies that cesium is still being released to the food chain. The Japanese government is using the MAFF results to keep fisheries closed off Fukushima and to closely monitor neighboring areas where levels are approaching the regulatory limits.

Knowledge of the patterns of radionuclide contamination and trends over time for different fish types helps to put risks arising from the released radioactivity in context. However, studies of cesium in fish are not enough. An understanding of sources and sinks of




Published by AAAS

cesium and other radionuclides is needed to predict long-term trends in fish and other seafood. Such knowledge would support smarter and better targeted decision-making, reduce public concern about seafood, and potentially help to revive local fisheries safely, with confidence, and in a timely manner.


**References and Notes**

1. N. Yoshida, J. Kanda, *Science* **336**, 1115 (2012).
2. K. O. Buesseler *et al.*, *Proc. Natl. Acad. Sci. U.S.A.* **109**, 5984 (2012).
3. K. O. Buesseler, M. Aoyama, M. Fukasawa, *Environ. Sci. Technol.* **45**, 9931 (2011).
4. Japan Ministry of Agriculture, "Results of the inspection on radioactivity materials in fisheries products" (press release March 2011 to March 2012); www.jfa.maff.go.jp/e/inspection/index.html.
5. Japan Ministry of Agriculture, "Results of the inspection on radioactivity materials in fisheries products" (28 September 2012); www.jfa.maff.go.jp/e/inspection/index.html.
6. Tokyo Electric Power Company, "Nuclide analysis results of fish and shellfish" (August 2012); www.tepco.co.jp/en/nu/fukushima-np/images/handouts_120821_01-e.pdf.
7. International Atomic Energy Agency, *Sediment Distribution Coefficients and Concentration Factors for Biota in the Marine Environment*, Technical Report Series No. 422 (IAEA, Vienna, 2004).
8. H. Doi, T. Takahara, K. Tanaka, *PLoS ONE* **7**, e29295 (2012).
9. D. J. Rowan, J. B. Rasmussen, *Can. J. Fish. Aquat. Sci.* **51**, 2388 (1994).
10. D. J. Rowan, J. B. Rasmussen, *J. Appl. Ecol.* **32**, 739 (1995).
11. Ministry of Education, Culture, Sports, Science and Technology, Japan (2012), "Readings of marine soil monitoring in sea area," http://radioactivity.mext.go.jp/en/list/260/list-1.html.
12. D. J. Madigan, Z. Baumann, N. S. Fisher, *Proc. Natl. Acad. Sci. U.S.A.* **109**, 9483 (2012).



**Acknowledgments:** Supported by the Gordon and Betty Moore Foundation. I thank S. Clifford for compilation of MAFF data and K. Kostel for assistance in writing.


**Supplementary Materials**

www.sciencemag.org/cgi/content/full/338/6106/480/DC1
Fig. S1
Reference

10.1126/science.1228250

NEUROSCIENCE

# Decoding the Neuronal Tower of Babel

Identification of a postsynaptic protein in the hippocampus reveals how neurotransmitter release from one neuron is tailored to different target cells.

**Chris J. McBain**

Individual neurons in the mammalian central nervous system communicate with their downstream targets by means of subcellular specializations in their axon. Arranged like pearls on a necklace, these presynaptic terminals enable the rapid release of neurotransmitter in response to an electrical action-potential wave front that travels from the cell body to the far reaches of the axon. A single axon may contact hundreds of downstream targets, including numerous distinct cell types. Though separated by only a few micrometers, each of these presynaptic release sites is often tuned to the particular cell type it innervates such that transmission may be robust onto one particular cell type yet weak at another, despite all terminals sensing the same action-potential waveform (*1*). This arrangement allows different terminals in the axon to behave independently and "translate" presynaptic action potentials into their own unique chemical language to effect both short- and long-term synaptic transmission and plasticity (*2*, *3*). Whether elements in the presynaptic terminal, postsynaptic membrane, or transynaptic proteins dictate this differential synaptic processing has been unclear. On page 536 in this issue, Sylwestrak and Ghosh (*4*) show that postsynaptic expression of the extracellular leucine-rich repeat fibronectin-containing 1 (Elfn1) plays an important role in establishing such target-specific differential transmission.

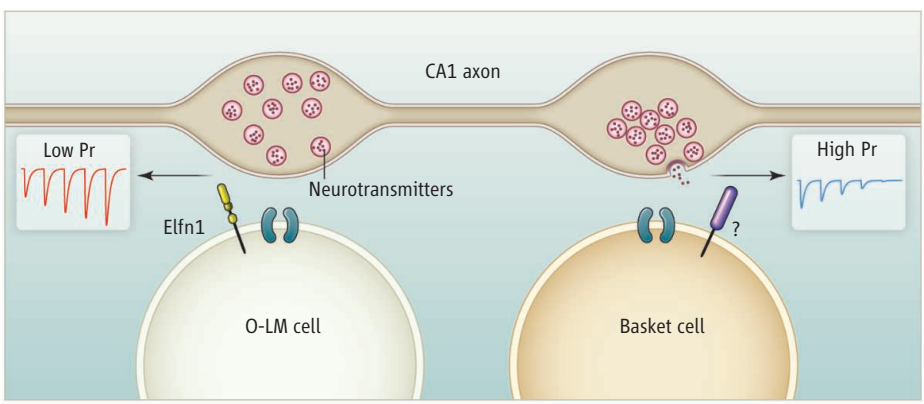


**Tailoring one neuron to two synapses.** In the hippocampus, somatostatin-containing O-LM and parvalbumin-containing basket cells receive common afferent input from CA1 pyramidal neurons. The postsynaptic expression of the leucine-rich repeat protein Elfn1 in O-LM cells acts to set the presynaptic initial transmitter release probability (Pr) low, ensuring short-term facilitation of synaptic transmission. In contrast, the absence of Elfn1, of the presence of an as yet undiscovered trans-synaptic protein, endows CA1 pyramidal neuron synapses onto basket cells with a high initial release probability, depressing synaptic transmission.

CA1 pyramidal neurons of the hippocampus form synapses with many downstream inhibitory interneuron targets, including the parvalbumin-containing fast-spiking basket cell and the somatostatin-positive oriens-lacunosum moleculare (O-LM) neuron. Under normal conditions, a train of presynaptic action potentials in the CA1 pyramidal neurons triggers robust synaptic transmission onto basket cells (such synapses are referred to as having a high initial release probability), such that larger synaptic events are triggered early in the train, which then rapidly wane as the train progresses (i.e., short-term depression). In contrast, synaptic events onto O-LM cells start small and grow as the train of action potentials progresses (a process termed short-term facilitation, and indicative of synapses with a low initial transmitter release probability). Sylwestrak and Ghosh demonstrate that Elfn1 is selectively expressed in O-LM inhibitory interneurons and that its punctate expression on dendrites reveals a strong enrichment at synapses where the neurotransmitter glutamate but not the neurotransmitter γ-aminobutyric acid is released. Targeted elimination of

Eunice Kennedy Shriver National Institute of Child Health and Human Development, Porter Neuroscience Center, Room 3C903, Lincoln Drive, Bethesda, MD 20892, USA. E-mail: mcbainc@mail.nih.gov

Elfn1 from O-LM neurons with a lentivirus construct containing short hairpin RNA increased the evoked excitatory postsynaptic current amplitude and strongly reduced the degree of short-term facilitation observed across a range of frequencies. Elimination of Elfn1 in early postnatal neurons had the greatest impact on transmission, suggesting an instructive role in the development and maturation of synaptic function. Elfn1 loss of function was not accompanied by changes in postsynaptic properties, consistent with a role for Elfn1 in establishing low–presynaptic release probability synapses onto O-LM cells (see the figure). Surprisingly, despite this apparent Elfn1 control over release probability, the absence of Elfn1 did not convert pyramidal neuron–O-LM synaptic activity to match that of pyramidal neuron–basket cell connections, which have an extremely high initial release probability. Rather, loss of Elfn1 normalized transmission across the train of stimuli, with only weak facilitation remaining. This suggests that other factors must be involved in establishing the high release probability at pyramidal neuron–basket cell targets. Consistent with a role for Elfn1 in establishing low–release probability synapses, overexpression of Elfn1 in basket cells converted their hallmark short-term synaptic depression into facilitation. The available data suggest that the default setting for excitatory synapses onto interneurons may occupy the middle ground of release probability, such that Elfn1 acts to lower release probability at O-LM synapses and an as yet unidentified element acts to elevate the release probability of basket cell synapses.

Although structural roles for proteins containing leucine-rich repeat (LRR) motifs in axon guidance, synapse target selection, maturation, and myelination are well established (*5*), functional roles for LRR proteins in regulating synaptic transmission are also not without precedent. For example, neurotrophins and their LRR-containing Trk receptors have both structural and functional roles in cortical circuits. Similarly, leucine-rich glioma inactivated 1 (LGI1) and ADAM22 interact with postsynaptic density protein 95 (PSD95) to regulate postsynaptic glutamate receptor subunit availability. In addition, interaction of LGI1 with the presynaptic voltage-gated potassium channel Kv1.1 influences presynaptic release probability in perforant path–granule cell synapses. How Elfn1 acts to influence release probability is currently unknown. Sylwestrak and Ghosh indicate that an interplay between Elfn1 and GluK2-receptor mediated short-term plasticity, but the underlying mechanism is unclear. The available data suggest that Elfn1 must have downstream diffusible or trans-synaptic partners that can act to regulate the availability of synaptic glutamate for presynaptic kainate receptors.

The two *Elfn* genes have highly complementary expression patterns in mammalian central neurons. Elfn2 is largely confined to cortical and hippocampal principal glutamatergic neurons (*6*). Although Sylwestrak and Ghosh show high enrichment of Elfn1 in somatostatin-containing O-LM cells, a wider pattern of expression among other unidentified inhibitory interneuron subtypes is suggested (*6*, *7*). Whether such expression coincides with other excitatory inputs with low release probabilities remains to be tested. Thus, the first step to decode target-specific synaptic transmission has been taken, with undoubtedly many more to follow.

**References**


1. H. J. Koester, D. Johnston, *Science* **308**, 863 (2005).
2. K. Tóth, C. J. McBain, *J. Physiol.* **525**, 41 (2000).
3. K. A. Pelkey, C. J. McBain, *J. Physiol.* **586**, 1495 (2008).
4. E. L. Sylwestrak, A. Ghosh, *Science* **338**, 536 (2012).
5. J. de Wit, W. Hong, L. Luo, A. Ghosh, *Annu. Rev. Cell Dev. Biol.* **27**, 697 (2011).
6. J. Dolan *et al.*, *BMC Genet.* **8**, 320 (2007).
7. Allen Brain Atlas, www.brain-map.org.


10.1126/science.1230338

MEDICINE

# Can Intellectual Property Save Drug Development?

Continually refining the focus of intellectual property during the drug development process should encourage productive collaborations and expedite the availability of new therapies.

**Garret A. FitzGerald**

The imbalance between the roughly constant rate of new drug approvals and the exploding cost estimates of drug development—mostly the cost of failure—has raised concern about the declining productivity of the pharmaceutical industry. Efforts to address the situation have included an investment in human capital—particularly those individuals who can project science across the translational divide (bench to clinic)—and investment in infrastructure, as exemplified by Clinical and Translational Science Awards in the United States and Biomedical Research Centers in the United Kingdom, and an increase in partnerships between academia and industry (*1*). However, radical reform of the iron rules of intellectual property (IP) worldwide will be necessary if we are to harvest and integrate the efforts of scientists and clinicians scattered across companies, universities, and countries, best qualified to generate new therapies.

Traditionally, large pharmaceutical companies embraced the entire process of drug discovery, development, approval, and marketing, but such large, "vertically" integrated companies are disintegrating. A recent market capital analysis of the 19 largest pharmaceutical companies indicated that investment was $1 billion for sales that amounted to only $75 million from 2005 to 2010—a decline of more than 70% in yield compared to the previous 8 years (*2*). This suggests that the current approach to drug development is vulnerable to abrupt changes in market forces, as has occurred in other markets including news media, movies, music, and transportation.

What might be a less costly and more efficient path to develop drugs? An ideal approach would be to engage talent, from discovery through to approval, from the experts most relevant to a particular challenge, irrespective of their geographic location or professional setting. Such a modular means has worked well in the nonprofit sector (such as the Medicines for Malaria Venture and One World Health), where altruism, the provision of capital by governments, charities, companies, the opportunity to trade shares of IP, and so-called credit default swaps (a type of insurance policy where the

The Institute for Translational Medicine and Therapeutics, Perelman School of Medicine Translational Research Center, 10th Floor, 3400 Civic Center Boulevard, Philadelphia, PA 19104–5158, USA. E-mail garret@upenn.edu

issuer—in this case, the drug developer—pays out when it defaults)—have prompted the collapse of IP barriers, adherence to timelines, and hand-off of results to the next partner in the chain of production. This procedure has enabled the rapid introduction of new drugs against malaria, tuberculosis, and Chagas disease into clinical trials. If a variation of this model could be exported to for-profit drug development, it could enable the assembly a range of stakeholders drawn from different sectors and geographies.

To launch this kind of collaborative model, it is important to consider how IP issues must change. Today, interactions between academia and private industry are often constrained by unrealistic expectations and outmoded structures of IP governance. The dominant source of IP in drug discovery and development is the "composition of matter," despite the extremely long odds of that matter becoming an approved drug. This approach focuses on the earliest stages of the process (discovery) and therefore can limit the sharing of data, reagents, and knowledge during research and development. Creative attempts to deal with this barrier have focused on expanding the scientific commons—the precompetitive space that is "IP free" and variations such as use of crowdsourcing, to solve problems, and "open innovation networks" (a prominent example is Linux, a free and open source software development and distribution collaboration) in which technologies and discoveries are shared (*3*). This is starting to happen. Licensing deals around the edges of the process feature in partnerships between industry and academia, but more fundamental reform is needed to deal with the hold that stakeholders still exert on IP. Unlike the altruistic sector, luring disparate partners to collaborate in the for-profit arena requires more than just providing resources to do the science. In the era of large, vertically integrated companies, a focus on the composition of matter was logical; in the unlikely event that a molecule became a drug, all employees who had shares in the company (not just the chemists) stood to profit. Moving to a collaborative model, how should partners from different sectors and countries become incentivized to pool efforts with the common purpose of bringing a new drug to market?

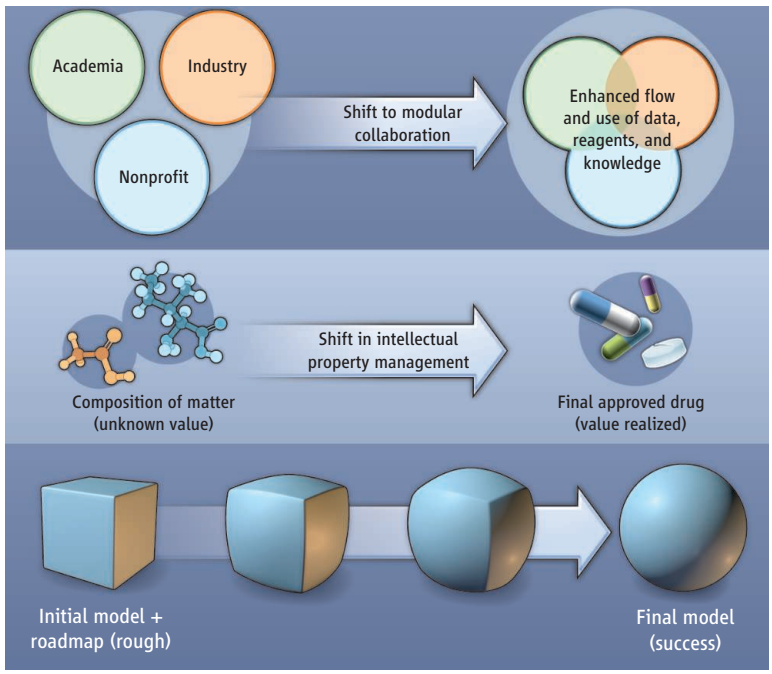


**Landscape change**. Open collaboration, refocusing intellectual property, and the use of modeling to generate roadmaps to success are needed to bring new drugs to market.

Perhaps we can learn from the success of another for-profit business—mobile devices such as smartphones and tablet computers. While developments in this field have been retarded in some cases by the patenting of concepts rather than composition of matter (*4*), its approach to product protection has lessons for drug development. Here, many components have attendant IP (such as voice recognition and touch screen), but the dominant IP is actually vested in the final product that people buy. If this process were applied to drug development, the dominant IP would shift from the initial composition of matter to the approved drug (see the figure). Given a particular challenge—say, to develop a vaccine for HIV or a better lipid-lowering drug—one could model prospectively the relative barriers to success during the development process and assign a percentage of the ultimate reward to each stage of development accordingly. In the example of an HIV vaccine, the major barrier might be seen at early stages of the process, and movement to the next stage may depend on further elucidation of the basic biology. In this case, more of the reward would be assigned prospectively to those who solve these problems. In the case of the lipid-lowering drug, a barrier might be predicted to arise later in the development process, such as defining populations in which the new drug worked well and safely so that the cost and design of a phase 3 clinical trial can be refined. Here, more of the reward would be assigned to clinical researchers. In both cases, the coalition of partners would move together through all stages of the development process and the model for distribution of reward could be iteratively refined in a Bayesian fashion (with prospective agreement of all the partners) and finalized upon drug approval.

If further studies of a new drug after its approval for clinical use are desirable, it could be directly incentivized by modeling the additional value realized if such studies were carried out. Additional value could be incrementally provided as insight into the populations that benefit is progressively refined. The application of modeling to drug discovery and development is not new. Systems biological approaches are increasingly applied in the selection of targets; pharmacokinetic and pharmacodynamic modeling is deployed in dose selection; and pharmacoeconomic modeling is used to estimate market size and potential.

The current approach to drug discovery and development is unsustainable. Radical solutions usually derive from the reality of crisis rather than the prospect of opportunity. Such a tipping point seems imminent in the drug industry. Current management of IP stifles and constrains interaction between industry and academia. Consideration of radical reform in this and other industries is timely (*5*). Here, it could remove this dead man's hand on the tiller and serve as a general framework to manage the transition to a modular, collaborative, and multisectoral approach to drug discovery and development.

**References**

1. G. A. FitzGerald, *Science* **320**, 1563 (2008).
2. J. Hewitt, J. D. Campbell, J. Cacciotti, www.oliverwyman.com/media/OW_EN_HLS_PUBL_2011_Beyond_the_Shadow_of_a_Drought(3).pdf (2012).
3. T. Bubela, G. A. FitzGerald, E. R. Gold, *Sci. Transl. Med.* **4**, 122cm3 (2012).
4. C. Digg, S. Lohr, "The patent used as a sword," *New York Times*, 7 October 2012; www.nytimes.com/2012/10/08/technology/patent-wars-among-tech-giants-can-stifle-competition.html.
5. "Does the law support inventors or investors?" *New York Times*, 10 October 2012; www.nytimes.com/roomfordebate/2012/10/10/does-the-law-support-inventors-or-investors.

10.1126/science.1231170

CREDIT: Y. HAMMOND/*SCIENCE*





Published by AAAS

IBI* SERIES WINNER

# Student-Directed Discovery of the Plant Microbiome and Its Products

Endophyte Discovery, an IBI Prize–winning module, allows novice scientists to engage in meaningful discovery through inquiry-based research experiences.

**Carol A. Bascom-Slack,[1] A. Elizabeth Arnold,[2] Scott A. Strobel[1]†**

Macroscopic organisms, even when healthy, harbor diverse microorganisms that influence their development, physiology, and fitness. This microbial diversity is accompanied by chemical diversity, which provides a platform for integrative research training spanning the biological and physical sciences. Our programs focus on the development of scientific inquiry skills through the lens of isolating microorganisms associated with plants and characterizing their bioactive natural products.

Endophytes are microbes, such as fungi and bacteria, that inhabit healthy plant tissue without causing disease (*1*). As symbionts, they constitute part of a diverse and ecologically important plant microbiome. Endophyte communities differ in composition among biomes and host species (*2*). They exhibit a wide range of host specificity and often enhance plant health (*2*, *3*). The total number of estimated fungal species is in the millions, yet fewer than 100,000 have been characterized (*4*).

Novel endophytes and their natural products can be isolated on standard microbiological media from the plants that surround our campuses and communities. This accessible biological and chemical diversity provides novice scientists with the raw materials for inquiry-based research experiences that engender project ownership, interdisciplinary training, and the excitement of meaningful discovery.

We have used endophyte discovery as the foundation for a one-semester course at Yale University (*5*); a 10-week summer program at Diné College, the tribal college of the Navajo Nation in rural northeastern Arizona; and a semester-long course at Tucson High Magnet School, an urban high school in Arizona that serves a highly diverse student body. Our collective experience points to the substantial difference between a demonstration laboratory, where experimental outcomes are known, and an inquiry-based opportunity where discovery, exploration, and long-term buy-in are hallmarks of the experience.

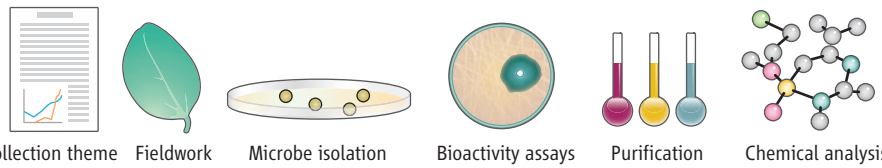


**Research objectives.** [Adapted from (*5*)]

Our programs synthesize lectures, fieldwork, and laboratory experiences. As students isolate and characterize endophytic microbes, evaluate their bioactivity, and examine their chemical diversity, they gain new technical skills that translate into broader research abilities. They develop the capacity to ask scientific questions, test hypotheses, synthesize information, and step beyond the limits of current knowledge. They traverse multiple success points that build progressively in intellectual and technical complexity, which allows them to gain confidence and take intellectual ownership from the earliest stages of their work. Our goal is for these novice scientists to leave behind a fear of "wrong" answers and move on to envision possibilities, exercise their own quality control, develop collaborations, and think critically. Success in our programs is not wholly defined by students' achievement of research goals (listed below), which can yield novel organisms, new compounds, and novel bioactivities—but by the intellectual development that characterizes the most important and often elusive aspects of scientific training.

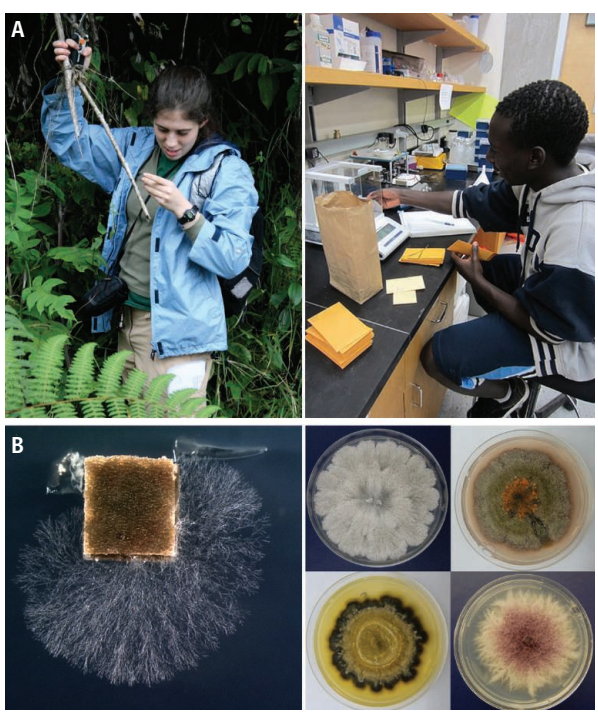


**Fieldwork.** (**A**) Students in the field and at the bench. (**B**) Endophytic fungus emerging from a tissue segment and four representative endophyte isolates.

Each of our programs is tailored to its specific target audience, but all are organized around six research objectives (see the first figure). Instructors are encouraged to tailor a course based on their area of expertise and the physical and personnel resources available at their home institution.

We use a parallel-project structure based on individualized but similar activities to simplify mentoring by the instructor and to facilitate peer mentoring among class members (*6*). Note that students need not complete all of the research objectives outlined below to gain a meaningful scientific experience: Adaptations of our courses at Diné College and Tucson High focus on objec-

[1]Department of Molecular Biophysics and Biochemistry, Yale University, New Haven, CT 06520, USA. [2]School of Plant Sciences, University of Arizona, Tucson, AZ 85721, USA.

*IBI, *Science* Prize for Inquiry-Based Instruction; www.sciencemag.org/site/feature/data/prizes/inquiry/

†Author for correspondence. E-mail: scott.strobel@yale.edu

PHOTO CREDIT: A. E. ARNOLD, S. A. STROBEL, R. CORBIN, AND J. RUSSELL





Published by AAAS

tives 1 to 4, for example, with students still gaining significantly in cognitive and technical skills through multidisciplinary, inquiry-based activities. The goals for our programs are as follows:

1. *Development of a plant collection theme.* Students first identify target plants to survey for endophytes. This preparation encourages them to consider diverse aspects of plant biology ranging from taxonomy to ethnobotany (Yale), or to frame ecological research questions with instructor support (Diné College and Tucson High). Allowing students to define and convey their collection themes provides a low-stakes opportunity to participate in empirical design.

2. *Fieldwork*. After a basic introduction to botany, students identify and collect plants for endophyte isolation [see the second figure (A)]. Our collection trips range from half-day excursions to botanical gardens, reserves, and state and national parks to multiweek expeditions to South American rainforests. Field experiences help students observe biology directly, appeal to students with diverse learning styles, and promote teamwork. We have found that fieldwork is transformative for students no matter what their future career choices might be.

3. *Endophyte isolation and characterization.* Endophytes are isolated by surface-sterilizing fresh plant tissue and plating small fragments on nutrient media [see the second figure (B)]. Students characterize the diverse microbes that emerge from the interior of symptomless tissue using traditional microbiology, microscopy, and molecular sequence analysis. They upload DNA sequence data to GenBank, thus contributing directly to the scientific knowledge base, and then use their data to construct phylogenetic trees that reveal the relations of newly discovered endophytes to known relatives. A hallmark of our programs is that individual student observations can be compiled to test larger research questions. We have published three research papers to date detailing novel observations resulting from the efforts of an entire class.

4. *Bioactivity assays.* Endophytes have a demonstrated, but underexplored, potential to make novel chemical products important for human sustainability (*7*). Students select and culture a subset of their endophytes on a larger scale for use in standard bioassays, testing culture filtrates and extracts for enzymatic activities relevant to industry, agriculture, and medicine (e.g., cellulase, ligninase, and protease activity or activity against human and plant pathogens). Each student also identifies an assay in conjunction with a collaborating faculty member and tests the library of extracts compiled by the entire class for activity. These diverse assays (e.g., anti-inflammatories, inhibition of β-amyloid oligomeric assembly, and effects on zebrafish development) allow students to exercise creative imagination and generate collaborations with peers and faculty. Positive results provide an impetus for further research projects beyond the course.

5. *Fractionation and purification.* Positive assays are followed by bioactivity-guided fractionation to isolate the active natural products with thin layer–, column-, and/or high-performance liquid chromatography.

6. *Chemical analysis.* Characterization of active natural products by analytical methods (e.g., mass spectroscopy, nuclear magnetic resonance analysis, and small-molecule x-ray crystallography) usually occurs after the course by alumni who continue their research projects. These analyses are technically challenging, but most students are remarkably motivated to provide a chemical explanation for their biological observations.

Assessment through the Classroom Undergraduate Research Experience survey (CURE) (*8*) indicates that alumni of the Yale program consistently self-report a readiness for more demanding research, greater self-confidence, and a better understanding of the research process. The vast majority (>80%) continue their research in subsequent semesters. Upon graduation, they matriculate into Ph.D. programs at a rate about three times that of other Yale graduates with a science degree. Diné College students highlight this experience in their applications to 4-year institutions and graduate school, and high school students use their experience as an entry point for science fairs, independent projects, and research after matriculating into college.

These discovery-based experiences centered on the biodiversity and chemical richness of endophytes have inspired a diversity of students with substantially different levels of scientific preparedness. Although execution of such an inquiry-based course requires a willingness to accept a level of uncertainty regarding research outcomes, with that uncertainty comes the potential for every student to make original and meaningful observations about the natural world.

## About the authors

Authors (left to right). **Carol Bascom-Slack** is a lecturer at Yale University and is a National Academy of Sciences Education Fellow. In addition to the course described here, she teaches a research-based biology course for freshmen and a microbiology course. **A. Elizabeth Arnold** (Betsy) is an Associate Professor in the School of Plant Sciences at The University of Arizona. Her research focuses on the diversity, ecology, evolution, systematics, and applications of endophytic fungi. **Scott A. Strobel** is the Henry Ford II Professor of Molecular Biophysics and Biochemistry at Yale and is a Howard Hughes Medical Institute Professor. His research explores application of endophytic fungi to production of alternative fuels and bioremediation.

### References and Notes


1. J. K. Stone, C. W. Bacon, J. F. J. White, in *Microbial Endophytes*, J. F. White, Ed. (Marcel Dekker, New York, NY, USA, 2000), pp. 3–29.
2. R. J. Rodriguez, J. F. J. White, Jr., A. E. Arnold, R. S. Redman, *New Phytol.* **182**, 314 (2009).
3. A. E. Arnold, *Fungal Biol. Rev.* **21**, 51 (2007).
4. D. L. Hawksworth, *Mycol. Res.* **105**, 1422 (2001).
5. S. A. Strobel, G. A. Strobel, *Nat. Chem. Biol.* **3**, 356 (2007).
6. D. I. Hanauer *et al.*, *Science* **314**, 1880 (2006).
7. G. Strobel, B. Daisy, *Microbiol. Mol. Biol. Rev.* **67**, 491 (2003).
8. D. Lopatto, *Cell Biol. Educ.* **3**, 270 (2004).



**Acknowledgments:** We thank K. Kucera, L. Boulanger, and the teaching fellows and students who have contributed to each program. S.A.S., C.A.B.-S., and colleagues are supported by a Professorship to S.A.S. from Howard Hughes Medical Institute and NSF grant 0853408. A.E.A. is supported by NSF (DEB-0702825, 1045766) and awards with colleagues B. Klein, M. Shimabukuro, and M. Wilch.


**Supplementary Materials**
www.sciencemag.org/cgi/content/full/338/6106/485/DC1

10.1126/science.1215227

PHOTO CREDIT: S. A. STROBEL, AND A. E. ARNOLD

IBI* SERIES WINNER

# A Mutant Search—*Caenorhabditis elegans* and Gene Discovery

Worm Mutants, an IBI Prize–winning module, offers Biology majors the opportunity to identify mutants and learn about genes that regulate biological functions.

**Candace C. LaRue and Pamela A. Padilla†**

With ~36,000 students enrolled, the University of North Texas is the fourth largest state university in Texas. To provide each of the >1800 undergraduate Biology majors the opportunity to participate in a discovery-based project, we developed "Worm Mutants," a worm mutant screen module for the required genetics laboratory, where students apply approaches used by geneticists to identify genes that regulate biological processes.

The genetics lab meets once a week for 4 hours; however, the worm mutant module requires additional time. Graduate student teaching assistants instruct the seven genetics lab sections offered each semester; each has a maximum of 24 students per lab section. Thus, as part of the required coursework for Biology majors, >300 students per year take part in the worm mutant screen project.

The module emphasizes scientific discovery while teaching the challenging concept of how mutant animals are used to identify genes that regulate biological processes [see Supplementary Materials (SM)]. Through an experimental approach, students learn the relations among gene, allele, and phenotype in wild-type and mutant organisms, by studying the nematode *Caenorhabditis elegans,* which is a well-researched model organism with considerable background information on its genetics and development. Students conduct a "forward" genetic screen, by starting with a predicted phenotype resulting from disruption of specific biological processes, and seek to identify, from a mutagenized population, a mutant with that phenotype. As a team of four, students devise a plan to identify a mutant worm with a phenotype potentially owing to a mutation in a gene involved with the biological process of interest to them. For example, students interested in how neurons regulate muscle movement look for a worm mutant that does not move normally.

**Lab team.** Undergraduate research team and graduate student teaching assistant working on a *C. elegans* project.

Recognizing the power of conducting a genetic screen to identify mechanisms for biological processes can be a challenge for undergraduate students, because they need to understand that model systems can be used to understand conserved genes, that analysis of a mutant with a specific phenotype can lead to a greater understanding of normal gene function, and that mutations in different genes involved with different cellular processes can result in a similar phenotype. For example, mutations affecting neurological function could also identify mutants that have muscle dysfunction or have motility issues for reasons not pertaining to neurological function. In addition to these conceptual challenges, student teams do not know if they will identify the mutant of interest and, therefore, there are no "right" answers to the lesson (see the first figure). Instead, the worm mutant screen challenges students to think about observable mutant phenotypes and biological processes.

The worm mutant screen is modeled after the pioneering work by the "Father of *C. elegans* genetics," Sydney Brenner, who demonstrated that induced mutations in *C. elegans* could be used to gain a molecular understanding of animal development (*1*). His work, along with that of John Sulston and Robert Horvitz, led to the elucidation of genetic pathways that regulate complex processes, such as organ development and function. Students are introduced to *C. elegans,* affectionately referred to as worms, by examining their anatomy, life cycle, and husbandry methods. Students also become familiar with the *C. elegans* genetic database, WormBase; relevant scientific papers; and *C. elegans* nomenclature. In a prior lab lesson, students are familiarized with wild-type and common mutant phenotypes (table S1) (*2*, *3*).

Students discuss the range of biological processes that intrigue them and which processes can be studied using *C. elegans* as a

Department of Biological Sciences, University of North Texas, Denton TX 76203, USA.

*IBI, *Science* Prize for Inquiry-Based Instruction; www.sciencemag.org/site/feature/data/prizes/inquiry/.

†Author for correspondence. E-mail: pamela.padilla@unt.edu

PHOTO CREDIT: JONATHAN REYNOLDS





Published by AAAS

model. Discussion points include known worm phenotypes (e.g., uncoordinated, sterility, egg-laying defects, and high incidence of males) and a predicted phenotype of interest to them (*4*). Students screen for a range of phenotypes: from the common (e.g., uncoordinated and dumpy) to the more challenging to isolate (abnormal pharynx pumping and sterility) to the unattainable owing to limited resources (e.g., altered responses to a particular molecule).

Students are encouraged to think critically and creatively as they develop a hypothesis and lay out an experimental plan. Students are required to read peer-reviewed publications (*1*, *4*) relevant to their topic of interest and to incorporate the information into their research proposal, which will be presented with their findings to the class.

Students are provided animals ($P_0$ generation) in which the germ line was mutagenized with the chemical EMS (see the second figure and SM). The mutagenized animals are grown for two generations to obtain offspring ($F_2$ generation) to visually screen, using stereomicroscopes, for a phenotype of interest (*4*). If the mutant is not identified, students are then encouraged to think about why the phenotype was not observed within their mutagenized population and to describe the mutants observed during the screening process. After students isolate a mutant animal, they observe the $F_3$ generation and determine whether the mode of inheritance is recessive or dominant. If the mode of inheritance is more complex, they describe their observations regarding inheritance pattern. Although isolation of a genetic mutant provides a path to many levels of further investigation, student experiments are limited to a general phenotype analysis because of resource constraints. To date, our undergraduate students have isolated many mutants with various phenotypes (see the second figure).

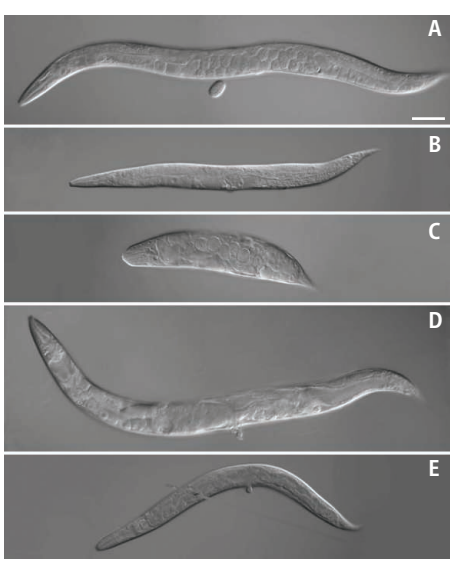


***C. elegans* mutants with observable phenotypes.** These were isolated by undergraduate students. (**A**) Wild-type; (**B**) small mutant (adults are small); (**C**) Dumpy mutant (adult animals are short and thick); (**D**) egg laying–defective mutant (adult animals rarely lay eggs, so embryos mature and hatch inside the hermaphrodite); (**E**) protruding vulva mutant. Scale bar, 50 μm.

Aside from the isolation of *C. elegans* mutants, student-learning experiences include teamwork, time management, recording of results, problem-solving, data collection, and scientific communication. Furthermore, students have shown innovation and creativity by using smart phones and video to capture images of lab tools, techniques, and experimental animals; have gained a sense of independence and ownership of discovery ("my mutant" is often heard); and have achieved experimental accomplishments not often observed with "cookbook" laboratory lessons. To demonstrate their communication skills, students' research proposals describe background, hypotheses, methods, preliminary data collection (their mutant identified), data interpretations, and future work proposed. We opted to have students write a research proposal, instead of a report, so that they understand the importance of preliminary data and gain practice proposing future experiments. The final research proposals reveal an understanding of the concept of a genetic screen and the nature of scientific inquiry. Team PowerPoint presentations describe their experimental approach, phenotype they screened for, results, and potential significance. Students are assessed on participation, proposal content, and team presentation (see SM).

Formal assessments of the student's ability to answer questions regarding genetic screens indicate a statistically significant increase in understanding key genetic concepts. We have found that this worm mutant screen is sustainable even with the challenge of implementation into a high-enrollment course with fixed and shared resources (e.g., stereomicroscopes and worm picks). Given the success of this module we intend to collect, freeze, and store some mutant strains isolated by the students so that we can expand the inquiry-based lesson to analyze the mutants. In conclusion, we found that the majority of students were more enthusiastic about this module, in comparison with past traditional lessons; that for some students it sparked an interest in joining a research lab; and that students became more aware of scientific research and the skill sets necessary for scientists, including communication, teamwork, and the development of scientific ideas.

## About the authors

**Pamela A. Padilla,** Ph.D., an Associate Professor in the Department of Biological Sciences at the University of North Texas, studies the genetic and environmental factors that influence oxygen deprivation response and survival in developing, adult, and aging animals using the *C. elegans* genetic model system. Aside from her research, she teaches genetics at the undergraduate and graduate level. Notably, she was awarded an NSF CAREER grant, which has a teaching component, to develop inquiry-based lessons for the genetics undergraduate laboratory course. **Candace C. LaRue** is a Ph.D. candidate in Padilla's lab at the University of North Texas. She has a Master of Science degree in Biology as well as a Life Science teaching certification. Evaluating how changes in teaching methods can improve student understanding of conceptually difficult concepts is central to her research. In addition, she is interested in assessing programs that include students of various levels into primary research.

**References and Notes**

1. S. Brenner, *Genetics* **77**, 71 (1974).
2. L. R. Girard *et al.*, *Nucleic Acids Res.* **35** (Database issue), D472 (2007).
3. K. Yook *et al.*, *Nucleic Acids Res.* **40** (Database issue), D735 (2012).
4. E. M. Jorgensen, S. E. Mango, *Nat. Rev. Genet.* **3**, 356 (2002).

**Acknowledgments:** This work has been supported in part by an NSF CAREER grant to P.A.P. We thank L. Finn for graphic art assistance for fig. S2. We thank the Department of Biological Sciences, Genetics teaching assistants, and the Lab Coordinator for support of this project and A. Colon-Carmona for comments.

**Supplementary Materials**
www.sciencemag.org/cgi/content/full/338/6106/487/DC1

10.1126/science.1215229

SCIENCE DIPLOMACY

# Fifty Years after Cuba Crisis, New Roles for S&T in Arms Control

**ATLANTA, GEORGIA—**Pierce Corden remembers well a mild night in late October 1962: President John F. Kennedy was addressing the nation, describing the placement of Soviet nuclear weapons in Cuba, just 90 miles from Florida, and warning of the potential for war. In the following days, a hush descended over the Georgetown University campus where Corden was a student. The fate of humanity seemed to hang in the balance.

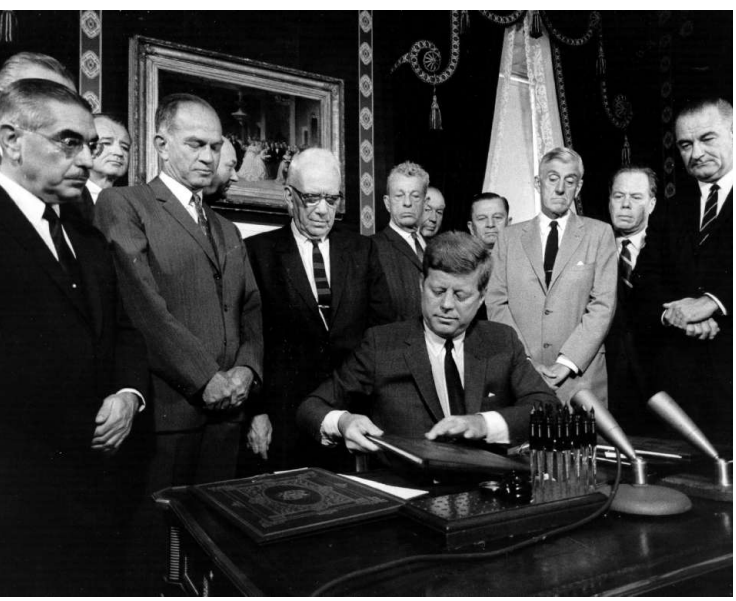

CREDIT: KEYSTONE/GETTY IMAGES

**Crisis and hope.** Almost a year after the Cuban missile crisis, in October 1963, U.S. President John F. Kennedy signed the Limited Test Ban Treaty with the Soviet Union and the United Kingdom. Other treaties and agreements followed in later years.

Fifty years after the Cuban missile crisis, retrospectives typically focus on how nuclear war was averted. But at a workshop cosponsored by AAAS, experts said the crisis also was an inflection point, leading to agreements to limit nuclear testing and curb proliferation and driving a cohort of scientists and engineers into the fields of arms control and science diplomacy.

While the Cold War has receded, arms control remains a global priority, driven by fears of terrorism, nuclear programs in Iran and North Korea, and creeping tensions between the United States and Russia. Technological advances and science diplomacy will be crucial to a new generation of nuclear security, said experts gathered at the Georgia Institute of Technology.

"In terms of U.S. diplomacy, some of the greatest assets we have are not only in our government agencies, but in our foundations, science associations, and other areas," said E. William Colglazier, science and technology adviser to Secretary of State Hillary Clinton. "We're going to have to use all of our assets if we're going to create a more peaceful world."

The workshop, held 3 to 4 October, attracted two dozen nuclear arms and security experts from government and diplomacy, industry, academia, and nongovernmental organizations for off-the-record discussions, followed by a presentation for about 150 Georgia Tech students and faculty members. The events were organized by the Center for International Strategy, Technology and Policy at Georgia Tech's Sam Nunn School of International Affairs and the AAAS Center for Science Diplomacy.

Corden, a physicist, has worked with U.S. and international arms control agencies for four decades; he's currently a visiting scholar at the AAAS Center for Science, Technology and Security Policy. He detailed how the crisis propelled the United States and the Soviet Union into a limited ban on nuclear testing and then to a series of arms control agreements in ensuing years.

Today, however, the nature of nuclear threats is far different than 50 years ago, said Adam N. Stulberg, codirector of the center at Georgia Tech. There are more nuclear players with "different idiosyncracies," Stulberg said. Nations or organizations that might have crude arsenals or "that don't subscribe to the established rules and norms" present different challenges to arms control verification, monitoring, and diplomacy.

In all, 183 nations have signed the Comprehensive Nuclear-Test-Ban Treaty, which seeks to prohibit all nuclear explosions, and 157 have ratified it. Ambassador Tibor Tóth, executive secretary of the Preparatory Commission for the Comprehensive Nuclear-Test-Ban Treaty Organization, said that with the exception of two nuclear tests by North Korea since 2006, the world has effectively frozen testing.

But, Tóth said, "we must put the genie of nuclear weapons tests back in the bottle, and we must seal the bottle." Without that, the world risks a new era of proliferation and testing. The risk is especially high in an arc from the Middle East through South Asia to East Asia, he added, where a number of key nations have not signed or ratified the treaty.

Critical to the success of the treaty is an ever-growing array of advanced monitoring stations and sensors—337 facilities in 89 nations when complete—that provides nuclear test detection capabilities by reading even faint atmospheric, seismic, or acoustic signals.

Experts at the workshop suggested scientific evaluation of vast amounts of data from a wide range of sources will be a means of detecting clandestine nuclear weapons activity. One of the most intriguing ideas is to sift through masses of social media data for subtle patterns or indicators.

Indeed, data-sharing between nations could be an important focus for science diplomacy, said Vaughan C. Turekian, director of the AAAS Center for Science Diplomacy and editor of its quarterly online publication *Science & Diplomacy*.

For example, he suggested, Cuba and the United States could negotiate agreements to share data on climate and fish migration. Cooperation on such projects could, in time, build trust on security issues.

"The distance that almost caused nuclear catastrophe is also a distance where we share so many resources and interests," Turekian said. "That's where this whole issue of science and diplomacy, and how it can help lead to peace and prosperity, is really important."





Published by AAAS

EDUCATION

# "Active Explorer" Project Turns Smart Phones into Classroom Research Tools

It's a common concern among parents and teachers: Smart phones in the classroom are bound to be a distraction. But a new project, developed by AAAS, turns the increasingly common technology into a powerful tool for hands-on science learning.

Students use the phones to collect data—anything from GPS coordinates for invasive plants in their neighborhoods to videos of a classroom experiment—to complete science "quests" developed by their teachers. They upload the information to a Web site where they can combine and share their discoveries as a slideshow, a comic book, or other creative presentations.

The "Active Explorer" project, launched in four Washington, D.C., schools this month, was designed to help students to become more active learners and collaborators, said Bob Hirshon, AAAS program director for technology and learning. He developed Active Explorer's Web and mobile platforms as part of a project supported by a grant from the Wireless Reach Initiative of the global communications company Qualcomm; kajeet, an educational smart phone company, will provide wireless service for the project.

Although the program is aimed at fourth- through seventh-grade science students, Hirshon said its open design could be used to create quests in the arts and social studies as well. No matter what the topic, he said, students who work on the quests "are building knowledge independently, rather than acquiring it solely from a book or exercise."

Eight teachers and 120 students at Friendship Blow Pierce Junior Academy, John Burroughs Elementary School, Sacred Heart Bilingual Catholic School, and The Washington Middle School for Girls are taking some of the first Active Explorer quests. One classroom is using it to document the results of an experiment that compares how candles made from different materials burn. Another class will collect information on plant and animal species in the school garden. For the students, Hirshon said, "it's a way of personalizing something that's really big, and taking something that is hard to wrap your head around and bringing it into your real life."

After evaluating the program in the four D.C. schools, Hirshon plans to add new features such as Spanish-language versions of the Web site and the mobile Android app, along with new ways to collect data within a quest.

*–Becky Ham*

CREDIT: BOB HIRSHON

## AAAS Council Reminder

The next meeting of the AAAS Council will take place during the AAAS Annual Meeting and will begin at 9:00 a.m. on 17 February 2013 in the Constitution Ballroom of the Sheraton Boston Hotel, 39 Dalton Street, Boston, Massachusetts.

Individuals or organizations wishing to present proposals or resolutions for possible consideration by the council should submit them in written form to AAAS Chief Executive Officer Alan I. Leshner by 26 November 2012. This will allow time for them to be considered by the Committee on Council Affairs at its winter meeting.

Items should be consistent with AAAS's objectives and be appropriate for consideration by the council. Resolutions should be in the traditional format, beginning with "Whereas" statements and ending with "Therefore be it resolved."

Late proposals or resolutions delivered to the AAAS Chief Executive Officer in advance of the February 2013 open hearing of the Committee on Council Affairs will be considered, provided that they deal with urgent matters and are accompanied by a written explanation of why they were not submitted by the November deadline. The Committee on Council Affairs will hold its open hearing at 2:30 p.m. on 16 February 2013 in the Republic Ballroom of the Sheraton Boston Hotel. A copy of the full council agenda will be available for inspection in the AAAS headquarters office in the Hynes Convention Center in Boston.

ELECTIONS

## Additional Candidates for AAAS Annual Election

The following candidates have been added to the ballot for the 2012 election of AAAS officers. Members registered in more than one section will receive ballots for elections for each section they are enrolled in. The 2012 AAAS election of general and section officers will be held later this fall. For a list of other candidates, please see AAAS News & Notes in the 31 August 2012 issue of *Science.*

### GENERAL ELECTION

*President:* Gerald R. Fink, Whitehead Institute/MIT; S. James Gates Jr., Univ. of Maryland, College Park

*Board of Directors:* Claire M. Fraser, Univ. of Maryland School of Medicine; Roberto Kolter, Harvard Medical School; Elizabeth F. Loftus, Univ. of California, Irvine; J. William (Bill) Schopf, Univ. of California, Los Angeles

*Committee on Nominations:* Bruce E. Bursten, Univ. of Tennessee, Knoxville; Judy R. Franz, American Physical Society; Barbara J. Grosz, Harvard Univ.; Thomas H. Jordan, Univ. of Southern California; Peter S. Kim, Merck Research Laboratories; Harvey F. Lodish, Whitehead Institute; Mario J. Molina, Univ. of California, San Diego; Richard H. Scheller, Genentech

### SECTION ELECTIONS

**Medical Sciences**

*Chair Elect:* Karen H. Antman, Boston Univ. School of Medicine; Janet S. Butel, Baylor College of Medicine

*Member-at-Large of the Section Committee:* Scott D. Emr, Cornell Univ.; Nancy L. Haigwood, Oregon Health and Science Univ.

*Electorate Nominating Committee:* Ruma Banerjee, Univ. of Michigan; Jeffrey I. Cohen, National Institute of Allergy and Infectious Diseases/NIH; Richard Kitsis, Albert Einstein College of Medicine; Joseph Loscalzo, Harvard Medical School





Published by AAAS

# Glial Progenitor Cell–Based Treatment and Modeling of Neurological Disease

Steven A. Goldman,* Maiken Nedergaard, Martha S. Windrem

The diseases of myelin are among the most prevalent and disabling conditions in neurology. These diseases include both the vascular and inflammatory demyelinating disorders of adulthood, as well as the childhood leukodystrophies and cerebral palsy. These fundamentally glial disorders may be amenable to treatment by glial progenitor cells (GPCs), which give rise to astroglia and myelin-producing oligodendrocytes. Given the development of new methods for generating and isolating human GPCs, the myelin disorders may now be compelling targets for cell-based therapy. In addition, the efficient engraftment and expansion of human GPCs in murine hosts has led to the development of human glial chimeric mouse brains, which provides new opportunities for studying the species-specific roles of human glia in cognition, as well as in disease pathogenesis.

Oligodendrocytes are the sole source of myelin in the adult central nervous system (CNS), and their loss or dysfunction is at the heart of a wide variety of child and adult diseases. In children, the hereditary leukodystrophies accompany cerebral palsy as major sources of neurological morbidity. In adults, oligodendrocytic loss and demyelination contribute to diseases as diverse as multiple sclerosis (MS), white matter stroke, and spinal cord injury (*1*). In addition, demyelination is also noted in degenerative disorders as varied as normal aging and Alzheimer's disease, and oligodendrocytic pathology has been associated with disorders as diverse as amyotrophic lateral sclerosis (*2*) and schizophrenia (*3*). As a result, the demyelinating diseases are especially attractive targets for cell-based therapeutic strategies. Several recent studies have supported the readiness with which axons can remyelinate after either congenital or acquired demyelination, if provided with myelinogenic cells (*4*, *5*). Glial progenitor cells (GPCs)—also referred to as either oligodendrocyte progenitor cells or NG2 cells (*6*)—have thus become promising reagents by which to restore myelin to demyelinated regions of the diseased or injured CNS.

## GPCs in Vivo

Glial progenitor cells arise from neural stem cells of the ventricular subependyma and disperse widely throughout the CNS, pervading both gray and white matter (*7*). In vivo, GPCs can generate both major macroglial phenotypes, astrocytes and oligodendrocytes, in a context-dependent fashion. Human glial progenitors comprise roughly 3% of all cells in the adult forebrain and may be isolated by surface antigen–targeted sorting techniques (*7*, *8*); by this means, their gene expression patterns, dominant signaling pathways, and homeostatic self-renewal mechanisms have all been studied in detail (*9*, *10*). In addition, both fetal and adult human GPCs have been found to efficiently generate myelinogenic oligodendrocytes upon transplantation (*11*). In practice, the relatively limited mitotic competence of adult GPCs and the scarcity of appropriate tissue samples limit the availability of adult GPCs for therapeutic purposes. Rather, fetal brain tissue, embryonic stem cells (ESCs), and induced pluripotential stem cells (iPSCs) encompass the more feasible sources of transplantable human GPCs (Fig. 1).

## Optimizing Cellular Agents for Treating Myelin Disorders

Disorders of myelin require extensive tissue repair and, in the case of the pediatric leukodystrophies, even whole neuraxis myelination. Although endogenous glial progenitors can remyelinate demyelinated lesions to some degree, the mitotic exhaustion and functional depletion of endogenous glial progenitors that may occur in acquired demyelination ultimately limits the extent and usefulness of spontaneous remyelination (*12*), thus necessitating the introduction of exogenous glial progenitors as therapeutic vectors. Yet to be safe and effective as therapeutic vectors, transplantable GPCs must be reliably deliverable in both purity and quantity (*1*). The surface antigen–based purification of human GPCs, on the basis of their selective expression of gangliosides recognized by monoclonal antibody A2B5, first allowed the isolation of these cells and their assessment in animal models of congenital hypomyelination (*5*, *13*). These studies revealed that fetal GPCs efficiently myelinated both the brain and the spinal cord, emigrated more widely and engrafted more efficiently than did adult cells, and exhibited context-dependent differentiation as astrocytes or oligodendrocytes, suggesting their usefulness in a broad array of myelin disorders (Fig. 2, A to C).

Yet despite the attractiveness of fetal GPCs as potential therapeutic vectors, they remain finite in both initial number and expansion competence, necessitating their periodic reacquisition from new donor tissues. As a result, recent efforts have focused on the production of myelinogenic GPCs from human ESCs (hESCs) and iPSCs. After the first report of myelination in the injured spinal cord by mouse ESCs (*14*), oligodendrocytes derived from hESCs were similarly directed to generate myelin in vivo (*15*, *16*). But although the findings were ground-breaking, these studies did not isolate GPCs or oligodendrocytes before transplant, nor did they follow animals over the time frames required to ensure the stability of the engrafted cells. This is cause for concern because any incidentally transplanted hESCs may retain the potential for undifferentiated expansion after implantation (*17*). Given this concern for tumorigenesis, stringent purification of lineage-restricted GPCs may be needed to ensure their safe use. Still, this point remains controversial. In 2009, the U.S. Food and Drug Administration approved a phase 1 safety trial evaluating the use of hESC-derived GPCs in spinal cord injury without such purification (*18*); although the trial was halted in 2011, its sponsor reported that its cessation was not related to safety. As a result, the need for pretransplant isolation of terminally differentiated phenotypes remains unsettled.

Human ESC-based therapy suffers also from the possibility of allograft rejection and, hence, the need for immunosuppression in graft recipients. Enthusiasm has thus developed for the use of autologous grafts of myelinogenic GPCs derived from human induced pluripotential cells (hiPSCs), potentially—though not assuredly (*19*)—obviating the need for immune suppression. These cells are generated by the reprogramming of somatic cells to a pluripotent ground state by the forced expression of a set of transcription factors that instruct stem cell phenotype (*20*). iPSCs were first generated from mouse (*21*) and human (*22*) fibroblasts and have since been differentiated into a variety of phenotypes, including neurons (*23*), astrocytes (*24*), and oligodendrocytes (*25*). Methods established for generating GPCs from hESCs have proven effective with hiPSCs as well and yield GPCs that are highly myelinogenic in vivo (*26*). This capability allows us to reasonably anticipate the use of iPSC-derived oligodendrocytes for autologous treatment, especially for nongenetic vascular, traumatic, and inflammatory demyelinations.


Center for Translational Neuromedicine, University of Rochester Medical Center, Rochester, NY 14642, USA.

*To whom correspondence should be addressed. E-mail: steven_goldman@urmc.rochester.edu

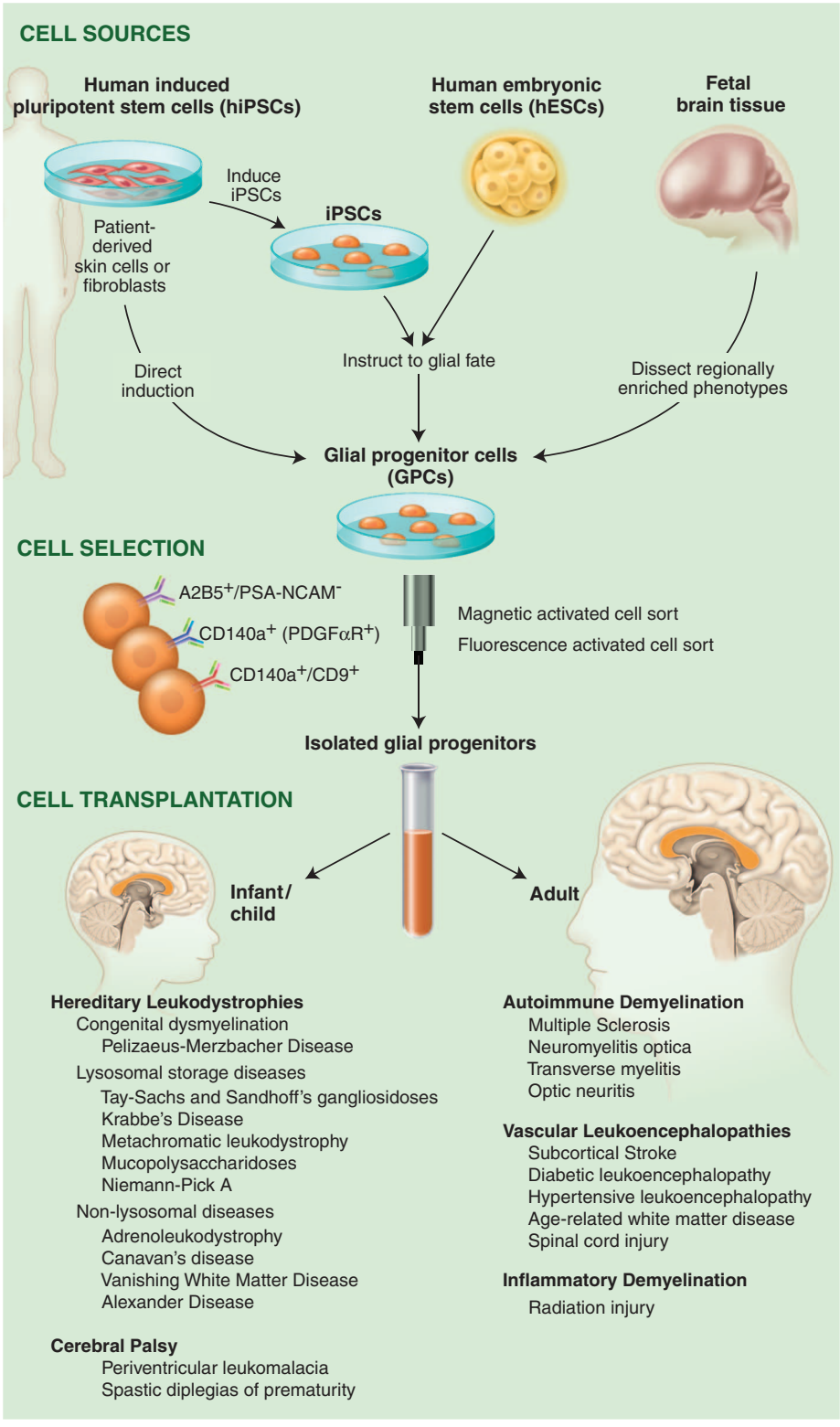


**Fig. 1.** Glial progenitor cell sources, phenotypes and clinical targets. GPCs may be directly sorted from tissue or generated from either hESCs or hiPSCs and then immunoselected based on their expression of either the A2B5 epitope or CD140a/PDGFαR. The CD140a phenotype includes all potential oligodendrocytes, whereas the tetraspanin CD9 identifies a pro-oligodendrocytic fraction (*10*). The choice of tissue-, hESC-, or iPSC-derived GPCs depends on whether allogeneic or autologous grafts are desired. Whereas autologous grafts of iPSC-derived GPCs might obviate the need for immunosuppression, their generation may take months, and their use in the hereditary leukodystrophies would first require correction of the underlying genetic disorder in the donor cell pool. At present, such genetic disorders of myelin may be better approached with allografted tissue- or hESC-derived GPCs.

Importantly though, iPSC-derived GPCs share many of the risks of those derived from hESCs, including aberrant differentiation and tumorigenesis (*27*). In addition, iPSCs retain epigenetic marks of the cells from which they derive (*28*), so that their cell type of origin may influence their differentiation competence (*29*). Indeed, iPSCs may differ from one another in their lineage competence, even when sourced from the same individual and tissue, making their standardization difficult. Recent studies have reported the direct induction of neurons from fibroblasts (*30*), and one may anticipate the development of analogous strategies of direct induction of glial progenitors and oligodendrocytes as well. By thereby avoiding the need for pluripotential intermediates, such direct induction of GPCs may accelerate the production of transplantable cells while mitigating their risk of tumorigenesis.

### Pediatric Disease Targets of GPC-Based Therapy

Tens of thousands of children in the U.S. suffer from diseases of myelin loss, including metabolic demyelinations, such as adrenoleukodystrophy; lysosomal storage disorders, such as metachromatic leukodystrophy, the neuronal ceroid lipofuscinoses, gangliosidoses, and Niemann-Pick and Krabbe's diseases; hypomyelinating diseases, such as Pelizaeus-Merzbacher disease; myelinoclastic disorders, including vanishing white matter disease, Alexander's disease, and Canavan's disease (*31*); and, most commonly, periventricular leukomalacia and cerebral palsy (*32*). Their mechanistic heterogeneity notwithstanding, all of these conditions include the prominent loss of oligodendrocytes and myelin, highlighting their attractiveness as potential targets for cell replacement (see Fig. 1, bottom).

In some metabolic disorders of myelin, such as Krabbe's disease, oligodendrocytes are essentially bystanders, killed by toxic metabolites generated by cells deficient in one or more critical enzymes (*31*). In others, such as Alexander's disease and vanishing white matter disease, myelin loss may be caused by astroglial pathology (*33*, *34*). Because glial progenitor engraftment is both widespread and associated with astrocytic and oligodendrocytic production, GPCs would seem an especially promising vehicle for dispersing astrocytes and oligodendrocytes throughout otherwise diseased and/or enzyme-deficient brain parenchyma. The lysosomal storage disorders present especially attractive targets in this regard, because wild-type (WT) lysosomal enzymes may be released by donor cells and taken up by deficient host cells through the mannose-6-phosphate receptor pathway. A relatively small number of donor glia may then provide sufficient enzymatic activity to correct the underlying catalytic deficit and storage disorder of a much larger number of host cells (*35*).

The cell-based rescue of enzymatically deficient host cells by WT donor neural stem cells (NSCs) was first noted in a mouse model of

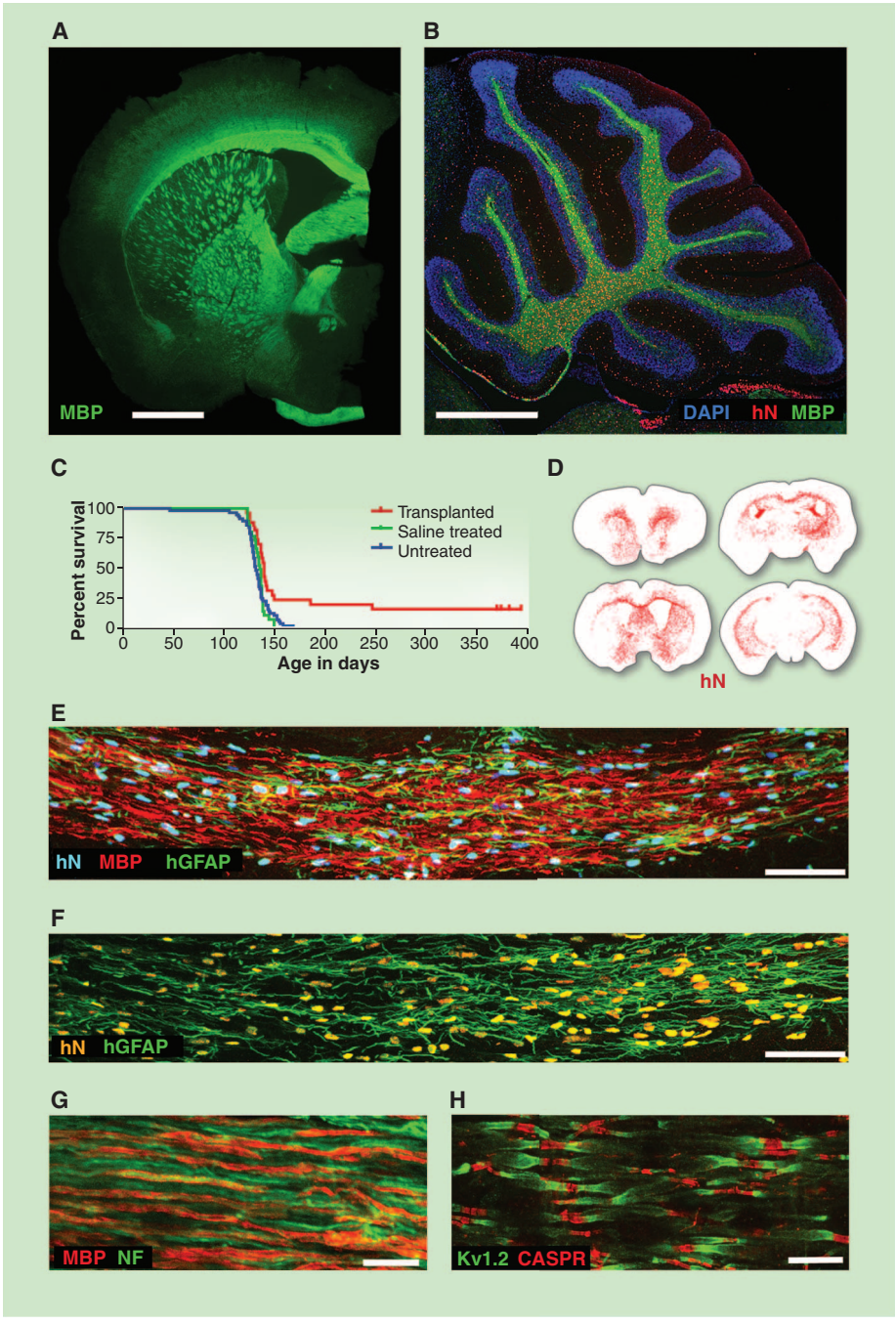


**Fig. 2.** Glial progenitor cell graft-mediated myelination of a dysmyelinated host. (**A**) A 13-month-old shiverer (*shi/shi*) × rag2$^{-/-}$ mouse, neonatally xenografted with A2B5$^{+}$/PSA-NCAM$^{-}$ hGPCs. MBP, myelin basic protein (shown in green). Shiverer mice do not express MBP; all immunolabeled myelin is of donor origin. (**B**) Sagittal view through the cerebellum. All cells were stained with 4′,6-diamidino-2-phenylindole (blue); donor cells were identified by human nuclear antigen (hN, red) and MBP (green). (**C**) Kaplan-Meier plot comparing survival of neonatally engrafted shiverer × rag2$^{-/-}$ mice to untreated and saline-injected controls. (**D**) CD140a-selected GPCs transplanted into neonatal shiverer × rag2$^{-/-}$ mice expanded and migrated extensively, rendering the brains chimeric. Red dots indicate individual human cells (hN); sacrificed at 3 months. (**E** and **F**) Coronal sections of a neonatally engrafted shiverer brain at 3 months, revealing donor-derived myelination (MBP, red) and astrocytic infiltration [human glial fibrillary acidic protein (GFAP), green] of the corpus callosum. (**G**) Myelin (MBP, red) produced by CD140a-selected hGPCs ensheathes mouse neurofilament-positive axons (NF, green), at 3 months. (**H**) Reconstituted nodes of Ranvier in the cervical spinal cord of a transplanted and rescued 1-year-old shiverer × rag2$^{-/-}$ mouse, showing paranodal Caspr protein and juxtaparanodal voltage-gated potassium channel protein Kv1.2, symmetrically flanking each axonal node. Untransplanted shiverer brains do not have organized nodes of Ranvier and, hence, cannot support saltatory conduction by central axons (Caspr, red; Kv1.2, green). Scale bars: (A) and (B), 1 mm; (E), 50 μm; (F) and (G), 10 μm; (H), 5 μm. (A) and (B), from (*54*); (C) and (H), from (*5*); (D) to (G), from (*10*).

mucopolysaccharidosis type VII, in which neonatally implanted cells restored lost enzymatic function to the recipient forebrain (*36*). Human NSCs also achieved substantial enzyme replacement in the β-hexosaminidase–deficient mouse with Sandhoff disease, with corresponding functional benefits (*37*). In the same vein, NSCs engineered to overexpress sphingomyelinase, engrafted into sphingomyelinase-deficient Niemann-Pick type A mice, yielded substantial reductions in misaccumulated sphingomyelin (*38*). Similarly, when NSCs were engrafted into a mouse model of neuronal ceroid lipofuscinosis (NCL), the cells dispersed broadly and ameliorated the lipofuscin misaccumulation of these animals (*39*). On that basis, a clinical trial to assess the use of human NSC allografts in treating infantile and late infantile NCL was undertaken (*40*). This phase 1 safety trial did not address therapeutic end points, but its initiation speaks to the efforts that may be anticipated in developing NSCs and GPCs as vehicles for intracerebral enzyme replacement in the metabolic leukodystrophies.

The intracerebral delivery of GPCs would seem an especially promising approach for treating those enzyme-deficiencies associated with early demyelination, which may require both enzyme replacement and structural remyelination. Metachromatic leukodystrophy (MLD), for example, is characterized by deficient expression of arylsulfatase A, which results in sulfatide misaccumulation and oligodendrocyte loss. Experimental models of MLD have responded well to GPC grafts, with broad dispersal and integration, as well as enzymatic rescue and sulfatide clearance (*41*). Krabbe's disease, characterized by galactocerebrosidase deficiency and early demyelination, is another storage disorder that may prove amenable to concurrent GPC-based enzymatic repletion and myelin restoration. When children with Krabbe's disease were transplanted with umbilical cord stem cells, they manifested slower disease progression, but the benefits of transplantation to children engrafted after symptom onset seemed minimal (*42*). Yet the intracerebral infiltration of umbilical cord stromal derivatives is modest, suggesting that treatment of these children with GPCs, which are able to achieve broad parenchymal dispersal as well as structural remyelination, might involve a more promising treatment strategy.

The experimental assessment of GPCs as vectors for remyelination has proceeded most aggressively in animal models of congenital hypomyelination. In an early study of cell-based myelin repair, mouse neural stem cells were transplanted into newborn shiverer mice, a hypomyelinated mutant deficient in myelin basic protein, and yielded context-dependent myelination (*43*). On that basis, we transplanted sorted human GPCs into neonatal shiverers, so as to assess the relative myelinogenic potential of GPCs (*13*). When delivered as highly enriched isolates, fetal human GPCs spread widely throughout the brain (Fig. 2, A, B, and D), developing as

astrocytes and oligodendrocytes in a context-dependent fashion. The donor-derived oligodendrocytes generated ultrastructurally mature myelin that effectively ensheathed host shiverer axons and formed nodes of Ranvier (Fig. 2H), which allowed the restoration of normal transcallosal conduction velocities in the transplanted mice (*5*, *13*). By using a five-site injection protocol to achieve broader dispersal of GPCs, we next established cell engraftment throughout the entire neuraxis, with myelination of the spinal cord and roots, as well as the entire brain, brainstem, cerebellum, and cranial nerve roots (*5*). This was associated with substantially prolonged survivals in transplanted mice, with phenotypic recovery and frank rescue of a large minority (Fig. 2C). These data strongly suggested the feasibility of neonatal GPC implantation in treating childhood disorders of myelin formation and maintenance. Later studies refined the criteria for selecting myelinogenic progenitors by identifying the platelet-derived growth factor α receptor (PDGFαR) epitope CD140a as recognizing the entire population of oligodendrocyte-competent progenitors (*10*). CD140a-sorted GPCs proved superior to those selected on the basis of A2B5 in both their efficiency and extent of myelination and were also highly migratory; thus, CD140a-sorted GPCs have supplanted the latter as a preferred cellular vector for therapeutic remyelination (Fig. 2, D to G).

Hence, the intracerebral delivery of GPCs may prove a viable approach to the treatment of a wide variety of enzymatic and storage disorders. In practice though, individual treatment regimens will need to be tailored to specific disease phenotypes and stages. Little data are available as to the numbers or proportion of WT cells required to achieve correction of enzymatic activity and substrate clearance in any storage disorder, and these values may need to be empirically derived for every disease target. Similarly, the extent of myelination required for effective treatment remains unclear, as do the extent and duration of immunosuppression required for allograft acceptance; these parameters may also vary with disease phenotype. These caveats notwithstanding, neural stem cell implantation is already under assessment as a means of myelin replacement in Pelizaeus-Merzbacher disease (*44*), and we anticipate that future efforts will similarly assess the efficacy of GPC grafts in this and related disorders.

### Adult Disease Targets of GPC-Based Treatment

In adults, oligodendrocytic loss contributes to diseases as diverse as hypertensive and diabetic white matter loss, traumatic spinal cord and brain injury, and MS and its variants. In addition, oligodendrocytic loss is prominent in the degenerative dementia associated with age-related white matter loss. All of these are potential targets of GPC replacement therapy, though the adult disease environment may limit this approach in ways not encountered in pediatric disease targets. For instance, the chronically ischemic brain tissue of diabetics with small vessel disease may require aggressive treatment of the underlying vascular insufficiency before any cell-replacement strategy may be considered. Similarly, the inflammatory disease environments of MS and many of the leukodystrophies present their own challenges, which need to be overcome before cell-based remyelination can succeed (*12*, *45*). Nonetheless, current disease-modifying strategies for treating both vascular and autoimmune diseases have advanced to the point where transplant-based remyelination of adult targets may now be feasible.

Interest in cell-based remyelination has been focused on MS, a debilitating disease characterized by both inflammatory myelinolysis and degenerative axonal loss. The attraction of MS as a therapeutic target derives from its high incidence and prevalence, with more than 300,000 cases in the U.S. alone. MS has been a difficult target for cell therapy, given its relapsing course and the limitations of introducing fresh cells into an inflammatory environment. Nonetheless, a new generation of immune modulators has substantially diminished disease recurrence, making cell replacement a tenable repair strategy. Natalizumab (anti-α4 integrin), alemtuzumab (anti-CD52), rituximab (anti-CD20), and fingolomod (a sphingosine-1-phosphate receptor modulator), have all been associated with significant reductions in relapse rate (*46*). These advances in the immunomodulatory control of MS suggest that focus may now shift from disease attenuation to the repair of demyelinated lesions.

The intracerebral delivery of GPCs into demyelinated brain may offer a feasible strategy for such myelin repair. When human GPCs were transplanted directly into lysolecithin-induced demyelinated lesions in the adult rat brain, the cells matured as oligodendrocytes and myelinated residual host axons, though with lower efficiency than in congenitally hypomyelinated brain (*11*). Similarly, in a new model of axon-sparing demyelination in adult cats, remyelination occurred efficiently from endogenous progenitors (*4*). Thus, GPCs seem to be effective cellular vectors for adult remyelination, though the complexity of the disease environment, which may include axonal loss, may make adult targets less approachable than their pediatric counterparts; this is especially true in aged patients (*12*, *47*). Thus, any cell-based strategies for treating adult demyelination will require not only disease modification, but also rigorous stratification to define those patients with sufficient axonal preservation to benefit from this approach.

Besides the myelinated tracts of the brain, the ascending sensory and descending motor tracts of the spinal cord are frequent victims of demyelination, whether from MS, neuromyelitis optica, or segmental injuries. In efforts to remyelinate the contused rat spinal cord, implanted GPCs have been found to disperse and generate both astrocytes and myelinogenic oligodendrocytes (*48*). Similarly, hESC-derived oligodendrocytes can remyelinate demyelinated cord lesions (*15*), with functional benefit (*49*). As noted, a safety trial of hESC-derived GPCs transplanted into patients with high-grade thoracic cord lesions was initiated on the basis of these observations (*18*). Although the therapeutic potential of a solely remyelinative strategy in patients with such high-grade lesions is unclear, such GPC grafts may hold great promise in carefully selected patients with isolated segmental demyelination.

### Human GPC-Engrafted Chimeric Mice as Systems for Assessing Human Glial Function

When hypomyelinated mutant mice are engrafted neonatally with human GPCs, the donor cells mature as both myelinating oligodendrocytes and fibrous astrocytes, ultimately yielding mice with substantially humanized white matter (*5*). Large numbers of human donor cells also remain as progenitors, which eventually predominate, displacing and ultimately replacing the endogenous mouse glial progenitor pool. This competitive advantage of human over murine glial progenitors is evident in WT and hypomyelinated mice, such that in the setting of normal glial turnover, the human GPCs also give rise to gray matter astrocytes, eventually resulting in substantial astrocytic as well as oligodendrocytic humanization of the recipient rodent brains (Fig. 2F).

The result of these events is that the xenografted mouse brains can become substantially humanized in their glial constituents (*5*). These human glial chimeras lend themselves to the investigation of questions that were never before approachable, for lack of an appropriate in vivo model of human glial function. First, what are the species-specific contributions of human glia to neural network function? Astrocytes clearly play a central role in synaptic efficiency and plasticity in mammals (*50*). Hominid evolution in particular has been attended by increasing astrocytic complexity, which may have contributed greatly to the evolution of higher cognitive functions in primates. Human astrocytes are larger and far more fibrous than those of infraprimate mammals and include more encompassed synapses (*51*). As such, is astrocytic specialization the basis for human cognitive evolution? The high degree of human glial chimerization of these brains will permit us to address this issue and should provide great opportunity for future studies of the species-specific roles of astrocytes in human cognition and disease alike. In addition, the advent of new technologies for generating glia from iPSCs suggests the potential for establishing chimeric mice with glia produced from iPSCs sourced from patients with specific neurological and psychiatric disorders, as a means of assessing the specific contributions of glia to the pathogenesis of those conditions. This approach may be of particular value in assessing the role of glia

in those neural diseases that are exclusive to humans, such as schizophrenia, whose phylogenetic appearance may parallel that of human astrocytic evolution.

Thus, the disorders of glia, and of myelin in particular, stand out as especially promising initial targets for cell-based therapy of neurological disease. With the use of a common strategy for GPC implantation, a broad set of both pediatric and adult disorders of the brain and spinal cord may prove amenable to structural repair. In addition, the human glial chimeric mice that have been established as a means of evaluating these transplant strategies may provide us with exciting new models for studying the species-specific roles of human glia and their progenitors in both normal physiology and disease.

*Note added in proof*: As this Review went to press, two new papers appeared that address the potential utility of propagated neural stem cells, as opposed to lineage-restricted glial progenitors, for myelinating congenitally hypomyelinated brain. Uchida *et al*. (*52*) describe the production of myelin in the brains of immunodeficient shiverer mice transplanted neonatally with human neural stem cells. Gupta *et al*. (*53*) then describe the early results of delivering these cells to the brains of children with Pelizaeus-Merzbacher disease, in a phase 1 safety trial that reports a favorable safety profile in the implanted children, as well as radiographic data suggestive of donor-derived myelin production in the graft recipients.

### References and Notes


1. N. Roy, M. Windrem, S. A. Goldman, in *Myelin Biology and Disorders*, R. Lazzarini, Ed. (Elsevier, Amsterdam, 2004), pp. 259–287.
2. Y. Lee *et al*., *Nature* **487**, 443 (2012).
3. D. Tkachev *et al*., *Lancet* **362**, 798 (2003).
4. I. D. Duncan, A. Brower, Y. Kondo, J. F. Curlee Jr., R. D. Schultz, *Proc. Natl. Acad. Sci. U.S.A.* **106**, 6832 (2009).
5. M. S. Windrem *et al*., *Cell Stem Cell* **2**, 553 (2008).
6. A. Nishiyama, M. Komitova, R. Suzuki, X. Zhu, *Nat. Rev. Neurosci.* **10**, 9 (2009).
7. N. S. Roy *et al*., *J. Neurosci.* **19**, 9986 (1999).
8. M. C. Nunes *et al*., *Nat. Med.* **9**, 439 (2003).
9. F. J. Sim *et al*., *Ann. Neurol.* **59**, 763 (2006).
10. F. J. Sim *et al*., *Nat. Biotechnol.* **29**, 934 (2011).
11. M. S. Windrem *et al*., *J. Neurosci. Res.* **69**, 966 (2002).
12. R. J. M. Franklin, C. Ffrench-Constant, *Nat. Rev. Neurosci.* **9**, 839 (2008).
13. M. S. Windrem *et al*., *Nat. Med.* **10**, 93 (2004).
14. O. Brüstle *et al*., *Science* **285**, 754 (1999).
15. G. I. Nistor, M. O. Totoiu, N. Haque, M. K. Carpenter, H. S. Keirstead, *Glia* **49**, 385 (2005).
16. M. Izrael *et al*., *Mol. Cell. Neurosci.* **34**, 310 (2007).
17. N. S. Roy *et al*., *Nat. Med.* **12**, 1259 (2006).
18. www.clinicaltrials.gov, NCT01217008.
19. T. Zhao, Z. N. Zhang, Z. Rong, Y. Xu, *Nature* **474**, 212 (2011).
20. J. C. I. Izpisúa Belmonte, J. Ellis, K. Hochedlinger, S. Yamanaka, *Nat. Rev. Genet.* **10**, 878 (2009).
21. K. Takahashi, S. Yamanaka, *Cell* **126**, 663 (2006).
22. J. Yu *et al*., *Science* **318**, 1917 (2007).
23. M. Wernig *et al*., *Proc. Natl. Acad. Sci. U.S.A.* **105**, 5856 (2008).
24. B. Y. Hu, Z. W. Du, S. C. Zhang, *Nat. Protoc.* **4**, 1614 (2009).
25. M. Czepiel *et al*., *Glia* **59**, 882 (2011).
26. M. S. Windrem *et al*., *Soc. Neurosci. Abstr.* 228.02 (2011).
27. V. B. Mattis, C. N. Svendsen, *Lancet Neurol.* **10**, 383 (2011).
28. M. Stadtfeld *et al*., *Nature* **465**, 175 (2010).
29. J. M. Polo *et al*., *Nat. Biotechnol.* **28**, 848 (2010).
30. Z. P. Pang *et al*., *Nature* **476**, 220 (2011).
31. J. Powers, in *Myelin Biology and Disorders*, R. Lazzarini, Ed. (Elsevier, Amsterdam, 2004), pp. 663–690.
32. J. C. Silbereis, E. J. Huang, S. A. Back, D. H. Rowitch, *Dis. Model. Mech.* **3**, 678 (2010).
33. J. Dietrich *et al*., *Nat. Med.* **11**, 277 (2005).
34. M. Bugiani *et al*., *J. Neuropathol. Exp. Neurol.* **70**, 69 (2011).
35. M. Jeyakumar, R. Dwek, T. Butters, F. Platt, *Nat. Rev. Neurosci.* **6**, 1 (2005).
36. E. Y. Snyder, R. M. Taylor, J. H. Wolfe, *Nature* **374**, 367 (1995).
37. J.-P. Lee *et al*., *Nat. Med.* **13**, 439 (2007).
38. L. S. Shihabuddin *et al*., *J. Neurosci.* **24**, 10642 (2004).
39. S. J. Tamaki *et al*., *Cell Stem Cell* **5**, 310 (2009).
40. www.clinicaltrials.gov, NCT00337636.
41. M. I. Givogri *et al*., *J. Neurosci.* **26**, 3109 (2006).
42. M. L. Escolar *et al*., *N. Engl. J. Med.* **352**, 2069 (2005).
43. B. D. Yandava, L. L. Billinghurst, E. Y. Snyder, *Proc. Natl. Acad. Sci. U.S.A.* **96**, 7029 (1999).
44. www.clinicaltrials.gov, NCT01391637.
45. C. W. Ip *et al*., *J. Neurosci.* **26**, 8206 (2006).
46. B. Weinstock-Guttman, M. Ramanathan, *Nat. Rev. Neurol.* **8**, 66 (2012).
47. J. M. Ruckh *et al*., *Cell Stem Cell* **10**, 96 (2012).
48. S. S. Han, Y. Liu, C. Tyler-Polsz, M. S. Rao, I. Fischer, *Glia* **45**, 1 (2004).
49. J. Sharp, J. Frame, M. Siegenthaler, G. Nistor, H. S. Keirstead, *Stem Cells* **28**, 152 (2010).
50. J. Kang, L. Jiang, S. A. Goldman, M. Nedergaard, *Nat. Neurosci.* **1**, 683 (1998).
51. N. A. Oberheim *et al*., *J. Neurosci.* **29**, 3276 (2009).
52. N. Uchida *et al*., *Sci. Transl. Med.* **4**, ra136 (2012).
53. N. Gupta *et al*., *Sci. Transl. Med.* **4**, ra137 (2012).
54. S. A. Goldman, *Arch. Neurol.* **68**, 848 (2011).


**Acknowledgments:** Work discussed in the Goldman lab was supported by grants from the National Institute of Neurological Disorders and Stroke (R01NS75345 and R01NS39559), the National Multiple Sclerosis Society, the Adelson Medical Research Foundation, the Mathers Charitable Foundation, and the New York State Stem Cell Research Program (NYSTEM). S.A.G. is an inventor on the following patents held by the University of Rochester and/or Cornell University: U.S. Patent 7,524,491 B2 ("Non-human animals with human glial chimeric brains"), U.S. Patent 8,206,699 ("Myelination of congenitally dysmyelinated forebrains using oligodendrocyte progenitor cells"), and U.S. Patent 8,263,402 ("A method for isolating and purifying oligodendrocytes and oligodendrocyte progenitor cells").

10.1126/science.1218071

# Detecting Causality in Complex Ecosystems

George Sugihara,[1]* Robert May,[2] Hao Ye,[1] Chih-hao Hsieh,[3]* Ethan Deyle,[1] Michael Fogarty,[4] Stephan Munch[5]

Identifying causal networks is important for effective policy and management recommendations on climate, epidemiology, financial regulation, and much else. We introduce a method, based on nonlinear state space reconstruction, that can distinguish causality from correlation. It extends to nonseparable weakly connected dynamic systems (cases not covered by the current Granger causality paradigm). The approach is illustrated both by simple models (where, in contrast to the real world, we know the underlying equations/relations and so can check the validity of our method) and by application to real ecological systems, including the controversial sardine-anchovy-temperature problem.

Identifying causality (*1*) in complex systems can be difficult. Contradictions arise in many scientific contexts where variables are positively coupled at some times but at other times appear unrelated or even negatively coupled depending on system state (movie S1). Baltic Sea fisheries, for example, exhibit radically different dynamic control regimes (top-down versus bottom-up) depending on the threshold abundance of planktivores, causing the correlations between fish and zooplankton to change sign (*2*). Such state-dependent behavior is a defining hallmark of complex nonlinear systems (*3*, *4*), and nonlinearity is ubiquitous in nature (*3*–*11*).

Ephemeral or "mirage" correlations are common in even the simplest nonlinear systems (*7*, *11*–*13*), such as shown in Fig. 1 for two coupled difference equations that exhibit chaotic behavior (*14*):

$$\begin{aligned} X(t+1) &= X(t)[r_x - r_x X(t) - \beta_{x,y} Y(t)] \\ Y(t+1) &= Y(t)[r_y - r_y Y(t) - \beta_{y,x} X(t)] \end{aligned} \quad (1)$$

When this happens, variables that may be positively coupled for long periods can spontaneously become anticorrelated or decoupled; this can create problems when fitting models to observational data (*15*).

Although correlation is neither necessary nor sufficient to establish causation, it remains deeply ingrained in our heuristic thinking (*8*, *13*, *16*, *17*). One might conclude, for example, that the variables in Fig. 1 have no causal relation because they are uncorrelated. Obviously, lack of correlation does not imply lack of causation. Because of this and for reasons just given, the use of correlation to infer causation is risky, especially as we come to recognize that nonlinear dynamics are ubiquitous.

[1]Scripps Institution of Oceanography, University of California, San Diego, 9500 Gilman Drive, La Jolla, CA 92093, USA. [2]Department of Zoology, University of Oxford, Oxford OX1 3PS, UK. [3]Institute of Oceanography and Institute of Ecology and Evolutionary Biology, National Taiwan University, No. 1, Sec. 4, Roosevelt Road, Taipei 106, Taiwan. [4]Northeast Fisheries Science Center, National Oceanic and Atmospheric Administration, 166 Water Street, Woods Hole, MA 02543, USA. [5]Southwest Fisheries Science Center, National Oceanic and Atmospheric Administration, 110 Shaffer Road, Santa Cruz, CA 95060, USA.

*To whom correspondence should be addressed. E-mail: gsugihara@ucsd.edu (G.S.); chsieh@ntu.edu.tw (C.H.)

An alternative approach, Granger causality (GC) (*18*), provides a framework that uses predictability as opposed to correlation to identify causation between time-series variables. GC is recognized as the primary advance on the causation problem since Berkeley (*1*).

Variable $X$ is said to "Granger cause" $Y$ if the predictability of $Y$ (in some idealized model) declines when $X$ is removed from the universe of all possible causative variables, $U$ (*18*). The key requirement of GC is separability, namely that information about a causative factor is independently unique to that variable (e.g., information about predator effects is not contained in time series for the prey) and can be removed by eliminating that variable from the model. Separability is characteristic of purely stochastic and linear systems, and GC can be useful for detecting interactions between strongly coupled (synchronized) variables in nonlinear systems. Separability reflects the view that systems can be understood a piece at a time rather than as a whole.

However, as Granger (*18*) realized early on, this approach may be problematic in deterministic settings, especially in dynamic systems with weak to moderate coupling. For example, GC gives ambiguous results for the system in Fig. 1 (see GC calculations S1). This is because separability is not satisfied in such systems, which, unlike the tradition in economics and single-species fisheries management, need to be considered as a whole. That is to say, in deterministic dynamic systems (even noisy ones), if $X$ is a cause for $Y$, information about $X$ will be redundantly present in $Y$ itself and cannot formally be removed from $U$—a consequence of Takens' theorem (*19*, *20*). To see this directly, we note simply that Eq. 1 can be rewritten as a model for $Y(t+1)$ in terms of $Y(t)$ and $Y(t-1)$ (see box S1 for a worked example). Therefore, information about $X(t)$ that is relevant to predicting $Y$ is redundant in this system and cannot be removed simply by eliminating $X$ as an explicit variable. When Granger's definition is violated, GC calculations are no longer valid, leaving the question of detecting causation in such systems unanswered.

In addition to nonseparability, ecosystems differ from the systems typically studied with Granger's approach in other important ways. First, in ecosystem dynamics, weak to moderate coupling is the norm. McCann (*21*) and others have developed a strong case for the ubiquity of weak coupling in ecological food webs and have demonstrated their importance for system stability. Second, ecosystems are typically subject to forcing by external driving variables such as temperature, precipitation, and upwelling [e.g., (*6*, *22*)]. Because many species share similar abiotic environments, this can lead to correlations and apparent synchrony among noninteracting species [e.g., the Moran effect (*23*)], complicating the task of sorting out the real interactions from spurious correlations. It is therefore important in ecology to have methods that (i) address nonseparable systems, (ii) identify weakly coupled variables, and (iii) distinguish interactions among species from the effects of shared driving variables.

Here, we examine an approach specifically aimed at identifying causation in ecological time series. We demonstrate the principles of our approach with simple model examples, showing that the method distinguishes species interactions from the effects of shared driving variables. Finally, we apply the method to ecological data from experimental and field studies, showing how it distinguishes top-down from bottom-up control in the classic *Paramecium-Didinium* experiment and clarifies the ongoing debate about the nature of interactions among sardine, anchovy, and sea surface temperature in the California Current ecosystem.

Our approach is not in competition with the many effective methods that use GC (see supplementary text); rather, it is specifically aimed at a class of system not covered by GC. As verified in GC calculations S1 to S5 and box S1, GC does not apply to this class of system.

**Dynamic causation and CCM.** GC applies if the world is purely stochastic. However, to the extent that it is deterministic and dynamics are not entirely random, there will be an underlying manifold governing the dynamics (representing coherent trajectories as opposed to a random tangle).

In dynamical systems theory, time-series variables (say, $X$ and $Y$) are causally linked if they are from the same dynamic system (*4*, *19*, *20*)—that is, they share a common attractor manifold $M$ (movies S1 to S3 illustrate this idea). This means that each variable can identify the state of the other (*3*, *19*, *20*, *24*, *25*) (e.g., information about past prey populations can be recovered from the predator time series, and vice versa). Additionally, when one variable $X$ is a stochastic environmental driver of a population variable $Y$, information about the states of $X$ can be recovered from $Y$, but not vice versa. For example, fish time series can be used to estimate weather, but not conversely. This runs counter to Granger's intuitive scheme (see explanation in box S1).

Our alternative approach, convergent cross mapping (CCM), tests for causation by measuring the extent to which the historical record of $Y$ values can reliably estimate states of $X$. This happens only if $X$ is causally influencing $Y$. In more detail, CCM looks for the signature of $X$ in $Y$'s time series by seeing whether there is a correspondence between the

"library" of points in the attractor manifold built from $Y$, $M_Y$, and points in the $X$ manifold, $M_X$, where these two manifolds are constructed from lagged coordinates of the time-series variables $Y$ and $X$, respectively (*3*, *19*, *24*) (movies S1 and S2).

Essentially, the idea is to see whether the time indices of nearby points on the $Y$ manifold can be used to identify nearby points on $M_X$. If so, then one can use $Y$ to estimate $X$ and vice versa. This procedure is illustrated in Fig. 2 and movie S3, with full technical details including an algorithm in (*26*).

Note that CCM is related to the general notion of cross prediction (*3*, *25*) but with important differences. First, CCM estimates "states" across variables and does not forecast how the system "evolves" on the manifold. This eliminates possible information loss from chaotic dynamics (Lyapunov divergence) and accommodates nondynamic (i.e., random) variables. More important, CCM involves convergence, a key property that distinguishes causation from simple correlation. Convergence means that cross-mapped estimates improve in estimation skill with time-series length $L$ (sample size used to construct a library) (Fig. 3A, fig. S2, and box S1). With more data, the trajectories defining the attractor fill in, resulting in closer nearest neighbors and declining estimation error (a higher correlation coefficient) as $L$ increases (Fig. 2). Thus, CCM becomes a necessary condition for causation. Indeed, failure to account for convergence explains conflicting results reported in the literature with related methods (supplementary text and fig. S5).

In practical applications, where shadow manifolds are low-dimensional approximations of the true system, convergence will be limited by observational error, process noise, and time-series length $L$. Thus, with limited or noisy field data, CCM is demonstrated by predictability that increases with $L$ (fig. S3). See (*26*) for a discussion of data requirements.

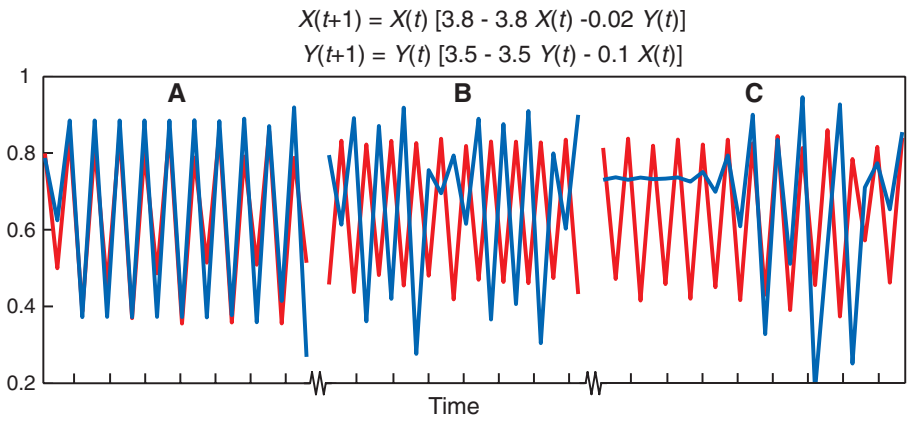


**Fig. 1.** Mirage correlations. (**A** to **C**) Three samples from a single run of a coupled two-species nonlinear logistic difference system with chaotic dynamics. Variables $X$ (blue) and $Y$ (red) appear correlated in the first time segment (A), anticorrelated in the second time segment (B), and lose all coherence in the third time segment (C) with alternating interspersed periods of positive, negative, and zero correlation. Although the system is deterministic and dynamically coupled, there is no long-term correlation ($n$ = 1000, ρ = 0.0054, $P$ = 0.864).

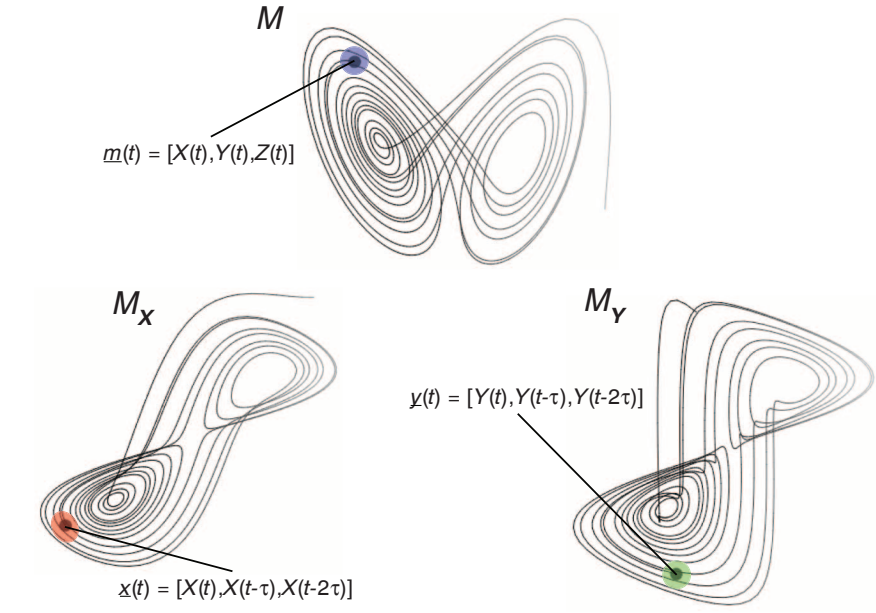


**Fig. 2.** Convergent cross mapping (CCM) tests for correspondence between shadow manifolds. This example based on the canonical Lorenz system (a coupled system in $X$, $Y$, and $Z$; eq. S7 without $V$) shows the attractor manifold for the original system ($M$) and two shadow manifolds, $M_X$ and $M_Y$, constructed using lagged-coordinate embeddings of $X$ and $Y$, respectively (lag = τ). Because $X$ and $Y$ are dynamically coupled, points that are nearby on $M_X$ (e.g., within the red ellipse) will correspond temporally to points that are nearby on $M_Y$ (e.g., within the green circle). That is, the points inside the red ellipse and green circle will have corresponding time indices (values for $t$). This enables us to estimate states across manifolds using $Y$ to estimate the state of $X$ and vice versa using nearest neighbors (*3*). With longer time series, the shadow manifolds become denser and the neighborhoods (ellipses of nearest neighbors) shrink, allowing more precise cross-map estimates (see movies S1 to S3).

In practical applications, where shadow manifolds are low-dimensional approximations of the true system, convergence will be limited by observational error, process noise, and time-series length $L$. Thus, with limited or noisy field data, CCM is demonstrated by predictability that increases with $L$ (fig. S3). See (*26*) for a discussion of data requirements.

**Framework for identifying causation, case (i) Bidirectional causality via functional coupling.** Bidirectional causality is analogous to the concept of "feedback" between two time series described by Granger (*18*) and is the primary case covered by Takens (*19*). Simply put, if variables are mutually coupled (e.g., predator and prey), they will cross map in both directions (Fig. 3A and fig. S1A). Thus, each variable can be estimated from the other (predator histories can estimate prey states). Figure 3B gives examples of the general case i.

Notice that as the strength of coupling increases, information becomes more distinct in the affected variables. As a result, their manifolds will contain stronger historical signatures of the causes. In Fig. 1 (Eq. 1), for example, where $\beta_{y,x} >> \beta_{x,y}$ the much stronger effect of species $X$ on $Y$ implies faster convergence for predicting $X$ than for $Y$ (Fig. 3A). Thus, all things equal, the relative skill of cross mapping can indicate the relative strength of causative effect (Fig. 3B).

**Framework for identifying causation, case (ii) Unidirectional causality.** Here, species $X$ influences the dynamics of $Y$, but $Y$ has no effect on $X$ (Fig. 3C and fig. S1B). This describes an amensal or commensal relationship, or where $X$ represents external environmental forcing.

Figure 3C examines the system when $\beta_{x,y} = 0$. Notice that with moderately strong forcing from $X$ (via $\beta_{y,x}$), even though $Y$ exerts no effect, there may still be partial cross mapping of $Y$ arising from the contemporaneous dependence of $Y$ on $X$. However, this statistical effect is not convergent (shown by the asymptotic level curves with respect to $L$ in Fig. 3E). With extremely strong forcing, the intrinsic dynamics of the forced variable become subordinate to the forcing variable, leading to the well-studied phenomenon of "synchrony" (*27*). The red plateau in Fig. 3E shows that bidirectional convergence can occur with strong forcing. Thus, strong forcing (synchrony) must be ruled out for CCM to unequivocally imply bidirectional coupling, although it still implies membership in a common dynamic system.

**Transitivity.** Notice that causation is transitive (e.g., if foxes prey on rabbits, and rabbits eat grass, then foxes and grass are causally linked). More formally, $X \Leftrightarrow Y \Leftrightarrow Z$ implies $X \Leftrightarrow Z$, whether or not $X$ and $Z$ interact directly. Similarly, for unidirectional

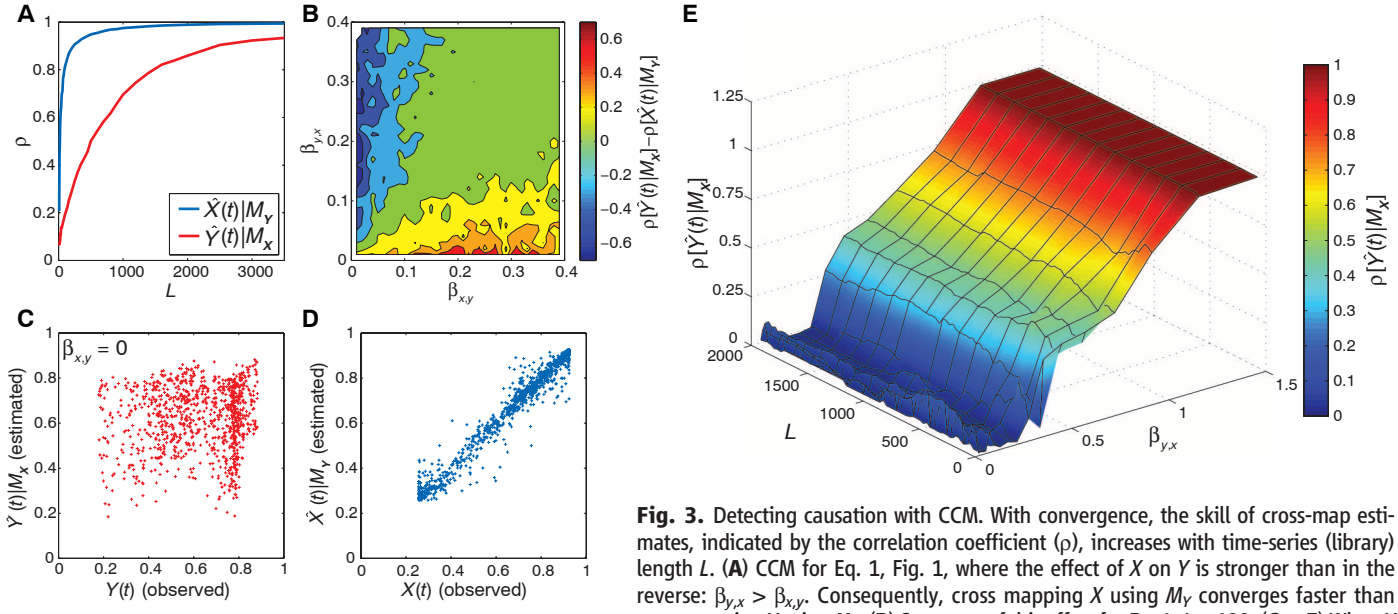


**Fig. 3.** Detecting causation with CCM. With convergence, the skill of cross-map estimates, indicated by the correlation coefficient (ρ), increases with time-series (library) length *L*. (**A**) CCM for Eq. 1, Fig. 1, where the effect of *X* on *Y* is stronger than in the reverse: $\beta_{y,x} > \beta_{x,y}$. Consequently, cross mapping *X* using $M_Y$ converges faster than cross mapping *Y* using $M_X$. (**B**) Summary of this effect for Eq. 1, $L = 400$. (**C** to **E**) When *Y* (red) has no effect on *X* (blue) (i.e., $\beta_{x,y} = 0$), (C) shows that cross mapping of *Y* using $M_X$ fails; however, the cross map of *X* succeeds (D) because the time series for *Y* contains information about the dynamics of *X*. (E) demonstrates nonconvergence of $\hat{Y}(t)$ as a function of forcing strength when $\beta_{x,y} = 0$. Convergence only occurs as a special case if strong forcing causes the system to collapse dimensionality (dark red plateau at high $\beta_{y,x}$), thus removing the dynamics of *Y*.

forcing, $X \Rightarrow Y$ and $Y \Rightarrow Z$ implies $X \Rightarrow Z$. Transitivity provides the basis for extending CCM to larger interaction networks, enabling us to distinguish variables that are coupled from those sharing a common driver. This is illustrated with two model examples below.

**Complex model examples: External forcing of noncoupled variables.** Consider the case where two species, *X* and *Y*, do not interact but are both driven by a common environmental variable *Z* (example 1 schematic in Fig. 4A). This occurs commonly in ecological systems [the Moran effect (*23*)] and remains problematic in studies of causation. Here we expect no cross mapping between species *X* and *Y* because there is no information flow between variables; however, information about the external forcing variable (*Z*) should still be recoverable from *X* and *Y*.

In fisheries, for example, noninteracting populations with common peak recruitment years due to favorable environmental conditions may be correlated even though they do not interact. The simple fisheries model in Fig. 4B illustrates this situation (*26*), where although the significant cross-correlation between species suggests that they might be coupled, cross mapping shows no evidence of convergence, proving that they are not coupled. This shows that CCM can distinguish true interaction from a simple correlation produced by shared driving variables.

Figure 4C provides an interesting further illustration of the method with a more complex five-species model [schematic in Fig. 4A, model details in (*26*)]. In this example, species 1, 2, and 3 represent a mutually interacting guild that externally force species 4 and 5, whereas 4 and 5 do not influence any other species. Species 1, 2, and 3 are akin to *Z* in the discussion above, with 4 and 5 akin to the externally forced noncoupled pair *X* and *Y*. Figure 4C shows that CCM is able to deduce the correct network of interactions getting all bidirectional and unidirectional links correct.

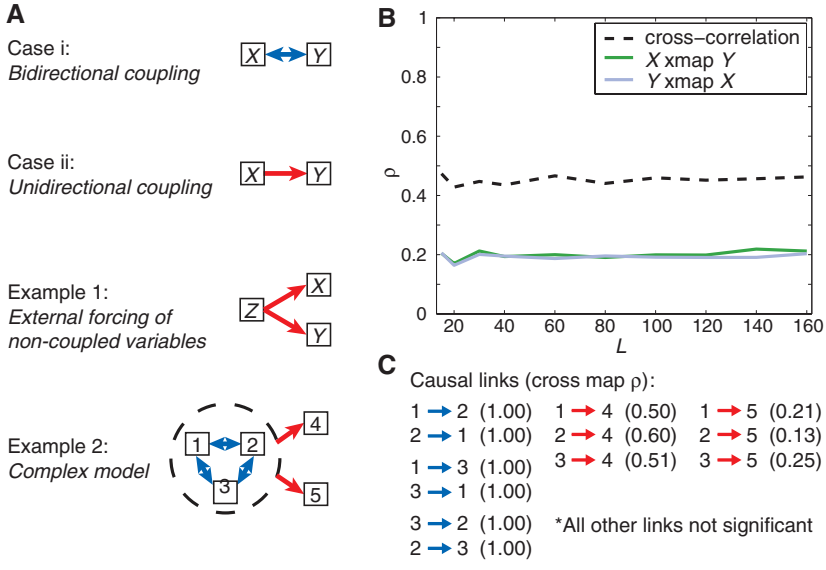


**Fig. 4.** Model causal networks. (**A**) Schematics of causal networks: two base cases and two model examples showing external forcing of noncoupled variables. (**B**) Cross-map results for example 1: external forcing of noncoupled variables. Cross-correlation erroneously suggests that *X* and *Y* are interacting, whereas cross mapping correctly shows that there is no interaction. (**C**) Cross-map results for the complex five-species model example. All significant ($P < 0.05$) mappings are given and indicate that species 1, 2, and 3 (the subsystem in the circle) all interact mutually (case i), but interact only asymmetrically as external forcing variables with respect to 4 and 5 (case ii), which do not interact directly themselves.

**Real-world examples: Demonstration with ecological data.** Keep in mind that attractors constructed from real data are approximations of dynamics occurring in higher dimensions. Thus, although observational error and process noise will limit the level of convergence attainable, low-dimensional approximations can still produce significant cross-map estimates of causal effects.

*Bidirectional causation in an experimental predator-prey system.* We apply the analysis to time series from the classic experimental predator-prey system, first studied in the 1920s by Gause and later improved by Veilleux (*28*), involving *Didinium* (predator) and *Paramecium* (prey) [methodological details in (*26*)].

The results in Fig. 5A suggest bidirectional coupling (case i), which accords with what is known. Moreover, the higher level of skill in

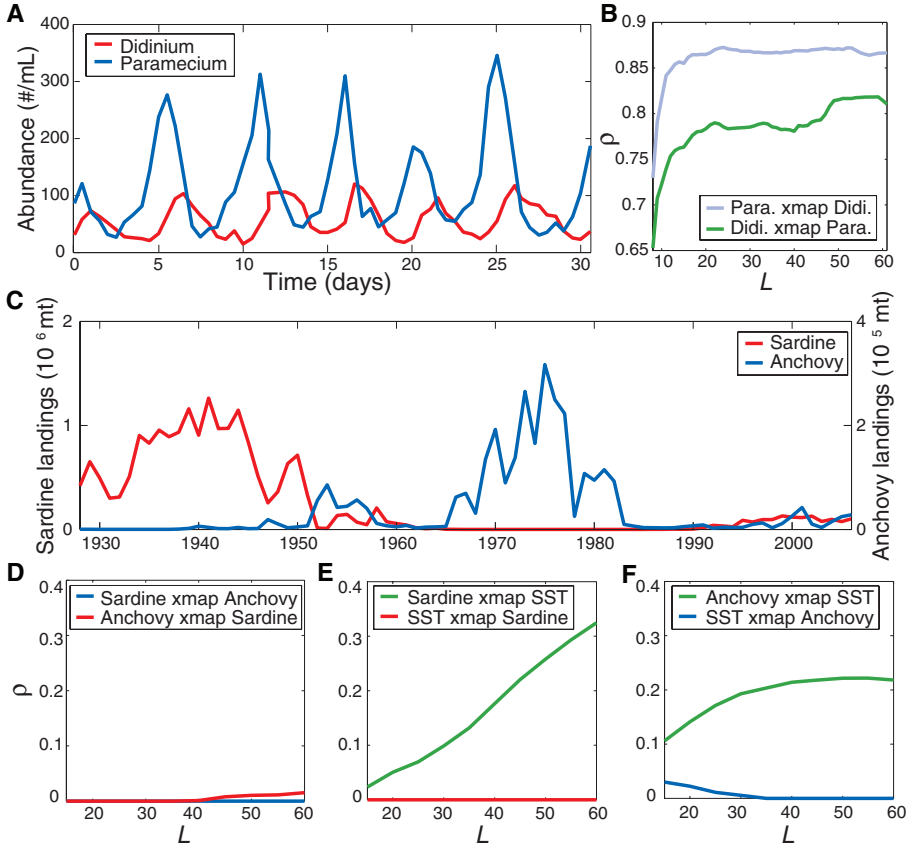


**Fig. 5.** Detecting causation in real time series. (**A**) Abundance time series of *Paramecium aurelia* and *Didinium nasutum* as reported in (*28*). (**B**) CCM of *Paramecium* and *Didinium* with increasing time-series length *L*. The pattern suggests top-down predator control. (**C**) California landings of Pacific sardine (*Sardinos sagax*) and northern anchovy (*Engraulis mordax*). (**D** to **F**) CCM (or lack thereof) of sardine versus anchovy, sardine versus SST (Scripps Pier), and anchovy versus SST (Newport Pier), respectively. This shows that sardines and anchovies do not interact with each other and that both are forced by temperature.

cross mapping *Didinium* from the *Paramecium* time series than the reverse (Fig. 5B) suggests that top-down control by the predator, *Didinium*, is stronger than bottom-up control by the prey, *Paramecium*. This finding is consistent with the experimental protocol and illustrates asymmetrical bidirectional coupling (case i).

*Complex causation in the sardine-anchovy system.* Here, we examine the relationship among Pacific sardine (*Sardinops sagax*) landings, northern anchovy (*Engraulis mordax*) landings, and sea surface temperature (SST) measured at Scripps Pier and Newport Pier, California (Fig. 5C).

Competing hypotheses have been advanced to explain the pattern of alternating dominance of sardine and anchovy across global fisheries on multidecadal time scales. Although the observed reciprocal abundance levels (Fig. 5A) resonates with ecological competition as an underlying mechanism, global synchrony in sardine and anchovy stanzas (*29*) suggests the operation of large-scale environmental forcing coupled with species-specific differences in optimal temperature levels. Recent evidence of regime-like behavior in these systems suggests the operation of nonlinear processes (*10*).

Similar to the global pattern, in California, 20th-century landings of Pacific sardine and northern anchovy show one population peaking when the other is low. Whereas some (*30*) have hypothesized that the species act in direct competition, others (*31*) have argued that the species react differently to common large-scale environmental forcing. Moreover, paleoecological time series based on fish scales preserved in the anoxic sediments of the Santa Barbara basin revealed that the negative cross-correlation witnessed in the 20th century disappears in these longer time series (*32*). Correlation with environmental factors has also been elusive. Jacobson and MacCall (*33*) used two approaches, a generalized additive model and a linearized Ricker stock-recruitment model with environmental terms, and detected correlation between 3-year running averages of the Scripps Pier SST versus sardine recruitment and spawning stock size. However, when the analysis was expanded to include recent stock assessments from 1992 to 2009, the relationships vanished (*34*). Although there are many possible explanations, such behavior is consistent with nonlinear dynamics and mirage correlation.

We address this controversy using the same analytical protocol used for the *Didinium-Paramecium* example (*26*). The results in Fig. 5D show no significant cross-map signal between sardine and anchovy landings, indicating that sardines and anchovies do not interact. In addition, as expected, there is no detectable signature from either sardine or anchovy in the temperature manifold; obviously, neither sardines nor anchovies affect SST. However, there is clear asymmetric CCM between sardines and SST as well as between anchovies and SST (Fig. 5, E and F), meaning that temperature information is encoded in both fishery time series. The recoverable temperature signature reveals a weak coupling of temperature to sardines and anchovies. Thus, although sardines and anchovies are not actually interacting, they are weakly forced by a common environmental driver, for which temperature is at least a viable proxy. Note that because of transitivity, temperature may be a proxy for a group of driving variables (i.e., temperature may not be the most proximate environmental driver). Our finding that SST influences sardine and anchovy population size (Fig. 5, E and F) is consistent with earlier findings of Jacobson and MacCall (*33*). Supporting evidence with other fishery-independent data are provided in the supplementary text (figs. S3 and S4).

Finally, it is important to note that the measurable nonlinear coupling of temperature to sardine stocks means that the effect of temperature varies with system state. Therefore, contrary to the current regulatory framework for sardines, a fixed temperature index will not suffice for sound management decisions. Rather, a dynamic (state-dependent) rule involving temperature is required.

**Final remarks on nonseparability.** One of the fundamental ideas in this work is that when causation is unilateral, $X \Rightarrow Y$ ("$X$ drives $Y$," as in case ii), then it is possible to estimate $X$ from $Y$, but not $Y$ from $X$. This runs counter to intuition (and GC), and suggests that if the weather drives fish populations, for example, we can use fish to estimate the weather but not conversely.

To further clarify how this works, consider the two-species logistic model described earlier (Eq. 1). We can recover the cross-map dynamics algebraically by rearranging Eq. 1 to give expressions for $Y(t)$ and $X(t)$, substituting these back into Eq. 1, and solving for $X(t)$ in terms of $Y(t)$ and $Y(t-1)$ (and conversely; see box S1).

In these expressions, the parameter $\beta_{x,y}$ governs the sensitivity of $X$ to changes in $Y$. As $\beta_{x,y}$ approaches 0, $X$ drives $Y$ unilaterally (case ii) and the cross-map estimate of $X$ remains well-behaved. But the cross-map model for $Y$ has a singularity when $\beta_{x,y} = 0$, meaning that cross mapping allows the driver to be reconstructed from the driven variable, but not the other way around (fish reflect weather states, but not conversely).

Finally, because Eq. 1 (parameterized as in Fig. 1) can be algebraically rearranged as a model for $X(t+1)$ purely in terms of $X(t)$ and $X(t-1)$, the information from $Y$ becomes redundant and can be removed without affecting our ability to predict $X(t+1)$. Thus, GC would conclude (incorrectly!) that $Y$ does not cause $X$ (GC calculation S1).

**Summary.** Despite the fundamental problems raised in Berkeley's 1710 *A Treatise on Principles of Human Knowledge* (*1*), correlation remains the analytical standard of modern science. This has be-

come more difficult to justify with increasing recognition that nonlinear dynamics are ubiquitous. Apparent relationships among variables can switch spontaneously in nonlinear systems as a result of mirage correlations or a threshold change in regime, and correlation can lead to incorrect and contradictory hypotheses. Growing recognition of the prevalence and importance of nonlinear behavior calls for a better criterion for evaluating causation where experimental manipulation is not possible.

Granger causality addresses Berkeley's issues with prediction rather than correlation as the criterion for causation in time series. This idea assumes that causes can be separated from effects, so that a variable is identified as causative if prediction skill declines when that variable is removed. This is possible in a purely stochastic world and is a powerful idea for systems that can be studied as independent pieces; however, it is not defined for all systems, and in particular not for deterministic dynamic systems (even noisy ones) where Takens' theorem applies (*19*, *20*). To address this, we examine an approach that exploits nonseparability by using CCM to test for membership to a common dynamical system. CCM is not a method competing with GC, but deals with interdependence often found in ecological study where GC is simply not applicable. Thus it is not surprising that as a further check, the GC calculations for all the model and real data examples considered in this work were largely unsuccessful (table S2 and GC calculations S1 to S5).

Although many empirical measures of species interactions exist (e.g., inferring interaction proxies from diet matrices), we suggest that causation inferred from time-series information provides a "bottom-line" picture of interactions that is more direct than those possible with proxies. The ability to resolve causal networks from their dynamical behavior has implications for system identification and ecosystem-based management, particularly where it is important to know which species interact as a group and need to be considered together. In resource management, as elsewhere, accurate knowledge of the causal network can be essential for avoiding unforeseen consequences of regulatory actions.

### References and Notes


1. G. Berkeley, *A Treatise on Principles of Human Knowledge* (1710).
2. M. Casini *et al.*, *Proc. Natl. Acad. Sci. U.S.A.* **106**, 197 (2009).
3. G. Sugihara, R. M. May, *Nature* **344**, 734 (1990).
4. P. A. Dixon, M. J. Milicich, G. Sugihara, *Science* **283**, 1528 (1999).
5. W. A. Brock, C. L. Sayers, *J. Monet. Econ.* **22**, 71 (1988).
6. B. T. Grenfell *et al.*, *Nature* **394**, 674 (1998).
7. A. Mysterud *et al.*, *Nature* **410**, 1096 (2001).
8. C. H. Hsieh, S. M. Glaser, A. J. Lucas, G. Sugihara, *Nature* **435**, 336 (2005).
9. G. I. Bischi, *et al.*, Eds., *Nonlinear Dynamics in Economics, Finance and Social Sciences* (Springer, Berlin, 2010).
10. D. A. S. Patil *et al.*, *Mon. Weather Rev.* **129**, 2116 (2001).
11. T. T. Lo, H. H. Hsu, *Atmos. Sci. Lett.* **11**, 210 (2010).
12. X. Rodo, M. Pascual, G. Fuchs, A. S. G. Faruque, *Proc. Natl. Acad. Sci. U.S.A.* **99**, 12901 (2002).
13. B. K. Wagner *et al.*, *Nat. Biotechnol.* **26**, 343 (2008).
14. A. L. Lloyd, *J. Theor. Biol.* **173**, 217 (1995).
15. Committee on Major U.S. Oceanographic Research Programs, National Research Council, *Global Ocean Science: Toward an Integrated Approach* (National Academies Press, Washington, DC, 1999).
16. Y. Chen *et al.*, *J. Neurosci. Methods* **150**, 228 (2006).
17. R. M. May, S. A. Levin, G. Sugihara, *Nature* **451**, 893 (2008).
18. C. W. J. Granger, *Econometrica* **37**, 424 (1969).
19. F. Takens, in *Dynamical Systems and Turbulence*, D. A. Rand, L. S. Young, Eds. (Springer-Verlag, New York, 1981), pp. 366–381.
20. E. R. Deyle, G. Sugihara, *PLoS ONE* **6**, e18295 (2011).
21. K. McCann, A. Hastings, G. R. Huxel, *Nature* **395**, 794 (1998).
22. C. H. Hsieh *et al.*, *Fish. Oceanogr.* **18**, 102 (2009).
23. P. A. P. Moran, *Aust. J. Zool.* **1**, 291 (1953).
24. N. H. Packard *et al.*, *Phys. Rev. Lett.* **45**, 712 (1980).
25. F. A. Ascioti *et al.*, *J. Plankton Res.* **15**, 603 (1993).
26. See supplementary materials on *Science* Online.
27. K. Josic, *Nonlinearity* **13**, 1321 (2000).
28. B. G. Veilleux, thesis, University of Alberta (1976).
29. R. A. Schwartzlose *et al.*, *S. Afr. J. Mar. Sci.* **21**, 289 (1999).
30. G. I. Murphy, J. D. Isaacs, Species replacement in marine ecosystems with reference to the California current. *Minutes of Meeting Marine Research Committee* **7**, 1 (1964).
31. R. Lasker, A. MacCall, in *Proceedings of the Joint Oceanographic Assembly, Halifax, August 1982: General Symposia* (Department of Fisheries and Oceans, Ontario, 1983), pp. 110–120.
32. T. R. Baumgartner *et al.*, *CCOFI Rep.* **33**, 24 (1992).
33. L. D. Jacobson, A. D. MacCall, *Can. J. Fish. Aquat. Sci.* **52**, 566 (1995).
34. S. McClatchie *et al.*, *Can. J. Fish. Aquat. Sci.* **67**, 1782 (2010).



**Acknowledgments:** We thank S. Sandin, L. Kaufman, A. MacCall, J. Melack, J. Schnute, L. Richards, A. Rosenberg, M. Kumagai, H. Liu, I. Altman, B. Fissel, S. Glaser, B. Carr, E. Klein, L. Storch, S. Kealhofer, M. Kogler, and C. Perretti for their comments and assistance with this work, and P. Sugihara for developing and producing the initial animations for movies S1 and S2. Supported by NSF grant DEB-1020372, NSF/NOAA CAMEO Award NA08OAR4320894, the McQuown Chair in Natural Science, the Sugihara Family Trust, and Quantitative Advisors (http://qadvisors.com) (G.S.); National Taiwan University and the National Science Council of Taiwan (C.H.); NSF graduate research fellowships (H.Y. and E.D.); and an EPA STAR graduate fellowship (E.D.).


### Supplementary Materials

www.sciencemag.org/cgi/content/full/science.1227079/DC1
Materials and Methods
Figs. S1 to S5
Tables S1 to S26
Box S1
GC Calculations S1 to S5
References (*35*–*76*)
Movies S1 to S3


6 July 2012; accepted 4 September 2012
Published online 20 September 2012;
10.1126/science.1227079




# REPORTS

# Biotinylated Rh(III) Complexes in Engineered Streptavidin for Accelerated Asymmetric C–H Activation


**Todd K. Hyster,[1,2] Livia Knörr,[2] Thomas R. Ward,[2]* Tomislav Rovis[1]***



**Enzymes provide an exquisitely tailored chiral environment to foster high catalytic activities and selectivities, but their native structures are optimized for very specific biochemical transformations. Designing a protein to accommodate a non-native transition metal complex can broaden the scope of enzymatic transformations while raising the activity and selectivity of small-molecule catalysis. Here, we report the creation of a bifunctional artificial metalloenzyme in which a glutamic acid or aspartic acid residue engineered into streptavidin acts in concert with a docked biotinylated rhodium(III) complex to enable catalytic asymmetric carbon-hydrogen (C–H) activation. The coupling of benzamides and alkenes to access dihydroisoquinolones proceeds with up to nearly a 100-fold rate acceleration compared with the activity of the isolated rhodium complex and enantiomeric ratios as high as 93:7.**


Thanks to the advent of genetic engineering, enzymes are attracting increasing attention as versatile synthetic tools, even displacing established organometal-catalyzed industrial processes (*1*). However, creating an enzyme for an abiotic reaction from a noncatalytic scaffold remains a major challenge (*2*–*5*). One class of strategies has relied on the incorporation of non-natural metal cofactors within a protein scaffold to afford artificial metalloenzymes (*6*–*9*). The main focus in the area has been improving the selectivity of the hybrid catalysts, rather than reaction rates, which are, by and large, dictated by the first coordination sphere interactions around the metal (*10*–*12*). Among the various cofactor localization strategies (*13*, *14*), the biotin-(strept)avidin technology has proven versatile: The geometry of the biotin-binding pocket is ideally suited to accommodate organometallic moieties, leaving enough room for substrate binding and activation (*15*–*19*).


[1]Department of Chemistry, Colorado State University, Fort Collins, CO 80523, USA. [2]Department of Chemistry, University of Basel, Basel CH-4056, Switzerland.

*To whom correspondence should be addressed. E-mail: rovis@lamar.colostate.edu (T.R.); thomas.ward@unibas.ch (T.R.W.)

In recent years, $[Cp^*RhCl_2]_2$, where Cp* is pentamethylcyclopentadienyl, has emerged as a versatile catalyst for electrophilic aromatic C–H activation reactions (*20*). Elegant work by the groups of Fagnou and Glorius showed that pivaloyl-protected benzhydroxamic acids may be efficiently coupled with alkenes to access dihydroisoquinolones in good yield at room temperature (*21*, *22*). An exogeneous base is required for the orthometallation step (*23*). Computations suggest that the C–H activation process occurs via a concerted metalation-deprotonation (CMD) mechanism (*24*). The presence of a base significantly lowers the activation energy of this step. As three coordination sites are required around the Cp*Rh moiety for catalysis (*25*), it has been difficult to introduce an asymmetric ligand, and no enantioselective version of this attractive benzannulation reaction has been reported thus far. In a biomimetic spirit, we hypothesized that incorporation of a biotinylated $[Cp^*RhX_2]_2$ combined with an engineered aspartate or glutamate residue might yield an asymmetric catalyst for the production of enantioenriched dihydroisoquinolones (Fig. 1).

We initially examined the viability of the $[RhCp^*Cl_2]_2$-catalyzed reaction between pivaloyl-protected benzhydroxamic acid (**1a**) and methyl acrylate (**2a**) to dihydroisoquinolone (**3a**) under aqueous conditions. Although this reaction is typically performed in MeOH or EtOH (*22*, *23*), we were pleased to find that the reaction proceeds to completion in a 4:1 mixture of $H_2O$/MeOH under basic conditions (200 mole % CsOAc), despite the sparing solubility of the substrates in this solvent mixture. Next, we designed a biotinylated analog $[RhCp^{*biotin}Cl_2]_2$ (*26*) for incorporation within streptavidin (Sav) (Fig. 1). Two equivalents of $[RhCp^{*biotin}Cl_2]_2$ were required to displace weakly bound 2-(4-hydroxyphenylazo)benzoic acid (HABA) in tetrameric streptavidin (*27*). This suggests that the dimeric catalyst precursor dissociates in aqueous solution to $RhCp^{*biotin}Cl_2(H_2O)$ and that the four biotin-binding sites of Sav can be loaded with the monomeric biotinylated catalyst precursor (*28*).

When we combined benzhydroxamic acid **1a** with 1.1 equivalents of methyl acrylate **2a** in a 4:1 mixture of $H_2O$:MeOH in the presence of tetrameric wild-type (WT) Sav and $[RhCp^{*biotin}Cl_2]_2$, only a trace amount of product was observed after 36 hours at room temperature (Table 1, entry 3). To increase conversion, we introduced a basic residue in the proximity of the rhodium moiety. As highlighted in an Auto-Dock (*29*) modeling study (Fig. 1D), residues $S112_A$ and $K121_B$ (of the adjacent Sav monomer B) lie closest to the metal center upon incorporation within WT Sav. We thus introduced by site-directed mutagenesis a basic residue at either of these positions. The presence of a glutamate residue at position 112 (S112E) has a marginal effect on the activity of the catalyst (Table 1, entry 5). Introduction of a glutamate residue at position 121 (i.e., K121E) again gives low conversion (Table 1, entry 7). Mutation to an aspartate at position 121 (i.e., K121D) improved the conversion to 89% after 72 hours (Table 1, entry 8). To confirm that this increase in activity was indeed caused by the presence of a carboxylate residue, we introduced an asparagine residue (i.e., K121N). Asparagine is sterically and electronically similar to aspartic acid but lacks the ability to facilitate the critical C–H activation step. As anticipated, K121N gave low conversion after 36 hours (Table 1, entry 9). The data thus suggest that the reaction is critically dependent on the precise localization of a carboxylate residue provided by Sav. We speculated that if the position of the carboxylate residue at position 121 could be further fine-tuned, increased conversions might result. This was realized upon combining a glutamate at position 121 with a lysine at position 118 (i.e., N118K-K121E). In addition to increased activity, this catalyst also gave enhanced levels of regioselectivity for alkene insertion (15:1) by comparison to the reaction in the absence of protein (4:1) (compare Table 1, entry 1 versus entry 10).

With a mutant exhibiting superior activity in hand, we were eager to determine whether the transformation could be rendered asymmetric thanks to the chiral nature of the active site. A



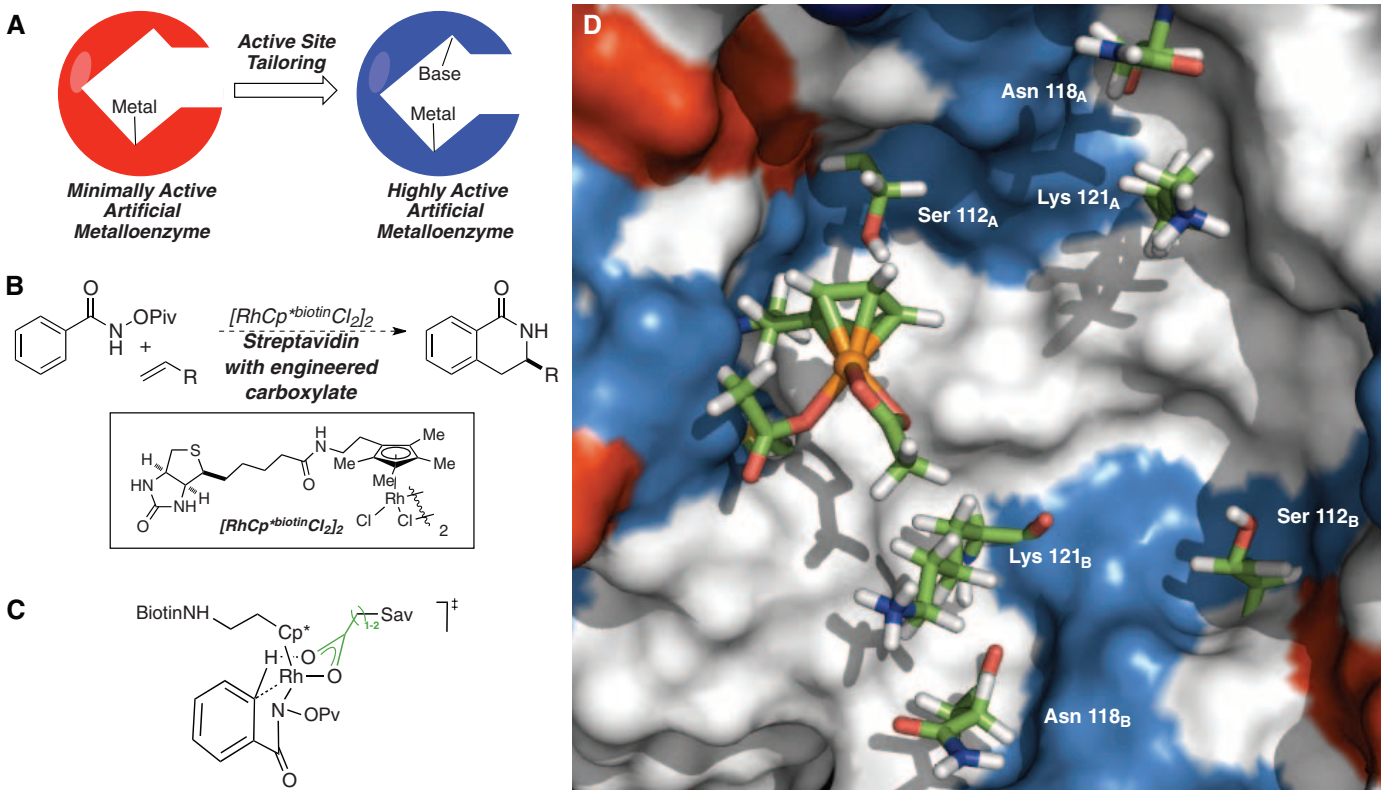


**Fig. 1.** (**A**) Synergistic action of a basic residue introduced by site-directed mutagenesis and a biotinylated $RhCp^{*biotin}Cl_2$ moiety acting as catalyst for an abiotic reaction. (**B**) Benzannulation reaction catalyzed by the artificial metalloenzyme for the synthesis of enantioenriched dihydroisoquinolones. (**C**) Postulated transition state for the C–H activation step. (**D**) Auto-Dock model of biotinylated $RhCp^{biotin}(OAc)_2$ complex anchored in the proposed active site of the streptavidin tetramer with key residues highlighted (adjacent complex in Sav monomer B omitted for clarity).

survey of our arsenal of Sav mutants revealed that the mutant with superior activity was also reasonably enantioselective (Table 1, entry 10). Because position 121 was identified as the best location for the carboxylate residue, we focused on position 112 to modify the chiral environment. A screen of nine mutants at position 112 using an acetate buffer revealed that aromatic residues gave superior reactivity by comparison to nonaromatic residues (30 to 50% yield), as well as enhanced enantioselectivity (Table 1, entries 12 to 20). Prolonged reaction times were required to achieve enhanced conversion. The best mutant under our conditions proved to be S112Y with 30% yield, 12:1 regioselectivity, and 88:12 enantiomeric ratio (er) (Table 1, entry 19). We hypothesized that if the superior activity imparted by the carboxylate mutation at position 121 could be combined in a synergistic way with the improved selectivity provided by S112Y, a highly active and selective artificial metalloenzyme might result (*30*). The use of S112Y-K121D gave good er but only in fair yield (Table 1, entry 21). Substituting the aspartic acid residue with glutamic acid resulted in a superior mutant that gave 80% yield with 20:1 regiomeric ratio and 90:10 enantiomeric ratio (Table 1, entry 22). The yield and er could be further improved by exchanging $H_2O$ with 3-(N-morpholino)propanesulfonic acid buffer to yield the desired product in 95% yield, 19:1 regioisomeric ratio (rr), and 91:9 er (Table 1, entry 23).

This transformation proved applicable to a variety of substrates (Fig. 2). Ethyl vinyl ketone was highly reactive under the reaction conditions, resulting in benzannulated product in good yield, high regioselectivity, but poor enantioselectivity. When methyl acrylate was replaced with benzyl acrylate, yield and enantioselectivity were diminished. Substitution on the benzamide was better tolerated under the reaction conditions. Bromo-substituted and naphthyl benzamides delivered product in good yield, with a modest erosion of er in comparison to the parent system. The enantioselectivity increased with para-substituted nitrobenzamides, albeit at the expense of lower yield. The remaining mass balance is represented by unreacted starting material.

The data presented above argue for the synergistic action of both the carboxylate side chain and the chiral cavity inside the metalloenzyme for optimal reactivity and selectivity. We sought further support for the role of the critical basic amino acid residue by conducting mechanistic studies. Using the monodeuterated benzamide $d_1$-**1a**, we observed a kinetic isotope effect ($k_H/k_D$) (KIE) value of 3.8 for the reaction with $[RhCp^{*biotin}Cl_2]_2$ under buffered conditions [1:4 MeOH:acetate buffer (pH = 5.9, 0.69 M) for the internal competition KIE study] (figs. S1 to S3). In the presence of WT Sav under identical conditions, a KIE value of 2.8 was obtained. With the most active mutant, N118K-K121E, a KIE value of 4.8 was found under acetate-free conditions (4:1 $H_2O$:MeOH). These

**Table 1.** Optimization of the performance of the artificial benzannulase.

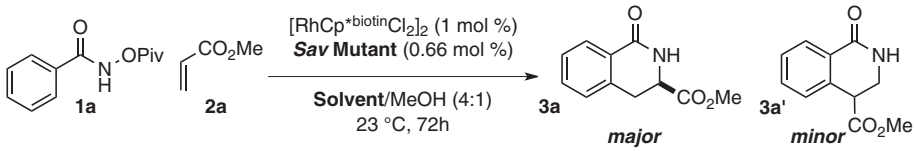


| entry | *Sav* Mutant | Solvent | yield (%)* | regioisomeric ratio (rr) | enantiomeric ratio (er) |
|---|---|---|---|---|---|
| 1 | - | Acetate Buffer | 80 | 4:1 | 51.5:48.5 |
| 2 | - | $H_2O$ | < 5% | - | - |
| 3 | WT† | $H_2O$ | < 5% | - | - |
| 4 | WT† | Acetate Buffer | 46 | 9:1 | 75:25 |
| 5 | S112E† | $H_2O$ | 10 | 15:1 | 78:22 |
| 6 | S112D† | $H_2O$ | < 5% | - | - |
| 7 | K121E† | $H_2O$ | 7 | 15:1 | 78:22 |
| 8 | K121D | $H_2O$ | 89 | 15:1 | 78:22 |
| 9 | K121N† | $H_2O$ | < 5% | - | - |
| 10 | N118K-K121E | $H_2O$ | 99 | 15:1 | 82:18 |
| 11 | N118K-K121E†,‡ | $H_2O$ | 8 | 6:1 | 52:48 |
| 12 | S112A | Acetate Buffer | 12 | 6:1 | 75:25 |
| 13 | S112C | Acetate Buffer | 6 | 10:1 | 71:29 |
| 14 | S112F | Acetate Buffer | 50 | 6:1 | 86:14 |
| 15 | S112K | Acetate Buffer | 6 | 6:1 | 76:24 |
| 16 | S112M | Acetate Buffer | 1 | 6:1 | 81:19 |
| 17 | S112T | Acetate Buffer | 35 | 6:1 | 79:21 |
| 18 | S112V | Acetate Buffer | 4 | 5:1 | 81:19 |
| 19 | S112Y | Acetate Buffer | 30 | 12:1 | 88:12 |
| 20 | S112W | Acetate Buffer | 32 | 12:1 | 86:14 |
| 21 | S112Y-K121D | $H_2O$ | 30 | 20:1 | 90:10 |
| 22 | S112Y-K121E | $H_2O$ | 80 | 20:1 | 90:10 |
| **23** | ***S112Y-K121E*** | ***MOPS Buffer*** | ***95*** | ***19:1*** | ***91:9*** |

*Yield determined by gas chromatography integration.
†Reaction conducted for 36 hours.
‡Sav preloaded with excess biotin for 10 min and then treated with $[RhCp^*biotinCl_2]_2$.

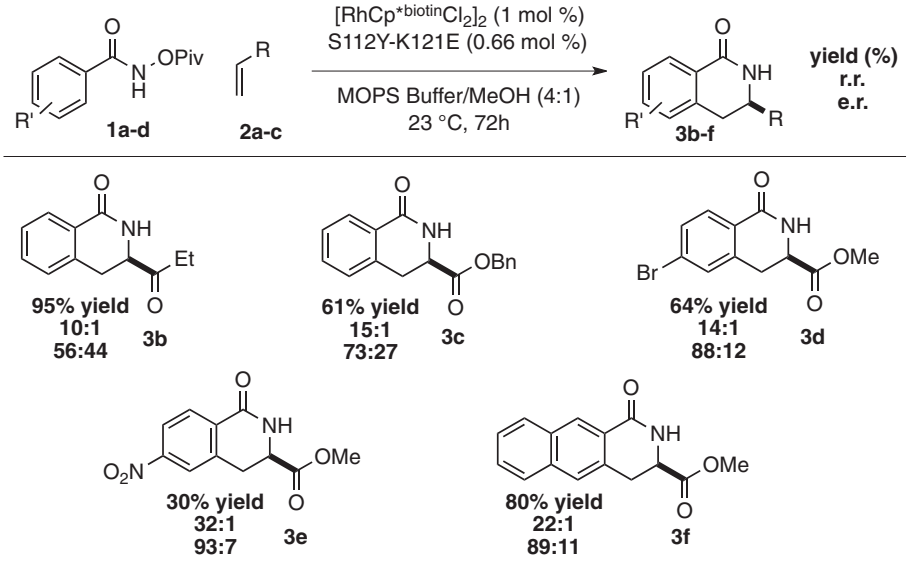


**Fig. 2.** Substrate scope.

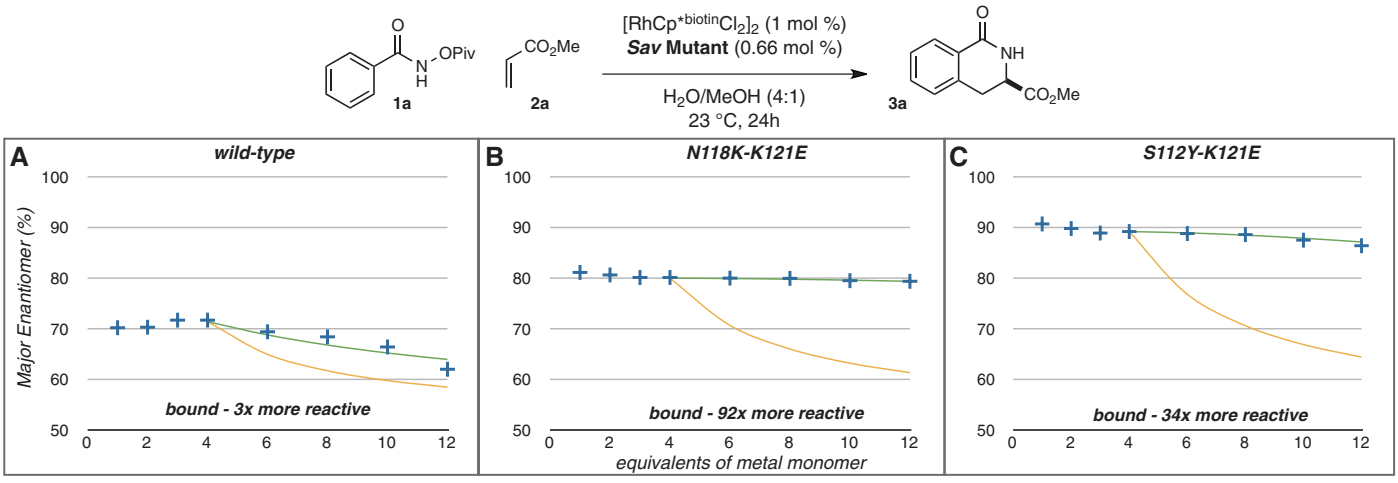


**Fig. 3.** Determination of the relative catalytic rates of free and Sav-bound catalysts using (**A**) WT Sav, (**B**) N118K-K121E, and (**C**) S112Y-K121E. Blue crosses, experimentally determined er; orange line, predicted er in the case of no protein rate acceleration [i.e., $k_{rel} = (k_{bound})/(k_{free}) = 1$]; green line, fitted er allowing the determination of $k_{rel}$.

results suggest a primary kinetic isotope effect in all cases. Subtle differences in the geometry of the CMD mechanism (Fig. 1C) is a likely source of the slightly different KIE values.

To provide further support for the critical role of the carboxylate residue within the enzyme's active site, we conducted competition experiments between protein-bound and free $[RhCp^{*biotin}Cl_2]_2$ catalyst precursors. The very limited solubility of the starting material precludes the use of classical Michaelis-Menten kinetic experiments. Because the free biotinylated catalyst leads to nearly racemic product (51.5:48.5 er) (Table 1, entry 1), whereas the Sav-bound catalyst leads to enantioenriched product, a comparison of the er as a function of the number of equivalents of $RhCp^{*biotin}Cl_2(H_2O)$ versus tetrameric Sav provides an estimate of the relative rates of the protein-bound ($k_{bound}$) and the free biotinylated catalyst ($k_{free}$) (*31*). These experiments were performed with WT Sav, N118K-K121E, and S112Y-K121E as host protein (Fig. 3, A, B, and C, respectively). Because the er with up to four equivalents $RhCp^{*biotin}Cl_2(H_2O)$ remains essentially constant, we conclude that the four Sav-bound catalysts operate independently (i.e., no cooperative effect) and induce the same level of enantioselectivity. Past four equivalents and if the relative rates $k_{bound}$ and $k_{free}$ are identical, the er is expected to sharply and asymptotically decrease (orange lines in Fig. 3). The rate acceleration provided by the protein-environment can be estimated by Eq. 1

$$\%(R)\text{calculated} = \frac{k_{bound}\bullet\mu_{bound}\bullet\%(R)_{bound} + k_{free}\bullet\mu_{free}\bullet\%(R)_{free}}{k_{bound}\bullet\mu_{bound} + k_{free}\bullet\mu_{free}} \quad (1)$$

where $k_{bound}$ and $k_{free}$ are the rate constants for the Sav-bound and the free catalyst, respectively. The parameters $\mu_{bound}$ and $\mu_{free}$ are the number of Sav-bound and free catalysts (i.e., at eight equivalents, $\mu_{bound} = \mu_{free} = 4$); $\%(R)_{bound}$ and $\%(R)_{free}$ are the $\%(R)$ for the Sav-bound and the free catalyst (i.e., $\%(R)_{free} = 0.515$, Table 1, entry 1). Using Eq. 1 and performing a least-square minimization on the calculated and experimentally determined $\%(R)$ (green line and blue crosses respectively, in Fig. 3) (also see table S1), we can determine the relative rates $k_{rel} = (k_{bound})/(k_{free})$. For WT Sav, we compute a 3-fold rate acceleration compared with the protein-free catalyst. This phenomenon of protein acceleration is enhanced in the presence of carboxylate-bearing Sav isoforms: In pure water and for N118K-K121E and S112Y-K121E, we compute rate accelerations of 92 and 34, respectively. The substantially increased rate is diagnostic of the key role of the active-site carboxylate in the turnover-limiting step, which we suggest is the C–H activation event. This confirms the hypothesis that the engineered carboxylate residue within the active site is key to generating a highly active and selective artificial benzannulase.

## References and Notes


1. C. K. Savile *et al.*, *Science* **329**, 305 (2010).
2. B. Seelig, J. W. Szostak, *Nature* **448**, 828 (2007).
3. H. S. Park *et al.*, *Science* **311**, 535 (2006).
4. S. D. Khare *et al.*, *Nat. Chem. Biol.* **8**, 294 (2012).
5. D. Röthlisberger *et al.*, *Nature* **453**, 190 (2008).
6. Y. Lu, N. Yeung, N. Sieracki, N. M. Marshall, *Nature* **460**, 855 (2009).
7. T. Heinisch, T. R. Ward, *Curr. Opin. Chem. Biol.* **14**, 184 (2010).
8. G. Roelfes, *Chem. Cat. Chem.* **3**, 647 (2011).
9. P. F. Mugford, U. G. Wagner, Y. Jiang, K. Faber, R. J. Kazlauskas, *Angew. Chem. Int. Ed.* **47**, 8782 (2008).
10. N. Yeung *et al.*, *Nature* **462**, 1079 (2009).
11. Y.-W. Lin *et al.*, *Proc. Natl. Acad. Sci. U.S.A.* **107**, 8581 (2010).
12. Y.-W. Lin *et al.*, *J. Am. Chem. Soc.* **132**, 9970 (2010).
13. P. J. Deuss, R. den Heeten, W. Laan, P. C. J. Kamer, *Chem. Eur. J.* **17**, 4680 (2011).
14. A. J. Boersma, R. P. Megens, B. L. Feringa, G. Roelfes, *Chem. Soc. Rev.* **39**, 2083 (2010).
15. M. E. Wilson, G. M. Whitesides, *J. Am. Chem. Soc.* **100**, 306 (1978).
16. C.-C. Lin, C.-W. Lin, A. S. C. Chan, *Tetrahedron Asymmetry* **10**, 1887 (1999).
17. M. T. Reetz, J. J. P. Peyralans, A. Maichele, Y. Fu, M. Maywald, *Chem. Commun.* **41**, 4318 (2006).
18. M. Skander *et al.*, *J. Am. Chem. Soc.* **126**, 14411 (2004).
19. T. R. Ward, *Acc. Chem. Res.* **44**, 47 (2011).
20. T. Satoh, M. Miura, *Chem. Eur. J.* **16**, 11212 (2010).
21. N. Guimond, S. I. Gorelsky, K. Fagnou, *J. Am. Chem. Soc.* **133**, 6449 (2011).
22. S. Rakshit, C. Grohmann, T. Besset, F. Glorius, *J. Am. Chem. Soc.* **133**, 2350 (2011).
23. T. K. Hyster, T. Rovis, *J. Am. Chem. Soc.* **132**, 10565 (2010).
24. D. Lapointe, K. Fagnou, *Chem. Lett.* **39**, 1118 (2010).
25. L. Xu, Q. Zhu, G. Huang, B. Cheng, Y. Xia, *J. Org. Chem.* **77**, 3017 (2012).
26. T. Reiner, D. Jantke, A. Raba, A. N. Marziale, J. Eppinger, *J. Organomet. Chem.* **694**, 1934 (2009).
27. N. M. Green, *Methods Enzymol.* **18A**, 418 (1970).
28. After optimization, the ideal conditions with WT Sav were found to be aqueous solvent [1:4 MeOH:acetate buffer (0.67M, pH=5.9)] with a 1.3:1 ratio of Sav binding sites to biotinylated rhodium monomer, delivering product in 23% yield with 9:1 regioselectivity after 36 hours. Identical product distribution was obtained upon using $[Cp^{*biotin}Rh(H_2O)_3]^{2+}$.
29. G. M. Morris *et al.*, *J. Comput. Chem.* **30**, 2785 (2009).
30. M. T. Reetz, *Angew. Chem. Int. Ed.* **50**, 138 (2011).
31. J. Collot, N. Humbert, M. Skander, G. Klein, T. R. Ward, *J. Organomet. Chem.* **689**, 4868 (2004).


**Acknowledgments:** We thank the National Institute of General Medical Sciences (GM80442), the Swiss National Science Foundation (grant 200020-126366), the National Center of Competence in Research Nanoscale Sciences, the Marie Curie Training Network (FP7-ITN-238434), Amgen, and Roche for support. We thank Johnson Matthey for a loan of rhodium salts and C. R. Cantor for the Sav gene. We thank M. J. Zimbron for providing an initial sample of $[RhCp^{*biotin}Cl_2]_2$ and for stimulating discussions.

## Supplementary Materials

www.sciencemag.org/cgi/content/full/338/6106/500/DC1
Materials and Methods
Figs. S1 to S3
Table S1
References (*32*–*36*)

15 June 2012; accepted 21 September 2012
10.1126/science.1226132

# Chiral Cyclopentadienyl Ligands as Stereocontrolling Element in Asymmetric C–H Functionalization

Baihua Ye and Nicolai Cramer*

Metal complexes coordinated by a single cyclopentadienyl (Cp) ligand are widely used, versatile catalysts, but their application to asymmetric reactions has been hindered by the difficulty of designing Cp substituents that effectively bias the coordination sphere. Here, we report on a class of simple $C_2$-symmetric Cp derivatives that finely control the spatial arrangement of the transiently coordinated reactants around the central metal atom. Rhodium(III) complexes bearing these ligands proved to be highly enantioselective catalysts for directed carbon-hydrogen (C–H) bond functionalizations of hydroxamic acid derivatives.

Since the discovery of ferrocene 70 years ago, cyclopentadienyl (Cp)–coordinated metal complexes contributed tremendously to the rise of organometallic chemistry. Countless transition-metal complexes have been prepared with Cp itself or its most popular pentamethylcyclopentadienyl analog (Cp*), and many of them are highly efficient catalysts for a broad range of transformations (*1*). Despite such favorable characteristics as stability and robustness, Cp ligands have been largely bypassed by other classes of ligands—such as diamines, phosphines, and carbenes—as carriers of chiral bias in asymmetric catalysis (*2*). The simple Cp or Cp* motif appears often in mixed-ligand designs comprising one or more additional coordination groups responsible for the chiral environment (*3*, *4*). However, only a few chiral Cp derivatives with non-coordinating substituents, and their corresponding metal complexes, have been synthesized (*5*–*11*), and they have rarely been applied as catalysts. With the exception of the Co(I)-catalyzed cyclotrimerizations reported by Heller, Hapke, and Gutnov (*12*–*14*), no notable chiral induction has been achieved with their respective late-transition metal complexes in catalytic reactions.

This discrepancy might derive from inherent difficulties linked to the design and synthesis of chiral Cp ligand derivatives. Although representing a long-standing problem in asymmetric catalysis, it has been systematically neglected. The striking opportunities inherent in addressing these shortcomings become clear by just considering half-sandwich complexes (*15*, *16*) with a $d^6$-electron count such as Cp Rh(III), Ir(III), Ru(II), and Co(I), which catalyze a range of important reactions (*17*–*23*). Often, these reactions require that, during the catalytic cycle, all three remaining coordination sites bind substrate(s) and reactants, leaving Cp as the sole permanent ligand on the metal. This characteristic makes the development of catalytic asymmetric versions enormously challenging because selectivity stems from the arrangement of the three other ligands around the central metal. Pseudotetrahedral complexes of the type $[(\eta^5\text{-}C_5H_5)ML^1L^2L^3]$ are chiral-at-metal (*24*, *25*), arising from a face-selective approach of the third ligand $L^3$ to the fluxional 16-electron intermediate, leading without a controlling element to a racemate.

Achieving high levels of stereoselectivity for this association is a key hurdle for successful asymmetric catalysis. The facial selectivity of the ligand association must be imposed by the chiral space crafted by an enantiopure Cp congener. We identified three criteria to design catalysts for an efficient enantioselective process: (i) use of $C_2$-symmetric Cp derivatives to avoid the complicating factor of diastereomer formation in coordination of the metal to either ligand face; (ii) restriction of rotation around the Cp moiety to lock in one of two substrate alignments, which must be highly preferred over the other, as this ratio reflects the maximum attainable selectivity; and (iii) steric blocking perpendicular to the Cp plane to induce approach of the incoming reactant $R_C$ from just one side. Taking these constraining factors into account, we hypothesized that a 1,2-disubstituted Cp ligand would favor the two orientations of the small and large substrate parallel to the positional locks ($S_S$ and $S_L$, structures **A** and **B**, Fig. 1). A

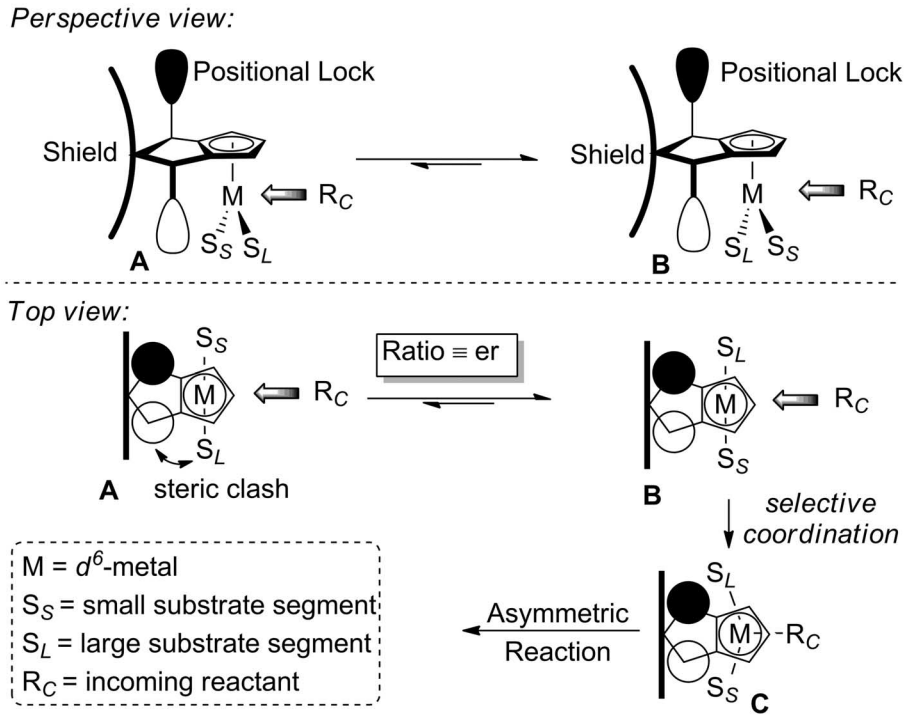


**Fig. 1.** Conceptual design of the chiral $Cp^{x*}$ complexes.

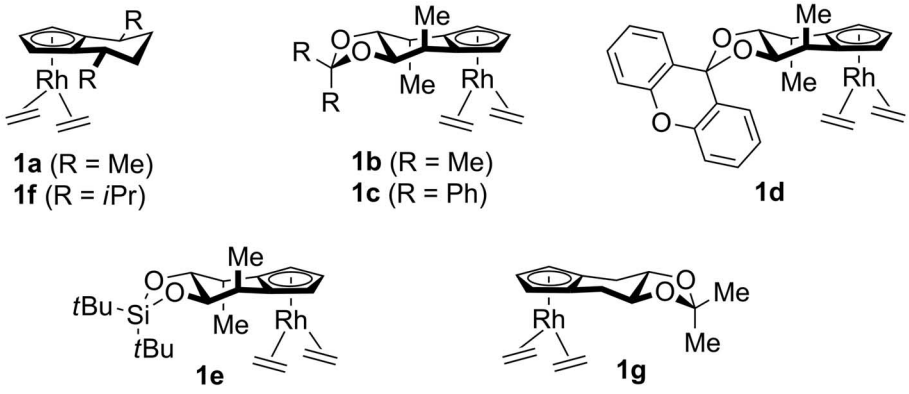


**Fig. 2.** Structure of the chiral $Cp^{x*}Rh(I)$ complexes **1a** to **1f**.

Ecole Polytechnic Fédérale de Lausanne, School of Basic Sciences, Institute of Chemical Sciences and Engineering, Laboratory of Asymmetric Catalysis and Synthesis, BCH 4305, CH-1015 Lausanne, Switzerland.

*To whom correspondence should be addressed. E-mail: nicolai.cramer@epfl.ch

bulky backbone should prevent the approach of the reactant $R_C$ from the back. The $C_2$-symmetric chiral space, illustrated by the upward- and downward-oriented positional locks, should preferentially orient the larger ligand $S_L$ away from the steric bulk and thus favoring conformer **B**. Association of $R_C$ would lead then to **C** as a single diastereomer, competent for selective downstream reactions (*26*).

We prepared a range of rhodium(I) complexes (**1a** to **1g**, Fig. 2) with different backside shielding from the corresponding $C_2$-symmetric cyclopentadiene precursors (*27*). These Rh(I) complexes are relatively air-stable and easy to handle. In keeping with our interest in C–H bond functionalization using rhodium catalysts (*28*, *29*), we chose the Cp*Rh(III)-catalyzed C–H functionalization (*30*) of hydroxamic acid derivative recently reported by Fagnou (*31*) and Glorius (*32*) as an optimal reaction to challenge the viability of our concept. In situ oxidation of complex **1** with dibenzoylperoxide (DBPO) delivered directly a competent catalyst, presumably Rh(III) *bis*-benzoate complex **5** (*33*).

Complex **1g**, bearing only remote stereochemical substitution, displayed as expected only negligible selectivity (table S1, entry 1). Installing steric bulk closer to the Cp ring improved the enantiomeric ratio (er) to 73:27 (table S1, entry 2). Unexpectedly, when the methyl group was replaced with any larger substituent—e.g., an isopropyl group—the enantioselectivity dropped sharply (table S1, entry 3). We next evaluated the influence of the rigidifying *trans*-acetal group. With the two oxygen atoms being in *syn*-relation to both methyl groups of the cyclohexene, these are forced into the pseudo-axial position, increasing the bulk near the metal center and giving increased selectivity of 90:10 er (table S1, entry 6). In addition to this conformational effect, the acetal group protects the metal from backside approach by the olefin. Different larger groups were evaluated as well, and a benzophenone acetal moiety (**1c**) proved to be optimal, providing **4aa** with 92:8 er (table S1, entry 7).

We next turned our attention to the size of the acyl substituent R of the oxygen atom of the hydroxamate substrate, which we expected would influence the ratio of the two specific orientations of the cyclometalated intermediate **7**. Several acyl and carbonate derivatives were tested, and the readily accessible Boc-derivative (R=O*t*Bu) was optimal, giving complex **1c** 96:4 er (entry 10). The high solubility of the starting Rh(I) complex allowed a wide variation of solvents with conserved selectivity (entries 12 to 15), although the yields proved highest in ethanol. The catalyst loading could be lowered to 1 mole % without diminishing the reaction performance (entry 16). The activation proceeds even at 0°C with a slightly increased selectivity (entry 17).

The scope of the reaction was explored with the optimized catalyst **1c** and is outlined in Table 1. On the olefin acceptor side, a variety of styrenes are competent reaction partners, and the observed enantioselectivity is consistently excellent (Table 1, entries 1 to 7). Some structurally and electronically different terminal and cyclic olefins were tested, performing reliably, albeit in some instances with slightly reduced enantioselectivity (entries 8 to 13). Uniquely, vinyl trimethyl silane gives **4aj** with the opposite regioselectivity (>10:1, entry 9). The process is also general for the aryl hydroxamates **2a** to **2h** and different electronic and steric variations have little influence on yield and selectivity (entries 13 to 20).

The catalytic cycle of the reaction is presumably initiated by oxidation of the $Cp^{x*}$Rh(I) complex **1** by DBPO, giving **5** (fig. S4). Based on published mechanistic studies of the racemic version of this transformation (*31*, *34*), ligand exchange binds substrate **2a**, forming **6**. Cyclometalation by concerted metalation deprotonation mechanism and loss of benzoic acid leads to the crucial cyclometalated 16-electron species **7**. In the enantioselectivity-determining step, coordination of the olefin in a highly diastereoselective manner leads to 18-electron chiral-at-metal complex **8**, and its incorporation forms **10** (*35*). With the benzoic acid present in

**Table 1.** Substrate scope of the enantioselective activation/addition.

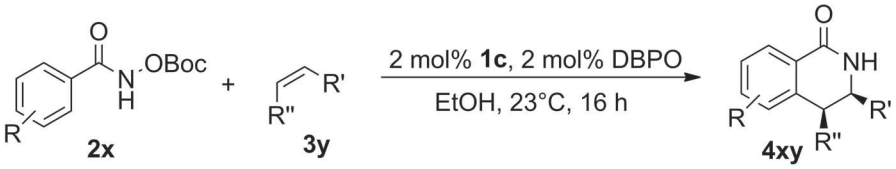


| Entry | R | R' | R'' | 4 | % yield* | er† |
|---|---|---|---|---|---|---|
| 1 | H | 3-Me-$C_6H_4$ | H | **4ab** | 91 | 95 : 5 |
| 2 | H | 4-Me-$C_6H_4$ | H | **4ac** | 89 | 96 : 4 |
| 3 | H | 4-*t*Bu-$C_6H_4$ | H | **4ad** | 91 | 95.5 : 4.5 |
| 4 | H | 4-MeO-$C_6H_4$ | H | **4ae** | 88 | 96 : 4 |
| 5 | H | 4-F-$C_6H_4$ | H | **4af** | 87 | 95.5 : 4.5 |
| 6‡ | H | 4-$CF_3$-$C_6H_4$ | H | **4ag** | 81 | 95 : 5 |
| 7‡,‖ | H | 2-naphthyl | H | **4ah** | 79 | 96.5 : 3.5 |
| 8‡ | H | C≡C-TIPS | H | **4ai** | 70 | 92 : 8 |
| 9‡ | H | H | $SiMe_3$ | **4aj** | 74 | 85 : 15 |
| 10‡ | H | 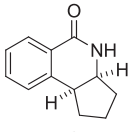 | | **4ak** | 83 | 91 : 9 |
| 11 | H | 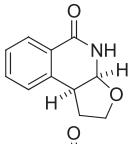 | | **4al** | 81 | 93 : 7 |
| 12‡ | H | 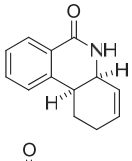 | | **4am** | 59 | 91.5 : 8.5 |
| 13 | 3-Me | 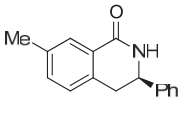 | | **4ba** | 80 | 96 : 4 |
| 14 | 4-Me | Ph | H | **4ca** | 85 | 97 : 3 |
| 15 | 4-MeO | Ph | H | **4da** | 68 | 96.5 : 3.5 |
| 16‖ | 4-$NO_2$ | Ph | H | **4ea** | 76 | 96.5 : 3.5 |
| 17 | 4-Br | Ph | H | **4fa** | 78 | 96.5 : 3.5 |
| 18 | 4-Cl | Ph | H | **4ga** | 81 | 96.5 : 3.5 |
| 19 | 4-F | Ph | H | **4ha** | 81 | 96 : 4 |
| 20 | | 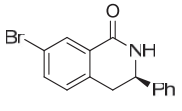 **4ia** 1 : 1.3 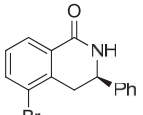 **4ia'** | | | 83 | 95 : 5 (**4ia**)<br>88.5 :11.5 (**4ia'**) |

* Isolated yields; † Determined by HPLC on a chiral stationary phase; ‡ with 5 mol% of **1c**; ‖ $CH_2Cl_2$ instead of EtOH.

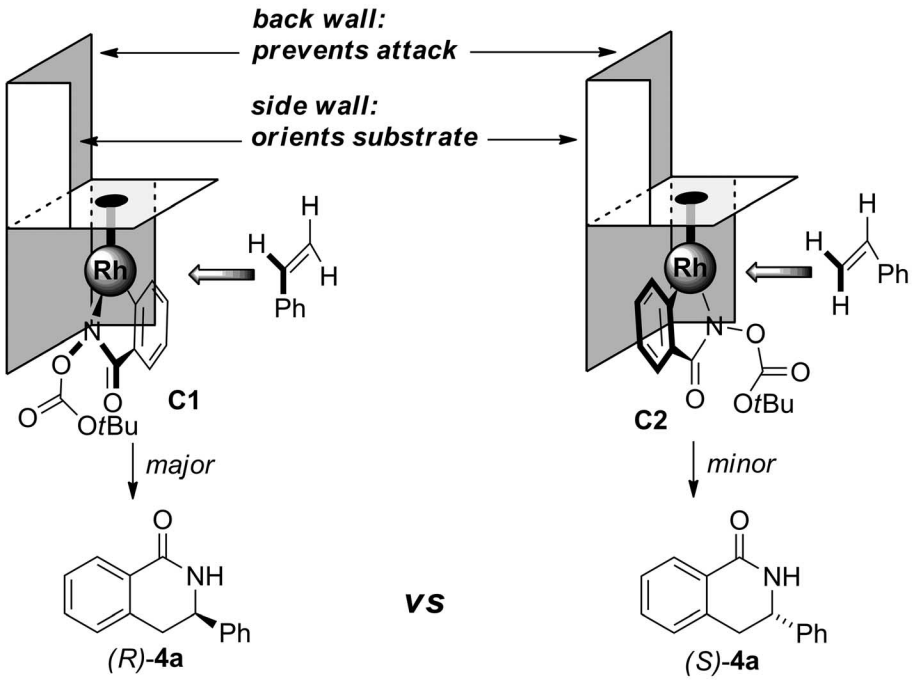


**Fig. 3.** Postulated model for the stereochemical preference with complex **1c**.

the reaction media, ligand exchange/protonation regenerates **5** and expels product **4** and *t*-butyl hydrogen carbonate, which collapses to $CO_2$ and *t*BuOH without changing the overall acidity of the medium during the course of the reaction. The absolute configuration of product **4a** was determined to be (*R*)-**4a** (*36*). The underlying selectivity of the reaction was visualized by a graphical model representing the complex **1c** (Fig. 3) (*37*). The back wall forces styrene to approach from the open face with the phenyl group oriented away from the Cp ring. Conformer **C1** having its hydroxamate moiety turned away from the steering side wall is the faster-reacting isomer, leading to (*R*)-**4a**.

In conclusion, we have described a class of chiral $Cp^{x*}$ analogs with low molecular weight that desymmetrize a rhodium(III)-catalyzed directed C–H bond functionalization. The reaction proceeds under mild conditions and is high yielding and enantioselective. This development should become a stepping-stone to unlock the potential of chiral Cp analogs as steering ligands in enantioselective late-transition metal catalysis with half-sandwich complexes.

### References and Notes


1. R. H. Crabtree, *The Organometallic Chemistry of the Transition Metals* (Wiley, New York, ed. 3, 2001).
2. E. N. Jacobsen, A. Pfaltz, H. Yamamoto, Eds., *Comprehensive Asymmetric Catalysis: Vol. I-III, Suppl. I-II,* (Springer, New York, 1999).
3. A. H. Hoveyda, J. P. Morken, *Angew. Chem. Int. Ed. Engl.* **35**, 1262 (1996).
4. U. Siemeling, *Chem. Rev.* **100**, 1495 (2000).
5. R. L. Halterman, K. P. C. Vollhardt, *Organometallics* **7**, 883 (1988).
6. R. L. Halterman, *Chem. Rev.* **92**, 965 (1992).
7. H. Schumann *et al.*, *Eur. J. Inorg. Chem.* **2002**, 211 (2002).
8. R. L. Halterman, L. D. Crow, *Tetrahedron Lett.* **44**, 2907 (2003).
9. A. Gutnov, B. Heller, H.-J. Drexler, A. Spannenberg, G. Oehme, *Organometallics* **22**, 1550 (2003).
10. A. Gutnov, H.-J. Drexler, A. Spannenberg, G. Oehme, B. Heller, *Organometallic* **23**, 1002 (2004).
11. G. P. McGlacken, C. T. O'Brien, A. C. Whitwood, I. J. S. Fairlamb, *Organometallics* **26**, 3722 (2007).
12. A. Gutnov *et al.*, *Angew. Chem. Int. Ed.* **43**, 3795 (2004).
13. B. Heller *et al.*, *Chemistry* **13**, 1117 (2007).
14. M. Hapke *et al.*, *J. Org. Chem.* **75**, 3993 (2010).
15. Sandwich complexes containing two Cp moieties such as *ansa*-ebthi metallocenes of Ti, Zr, or Hf are versatile catalysts for several asymmetric reactions. For an overview, see (*16*).
16. A. H. Hoveyda, J. P. Morken, *Angew. Chem. Int. Ed. Engl.* **35**, 1262 (1996).
17. C. P. Lenges, M. Brookhart, *J. Am. Chem. Soc.* **119**, 3165 (1997).
18. H. Chen, S. Schlecht, T. C. Semple, J. F. Hartwig, *Science* **287**, 1995 (2000).
19. J. F. Hartwig *et al.*, *J. Am. Chem. Soc.* **127**, 2538 (2005).
20. B. M. Trost, M. U. Frederiksen, M. T. Rudd, *Angew. Chem. Int. Ed.* **44**, 6630 (2005).
21. A. H. Roy, C. P. Lenges, M. Brookhart, *J. Am. Chem. Soc.* **129**, 2082 (2007).
22. A. D. Bolig, M. Brookhart, *J. Am. Chem. Soc.* **129**, 14544 (2007).
23. M. Zhou, N. D. Schley, R. H. Crabtree, *J. Am. Chem. Soc.* **132**, 12550 (2010).
24. H. Brunner, *Angew. Chem. Int. Ed.* **38**, 1194 (1999).
25. E. B. Bauer, *Chem. Soc. Rev.* **41**, 3153 (2012).
26. Although Fig. 1 depicts solely the differences of the two most stable conformers, we assume that reactions proceed under Curtin-Hammett conditions. Therefore, no judgment on the reactive conformer, the one with a lower transition state, is possible.
27. Materials and methods are available as supplementary materials on *Science* Online. For the syntheses and an x-ray structure of **1c**, see figs. S1 to S3.
28. D. N. Tran, N. Cramer, *Angew. Chem. Int. Ed.* **49**, 8181 (2010).
29. D. N. Tran, N. Cramer, *Angew. Chem. Int. Ed.* **50**, 11098 (2011).
30. G. Song, F. Wang, X. Li, *Chem. Soc. Rev.* **41**, 3651 (2012).
31. N. Guimond, S. I. Gorelsky, K. Fagnou, *J. Am. Chem. Soc.* **133**, 6449 (2011).
32. S. Rakshit, C. Grohmann, T. Besset, F. Glorius, *J. Am. Chem. Soc.* **133**, 2350 (2011).
33. Related Cp*Rh(III) *bis*-carboxylate complexes are most likely the active catalytic species in the racemic reaction and are usually generated in situ from $\{[Cp^*Rh(Cl_2)]_2\}$ by silver salts and carboxylate additives.
34. D. Lapointe, K. Fagnou, *Chem. Lett.* **39**, 1118 (2010).
35. L. Xu, Q. Zhu, G. Huang, B. Cheng, Y. Xia, *J. Org. Chem.* **77**, 3017 (2012).
36. F. A. Davis, Y. W. Andemichael, *J. Org. Chem.* **64**, 8627 (1999).
37. J. A. Gladysz, B. J. Boone, *Angew. Chem. Int. Ed. Engl.* **36**, 550 (1997).


**Acknowledgments:** This work is supported by the European Research Council (ERC) under the European Community's Seventh Framework Program (FP7 2007–2013)/ERC Grant agreement 257891. We thank R. Scopelliti for x-ray crystallographic analysis of **1c**. CCDC 898196 contains the crystallographic data for **1c**. These data can be obtained free of charge from the Cambridge Crystallographic Data Centre, www.ccdc.cam.ac.uk/data_request/cif.

### Supplementary Materials

www.sciencemag.org/cgi/content/full/338/6106/504/DC1
Materials and Methods
Figs. S1 to S3
References (*38*–*43*)

4 July 2012; accepted 10 September 2012
10.1126/science.1226938

# Fluorescence Enhancement at Docking Sites of DNA-Directed Self-Assembled Nanoantennas

**G. P. Acuna,* F. M. Möller, P. Holzmeister, S. Beater, B. Lalkens, P. Tinnefeld***

We introduce self-assembled nanoantennas to enhance the fluorescence intensity in a plasmonic hotspot of zeptoliter volume. The nanoantennas are prepared by attaching one or two gold nanoparticles (NPs) to DNA origami structures, which also incorporated docking sites for a single fluorescent dye next to one NP or in the gap between two NPs. We measured the dependence of the fluorescence enhancement on NP size and number and compare it to numerical simulations. A maximum of 117-fold fluorescence enhancement was obtained for a dye molecule positioned in the 23-nanometer gap between 100-nanometer gold NPs. Direct visualization of the binding and unbinding of short DNA strands, as well as the conformational dynamics of a DNA Holliday junction in the hotspot of the nanoantenna, show the compatibility with single-molecule assays.

Single-molecule fluorescence measurements report on kinetic processes without the need for synchronization, lifetimes of intermediates, structure, stoichiometry of subpopulations, and the choreography of biomolecular processes (*1*, *2*). Yet, only a small number

of successful commercial applications, such as real-time single-molecule sequencing and single-molecule–based super-resolution imaging, have emerged that rely on single-molecule detection (*3*, *4*). Single-molecule fluorescence applications pose two major limitations including (i) the concentration range of the fluorescent species suitable for single-molecule detection (typically in the picomolar to nanomolar regime) and (ii) the high brightness and photostability requirements for the fluorescent marker.

The field of nanophotonics offers several solutions to overcome both the concentration limitation and the brightness requirement. Circular holes of 50- to 200-nm diameter in a metal cladding film deposited on a transparent substrate (so called zero-mode waveguides), for example, reduce the observation volumes and enable monitoring of enzymatic reactions at high substrate concentration (*5*). This technique led to the visualization of transcription and translation at the single-molecule level (*3*, *6*). However, the production and handling of these nanophotonics structures is costly and serial by nature. Because molecules are not specifically placed in the center of the structures, they undergo varying levels of fluorescence quenching because of the distribution of distances to the metallic walls yielding heterogeneous signals. Furthermore, zero-mode waveguide occupancy is limited by Poissonian statistics to a fraction of the waveguides to guarantee that only one molecule is present within one hole.

Besides the exclusion of light in zero-mode waveguides, metallic nanostructures can also enhance fluorescence by creating plasmonic nanoantennas that highly enhance local fields (*7*, *8*). Lithographically fabricated nanoantennas not only enhance the excitation field in a very small volume but can also direct single-molecule emission (*9*) and increase quantum yields for the detection of low–quantum yield dyes (*10*, *11*). Again, demanding nanolithography is required, and the problem remains how to place the molecules of interest with nanometer accuracy in the hotspot of the antenna structure (*7*). Current approaches to fabricate fluorescence enhancing structures via self-assembly or wet chemical synthesis do not achieve the required structural control, cannot provide docking sites in the hotspot, and fail to provide a reliable stoichiometry control for particles bigger than 40 nm (*12*–*15*).

In this work, we used a self-assembly scheme based on the DNA origami technique (*16*, *17*) to construct nanoantennas with docking sites (NADS) for biomolecular assays. The DNA origami allows a precise arrangement of dimers of arbitrary size at a defined interparticle distance, a docking site for objects of interest in the plasmonic hotspot between gold nanoparticles (Au NPs), as well as specific attachment sites for surface immobilization. Based on this platform, we studied the fluorescence enhancement by Au NPs of different size. The docking sites serve for placement of single-dye molecules or biomolecular assays such as a DNA binding assay or a Holliday junction.

A three-dimensional, pillar-shaped DNA origami (Fig. 1A) was folded from one M13mp18-derived scaffold strand and 207 staple strands [see supplementary materials and methods for experimental details (*18*)]. The DNA origami pillar has a length of 220 nm, a 15-nm diameter consisting of a 12-helix bundle, and three extra 6-helix bundles on the base, leading to a base diameter of 30 nm. The base contains 15 biotin-modified staple strands for selective immobilization of the pillar on cover slips coated with biotinylated bovine serum albumin and neutravidin (lower-right inset of Fig. 1A). During hybridization, a dye-labeled strand (ATTO647N) and three to six capturing strands (original staple strands extended by an extra 15 bases) were additionally incorporated at the half height of the pillar (see upper-right inset of Fig. 1A and fig. S1). After immobilization, DNA functionalized Au NPs were bound to the pillar by hybridization to the capturing strands (*18*). We used three capturing strands per Au NP to increase the rigidity of the interaction between DNA origami and Au NPs (*19*). This procedure minimizes sample consumption and avoids aggregation, even for large particles (*19*). The DNA origami design enables the alignment of the NADS with respect to the electric field polarization.

Plasmonic nanostructures create highly enhanced local fields, which can lead to fluorescence brightness enhancement, depending on how the excitation as well as the radiative and nonradiative rates of the fluorescent dye are influenced (*20*). In general, a stronger enhancement occurs for larger NPs; additionally, the enhancement is more pronounced if the spacing between the two Au NPs is reduced (*21*, *22*). We designed a gap of 23 nm between the NPs as a compromise of strong fluorescence enhancement and sufficient space for accommodation of a biomolecular assay. We used numerical simulations to estimate the influence of single metallic NPs and NP dimers on the excitation and emission of single fluorescent dyes. Figure 1B shows the normalized electric field intensity at the equator plane of a monomer (left) and dimer (right) when illuminated with a plane wave from below at the laser excitation wavelength of 640 nm. In our arrangement, the fluorescence brightness enhancement of a dye placed in the vicinity of a NP system can be approximated by the product of the quantum yield enhancement and the normalized electric field intensity enhancement (*21*, *23*). A single 80-nm NP, for example, is expected to induce a maximum fluorescence enhancement of 10-fold relative to the unperturbed dye, and a plateau with an enhancement around 115 is simulated for a dye with radial orientation in the gap of a dimer with 23-nm separation (Fig. 1C). Very close to the NP, the fluorescence intensity drops to nearly zero because quenching dominates (*21*).

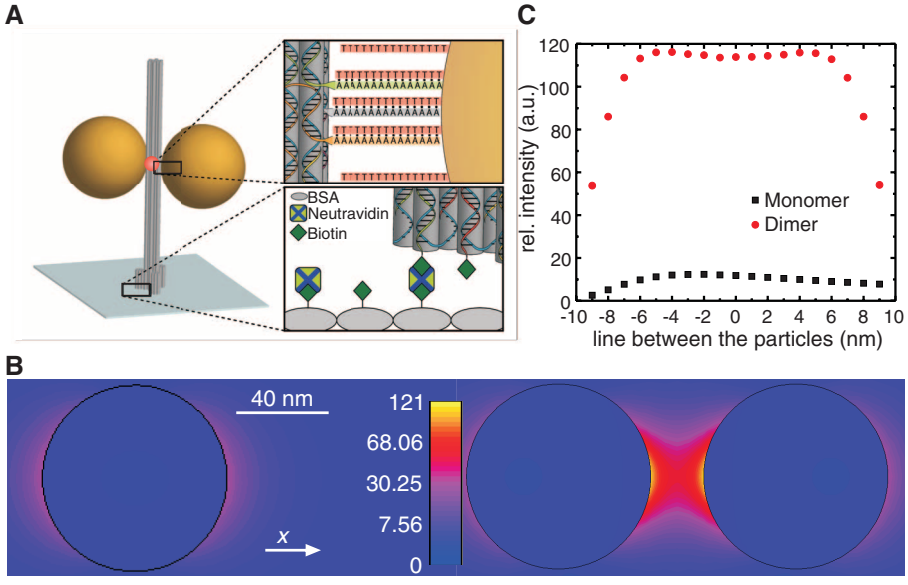


**Fig. 1.** (**A**) Sketch of the DNA origami pillar with two Au NPs forming a dimer. The dye (red sphere) is located between the NPs within the central bundle of the pillar. (Upper right inset) Binding of the NP to the DNA origami structure through three capturing strands. (Lower right inset) Binding of DNA origami to the neutravidin functionalized cover slip. BSA, bovine serum albumin. (**B**) Numerical simulation of electric field intensity for a monomer (left) and dimer (right) for 80-nm-diameter gold NPs and an interparticle spacing of 23 nm (dimer). The incoming light was horizontally polarized at a wavelength of 640 nm. (**C**) Numerical simulations of the fluorescence enhancement along the gap connecting the NPs for a dye oriented in the radial direction. a.u., arbitrary units.

NanoBioSciences Group, Institute for Physical and Theoretical Chemistry, Technische Universität Braunschweig, Hans-Sommer-Strasse 10, 38106 Braunschweig, Germany.

*To whom correspondence should be addressed. E-mail: g.acuna@tu-bs.de (G.P.A.); p.tinnefeld@tu-bs.de (P.T.)

We used a 640-nm pulsed diode laser with circular polarization to excite fluorescence from the ATTO647N molecules in a custom-built confocal microscope. Figure 2A shows a fluorescence image of a low concentration of self-assembled nanoantennas with capturing strands for two 80-nm Au NPs. The image exhibits spots of a broad range of intensities and sometimes fluorescence intermittencies, which indicates the presence of a single fluorescent dye for even the brightest spots. We used phosphate buffered saline as the solvent, because ATTO647N exhibits pronounced blinking and moderate photostability so that single-molecule emission is readily visualized (*24*). The fluorescence transients shown in Fig. 2, B to D, were recorded from a dim spot, a spot with intermediate intensity, and a bright spot, as indicated in the image of Fig. 2A. All three dye molecules showed single-step photobleaching and revealed markedly different average intensities of 3.5, 11, and 200 kHz, respectively. The 3.5-kHz intensity was the typical fluorescence count rate of ATTO647N attached to the DNA origami pillar without NPs at otherwise identical conditions. The assignment of the dim spots to DNA origami pillars without NPs is supported by the long fluorescence lifetime of 3.80 ns, typical for ATTO647N (inset of Fig. 2B). The molecules depicted in Fig. 2, C and D, are substantially brighter and exhibit reduced fluorescence lifetimes of 1.17 and 0.22 ns obtained by deconvolution with the instrument response function [see fluorescence decays in the insets of Fig. 2, C and D (*18*)]. These transients represent emission from NADS carrying one and two gold NPs, respectively.

To further study the effect of the NPs on the fluorescent dyes and to substantiate our assignment to the number of NPs, we analyzed the emitted intensities and fluorescence lifetimes of several images for NADS samples with one and two binding sites for 80-nm gold NPs (Fig. 3). The sample with one binding site for Au NPs exhibits two maxima in the fluorescence lifetime histogram (Fig. 3A). The long fluorescence lifetime represents DNA origami pillars without a NP, and the population with a fluorescence lifetime with a maximum at 1.0 ns represents the population with one Au NP (Fig. 3A, red data points). The sample with two NP binding sites exhibits an additional maximum at 0.2 ns that we assign to DNA origami pillars with two NPs bound. Classification of molecules and the correlation of the fluorescence intensity and the fluorescence lifetime (Fig. 3A) directly show that fluorescent dyes bound to NADS with one NP were substantially brighter than ordinary ATTO647N dye molecules. NADS with two NPs provoke an even stronger fluorescence enhancement.

For quantifying the fluorescence brightness enhancement, we sorted the spots from the intensity lifetime plots by the number of NPs into separate intensity histograms as indicated in Fig. 3A. The average intensity of the population without NPs served as an internal reference to which the intensity of the other populations was normalized. This possibility for internal referencing and the ability to separate subpopulations were also the reasons why we did not aim for 100% binding efficiency of NPs to NADS, although we obtained higher binding efficiencies by longer incubation with higher NP concentrations (see fig. S2). Analogous results of the average fluorescence enhancement with specified NP diameters of 20, 40, 60, 80, and 100 nm (experimentally determined diameters were 19.4 ± 1.7, 43.5 ± 4.6, 61.5 ± 7.0, 80.1 ± 7.4, and 105 ± 10.4 nm; see fig. S3 for particle characterization) are shown in Fig. 3B for monomers and in Fig. 3C for dimers. For the smallest NPs, a reduction in the fluorescence brightness is observed, whereas for the bigger NPs, a clear enhancement occurred (*21*). For the 100-nm NPs, the average fluorescence brightness enhancement is 8-fold for the monomer and 28-fold for the dimer, with some dimers exhibiting more than 100-fold enhancement (see fig. S4). The distribution of enhancement factors is ascribed to the inhomogeneity of the Au NPs in size, shape, and distance, as well as to a possible deviation of the DNA origami pillar from vertical orientation on the surface.

To compare the measured enhancement with theoretical expectations, we performed numerical simulations (Fig. 1, B and C). These simulations determined the fluorescence enhancement for a radial and tangential orientation of the dye's transition dipole (Fig. 3, B and C). In the first case, we observed a slight increase in the relative quantum yield accompanied by a drastic reduction in the fluorescence lifetime (fig. S5). For the tangential orientation, the relative quantum yield was dramatically decreased, whereas the lifetime was only slightly reduced. Because of the nature of the experiment, the dipole moment of the fluorophore was randomly oriented and rotating. ATTO647N attached to DNA had a typical rotational correlation time of 0.8 ns (*25*), which is of similar magnitude as the decay rates in the NADS. Thus, the probability of absorption and decay was biased toward radially oriented dyes, and a quickly rotating dye would show fluorescence enhancement resembling the results of the radial rather than the tangential simulation, with the simulation for the radial (or tangential) orientation representing an upper (or lower) enhancement limit. This upper limit is in good agreement with the highest measured values for each NP diameter, and we expect that the average measured values fall between the simulations for the radial and tangential dye orientation (Fig. 3, B and C).

We demonstrate the biocompatibility of the NADS by a transient DNA binding as well as a single-molecule fluorescence resonance energy transfer (FRET) assay. First, we observed binding and unbinding of single-stranded DNA (ssDNA) to the hotspot created by the NP dimer (*26*). For this reason, we modified the previous DNA origami pillar by replacing the ATTO647N dye inside the DNA bundle by five ssDNA strands (nine base pairs long) attached to the central bundle in the hotspot (Fig. 4A and fig. S1). We visualized binding and unbinding of single ATTO655-labeled counterstrands at a concentration of 100 nM (*26*). Figure 4B shows a fluorescence intensity transient in which the background of the freely diffusing, complementary strands has been subtracted, and the remaining intensity is normalized to the intensity of a single ATTO655 dye in the absence of NPs (the ordinate directly reports on the fluorescence enhancement). Short fluorescence bursts report on transient binding of the labeled ATTO655 strand to one of the protruding DNA strands in the hotspot of the NADS, showing that biomolecular interaction can be visualized at the docking sites of the NADS.

To demonstrate that the fluorescence bursts were related to the nanoantenna, we rotated linear excitation polarization at a frequency of 50 Hz using an electro-optical modulator. The zoom in Fig. 4C reveals binding events with a relative intensity enhancement of 60-fold. A further zoom

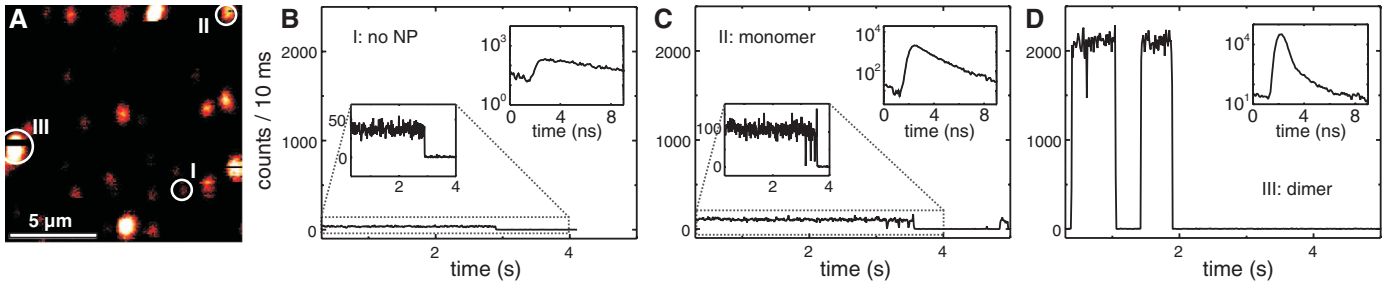


**Fig. 2.** (**A**) Confocal fluorescence image of NADS with binding sites for two NPs. Three spots with different intensities are highlighted: I (no NP), II (one NP), and III (two NPs). (**B** to **D**) Corresponding intensity transients together with their fluorescence decays (insets).

in Fig. 4D shows the effect of the rotating incident electric field polarization. Whereas a single fluorophore wiggling and rotating around the linker commonly exhibits fluorescence independent of the excitation polarization, the plasmon coupling depends strongly on the relative orientation of the incident light field, NP, and dye. At the hotspot of the dimer, an enhancement of the electric field occurs when the incident electric field is parallel to the dimer (Fig. 1B), leading to the highest fluorescence signal. As the polarization rotated, the plasmon coupling between the NPs decreased, as did the enhancement of the electric field and the fluorescence signal until the perpendicular orientation was reached, leading to a minimum.

In a single-molecule FRET assay, we visualized fluctuation of a Holliday junction (HJ) (*27*) bound to the hotspot of a dimer NADS (Fig. 4E and fig. S1). The HJ was directly incorporated to the DNA origami structure as in (*28*) and was labeled with Cy3 and Cy5 dyes (*18*). The anticorrelated intensity changes of the green (donor excitation/donor emission) and red (donor excitation/acceptor emission) detection channels shown in Fig. 4F directly reflected the HJ conformational dynamics in the presence of 100 mM magnesium (*27*). In addition, we used the intensity transient of direct acceptor excitation to estimate fluorescence enhancement as well as fluorescence lifetime (inset in Fig. 4F). Transients with a NP dimer bound such as the HJ depicted in Fig. 4G showed similar fluctuations at much higher fluorescence count rates. Despite faster bleaching at higher count rates, switching between the two conformations occurred at a similar rate of 3 Hz.

NADS created fluorescence enhancement in ultrasmall hotspots in the zeptoliter range that could be used for single-molecule detection at elevated dye concentrations. Additional time-gated detection making use of the difference of the fluorescence lifetimes inside and outside of the hotspot could almost fully recover

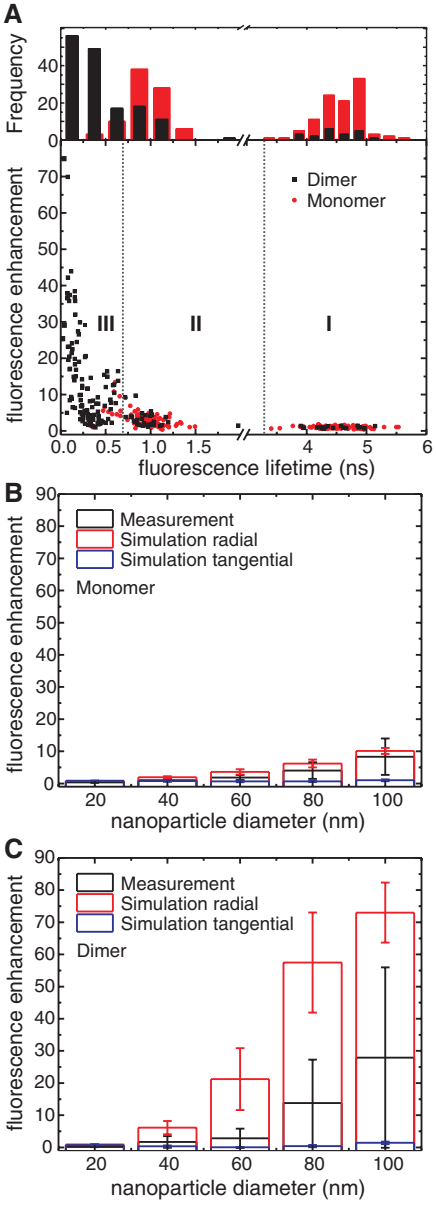


**Fig. 3.** (**A**) Scatter plot of fluorescence intensity versus lifetime with a corresponding lifetime histogram of the ATTO647N-labeled DNA origami pillar with binding sites for one (monomer) and two (dimer) particles. Au NPs with 80-nm diameters were used. Based on the lifetime, three populations are identified. The mean fluorescence enhancement (normalized) for different NP sizes, together with numerical simulations assuming a radial or tangential orientation of the dye's dipole, is shown for a monomer (**B**) and a NP dimer (**C**). Error bars indicate the SD for the measurements and consider the size distribution of NPs for the simulations.

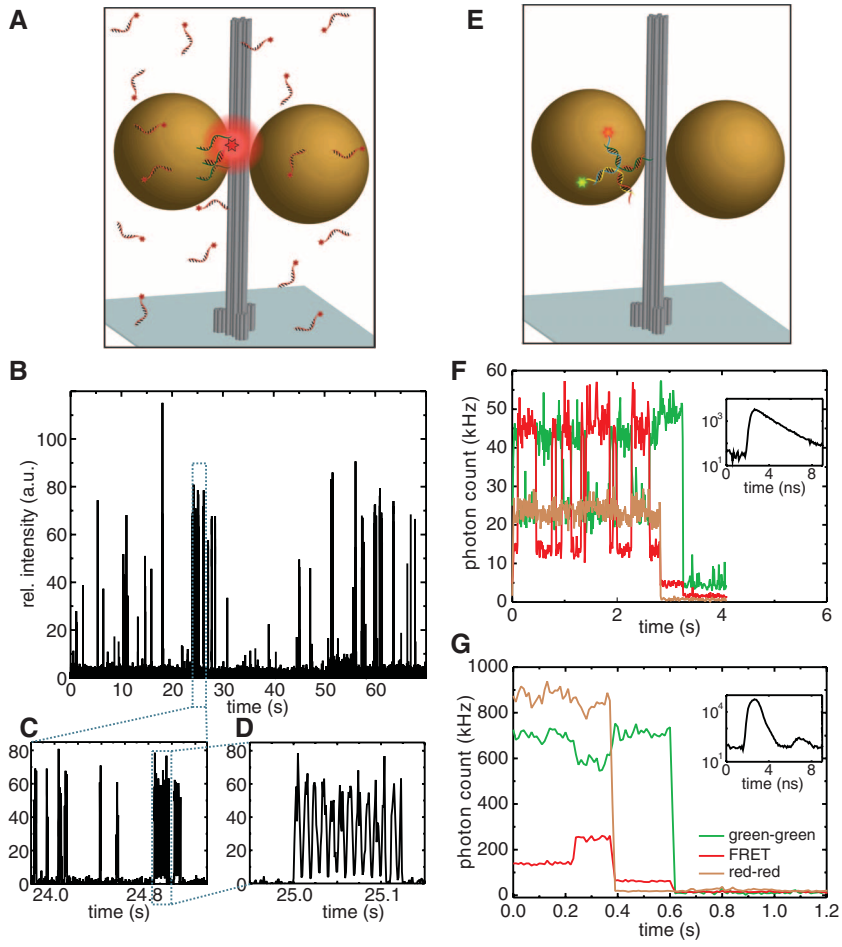


**Fig. 4.** (**A**) Sketch of the modified DNA pillar for the DNA binding assay. ssDNA sequences modified with ATTO655 (red) at 100 nM transiently hybridize with complimentary sequences (green) at the hotspot between the NPs. (**B**) Fluorescence intensity transient showing several binding and unbinding events on a DNA origami pillar with two NPs. Background was subtracted, and the intensity was normalized to the fluorescence without NPs. (**C** and **D**) Enlarged views reveal the magnitude of enhancement, as well as the effect of rotating linear excitation polarization. (**E**) Sketch of the DNA origami dimer with an incorporated HJ labeled with green and red dyes. Fluorescent intensity and FRET transients show oscillations of the HJ for a pillar with no NPs (**F**) and a NP dimer (**G**). The green, red, and brown transients represent donor excitation/donor emission, donor excitation/acceptor emission (FRET), and acceptor excitation/acceptor emission, respectively. Fluorescence decays of acceptor excitation/acceptor emission are shown in the insets.

the signal-to-noise ratio at close to micromolar concentrations (fig. S6). Alternatively, very fast kinetics—for example, in protein folding—could be resolved if the signal was large enough (*29*). Increasing the excitation power to only 7 μW (10 kW/cm$^2$) yielded fluorescence signals of up to 10.6 MHz, allowing the direct visualization of 10-μs blinking events (see fig. S7).

Self-assembled nanoantennas with docking sites based on DNA origami scaffolds represent an inexpensive and versatile platform to study plasmonic effects of metallic NP systems. The approach offers a simple solution to one of the urgent needs, that is, the ability to couple optical sources to nanoantennas. We have studied the dependence of the fluorescence intensity and lifetime of single dyes placed in the vicinity of gold NP monomers and dimers of varying sizes. We achieved fluorescence enhancement of up to 117-fold for 100-nm dimers that enables higher count rates in single-molecule applications and relaxes the requirements for single-molecule–compatible fluorescent dyes. Our results are in good agreement with numerical simulations and show that substantial fluorescence enhancement can be achieved, even at an interparticle distance of 23 nm that allows for the accommodation of biomolecular assays. The reduction of the hot-spot size far beyond diffraction-limited dimensions and the improved signal-to-noise ratio pave the way for sensor applications and nanoscale light control and extend the concentration range of single-molecule measurements toward the biologically relevant micromolar regime.

### References and Notes


1. C. Joo, H. Balci, Y. Ishitsuka, C. Buranachai, T. Ha, *Annu. Rev. Biochem.* **77**, 51 (2008).
2. P. Tinnefeld, M. Sauer, *Angew. Chem. Int. Ed.* **44**, 2642 (2005).
3. J. Eid *et al.*, *Science* **323**, 133 (2009).
4. B. Huang, H. Babcock, X. Zhuang, *Cell* **143**, 1047 (2010).
5. M. J. Levene *et al.*, *Science* **299**, 682 (2003).
6. S. Uemura *et al.*, *Nature* **464**, 1012 (2010).
7. L. Novotny, N. van Hulst, *Nat. Photonics* **5**, 83 (2011).
8. J. A. Schuller *et al.*, *Nat. Mater.* **9**, 193 (2010).
9. T. H. Taminiau, F. D. Stefani, F. B. Segerink, N. F. van Hulst, *Nat. Photonics* **2**, 234 (2008).
10. A. G. Curto *et al.*, *Science* **329**, 930 (2010).
11. A. Kinkhabwala *et al.*, *Nat. Photonics* **3**, 654 (2009).
12. M. Ringler *et al.*, *Phys. Rev. Lett.* **100**, 203002 (2008) and references therein.
13. H. Lin *et al.*, *ChemPhysChem* **13**, 973 (2012) and references therein.
14. H. Cang *et al.*, *Nature* **469**, 385 (2011) and references therein.
15. M. P. Busson, B. Rolly, B. Stout, N. Bonod, S. Bidault, *Nat. Commun.* **3**, 962 (2012) and references therein.
16. P. W. Rothemund, *Nature* **440**, 297 (2006).
17. S. M. Douglas *et al.*, *Nature* **459**, 414 (2009).
18. See the supplementary materials on *Science* Online.
19. G. P. Acuna *et al.*, *ACS Nano* **6**, 3189 (2012).
20. E. A. Coronado, E. R. Encina, F. D. Stefani, *Nanoscale* **3**, 4042 (2011).
21. P. Anger, P. Bharadwaj, L. Novotny, *Phys. Rev. Lett.* **96**, 113002 (2006).
22. A. Bek *et al.*, *Nano Lett.* **8**, 485 (2008).
23. S. Kühn, U. Håkanson, L. Rogobete, V. Sandoghdar, *Phys. Rev. Lett.* **97**, 017402 (2006).
24. J. Vogelsang *et al.*, *Angew. Chem. Int. Ed.* **47**, 5465 (2008).
25. N. Di Fiori, A. Meller, *Biophys. J.* **98**, 2265 (2010).
26. R. Jungmann *et al.*, *Nano Lett.* **10**, 4756 (2010).
27. S. A. McKinney, A.-C. Déclais, D. M. J. Lilley, T. Ha, *Nat. Struct. Biol.* **10**, 93 (2003).
28. A. Gietl, P. Holzmeister, D. Grohmann, P. Tinnefeld, *Nucleic Acids Res.* **40**, e110 (2012).
29. H. S. Chung, K. McHale, J. M. Louis, W. A. Eaton, *Science* **335**, 981 (2012).


**Acknowledgments:** We thank A. Gietl, J. J. Schmied, D. Grohmann, T. Liedl, and F. Stefani for fruitful discussion; A. Tiefnig for sample preparation; F. Demming for assistance with the numerical simulations; and S. Carregal Romero for the transmission electron microscopy images. This work was carried out at the NanoBioScience group, Braunschweig University of Technology, and was supported by a starting grant (SiMBA) of the European Research Council, the Volkswagen Foundation, and the Center for NanoScience. Technische Universität Braunschweig, G.P.A., and P.T. have filed a provisional patent application, EP1260316.1., on the described method of creating hotspots using self-assembled DNA origami.

### Supplementary Materials

www.sciencemag.org/cgi/content/full/338/6106/506/DC1
Materials and Methods
Figs. S1 to S9
Table S1
References (*30*–*34*)

9 August 2012; accepted 25 September 2012
10.1126/science.1228638

# Feathered Non-Avian Dinosaurs from North America Provide Insight into Wing Origins

**Darla K. Zelenitsky,[1]* François Therrien,[2]* Gregory M. Erickson,[3] Christopher L. DeBuhr,[1] Yoshitsugu Kobayashi,[4] David A. Eberth,[2] Frank Hadfield[5]**

**Previously described feathered dinosaurs reveal a fascinating record of feather evolution, although substantial phylogenetic gaps remain. Here we report the occurrence of feathers in ornithomimosaurs, a clade of non-maniraptoran theropods for which fossilized feathers were previously unknown. The *Ornithomimus* specimens, recovered from Upper Cretaceous deposits of Alberta, Canada, provide new insights into dinosaur plumage and the origin of the avian wing. Individuals from different growth stages reveal the presence of a filamentous feather covering throughout life and winglike structures on the forelimbs of adults. The appearance of winglike structures in older animals indicates that they may have evolved in association with reproductive behaviors. These specimens show that primordial wings originated earlier than previously thought, among non-maniraptoran theropods.**

Non-avian dinosaurs have been found in a variety of sediments worldwide, but skeletons with well-preserved feathers have been restricted to fine-grained deposits, primarily the Upper Jurassic and Lower Cretaceous lacustrine deposits of Liaoning, China (*1*–*8*). Although feathered dinosaur specimens have helped substantiate the dinosaurian origin of birds (*2*, *3*, *9*–*12*), their restricted occurrence has left notable gaps in the record of early feather evolution, particularly among non-maniraptoran theropods (such as Ornithomimosauria or Carnosauria). Here we report on the presence of feathers in ornithomimosaurs (bird-mimic dinosaurs), based on specimens found in Upper Cretaceous fluvial channel deposits of Alberta, Canada, a discovery that expands the known phylogenetic, depositional, and geographic range of feathered non-avialans. Three skeletons, referable to juvenile and adult *Ornithomimus edmontonicus* (*8*), and housed at the Royal Tyrrell Museum of Palaeontology (TMP), collectively preserve evidence of filamentous and shafted feathers in this taxon. This occurrence of feathered non-avian dinosaurs in North America reveals the nature of ornithomimosaur plumage, provides insight into the origin of wings in Theropoda, and demonstrates new potential for the discovery of well-preserved feathered dinosaur specimens in fluvial (coarser-grained) deposits.

Two of the *Ornithomimus* specimens preserve filamentous feathers [type 1 or 2 feathers (*11*, *12*)]. The first is the partial skeleton (TMP 2009.110.1) of a young juvenile (~1 year old) (*8*), which has filaments covering the axial and appendicular skeleton (Fig. 1). These integumentary structures, morphologically similar to the primitive filamentous feathers described in the Liaoning theropods (*1*, *2*), are preserved as a dense array of hundreds of filaments in a thin (up to 2 mm) ferruginous coating that follows

[1]Department of Geoscience, University of Calgary, Calgary, Alberta T2N 1N4, Canada. [2]Royal Tyrrell Museum of Palaeontology, Drumheller, Alberta T0J 0Y0, Canada. [3]Department of Biological Science, Florida State University, Tallahassee, FL 32306–4295, USA. [4]Hokkaido University Museum, Hokkaido University, Sapporo, Hokkaido 060 0810, Japan. [5]Palcoprep, Drumheller, Alberta T0J 0Y0, Canada.

*To whom correspondence should be addressed. E-mail: dkzeleni@ucalgary.ca (D.K.Z.); francois.therrien@gov.ab.ca (F.T.)

the three-dimensional (3D) contour of the body (Fig. 1, D to F). These structures (up to 50 mm in length and 0.5 mm in width) drape ventrally over the left side, perpendicular to the vertebral column, and run parallel or subparallel to one another. They are curved or contorted on some areas of the body, indicating that the original structures were supple (Fig. 1, D and F, and figs. S1 and S2). On the distal forelimbs, the filaments are shorter (up to 15 mm) than those on the body, and part at a low angle along the midline (Fig. 1E and fig. S3). Many of the filaments on the right manus show a central calcite streak (Fig. 1E and fig. S4), which indicates that the structures had a hollow core, as proposed for primitive filamentous feathers (*1*, *8*, *11*, *13*, *14*). The preservation of feathers within a ferruginous residue in a sandstone represents a previously undescribed preservational mode for non-avian feathers; however, other dinosaur soft tissues have been found associated with such residues (*15*–*17*).

A second specimen (TMP 2008.70.1) is an incomplete adult skeleton lacking forelimbs (*8*), which displays filamentous feathers preserved as faint 2D carbonized traces along the neck, back, and anterior thorax (Fig. 2). The filaments, morphologically similar to those of TMP 2009.110.1 and the Liaoning theropods (*1*, *2*), measure up to 50 mm long and 0.5 mm wide (*8*). They are in close contact with the bone on the ventral side of the skeleton and start approximately 20 mm from the bone on the dorsal side. Their orientation varies from subparallel to 50° relative to the bone surfaces, and their curvature indicates that the original structures were supple (Fig. 2B). Feather preservation resembles that of the Liaoning theropods (*1*, *2*), although the filaments in TMP 2008.70.1 are faint, sparsely distributed, and preserved in a sandstone matrix.

Evidence of shafted feathers {i.e., feathers with a rigid shaft, with or without interlocking barbules [type 3 feathers or higher (*11*, *12*)]} is preserved on the forelimb bones of an adult *Ornithomimus* skeleton (TMP 1995.110.1, Fig. 3). This specimen has an array of approximately 70 2D carbonized traces [a common preservational style for feathers (*8*, *18*, *19*)] as linear markings on the surfaces of the ulna and radius (Fig. 3, B and C). The markings on the ulna are located on the dorsal and posterior sides and change orientation gradually along its length, from posterodistally near the proximal end to longitudinally toward the distal end, whereas those on the radius are located on the dorsal side and are all oriented anterodistally. Their distribution and orientation are similar to the insertion pattern of covert feathers (*20*, *21*), which form the bulk of the feather covering in modern bird wings. The shapes of the individual markings are consistent with

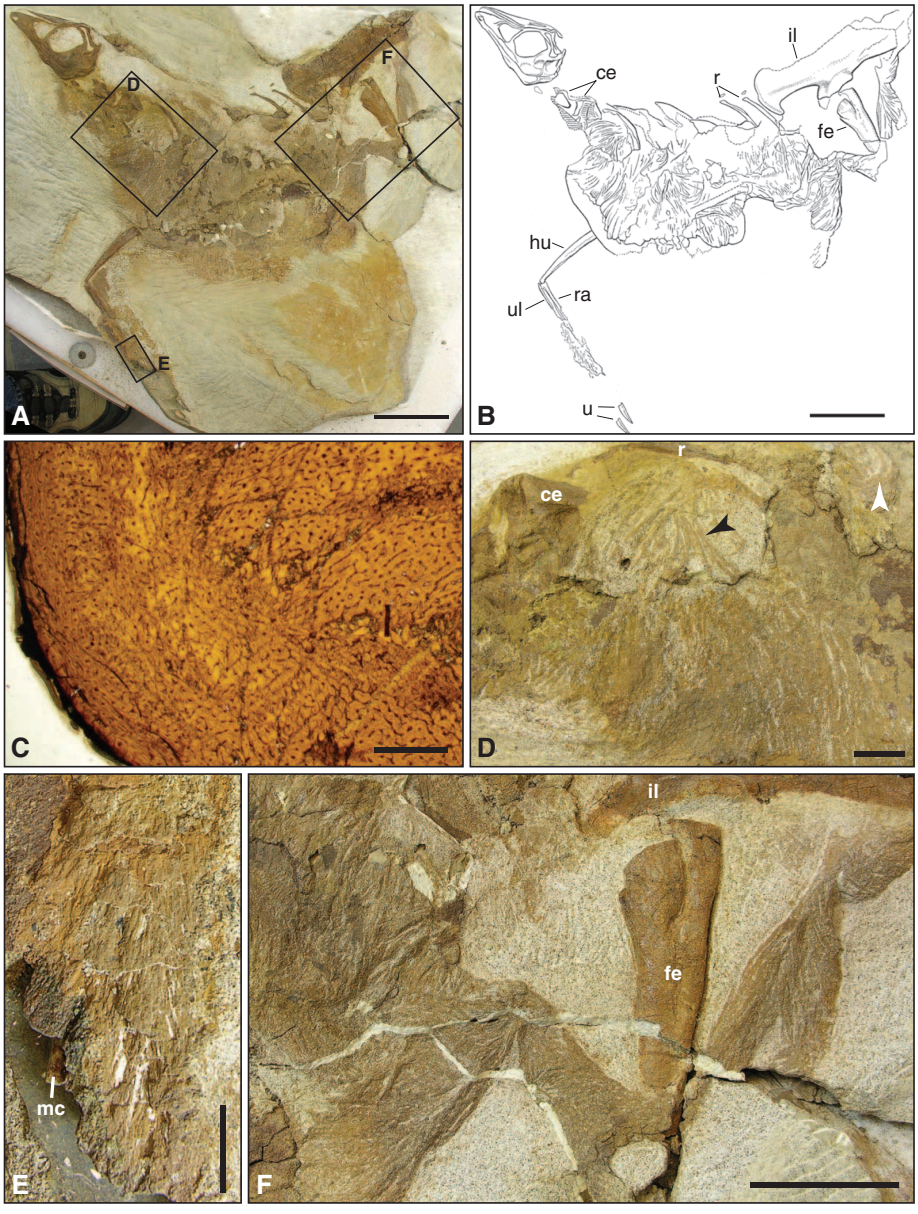


**Fig. 1.** Juvenile *Ornithomimus* (TMP 2009.110.1) preserving filamentous feather traces in ferruginous residue. (**A**) Photograph and (**B**) illustration of specimen showing the distribution and orientation of filamentous feathers and the location of insets. Scale bar, 10 cm. (**C**) Histological photomicrograph of metatarsal, showing highly vascularized bone lacking growth lines, indicating an individual less than 1 year old. Scale bar, 0.5 mm. (**D**) Close-up of filaments draping ventrally over the neck region, with curved filaments (white arrow) and possible filament bundles (black arrow). Scale bar, 2 cm. (**E**) Close-up of distal right forelimb, displaying filaments fanning out from the midline. Calcite infilled some feathers. Scale bar, 1 cm. (**F**) Close-up of feather filaments following the contour of abdomen and thigh. Scale bar, 5 cm. Interpretive line drawings of (D) to (F) are available in (*8*). ce, cervical vertebrae; fe, femur; hu, humerus; il, ilium; mc, metacarpal; ra, radius; r, rib; ul, ulna; u, ungual phalange.

the morphology of the rigid shafts of such feathers. The markings are up to 6.5 mm long and up to 1.5 mm wide (*8*) and are much wider than the filamentous feathers (0.5 mm) in the other two specimens. Almost all are linear features with well-defined (nondiffuse) edges, indicating that the original structures were elongate and straight. Some markings have an open central area and/or have U- or hook-shaped components (Fig. 3C). Such 2D shapes are consistent with traces that would be left by longitudinal or oblique sections of an originally elongate and hollow structure, such as a feather calamus (*8*). Based on the distribution, orientation, anatomical location, size, and shape of these markings on the bones, we interpret them as traces of the calami of covert feathers that covered the forearm in *Ornithomimus*.

The *Ornithomimus* specimens reveal two distinct plumages during ontogeny (Fig. 4, A and B). Young juveniles (~1 year old) had a plumage of filamentous feathers, whereas adults possessed both filamentous feathers and a pennibrachium [a winglike structure consisting of elongate feathers (*22*)]. This evidence for an ontogenetic change in plumage shows that immature individuals did not possess all the feather types present in adults. This indicates that the absence of specific feather types (such as remiges) in other feathered nonavian theropod taxa, especially those primarily known from immature individuals, could be partially due to their early ontogenetic stage, thus potentially complicating reconstruction of the evolutionary history of feathers and early wings.

The presence of a pennibrachium in ornithomimosaurs, previously reported only among maniraptorans (*22*), indicates that winglike structures originated earlier than previously known (Fig. 4C). Several roles have been proposed for primitive wings [gliding (*23*, *24*), predatory behaviors (*25*, *26*), or terrestrial locomotion (*27*, *28*)], but their occurrence in a clade of ground-dwelling herbivorous (*29*) non-maniraptorans suggests that they did not originate for predatory behaviors or aerial locomotion. The *Ornithomimus* specimens show a late appearance of shafted wing feathers during ontogeny (occurring in adults but absent in 1-year-old juveniles) as compared to birds, in which these feathers develop early, within a few weeks of hatching (*28*, *30*, *31*), to be used for aerial (*31*) or terrestrial (*28*) locomotion. Although ornithomimosaurs may have also used their feathered forelimbs for terrestrial locomotion as in some birds (chukar and ostrich) (*27*, *28*, *32*, *33*), the ontogenetically late appearance of the pennibrachia suggests that they may have initially evolved as a secondary sexual characteristic. As such, these winglike structures would have been used for reproductive activities (such as courtship, display, and brooding) and were only later, among maniraptorans, coopted for other roles, including flight.

Until now, non-avian dinosaurs with well-preserved feathers had been recovered exclusively from fine-grained deposits, primarily in northeastern China (*1*–*8*). The present report of feathered ornithomimosaurs found in channel sandstones from North America reveals that specimens bearing well-preserved feather impressions also occur in fluvial (coarser-grained) deposits. Such deposits have historically yielded a great abundance of dinosaur skeletons (*34*), yet associated feathers have heretofore gone unnoticed, perhaps because they are generally expected to be preserved only in finer-grained sediments (*18*, *19*). The discovery of feathered dinosaurs in sandstone indicates that their integumentary structures may be more readily preserved than previously anticipated. Perhaps the apparent absence of feathers in many specimens is due to their nonrecognition and subsequent destruction during fossil preparation. This potential for feather preservation in fluvial deposits, combined with the sheer abundance of non-avian dinosaurs found in such rocks, reveals great new possibilities for the discovery of feathered dinosaurs worldwide.

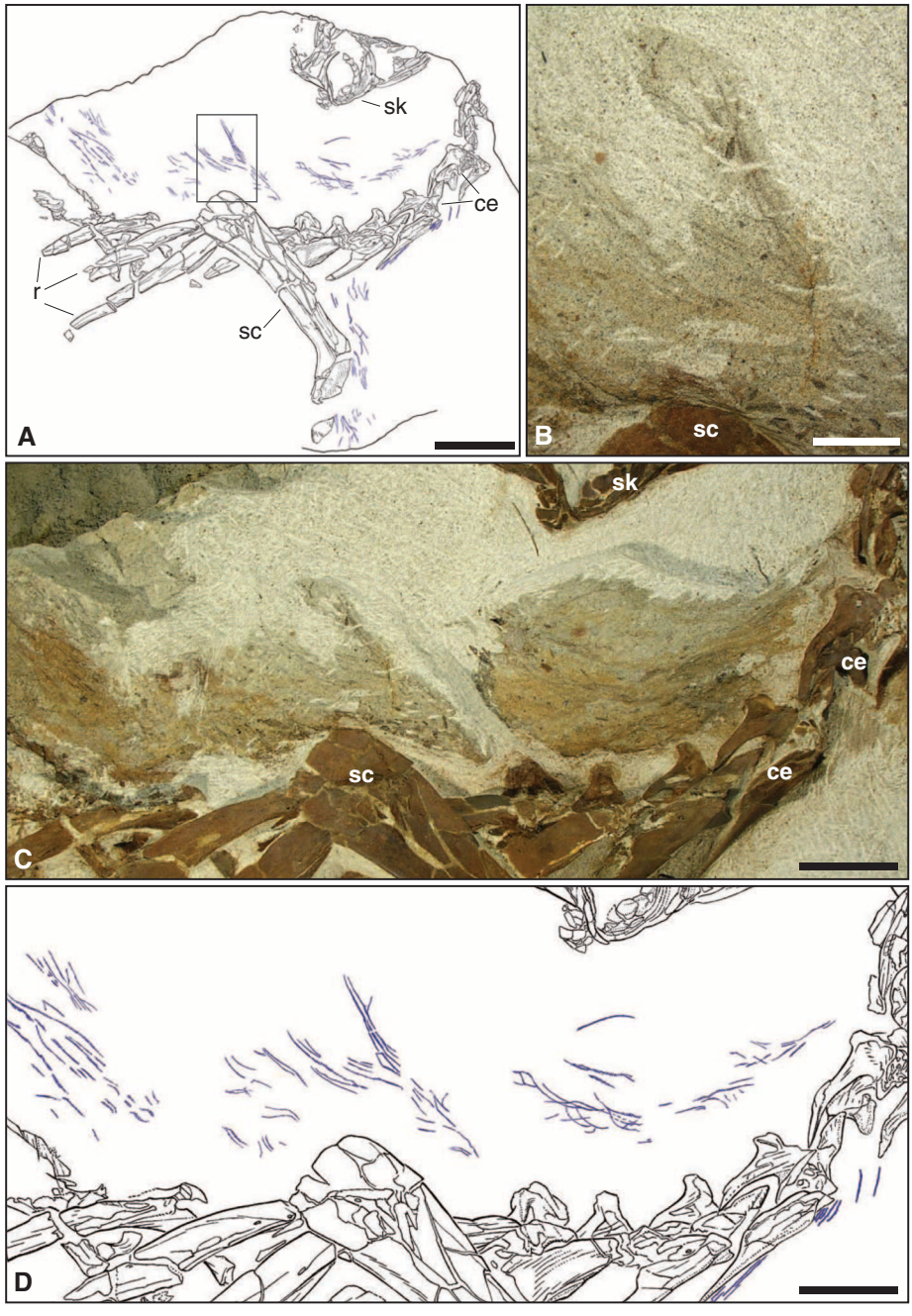


**Fig. 2.** Adult *Ornithomimus* (TMP 2008.70.1), preserving carbonized filamentous feathers. (**A**) Illustration of specimen showing the distribution and orientation of filamentous feathers (blue). Scale bar, 10 cm. (**B**) Close-up of curved filamentous feathers in inset from (A). Scale bar, 2 cm. (**C**) Photograph and (**D**) illustration of filamentous feathers along the dorsal side of the vertebral column. Scale bar, 5 cm. ce, cervical vertebrae; r, rib; sc, scapula; sk, skull.

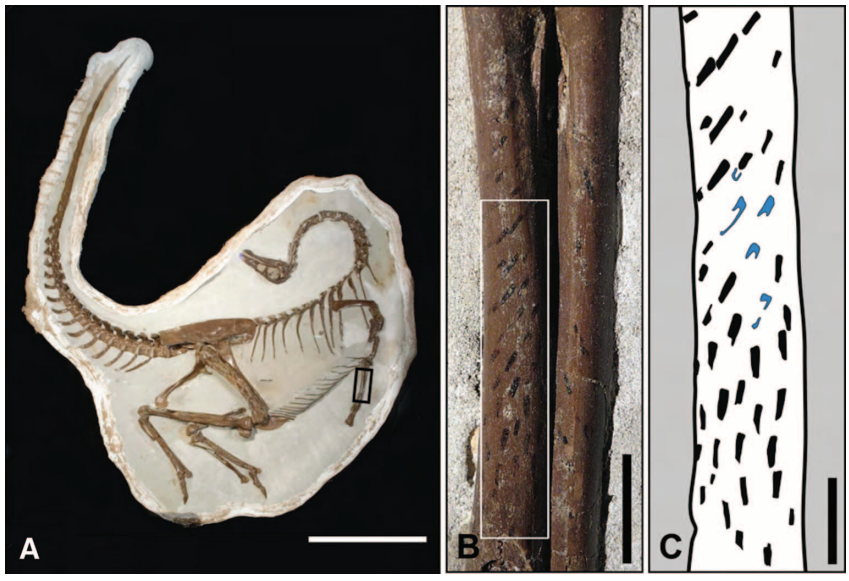


**Fig. 3.** Adult *Ornithomimus* skeleton (TMP 1995.110.1), preserving evidence of shafted feathers. (**A**) Region of markings on the forelimb bones, delineated by a black rectangle. Scale bar, 50 cm. (**B**) Close-up of ulna (on left) and radius showing markings. Scale bar, 2 cm. (**C**) Schematic drawing of inset from (B), illustrating the shape, orientation, and distribution of markings on a portion of the ulna. U- and hook-shaped components are shown in blue. Scale bar, 1 cm.

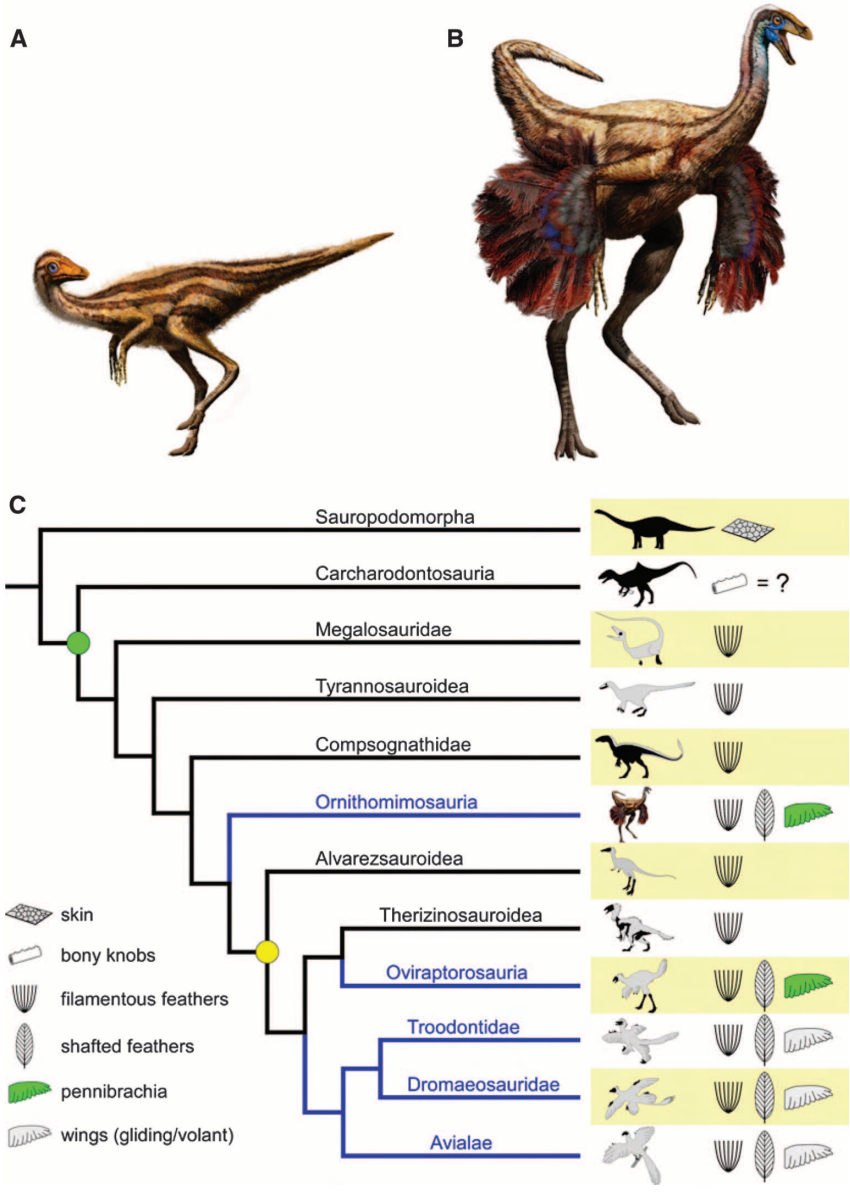


**Fig. 4.** Ornithomimosaur plumage and its phylogenetic context. Artistic representations of (**A**) juvenile plumage and (**B**) adult plumage, both illustrated by Julius Csotonyi. (**C**) Phylogenetic distribution of major feather types and wings/pennibrachia in theropods. "Filamentous feathers" refer to all feathers that lack a rigid shaft [types 1, 2, and 3b of (*11*) and morphotypes 2 to 7 of (*3*)], whereas "shafted feathers" refer to all feathers that possess a rigid shaft [types 3a, 3a+b, 4, and 5 of (*11*) and morphotypes 8 and 9 of (*3*)]. Theropod phylogeny is from (*35*), and the reported occurrences of feathers are from (*2*, *36*). The basalmost occurrence of winglike structures among Theropoda is in Ornithomimosauria. Forearm protuberances in a basal carcharodontosaur have been suggested to be associated with non-scale skin appendages (*37*) of unknown type. Green node, Theropoda. Yellow node, Maniraptora. Blue branches indicate clades that possess wings/pennibrachia. Gray wings denote clades in which at least one taxon used wings for aerial locomotion.

**References and Notes**

1. M. A. Norell, X. Xu, *Annu. Rev. Earth Planet. Sci.* **33**, 277 (2005).
2. X. Xu, Y. Guo, *Vertebrat Palasiatica* **47**, 311 (2009).
3. X. Xu, X. Zheng, H. You, *Nature* **464**, 1338 (2010).
4. Z. Zhou, P. M. Barrett, J. Hilton, *Nature* **421**, 807 (2003).
5. Z. Fucheng, Z. Zhonghe, G. Dyke, *Geol. J.* **41**, 395 (2006).
6. X. Xu *et al.*, *Nature* **484**, 92 (2012).
7. D. Hu, L. Hou, L. Zhang, X. Xu, *Nature* **461**, 640 (2009).
8. See the supplementary materials on *Science* Online.
9. Q. Ji, P. J. Currie, M. A. Norell, J. Shu-An, *Nature* **393**, 753 (1998).
10. P. J. Chen, Z. M. Dong, S. N. Zhen, *Nature* **391**, 147 (1998).
11. R. O. Prum, A. H. Brush, *Q. Rev. Biol.* **77**, 261 (2002).
12. R. O. Prum, *J. Exp. Zool.* **285**, 291 (1999).
13. M. H. Schweitzer *et al.*, *J. Exp. Zool.* **285**, 146 (1999).
14. X. Xu, Z. Tang, X. Wang, *Nature* **399**, 350 (1999).
15. C. Dal Sasso, M. Signore, *Nature* **392**, 383 (1998).
16. D. E. G. Briggs, P. R. Wilby, B. P. Pérez-Moreno, J. L. Sanz, M. Fregenal-Martínez, *J. Geol. Soc. London* **154**, 587 (1997).
17. A. W. A. Kellner, *Nature* **379**, 32 (1996).
18. P. G. Davis, D. E. G. Briggs, *Geology* **23**, 783 (1995).
19. A. W. A. Kellner, in *Mesozoic Birds above the Heads of Dinosaurs,* L. M. Chiappe, L. M. Witmer, Eds. (Univ. of California Press, Berkeley, CA, 2002), pp. 389–404.
20. A. M. Lucas, P. R. Stettenheim, *Avian Anatomy. Integument, Part I* (U.S. Government Printing Office, Washington, DC, 1972).
21. R. S. Wray, *Proc. Zool. Soc. London* **55**, 343 (1887).
22. C. Sullivan, D. W. E. Hone, X. Xu, F. Zhang, *Proc. Biol. Sci.* **277**, 2027 (2010).
23. W. J. Bock, *Syst. Zool.* **14**, 272 (1965).
24. X. Xu *et al.*, *Nature* **421**, 335 (2003).
25. D. W. Fowler, E. A. Freedman, J. B. Scannella, R. E. Kambic, *PLoS ONE* **6**, e28964 (2011).
26. J. H. Ostrom, *Q. Rev. Biol.* **49**, 27 (1974).
27. K. P. Dial, *Science* **299**, 402 (2003).
28. A. M. Heers, K. P. Dial, *Trends Ecol. Evol.* **27**, 296 (2012).
29. L. E. Zanno, P. J. Makovicky, *Proc. Natl. Acad. Sci. U.S.A.* **108**, 232 (2011).
30. J. E. Duerden, *Agric. J. Union S. Afr.* **1**, 29 (1911).
31. F. B. Gill, *Ornithology* (W.H. Freeman, New York, ed. 3, 2007).
32. P. Cho, R. Brown, M. Anderson, *Zoo Biol.* **3**, 133 (1984).
33. S. Davies, *Ratites and Tinamous* (Oxford Univ. Press, Oxford, 2002).
34. D. E. Fastovsky, in *The Age of Dinosaurs. Short Courses in Paleontology 2,* S. J. Culver, Ed. (Paleontological Society, Knoxville, TN, 1989), pp. 22–33.
35. A. H. Turner, D. Pol, J. A. Clarke, G. M. Erickson, M. A. Norell, *Science* **317**, 1378 (2007).
36. O. W. M. Rauhut, C. Foth, H. Tischlinger, M. A. Norell, *Proc. Natl. Acad. Sci. U.S.A.* **109**, 11746 (2012).
37. F. Ortega, F. Escaso, J. L. Sanz, *Nature* **467**, 203 (2010).



**Acknowledgments:** We thank P. Andrew (landowner), D. Brinkman (logistical support), J. Csotonyi (artwork), D. MacLeod (specimen preparation), M. Newbrey (discussions), D. Sloan (technical illustrations), and K. Womble (graphics). Research was funded by the Royal Tyrrell Museum of Palaeontology, a Natural Sciences and Engineering Research Council of Canada Discovery grant (D.K.Z.), the University of Calgary Start-up Fund (D.K.Z.), and an NSF Division of Earth Sciences grant (EAR 0959029) (G.M.E.). TMP 1995.110.1, TMP 2008.70.1, and TMP 2009.110.1 are permanently deposited at the Royal Tyrrell Museum, Drumheller, Alberta, Canada.


**Supplementary Materials**

www.sciencemag.org/cgi/content/full/338/6106/510/DC1
Supplementary Text
Figs. S1 to S6
Tables S1 and S2
References (*38*–*60*)


30 May 2012; accepted 30 August 2012
10.1126/science.1225376


# *Australopithecus afarensis* Scapular Ontogeny, Function, and the Role of Climbing in Human Evolution


**David J. Green[1]* and Zeresenay Alemseged[2]**



**Scapular morphology is predictive of locomotor adaptations among primates, but this skeletal element is scarce in the hominin fossil record. Notably, both scapulae of the juvenile *Australopithecus afarensis* skeleton from Dikika, Ethiopia, have been recovered. These scapulae display several traits characteristic of suspensory apes, as do the few known fragmentary adult australopith representatives. Many of these traits change significantly throughout modern human ontogeny, but remain stable in apes. Thus, the similarity of juvenile and adult fossil morphologies implies that *A. afarensis* development was apelike. Additionally, changes in other scapular traits throughout African ape development are associated with shifts in locomotor behavior. This affirms the functional relevance of those characteristics, and their presence in australopith fossils supports the hypothesis that their locomotor repertoire included a substantial amount of climbing.**


Scapular morphology corresponds closely with locomotor habits, often irrespective of phylogeny (*1*–*7*). However, our understanding of this important element in hominin evolution is limited by the paucity of scapular fossil remains. Upon its discovery, the right scapula associated with the juvenile *Australopithecus afarensis* skeleton from Dikika, Ethiopia (DIK-1-1, "Selam") represented the most complete such fossil known for this well-documented early hominin species (*8*). Furthermore, comparison of this complete juvenile with adult australopith fossils promised to shed light on *A. afarensis* growth and development (*8*, *9*). Continued preparation has since freed both scapulae from the matrix encasing much of the axial skeleton (Fig. 1).

Before DIK-1-1's discovery, the limited number of available fossil scapulae provided only tentative clues that the australopith shoulder was apelike (*10*). In addition, we lack a clear understanding of what the scapular morphology of the last common ancestor (LCA) of *Pan* and *Homo* looked like, making it difficult to determine whether australopiths retained apelike features from the LCA or if these features evolved independently (*11*–*14*). Furthermore, limited information on the postcranial architecture, developmental pathways, and the manner in which behavioral variation contributes to morphological diversity among extant hominoids presents a challenge for reconstructing locomotor patterns in extinct taxa. Here, we describe further the DIK-1-1 scapulae and infer the locomotor behavior of *Australopithecus* through comparisons with other fossil hominins—including the new specimen from Woranso-Mille, Ethiopia (KSD-VP-1/1) (*15*)—and modern apes and humans (*16*). We track the ontogeny of scapular shape among extant hominoids to evaluate how juvenile scapular morphology compares with the adult form. We also evaluate functionally relevant characters throughout development to identify various genetic and epigenetic influences on hard-tissue morphology. These approaches consider how ontogenetic shifts in locomotor behavior (e.g., in *Pan* and *Gorilla*) influence scapular shape, providing context for evaluating the morphology of more fragmentary adult fossils and a more comprehensive view for inferring the locomotor implications of australopith shoulder anatomy.

The original analysis of the right DIK-1-1 scapula showed it to be most similar to that of juvenile *Gorilla* (*8*), but the two principal component axes describing its shape explained only ~7% of variance, drawing criticism (*15*). We performed two canonical variates analyses (CVAs) among juvenile and adult representatives of modern *Homo*, *Pan*, *Gorilla*, and *Pongo*, as well as DIK-1-1 and the immature *H. ergaster* (early *H. erectus*) scapula of the Turkana Boy (KNM-WT 15000) (*17*). In the first CVA, *Homo* and *Pongo* separated from *Pan* and *Gorilla* along the first root axis, which accounted for 70.3% of the variation; *Pongo* and *Pan* separated from *Homo* and *Gorilla*, respectively, along the second root axis (16.0%; Fig. 2A). The DIK-1-1 scapulae did not significantly differ from one another ($P = 0.81$) and were most similar to those of *Gorilla* juveniles (table S6); KNM-WT 15000 fell among the juvenile *Homo* data (Fig. 2A). The second CVA considered fewer variables to include the less complete KSD-VP-1/1,


[1]Department of Anatomy, Midwestern University, Downers Grove, IL 60515, USA. [2]Department of Anthropology, California Academy of Sciences, San Francisco, CA 94118, USA.

*To whom correspondence should be addressed. E-mail: dgreen1@midwestern.edu

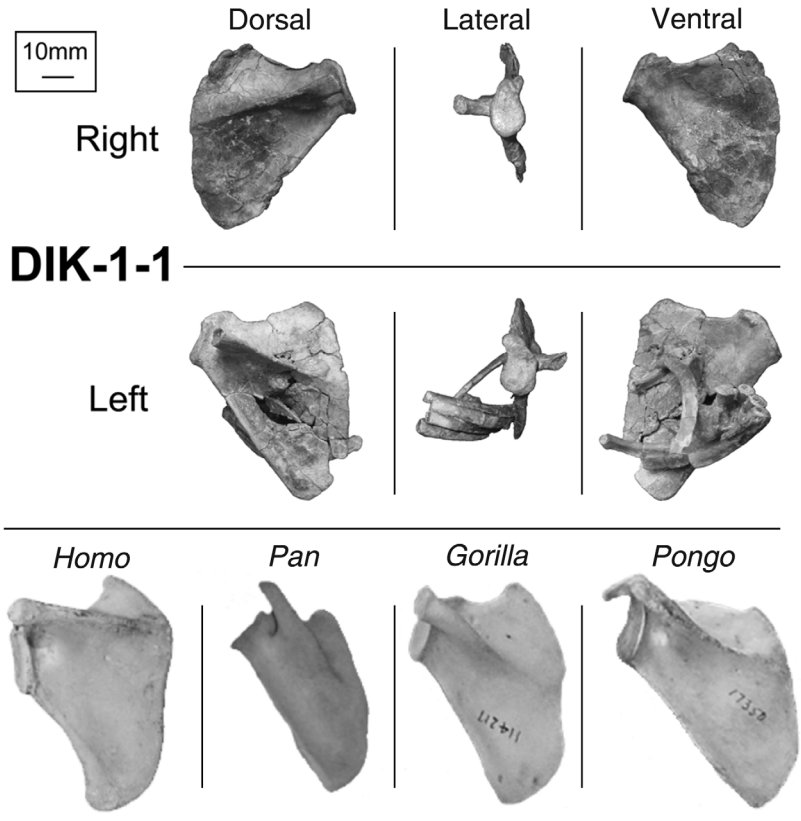


**Fig. 1.** The DIK-1-1 scapulae; top and middle row images show dorsal, lateral, and ventral views of the recently prepared right and left scapulae, respectively. The left scapula was more recently prepared and some rib and vertebral elements are still adhering to it (this did not impede the measurements presented). Images along the bottom row are scapulae of comparably aged *Homo*, *Pan*, *Gorilla*, and *Pongo* individuals.

but did not distinguish the groups as effectively. *Homo* separated from the African apes along the first root, which explained 84.2% of the variation, and *Pongo* fell between the two groups with considerable overlap (Fig. 2B). The two DIK-1-1 scapulae did not significantly differ ($P$ = 0.42) and fell among the *Pongo* and *Gorilla* data (table S8). KNM-WT 15000 was again most similar to *Homo* juveniles, whereas KSD-VP-1/1 fell near the intersection of adult *Homo* and *Pongo*.

These multivariate analyses confirm that there are two distinct scapular shapes among living and extinct hominoids (tables S5 and S6). The scapulae of the African apes, and to a lesser extent, *Pongo*, differ from those of *Homo* in possessing more cranially oriented glenoid fossae, which may be an adaptation to more effectively distribute strain over the joint capsule during climbing and reaching when the upper limb is loaded (Fig. 3) (*18*). Suspensory great apes also possess obliquely oriented scapular spines (fig. S1) with superoinferiorly narrow infraspinous fossae and relatively broader supraspinous fossae (Fig. 4). The orientation of the scapular spine is associated with the relative size and shape of the dorsal scapular fossae and the corresponding muscles, as a more obliquely oriented spine provides a direct line of action for these muscles in preventing displacement of the humeral head during suspensory behaviors (*19*–*21*).

Other fragmentary *Australopithecus* fossils (*A. afarensis*: A.L. 288-1; *A. africanus*: Sts 7 and Stw 162) were included in bivariate comparisons (table S1). All australopiths possessed more cranially oriented shoulder joints relative to modern humans (Fig. 3) (*17*). Both DIK-1-1 scapulae fell within the *Gorilla* confidence interval (CI), whereas

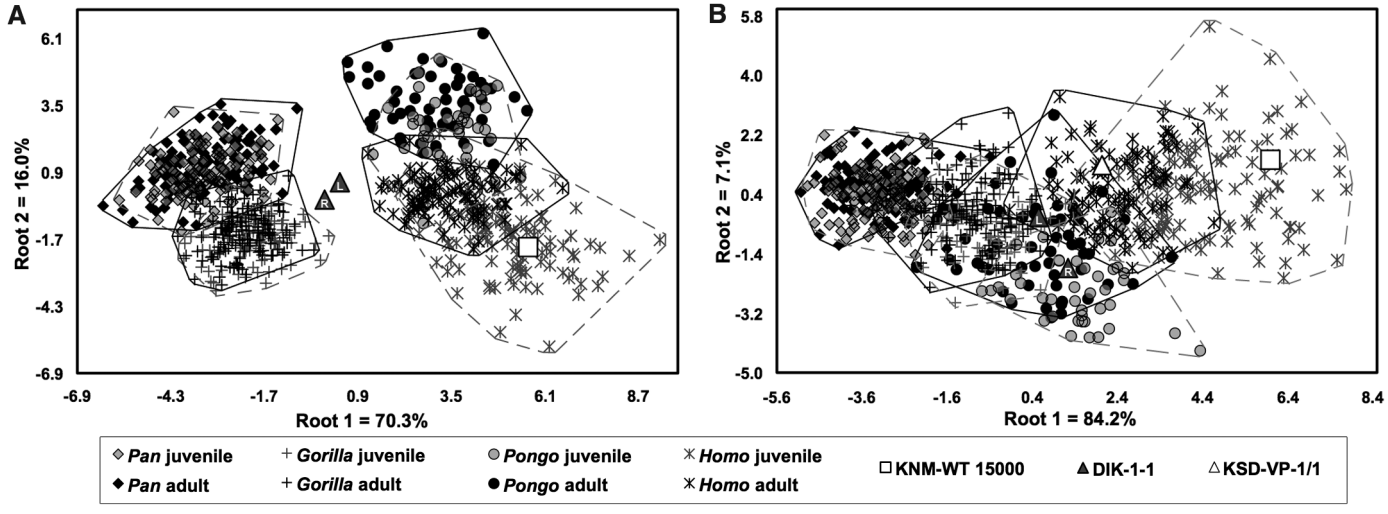


**Fig. 2.** Canonical variates analysis (CVA) plots. (**A**) The first CVA considered three angular and 10 size-corrected, linear measures (table S5). *Homo*, KNM-WT 15000, and *Pongo* separated from *Pan*, *Gorilla*, and DIK-1-1 positively along the first root. *Homo* could be further distinguished from *Pongo* along the second root, as could *Pan* from *Gorilla*. The DIK-1-1 scapulae were most similar to those of *Gorilla* juveniles, whereas KNM-WT 15000 fell among the juvenile *Homo* data. (**B**) A second CVA considered five angular measures and also the less complete Woranso-Mille specimen, KSD-VP-1/1 (table S7). Although this CVA did not distinguish the extant taxa as effectively as the previous analysis, *Homo* separated from the African apes along the first root and *Pongo* fell intermediately between the two groups. The two DIK-1-1 scapulae did not significantly differ from one another and fell among the *Pongo* and *Gorilla* data. KNM-WT 15000 was most similar to *Homo* juveniles, whereas KSD-VP-1/1 fell near the intersection of adult *Homo* and *Pongo*. See also tables S6 and S8.

KNM-WT 15000's shoulder joint was most similar to that of modern humans (Fig. 3 and table S9). Shoulder joint orientation does not significantly change in *Pan* or *Gorilla* throughout ontogeny, and it becomes slightly more cranially oriented in *Pongo* during the middle ontogenetic stages, but returns to the juvenile configuration in adulthood. In contrast, *Homo* shoulder joints become significantly more cranially oriented throughout ontogeny ($P < 0.001$), but remain more laterally oriented than those of the other hominoids at all stages (Fig. 3, fig. S2, and table S10). Starting from DIK-1-1, a humanlike ontogenetic pattern would imply that adult *A. afarensis* individuals should have more cranially oriented shoulder joints than those displayed by either A.L. 288-1 or KSD-VP-1/1. However, both juvenile and adult *A. afarensis* representatives have comparably oriented shoulder joints, suggesting that this trait remained relatively stable during ontogeny. This implies a developmental pattern for *A. afarensis* similar to that exhibited by the living African apes, but both developmental scenarios point toward a distinctly apelike shoulder joint configuration for *A. afarensis* throughout ontogeny (Fig. 3 and table S9).

It has been debated whether the cranially facing shoulder joint of A.L. 288-1 (Lucy) is an allometric result of the specimen's diminutive size, rather than an indicator of arboreal adaptations (*15*, *22*, *23*). Our results support the functional inference: Both Sts 7 and Stw 162 are larger than A.L. 288-1, yet possess more cranially oriented shoulder joints. Additionally, the Lucy-sized LB6/4 scapula (*H. floresiensis*) has a "hyperhuman," laterally facing shoulder joint (Fig. 3 and table S9) [(*24*), p. 725; (*25*)]. Moreover, the youngest modern humans had the most laterally positioned shoulder joints, further distinguishing them from juvenile great apes and DIK-1-1 (Fig. 3 and table S9). These findings contradict the hypothesis that cranially oriented shoulder joints are a by-product of small size. Thus, we conclude that *A. afarensis* possessed an apelike, cranially oriented scapula, distinct from the configuration seen in modern and fossil *Homo*.

Both DIK-1-1 scapular spines are oriented significantly more obliquely than in *Homo*, with angle values within the *Pongo* CI. In contrast, KNM-WT 15000 has a significantly more transversely oriented spine that even exceeded the modern human range (fig. S1 and table S9). The KSD-VP-1/1 scapula is described as having a more transversely oriented spine (*15*), whereas the spine of A.L. 288-1 is more obliquely oriented, falling just above the *Pongo* CI (table S9). The Sts 7 spine is the most oblique of the australopiths and fell within the *Gorilla* CI (table S9). Scapular spine orientation does not change significantly in the great apes throughout ontogeny, but modern human scapular spines shifted significantly more obliquely ($P < 0.01$; fig. S3 and table S10). As observed for shoulder joint orientation, the relative orientation of juvenile and adult *A. afarensis* scapular spines might be partially explained by a more apelike ontogenetic trajectory than that exhibited by modern humans (figs. S1 and 3 and tables S9 and S10).

Scapular spine orientation is a principal determinant of dorsal scapular fossa shape (*21*). In particular, the infraspinatus muscle has been shown to be primarily involved in shoulder joint stabilization during suspensory activities (*20*). DIK-1-1's infraspinous fossae are narrow relative to glenoid size and most similar to those of *Gorilla* and *Pongo* juveniles, whereas KNM-WT 15000 has an extremely broad fossa (Fig. 4 and tables S1 and S9). Supraspinous breadth generally increases in all taxa throughout ontogeny, whereas infraspinous breadth does not show any significant increase from stage to stage in *Homo* or *Pongo* (table S10). In contrast, infraspinous breadth increases significantly throughout both *Pan* and *Gorilla* ontogeny ($P < 0.03$; fig. S4 and table S10). The ratio of supraspinous:infraspinous breadth (SIB) increases throughout ontogeny in *Homo*, does not significantly change in *Pongo*, but significantly decreases in both *Pan* and *Gorilla*. Given the increase in relative supraspinous breadth in *Pan* and *Gorilla*, the decrease in the SIB ratio similarly

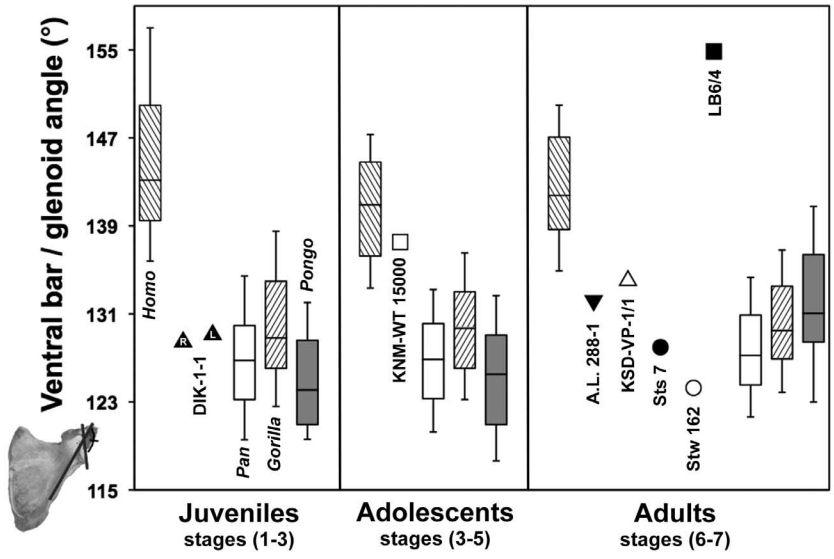


**Fig. 3.** Box plots of ventral bar/glenoid angle across extant taxa and fossil individuals for juvenile, adolescent, and adult age groups. All of the *Australopithecus* fossils differ significantly from modern human scapulae and are more similar to the suspensory apes with cranially oriented shoulder joints. In contrast, modern humans, KNM-WT 15000, and LB6/4 display more laterally oriented joints.

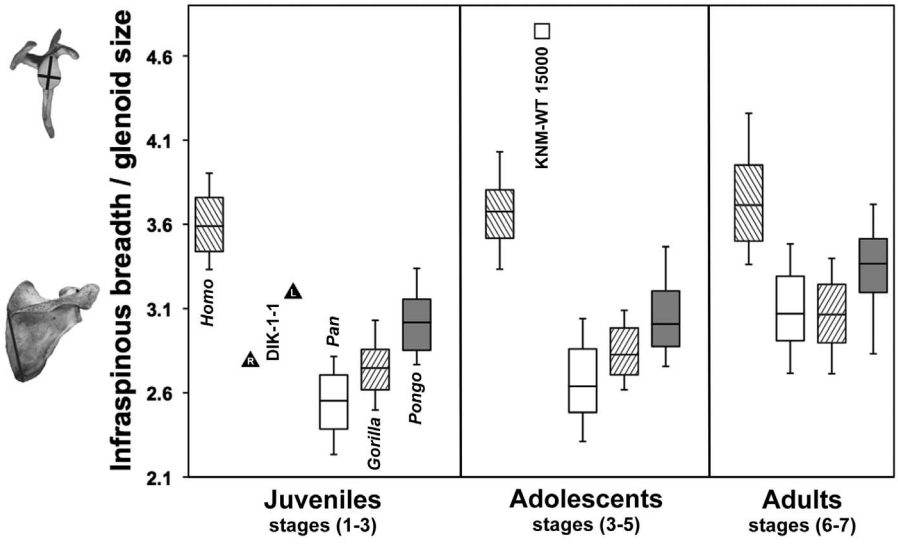


**Fig. 4.** Box plots of relative infraspinous fossa breadth across extant taxa for juvenile, adolescent, and adult age groups and the DIK-1-1 and KNM-WT 15000 fossils. The two DIK-1-1 scapulae differ from one another, but both possess relatively narrow infraspinous regions that are more similar to those of the suspensory apes, whereas KNM-WT 15000 possesses a very broad infraspinous fossa that exceeded even the modern human range.

highlights the relative increase in infraspinous breadth (table S10).

These developmental patterns further inform the link between shoulder morphology and locomotor behavior. Arboreal hominoids possess narrower infraspinous regions, in contrast to the broad fossae displayed by modern humans (*6*, *19*, *26*). Further, the increase in infraspinous breadth during *Pan* and *Gorilla* ontogeny corresponds with a behavioral shift from a principally arboreal lifestyle at younger ages to an adult locomotor repertoire predominated by terrestrial knuckle-walking (*27*, *28*). The infraspinatus muscle is consistently recruited to stabilize the shoulder joint during both suspensory and knuckle-walking behaviors in chimpanzees (*20*, *29*), so the change in African ape infraspinous fossa shape might represent an adaptive optimization of the scapular blade. A narrow infraspinous region with an obliquely oriented scapular spine is a more effective configuration for infraspinatus' role in stabilizing the shoulder joint during suspensory activities (*19*, *20*). In contrast, an enlarged infraspinous fossa allows the muscle to pass broadly behind the humeral head, which might facilitate joint integrity when the arm is loaded from below as individuals engage more regularly in knuckle-walking activities (*19*).

The change in infraspinous fossa shape during African ape ontogeny may represent a response to the changing loading regimes of a dynamic locomotor repertoire. This interpretation is supported by experimental evidence, where differences in shoulder activity during growth corresponded with significant infraspinous fossa shape changes in mice (*30*). Thus, in addition to a more cranially oriented shoulder joint and an oblique scapular spine, we propose that DIK-1-1's relatively narrow infraspinous region is a functionally meaningful characteristic. This configuration further highlights its overall apelike appearance while also distinguishing it from juvenile modern humans and the considerably more derived KNM-WT 15000 adolescent.

Comparing the DIK-1-1 scapulae to those of adult conspecifics suggests that growth of the *A. afarensis* shoulder may have followed a developmental trajectory more like that of African apes than modern humans. This conclusion is consistent with evidence purporting that *A. afarensis* dental development was also apelike (*31*). Additionally, behavioral changes that occur throughout African ape ontogeny could be linked with morphological shifts, indicating that some scapular blade characteristics track locomotor habits, even during an organism's lifetime. The apelike appearance of the most complete *A. afarensis* scapulae strengthens the hypothesis that these hominins participated in a behavioral strategy that incorporated a considerable amount of arboreal behaviors in addition to bipedal locomotion.

### References and Notes


1. E. H. Ashton, C. E. Oxnard, *Proc. Zool. Soc. Lond.* **142**, 49 (1964).
2. V. Inman, J. Saunders, L. Abbott, *J. Bone Joint Surg. Am.* **26**, 1 (1944).
3. C. E. Oxnard, *Am. J. Phys. Anthropol.* **26**, 219 (1967).
4. D. Roberts, Structure and function of the primate scapula, in *Primate Locomotion*, F. A. Jenkins, Ed. (Academic Press, New York, 1974), pp. 171–200.
5. A. Schultz, *Hum. Biol.* **2**, 303 (1930).
6. N. M. Young, thesis, Harvard University (2002).
7. N. M. Young, *Am. J. Phys. Anthropol.* **136**, 247 (2008).
8. Z. Alemseged *et al.*, *Nature* **443**, 296 (2006).
9. C. V. Ward, *Yearb. Phys. Anthropol. S* **35**, 185 (2002).
10. S. G. Larson, *Evol. Anthropol.* **16**, 172 (2007).
11. B. Latimer, in *Origine(s) de la bipédie chez les hominidés,* Y. Coppens, B. Senut, Eds. (CNRS, Paris, 1991), pp. 169–176.
12. C. O. Lovejoy, *Sci. Am.* **259**, 118 (1988).
13. J. T. Stern, *Evol. Anthropol.* **9**, 113 (2000).
14. R. L. Susman, J. T. Stern, in *Origine(s) de la bipédie chez les hominidés*, Y. Coppens, B. Senut, Eds. (CNRS, Paris, 1991), pp. 121–131.
15. Y. Haile-Selassie *et al.*, *Proc. Natl. Acad. Sci. U.S.A.* **107**, 12121 (2010).
16. The new *A. sediba* shoulder blade from Malapa, South Africa (*32*) was not included in the present study, but represents another significant addition to the scapular fossil record.
17. Materials and methods are available as supplementary materials on *Science* Online
18. K. D. Hunt, *Am. J. Phys. Anthropol.* **86**, 521 (1991).
19. S. G. Larson, *Am. J. Phys. Anthropol.* **98**, 13 (1995).
20. S. G. Larson, J. T. Stern Jr., *Am. J. Anat.* **176**, 171 (1986).
21. S. G. Larson, J. T. Stern Jr., W. L. Jungers, *Am. J. Phys. Anthropol.* **85**, 71 (1991).
22. S. E. Inouye, B. T. Shea, *Int. J. Primatol.* **18**, 629 (1997).
23. R. P. Mensforth, B. Latimer, S. Senturia, *Am. J. Phys. Anthropol.* **81**, 267 (1990).
24. S. G. Larson *et al.*, *J. Hum. Evol.* **53**, 718 (2007).
25. M. J. Morwood *et al.*, *Nature* **437**, 1012 (2005).
26. D. J. Green, thesis, The George Washington University (2010).
27. D. M. Doran, *J. Hum. Evol.* **23**, 139 (1992).
28. D. M. Doran, *J. Hum. Evol.* **32**, 323 (1997).
29. S. G. Larson, J. T. Stern Jr., *J. Zool.* **212**, 629 (1987).
30. D. J. Green, B. G. Richmond, S. L. Miran, *J. Exp. Zool. B Mol. Dev. Evol.* (2012).
31. C. Dean *et al.*, *Nature* **414**, 628 (2001).
32. L. R. Berger *et al.*, *Science* **328**, 195 (2010).



**Acknowledgments:** We thank C. Kiarie and the staff at the National Museum of Ethiopia for help during the preparation of these fragile fossils. We greatly appreciate critical comments offered by B. Richmond, B. Wood, R. Bernstein, M. Hamrick, L.P. Hernandez, and three anonymous reviewers on this manuscript and A. Gordon for analytical assistance. We thank D. Hunt, L. Gordon, E. Westwig, I. Tattersall, G. Garcia, J. Chupasko, M. Omura, Y. Haile-Selassie, L. Jellema, M. Harman, A. Gill, E. Mbua, S. Muteti, M. Yilma, P.V. Tobias, B. Zipfel, S. Potze, and T. Perregil for coordinating museum visits. We also acknowledge the NSF IGERT grant (9987590), NSF Doctoral Dissertation Improvement Grant (BCS-0824552), NSF (BCS-0914687), The Leakey Foundation, the Wenner-Gren Foundation, The George Washington University, Midwestern University, and the California Academy of Sciences for funding support. This paper was written by D.J.G. and Z.A. Fossil data were collected and described by D.J.G. and Z.A. Extant primate data were collected and analyzed by D.J.G. The data reported in this paper are summarized in the supplementary materials; raw data are available on request to D.J.G.


### Supplementary Materials

www.sciencemag.org/cgi/content/full/338/6106/514/DC1
Materials and Methods
Supplementary Text
Figs. S1 to S4
Tables S1 to S10
References (*33*–*41*)


9 July 2012; accepted 31 August 2012
10.1126/science.1227123


# Status and Solutions for the World's Unassessed Fisheries


**Christopher Costello,[1]* Daniel Ovando,[1] Ray Hilborn,[2] Steven D. Gaines,[1] Olivier Deschenes,[3] Sarah E. Lester[1,4]**



**Recent reports suggest that many well-assessed fisheries in developed countries are moving toward sustainability. We examined whether the same conclusion holds for fisheries lacking formal assessment, which comprise >80% of global catch. We developed a method using species' life-history, catch, and fishery development data to estimate the status of thousands of unassessed fisheries worldwide. We found that small unassessed fisheries are in substantially worse condition than assessed fisheries, but that large unassessed fisheries may be performing nearly as well as their assessed counterparts. Both small and large stocks, however, continue to decline; 64% of unassessed stocks could provide increased sustainable harvest if rebuilt. Our results suggest that global fishery recovery would simultaneously create increases in abundance (56%) and fishery yields (8 to 40%).**


When sustainably managed, marine fisheries provide a major source of food and livelihoods for hundreds of millions of people worldwide (*1*). When poorly managed, these benefits to people and ecosystems are severely compromised (*2*). Despite this tremendous global impact, there is considerable debate among conservation and fisheries scientists about the status of global fisheries [e.g., (*3*)]. To date, assessing the biological status of fisheries has relied either on detailed stock assessments, which combine structural population models with data to estimate a species' population size and trajectories under different harvest scenarios, or on local knowledge and less formal analysis (*4*). A recent synthesis of global fisheries with formal assessments


[1]Bren School of Environmental Science and Management, University of California, Santa Barbara, CA 93106, USA. [2]School of Aquatic and Fishery Sciences, University of Washington, Seattle, WA 98195, USA. [3]Department of Economics, University of California, Santa Barbara, CA 93106, USA. [4]Marine Science Institute, University of California, Santa Barbara, CA 93106, USA.

*To whom correspondence should be addressed. E-mail: costello@bren.ucsb.edu

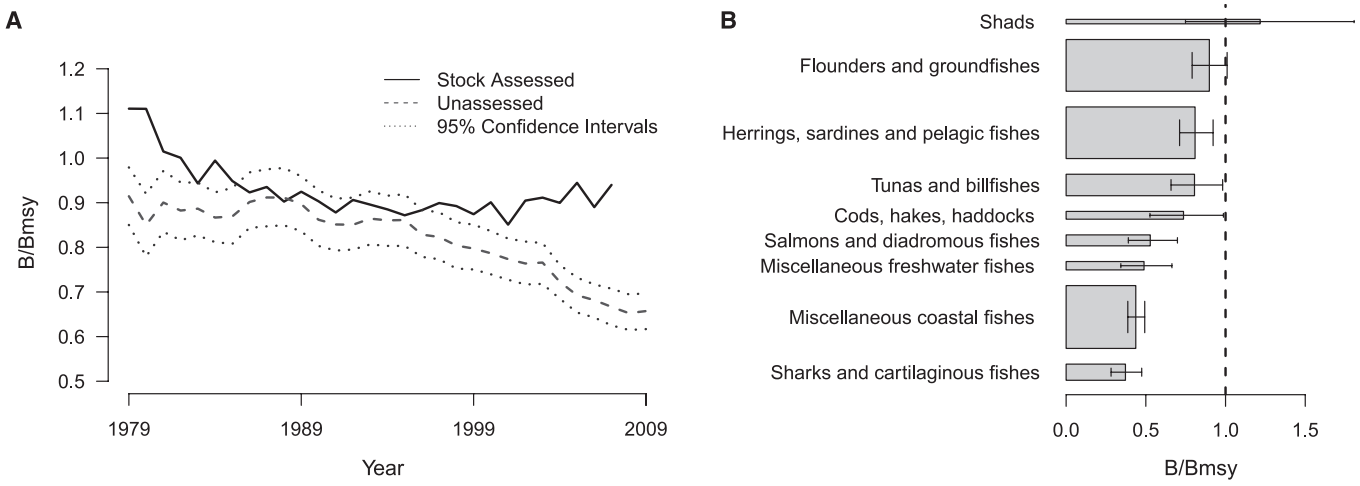


**Fig. 1.** (**A**) Time trend of median $B/B_{msy}$ for stock assessed and unassessed fisheries. (**B**) Histogram of median predicted $B/B_{msy}$ in 2009 for species categories of unassessed fisheries. Bar widths are proportional to the number of fisheries in each category.

reveals that although 63% have a biomass ($B$) below what would produce maximum sustainable yields (MSY), nearly half of these (45%) have lowered exploitation rates sufficient for recovery (*3*). A complementary analysis by the U.N. Food and Agriculture Organization (FAO) found that 32% of 441 studied stocks are either overexploited (28%), depleted (3%), or recovering (1%) (*4*). However, it is unclear whether these results extend to the remainder of global fisheries; although 20% of global catch comes from assessed species (*5*, *6*), <1% of species have assessments, largely owing to intensive data requirements and cost. Here, we explore the status of thousands of previously unassessed fisheries and use the estimates to inform the challenges and benefits surrounding global fisheries recovery.

The scientific literature includes widespread speculation on global fisheries status because of considerable ecological, social, and food security implications. One approach relies on indirect measures of fishery status (e.g., fraction of fisheries with declined catch, mean trophic level of catch, percentage of primary production appropriated by fishery catches) (*2*, *7*–*12*), but these approaches have many potentially confounding explanations. For example, declining catch is a necessary but not sufficient indicator of collapsed fisheries, resulting in unreliable estimates of stock status (*13*). A different approach uses status estimates from a smaller collection of "data-rich" fisheries (with formal assessments) as indicators for all fisheries (*13*), which also leads to unreliable predictions if data-rich fisheries differ fundamentally from unassessed fisheries (*3*).

Building on this literature, we developed a multivariate regression approach to identify predictors of stock status ($B/B_{msy}$) from assessed fisheries and use these models to estimate the status of unassessed fisheries (*14*). We couple the compilation of existing stock assessments (*5*) to an extensive database of characteristics of each unassessed fishery, such as time series of catch and fishery development (*6*) and species' life-history traits (*15*). Building on fishery science, our method assumes that the status of a population is a function of its life-history traits and harvest history, and the manner in which these variables collectively affect fishery status is consistent across species with similar characteristics.

**Fig. 2.** Time trend of median $B/B_{msy}$ for unassessed fisheries (red) and assessed fisheries (black) with small landings (i.e., lifetime landings for a fishery is less than the median lifetime landings for all fisheries; solid line) and large landings (dashed line).

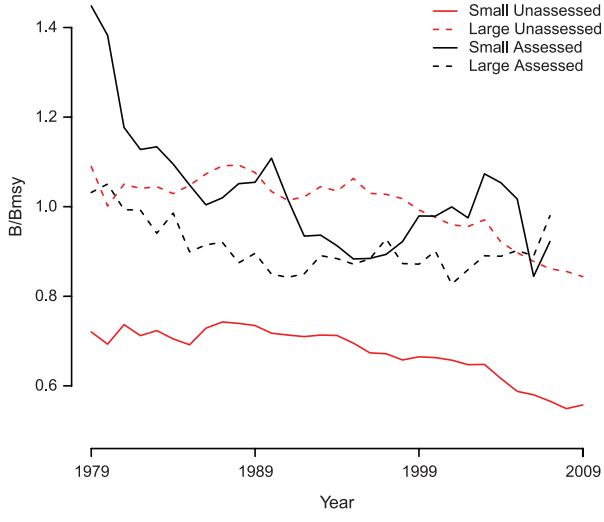


Our approach uses the same kinds of variables (life history, fishery catch, etc.) as do stock assessments. Yet the approach departs fundamentally from traditional stock assessment because at no time do we specify a structural model linking these variables to stock status and we have no indices of abundance trends. By building a panel (i.e., longitudinal data set), our approach captures both time-series effects (e.g., how long the fishery has operated) and cross-sectional effects (e.g., anchovies and sharks may respond differently to the same series of catch). This approach does not produce precise estimates for individual fisheries and therefore is not a substitute for formal assessment. However, it does provide a method for estimating the status of collections (including the global status) of previously unassessed stocks.

Regression models estimating $\log(B/B_{msy})$ predict stock status for assessed fisheries; we use six models of varying complexity (*14*) that are consistent with the scientific literature [e.g., (*16*–*18*)]. Specifically, $B/B_{msy}$ is higher when catch shows an upward trajectory and lower when current catches are consistently lower than historic levels. Small, quickly maturing species that can recover rapidly from mismanagement have higher $B/B_{msy}$ than slow-growing species that take longer to reach sexual maturity and have lower sustainable exploitation rates.

To predict the status of unassessed fisheries, we compiled a companion database of 7721 marine fisheries from the FAO landings database (*6*). There are strong caveats around aspects of these data (*19*), but they remain the best source of global fisheries catch records. This database determines the finest resolution for analysis—species caught by a country within an FAO region (fig. S2).

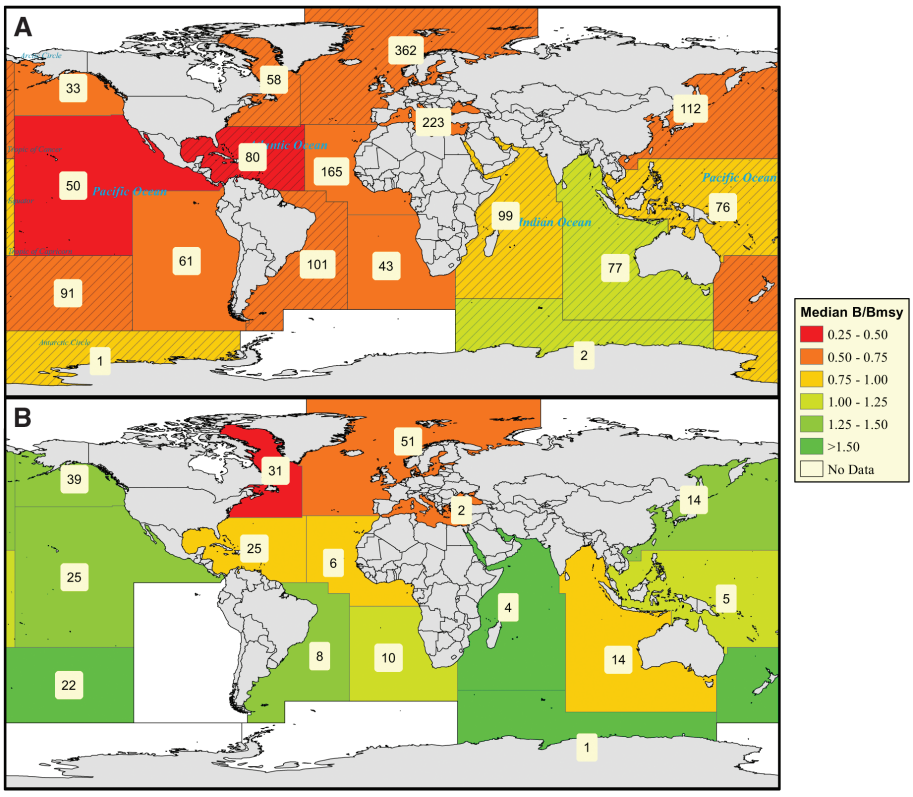


**Fig. 3.** Map of median $B/B_{msy}$ of (**A**) unassessed fisheries in 2009 and (**B**) stock assessed fisheries (2000 to 2007) for FAO regions. Hashing indicates the model accounts for less than 40% of total reported landings in that region.

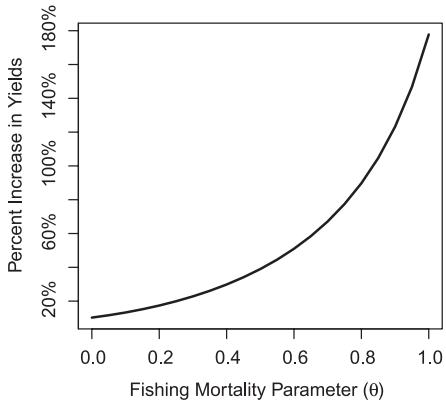


**Fig. 4.** Percentage increase in fishery yields from moving to $B_{msy}$ across a spectrum of possible fishing mortality rates. θ measures the fractional difference between fishing mortality to hold current biomass in steady state and fishing mortality at collapse.

After focusing exclusively on finfish and aggregating across countries for highly mobile species, our final data set contains 1793 distinct unassessed marine fisheries from around the world, comprising 23% of global landings (*6*). For each unassessed fishery, we applied the most data-rich model possible, yielding time-series estimates of $B/B_{msy}$ for each fishery.

We found that 64% of unassessed fisheries have a stock biomass less than $B_{msy}$ (*14*)—nearly identical to the comparable statistic (63%) for assessed fisheries (*3*). We also found that 18% [confidence interval (CI): 0.17 to 0.20] of unassessed stocks are collapsed (i.e., $B/B_{msy} < 0.2$), which is intermediate to other estimates [5% by (*17*), 14% by (*3*), and 30% by (*7*)]. Overall, we predict a median $B/B_{msy}$ of 0.64 (CI: 0.61 to 0.69) for the world's unassessed fisheries in 2009—substantially lower than the median value of 0.94 exhibited by assessed fisheries in 2007, the nearest year for which data are available (Fig. 1A). Trends in assessed and unassessed stocks diverged in the mid-1990s; one possible explanation is a shift of effort from assessed (and well-managed) fisheries to unassessed ones (*20*).

We used our model to estimate status by categories such as species category, fishery size, socioeconomic conditions of the host nation, and geographic region. Although most species categories would benefit from management reform, small schooling fish such as herrings and sardines have relatively higher biomass than many slow-growing large-bodied fishes such as sharks (Fig. 1B). Larger-than-average unassessed fisheries have a median biomass near MSY ($B/B_{msy} = 0.83$; CI: 0.77 to 0.92; Fig. 2). Smaller stocks, which are critically important for biodiversity and small-scale seafood security, tend to be in much worse condition ($B/B_{msy} = 0.55$; CI: 0.51 to 0.60). These effects of fishery size hold over time, and both groups show continuing declines in biomass. We found that unassessed fisheries in the developing world ($B/B_{msy} = 0.70$, CI: 0.60 to 0.80) may have higher stock biomasses, on average, than those in developed countries ($B/B_{msy}$ of 0.56; CI: 0.51 to 0.62; supplementary text). Geographically, the eastern Indian Ocean, including India, southern Indonesia, and Western Australia, have relatively high $B/B_{msy}$, whereas the Northwestern Atlantic, including the Northeastern United States and Canada, has among the lowest median $B/B_{msy}$ (Fig. 3). In general, there are stark contrasts between the median status of assessed and unassessed stocks, even in regions noted for well-managed assessed stocks (e.g., New Zealand and Alaska; Fig. 3). However, our data coverage in some regions is low (Fig. 3), and thus geographical comparisons warrant caution.

We used five approaches to validate the accuracy of model predictions, including within sample validation for assessed fisheries, bias tests for fishery size and data errors, jackknife analyses, comparisons with FAO assessments, and comparisons with $B/B_{msy}$ estimates from inside and outside more than 50 marine reserves around the world. Each of these validations generally supported the value of this new assessment tool (supplementary text).

The ability to estimate the status of thousands of unassessed stocks allows us to address a number of globally important policy questions. An immediate consequence of $B/B_{msy} < 1.0$ is the increase in fishery yield and fish biomass that would result from recovery. Using $B_{msy}$ as a target for rebuilding fisheries, the percentage increase in stock biomass that would result from reform is simply: $\%\text{Increase} = 100(B_{msy}/B - 1)$. For example, recovering the median fishery in our analysis ($B/B_{msy} = 0.64$) would generate a 56% increase in biomass left in the ocean.

Fishery recovery also ultimately increases yields. Many regions of the world with low $B/B_{msy}$ also face pressing food security challenges, which will increase dramatically given projected changes in human populations and wealth in the coming decades (*21*). We find that in some fisheries, yields could more than double (supplementary text), although it is worth noting that total global seafood production is dominated by a small number of large stocks. Forecasting the potential response for the median fishery requires estimating the current fishing mortality. Using the very conservative assumption that current mortality would stabilize $B/B_{msy}$ at its current value, recovering the median fishery would increase yield by 15% and recovering all fisheries would increase yield by 8%. The continued declines in biomass for both large and small unassessed stocks, however, suggest that current mortality is substantially higher. If instead we assume that unassessed fisheries are 50% closer to the fishing effort that would lead to their collapse, the predicted increase in yield from recovery is 51% for the median fishery and 40% globally (Fig. 4; supplementary text).

Our analysis suggests large potential conservation and food benefits from improving the management of the world's unassessed fisheries. To realize these benefits requires successful approaches for fisheries reform. Limiting entry and using individual transferable quotas have been shown to benefit data-rich fisheries within developed countries (*22*). These approaches, however, may prove more challenging to implement for unassessed fisheries in developing countries, because they inherently require strong governance, rule of law, and monitoring. Rather, approaches such as territorial user right fisheries (TURFs) (*23*), fisheries cooperatives (*24*), TURFs coupled with no-take reserves (*25*), and co-management approaches (*26*) are likely to be more broadly appropriate tools. In addition, coupling recent advances in data-poor assessment (*27*) with these management instruments will be critical to success.

### References and Notes


1. R. Arnason, K. Kelleher, R. Willmann, *The Sunken Billions: The Economic Justification for Fisheries Reform* (World Bank, Washington, DC, 2009).
2. D. Pauly, R. Watson, J. Alder, *Philos. Trans. R. Soc. Lond. B Biol. Sci.* **360**, 5 (2005).
3. B. Worm *et al.*, *Science* **325**, 578 (2009).
4. FAO, *The State of World Fisheries and Aquaculture 2010* (Food and Agriculture Organization of the United Nations, Rome, 2010).
5. D. Ricard, C. Minto, O. Jensen, J. Baum, *Fish Fish.* 10.1111/j.14672011.00435.x (2011).
6. FAO, *FAO Statistics and Information Service of the Fisheries and Aquaculture Department. Total Fishery Production 1950-2009. FISHSTAT Plus* (Food and Agriculture Organization of the United Nations, Rome, 2011); www.fao.org/fishery/statistics/software/fishstat/en.
7. B. Worm *et al.*, *Science* **314**, 787 (2006).
8. U. T. Srinivasan, W. W. L. Cheung, R. Watson, U. R. Sumaila, *J. Bioecon.* **12**, 183 (2010).
9. W. Swartz, E. Sala, S. Tracey, R. Watson, D. Pauly, *PLoS ONE* **5**, e15143 (2010).
10. E. Chassot *et al.*, *Ecol. Lett.* **13**, 495 (2010).
11. T. A. Branch *et al.*, *Nature* **468**, 431 (2010).
12. D. Pauly, V. Christensen, J. Dalsgaard, R. Froese, F. Torres Jr., *Science* **279**, 860 (1998).
13. T. A. Branch, O. P. Jensen, D. Ricard, Y. M. Ye, R. Hilborn, *Conserv. Biol.* **25**, 777 (2011).
14. Materials and methods are available as supplementary materials on *Science* Online.
15. R. Froese, D. Pauly, *FishBase* (2010); www.fishbase.org.
16. M. L. Pinsky, O. P. Jensen, D. Ricard, S. R. Palumbi, *Proc. Natl. Acad. Sci. U.S.A.* **108**, 8317 (2011).
17. J. T. Thorson, T. A. Branch, O. P. Jensen, T. Quinn, *Can. J. Fish. Aquat. Sci.* **69**, 645 (2012).
18. T. R. McClanahan, J. O. Omukoto, *Conserv. Biol.* **25**, 945 (2011).
19. L. Garibaldi, *Mar. Policy* **36**, 760 (2012).
20. S. C. Anderson, J. M. Flemming, R. Watson, H. K. Lotze, *PLoS ONE* **6**, e14735 (2011).
21. D. Tilman, C. Balzer, J. Hill, B. L. Befort, *Proc. Natl. Acad. Sci. U.S.A.* **108**, 20260 (2011).
22. C. Costello, S. D. Gaines, J. Lynham, *Science* **321**, 1678 (2008).
23. J. Cancino, H. Uchida, J. E. Wilen, *Mar. Resour. Econ.* **22**, 391 (2007).
24. D. Ovando *et al.*, *Mar. Policy* (2012).
25. C. Costello, D. Kaffine, *Aust. J. Agric. Resour. Econ.* **54**, 321 (2010).
26. N. L. Gutiérrez, R. Hilborn, O. Defeo, *Nature* **470**, 386 (2011).
27. J. R. Wilson, J. D. Prince, H. S. Lenihan, *Mar. Coast. Fish.* **2**, 14 (2010).


**Acknowledgments:** We thank seminar participants at the University of British Columbia, S. R. Walton, A. Leland, T. Branch, Y. Ye, and T. Essington for helpful suggestions. We gratefully acknowledge the Waitt, Moore, Walton, Oak, and Packard Foundations, California Environmental Associates, and NSF grant 1041570 (to R.H.) for financial support. Detailed results, as well as the locations of source data used in this analysis, can be found in the supplementary materials and methods and text.

### Supplementary Materials

www.sciencemag.org/cgi/content/full/science.1223389/DC1
Materials and Methods
Supplementary Text
Figs. S1 to S13
Tables S1 to S12
References (*28*–*32*)

16 April 2012; accepted 4 September 2012
Published online 27 September 2012;
10.1126/science.1223389

# The APC/C Inhibitor XErp1/Emi2 Is Essential for *Xenopus* Early Embryonic Divisions

**Thomas Tischer,* Eva Hörmanseder,* Thomas U. Mayer†**

**Mitotic divisions result from the oscillating activity of cyclin-dependent kinase 1 (Cdk1). Cdk1 activity is terminated by the anaphase-promoting complex/cyclosome (APC/C), a ubiquitin ligase that targets cyclin B for destruction. In somatic divisions, the early mitotic inhibitor 1 (Emi1) and the spindle assembly checkpoint (SAC) regulate cell cycle progression by inhibiting the APC/C. Early embryonic divisions lack these APC/C-inhibitory components, which raises the question of how those cycles are controlled. We found that the APC/C-inhibitory activity of XErp1 (also known as Emi2) was essential for early divisions in *Xenopus* embryos. Loss of XErp1 resulted in untimely destruction of APC/C substrates and embryonic lethality. XErp1's APC/C-inhibitory function was negatively regulated by Cdk1 and positively by protein phosphatase 2A (PP2A). Thus, Cdk1 and PP2A operate at the core of early mitotic cell cycles by antagonistically controlling XErp1 activity, which results in oscillating APC/C activity.**

After fertilization and a prolonged first cell cycle, *Xenopus* embryos progress through 11 rapid divisions devoid of gap phases. Cycle 13 marks mid-blastula transition (MBT), when cycles become longer and gap phases are resumed (*1*–*3*). Although it is clear that cyclin-dependent kinase 1 (Cdk1) is the universal cell cycle regulator, it remains unknown how pre-MBT divisions lacking inhibitory phosphorylations of Cdk1 (*2*, *4*) as well as the anaphase-promoting complex/cyclosome (APC/C)–inhibitory activities of Emi1 and SAC (*3*, *5*, *6*) are controlled. Before fertilization, XErp1 mediates the metaphase II arrest of mature *Xenopus* eggs by directly inhibiting the APC/C (*7*). Surprisingly, XErp1 is completely degraded at fertilization but reaccumulates in early embryos (*8*–*12*), yet egg extract studies suggest that XErp1 has no function in mitosis (*9*).

Department of Biology and Konstanz Research School Chemical Biology, University of Konstanz, Universitätsstr. 10, 78457 Konstanz, Germany.

*These authors contributed equally to this work.
†To whom correspondence should be addressed. E-mail: thomas.u.mayer@uni-konstanz.de

To understand the regulation of early mitotic divisions, we first examined XErp1 levels in *Xenopus* embryos by immunoblot analyses. After its destruction at fertilization, XErp1 reaccumulated to levels comparable to those in unfertilized eggs and started to disappear again at MBT, which is marked by the destruction of cyclin E1 and replacement of cyclin A1 by cyclin A2 (Fig. 1A). To test whether XErp1 expression is critical for early mitotic cycles, we injected antisense morpholino-oligos (MO) targeting *XErp1* mRNA (XErp1-MO) or control sense MO into one-cell embryos (*13*). At 24 hours post-fertilization (hpf), 92% of the control MO–injected embryos displayed small blastopores (Fig. 1, B and C), revealing that these embryos completed the first major morphogenetic transformation (i.e., blastopore closure). In contrast, 90% of XErp1-depleted embryos failed to undergo blastopore closure but underwent apoptosis at gastrulation (Fig. 1, B to D; fig. S1, A and B; and movie S1). To confirm that loss of XErp1 accounted for the observed phenotype, we co-injected embryos with XErp1-MO and wild-type (WT) *XErp1* mRNA (myc-XErp1$^{WT}$) that was not targeted by the MO (Fig. 1D). Expression of myc-tagged full-length XErp1$^{WT}$ efficiently rescued blastopore closure in XErp1-depleted embryos (Fig. 1, B and C). Thus, XErp1 is essential for *Xenopus* early embryonic cycles.

Next, we analyzed whether these divisions depend on XErp1's APC/C-inhibitory activity. Indeed, the majority of XErp1-depleted embryos expressing XErp1 mutated in its zinc-binding region (ZBR$^-$) or destruction box (Δbox$^-$)—both of

which are deficient in APC/C inhibition (*7*, *11*) (fig. S5)—failed to undergo blastopore closure, whereas Fbox-mutant XErp1, which is not compromised in APC/C inhibition (*7*), efficiently rescued the loss of XErp1 (Fig. 1, B and C, and fig. S1, C to E). Consequently, relative to control embryos, XErp1-depleted embryos displayed reduced levels of the APC/C substrate cyclin B2 (Fig. 2A) and increased cell cycle lengths (fig.

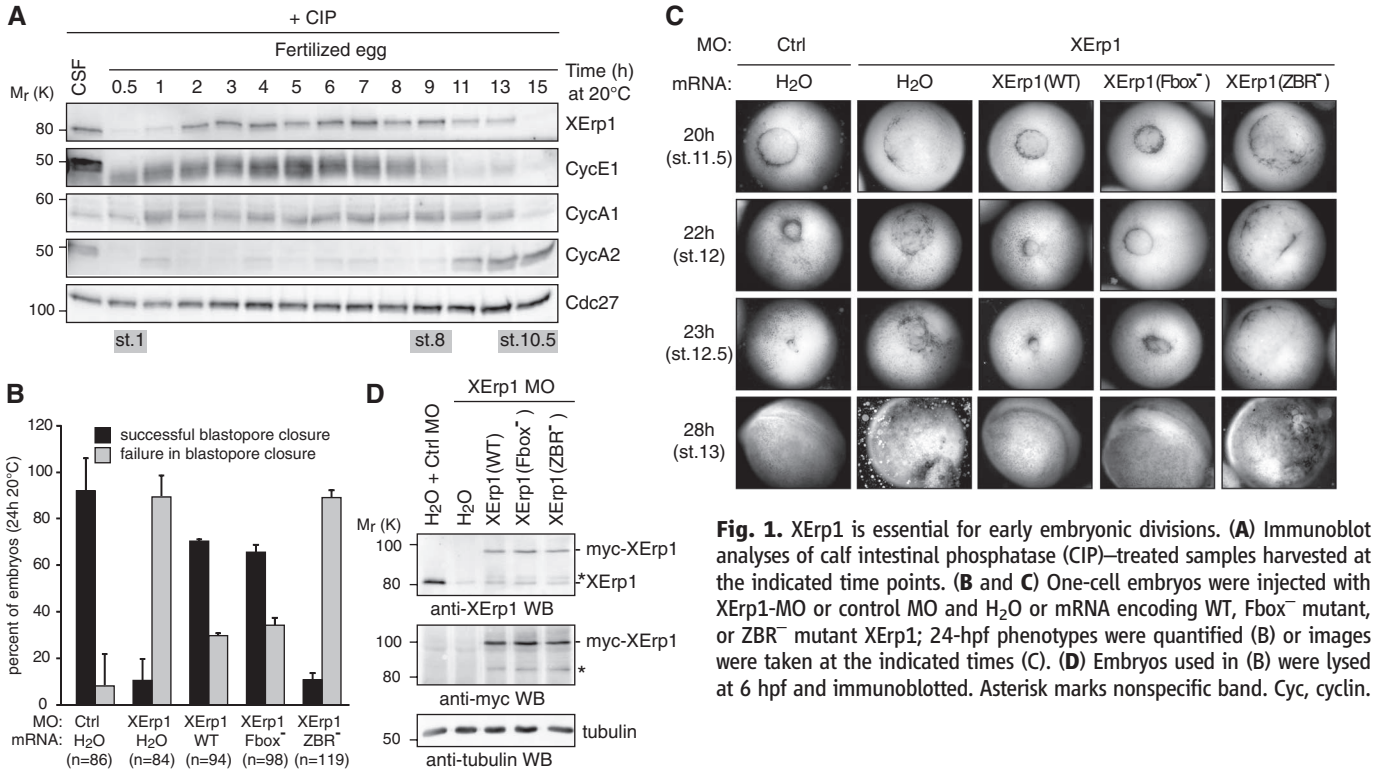


**Fig. 1.** XErp1 is essential for early embryonic divisions. (**A**) Immunoblot analyses of calf intestinal phosphatase (CIP)–treated samples harvested at the indicated time points. (**B** and **C**) One-cell embryos were injected with XErp1-MO or control MO and $H_2O$ or mRNA encoding WT, Fbox$^-$ mutant, or ZBR$^-$ mutant XErp1; 24-hpf phenotypes were quantified (B) or images were taken at the indicated times (C). (**D**) Embryos used in (B) were lysed at 6 hpf and immunoblotted. Asterisk marks nonspecific band. Cyc, cyclin.

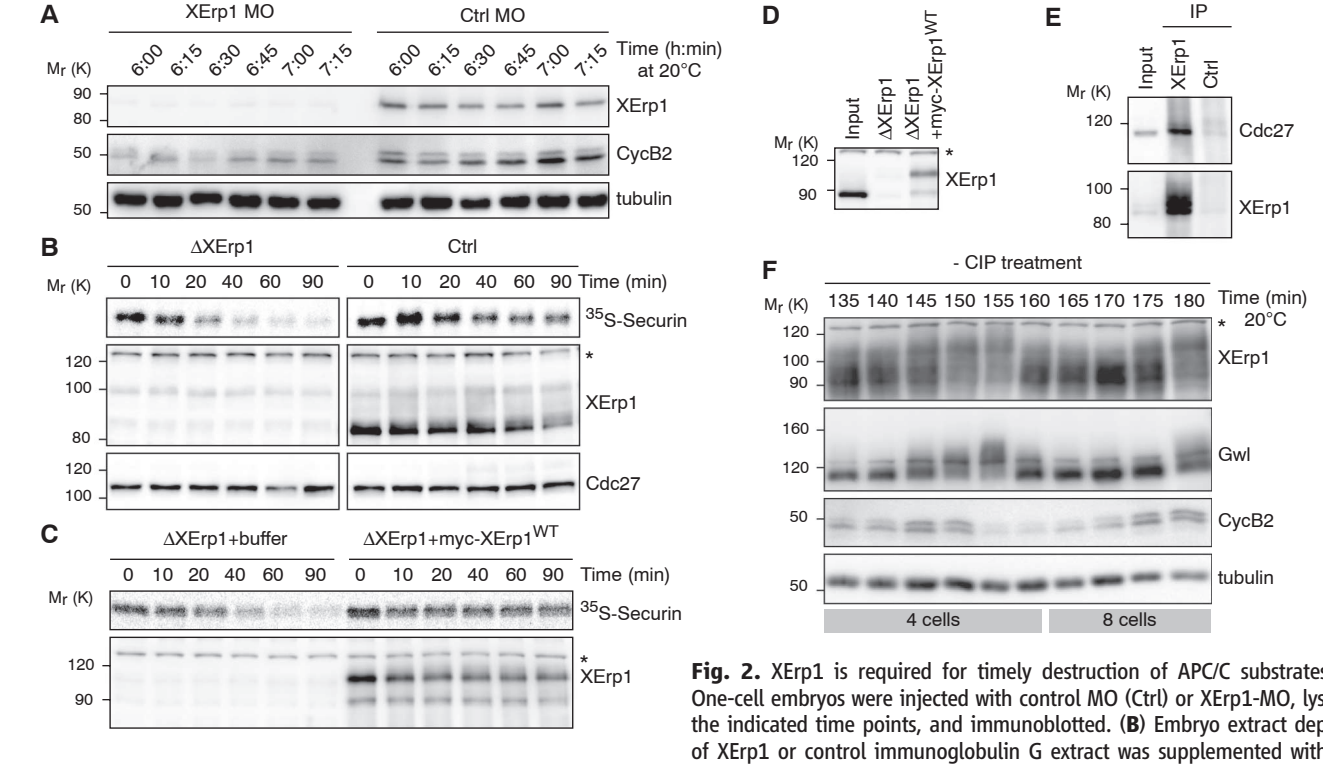


**Fig. 2.** XErp1 is required for timely destruction of APC/C substrates. (**A**) One-cell embryos were injected with control MO (Ctrl) or XErp1-MO, lysed at the indicated time points, and immunoblotted. (**B**) Embryo extract depleted of XErp1 or control immunoglobulin G extract was supplemented with $^{35}$S-labeled securin and at the indicated time points, samples were analyzed by immunoblot and autoradiography analysis. (**C**) XErp1-depleted extract was supplemented with buffer or IVT myc-XErp1$^{WT}$ and samples were analyzed as in (B). (**D**) Extract from (C) was treated with CIP and immunoblotted for XErp1. Asterisk marks nonspecific band. (**E**) At 4 hpf, embryos were lysed, and XErp1 and control immunoprecipitates were immunoblotted for XErp1 and Cdc27. (**F**) Non–CIP-treated embryo lysates were immunoblotted. Gwl, greatwall kinase.

S2, A and B). To further confirm this finding, we established an embryonic extract system that allowed us to monitor APC/C activity by analyzing the stability of in vitro translated (IVT) $^{35}$S-labeled securin. Depletion of XErp1 caused APC/C activation indicated by the destruction of $^{35}$S-labeled securin, and this effect could be rescued by IVT myc-XErp1$^{WT}$ (Fig. 2, B to D). Consequently, XErp1 immunopurified from embryo extract associated with the APC/C core subunit Cdc27 (Fig. 2E). Thus, the APC/C inhibitor XErp1 is critical for timely destruction of APC/C substrates in early *Xenopus* embryos.

In metaphase II, Cdk1 transiently activates the APC/C to compensate for continuous cyclin B synthesis by phosphorylating XErp1 at Ser$^{213}$, Thr$^{239}$, Thr$^{252}$, Thr$^{267}$, Thr$^{545}$, and Thr$^{551}$ ($ST_5$), which decreases its half-life and affinity for the APC/C (*14*, *15*). Negative regulation by Cdk1 is antagonized by protein phosphatase 2A (PP2A), which, upon phosphorylation of XErp1 by p90Rsk, binds to XErp1 and keeps dephosphorylating it (*8*, *11*, *14*–*16*). Because XErp1 remained at constant levels during early divisions (fig. S3A) but underwent cell cycle–dependent changes in its electrophoretic mobility (Fig. 2F and fig. S3B), we speculated that XErp1 might be regulated by Cdk1 and PP2A. If this applies, expression of XErp1 mutated at the six Cdk1 phosphorylation sites ($ST_5 \rightarrow 6A$) should cause a cell cycle arrest due to constitutive APC/C inhibition. Indeed, 6-hpf XErp1-depleted embryos expressing myc-XErp1$^{6A}$ displayed gigantic cells and elevated cyclin B2 levels (Fig. 3, A and B, and fig. S3, C and D). This cell cycle arrest was caused by APC/C inhibition, because expression of myc-XErp1$^{6A,ZBR-}$ had no effect (Fig. 3, A and B, and fig. S3C). To further confirm these findings, we analyzed the stability of APC/C substrates in embryo extract where we elevated Cdk1 activity by the addition of nondegradable cyclin B (CycB$^{\Delta 90}$). Intriguingly, 25 nM CycB$^{\Delta 90}$ was sufficient to induce the degradation of cyclin B2 and $^{35}$S-labeled securin (Fig. 3C). Elevated Cdk1 activity correlated with the phosphorylation of XErp1 (Fig. 3C) and its dissociation from the APC/C, as shown by Cdc27 immunoprecipitation experiments from extract and embryos supplemented with CycB$^{\Delta 90}$ (Fig. 3, D and G). Thus, Cdk1 negatively regulates XErp1's APC/C-inhibitory function.

An additional corollary of our model is that PP2A activity is required to antagonize Cdk1. In fact, treatment of embryo extract with 1 μM of the PP2A inhibitor okadaic acid (OA) quickly induced the hyperphosphorylation of XErp1 and the destruction of cyclin B2 and $^{35}$S-labeled securin (Fig. 3E). As shown by Cdc27 immunoprecipitation experiments, PP2A inhibition in embryos or extract resulted in the dissociation of XErp1 from the APC/C (Fig. 3, F and G). Notably, prolonged PP2A inhibition by OA induced the destabilization of XErp1 in embryos and extract (fig. S3E). Although this mechanism seems not to be relevant for rapid pre-MBT divisions where XErp1 levels remain constant (fig. S3A), this observation suggests that Cdk1 in the absence of PP2A activity can affect the turnover of XErp1. In *Xenopus* egg extract, the PP2A holoenzyme is targeted to XErp1 via the B′56 subtype of regulatory subunits (*15*). To test whether the same applies for embryonic divisions, we performed immunoprecipitation experiments from embryo extract expressing FLAG-tagged B′56ε. Endogenous XErp1 efficiently coimmunoprecipitated with FLAG-B′56ε but not with FLAG-B55δ (Fig. 3H). XErp1 residues Ser$^{335}$, Thr$^{336}$, Ser$^{342}$, and Ser$^{344}$ ($STS_2$) are critical for PP2A recruitment in meiosis (*14*, *15*). To test whether these residues are also critical for the mitotic interaction between XErp1 and PP2A-B′56, we performed pull-down experiments from embryo extract using

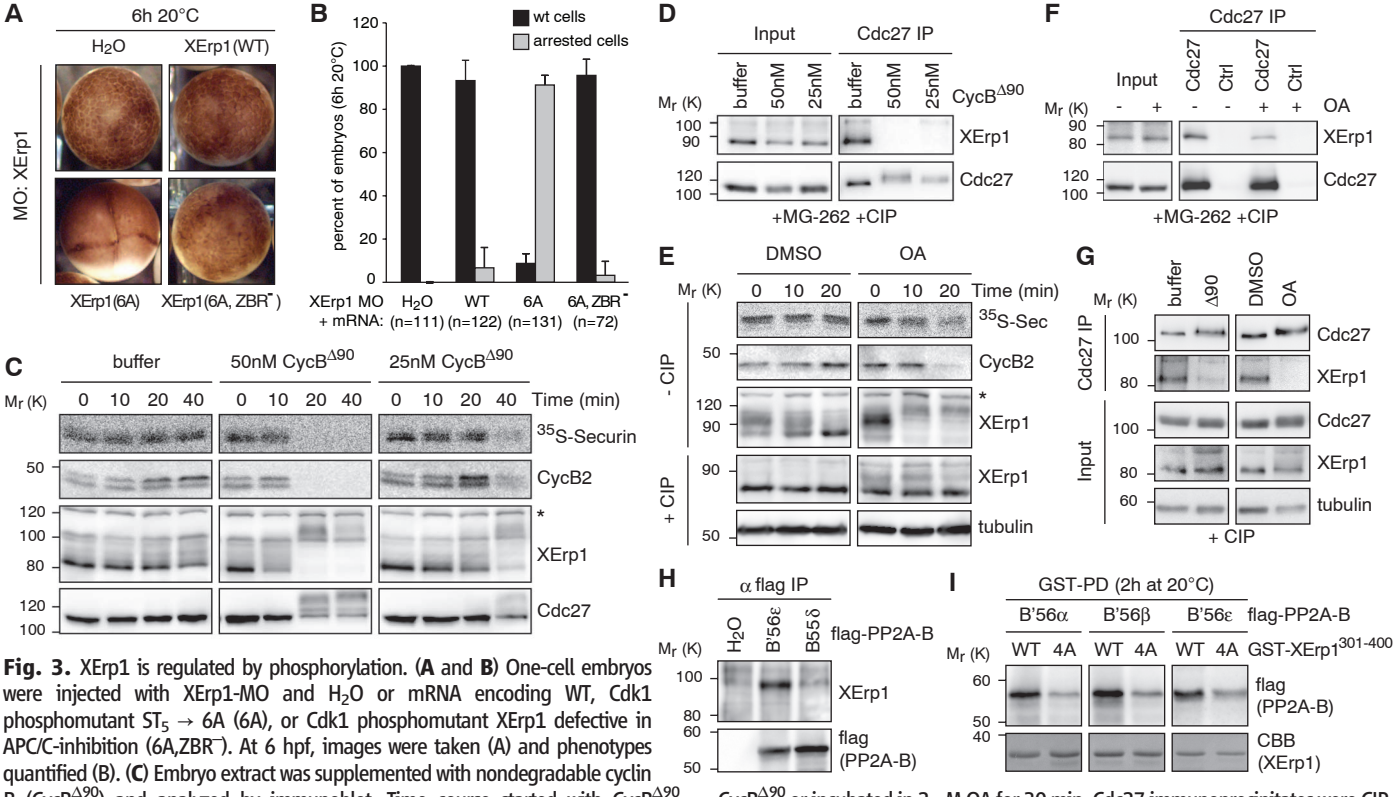


**Fig. 3.** XErp1 is regulated by phosphorylation. (**A** and **B**) One-cell embryos were injected with XErp1-MO and $H_2O$ or mRNA encoding WT, Cdk1 phosphomutant $ST_5 \rightarrow 6A$ (6A), or Cdk1 phosphomutant XErp1 defective in APC/C-inhibition (6A,ZBR$^-$). At 6 hpf, images were taken (A) and phenotypes quantified (B). (**C**) Embryo extract was supplemented with nondegradable cyclin B (CycB$^{\Delta 90}$) and analyzed by immunoblot. Time course started with CycB$^{\Delta 90}$ addition. (**D**) Cdc27 was immunoprecipitated from extracts treated as in (C) and supplemented with MG-262. Samples were CIP-treated before immunoblotting for Cdc27 and XErp1. (**E**) Embryo extract was supplemented with 1 μM OA or dimethyl sulfoxide (DMSO) as solvent control, and samples were CIP-treated as indicated and analyzed as in (C). (**F**) From extracts treated as in (E) and supplemented with MG-262, Cdc27 was immunoprecipitated. Samples were CIP-treated and immunoblotted for XErp1 and Cdc27. (**G**) One-cell embryos were injected with 50 nM CycB$^{\Delta 90}$ or incubated in 2 μM OA for 30 min. Cdc27 immunoprecipitates were CIP-treated and analyzed by immunoblot. (**H**) mRNA encoding FLAG-tagged PP2A B subunits or $H_2O$ (control) was incubated in embryo extract and immunoprecipitated using antibodies to FLAG. Precipitates were analyzed for XErp1 and FLAG epitope. (**I**) Extracts were incubated with B′56 mRNAs and GST-tagged XErp1$^{301-400}$ WT or PKA phosphomutant (4A) XErp1. After reisolation of GST-tagged proteins, interacting B′56 subunits were analyzed by immunoblot. Inputs [(H) and (I)] are shown in fig. S3, F and G. CBB, Coomassie Brilliant Blue.

glutathione *S*-transferase (GST)–tagged WT and mutant ($STS_2 \rightarrow 4A$) XErp1 fragments (residues 301 to 400). As shown in Fig. 3I, FLAG-B′56α, FLAG-B′56β, and FLAG-B′56ε efficiently associated with the WT fragment but not the 4A fragment.

Fertilization triggers destruction of cMos (*17*)—the upstream kinase of the MAPK-p90Rsk pathway—which raises a question about which kinase is critical for XErp1 activity in mitosis. XErp1 residues $Ser^{335}$, $Thr^{336}$, $Ser^{342}$, and $Ser^{344}$, which are critical for PP2A-B′56 recruitment (Fig. 3I), are flanked by highly conserved residues matching the protein kinase A (PKA) consensus phosphorylation motif (*18*) (fig. S4A). To test whether XErp1 is a substrate of PKA, we performed in vitro assays using full-length XErp1 fused to maltose-binding protein (MBP). MBP-$XErp1^{WT}$ but not MBP-$XErp1^{4A}$ was efficiently phosphorylated by PKA in vitro (Fig. 4A). To analyze whether XErp1 phosphorylation in embryos is mediated by PKA, we incubated MBP-$XErp1^{BD}$ (residues 319 to 375) in [γ-$^{32}$P]adenosine triphosphate (ATP)–supplemented control or PKA-depleted embryo extract (Fig. 4B). The WT but not the 4A mutant was efficiently phosphorylated in control-depleted extract (Fig. 4C). PKA depletion diminished MBP-$XErp1^{BD,WT}$ phosphorylation, which was specific for PKA depletion (Fig. 4C). Thus, PKA phosphorylates XErp1 at sites relevant for PP2A-B′56 binding (see Fig. 3I), which suggests that PKA might promote the recruitment of PP2A to XErp1.

To test this idea, we incubated in vitro PKA-phosphorylated MBP-$XErp1^{BD}$ in embryo extract and analyzed PP2A levels associated with re-isolated MBP-$XErp1^{BD}$. Under stringent conditions where PP2A did not associate with unphosphorylated MBP-$XErp1^{BD,WT}$, prephosphorylation of MBP-$XErp1^{BD,WT}$ but not of $XErp1^{BD,4A}$ drastically increased the amount of copurified PP2A (Fig. 4D). Consequently, expression of full-length myc-$XErp1^{4A}$ failed to rescue loss of endogenous XErp1 in embryos (Fig. 4E and fig. S4, B and C). Expression of full-length myc-XErp1 mutated at either motif $Ser^{335}$/$Thr^{336}$ (S335/T336A) or $Ser^{342}$/$Ser^{344}$ (S342/S344A) was also inefficient in complementing loss of endogenous XErp1, and the corresponding MBP-$XErp1^{BD}$ fragments were less efficiently phosphorylated by PKA in vitro than were MBP-$XErp1^{BD,WT}$ fragments (fig. S4, D to G). Thus, although $Ser^{342}$/$Ser^{344}$ does not match the PKA consensus motif, our data—in line with previous reports (*11*)—suggest that phosphorylation of both motifs is important for the APC/C-inhibitory function of XErp1. Finally, we tested the prediction that PKA inhibition should result in a phenotype reminiscent of that of XErp1-depleted embryos. To this end, we analyzed embryos treated with the PKA inhibitors H89 or PKI (*19*, *20*). At 24 hpf, the majority of PKA-inhibited embryos failed to undergo blastopore closure and died (Fig. 4F and fig. S4H). Immunoblot analyses confirmed efficient PKA inhibition in these embryos (Fig. 4G). Prolonged PKA inhibition—like that of PP2A (fig. S3E)—resulted in reduced levels of XErp1 (Fig. 4G), further confirming our idea that PKA, via PP2A-B′56, antagonizes Cdk1's negative effect on XErp1 in mitosis.

Our studies identify XErp1 as a mitotic APC/C inhibitor essential for the fast embryonic pre-MBT divisions. According to our model (Fig. 4H), XErp1-mediated APC/C inhibition allows cyclin B accumulation and thus entry into mitosis. At early mitosis, Cdk1's inhibitory effect on XErp1 is efficiently antagonized by PP2A-B′56. Once Cdk1 reaches maximal activity, it prevails over PP2A and thereby triggers APC/C activation. During mitotic exit, XErp1 must remain inactive despite decreasing Cdk1 activity, which suggests the existence of a molecular switch that inactivates PP2A-B′56 and/or PKA at anaphase. In embryo extract, PKA activity remained constant during early divisions (fig. S4I), indicating that PP2A-B′56 might be the target of such a mechanism. At mitotic entry, Cdk1 promotes inactivation of its

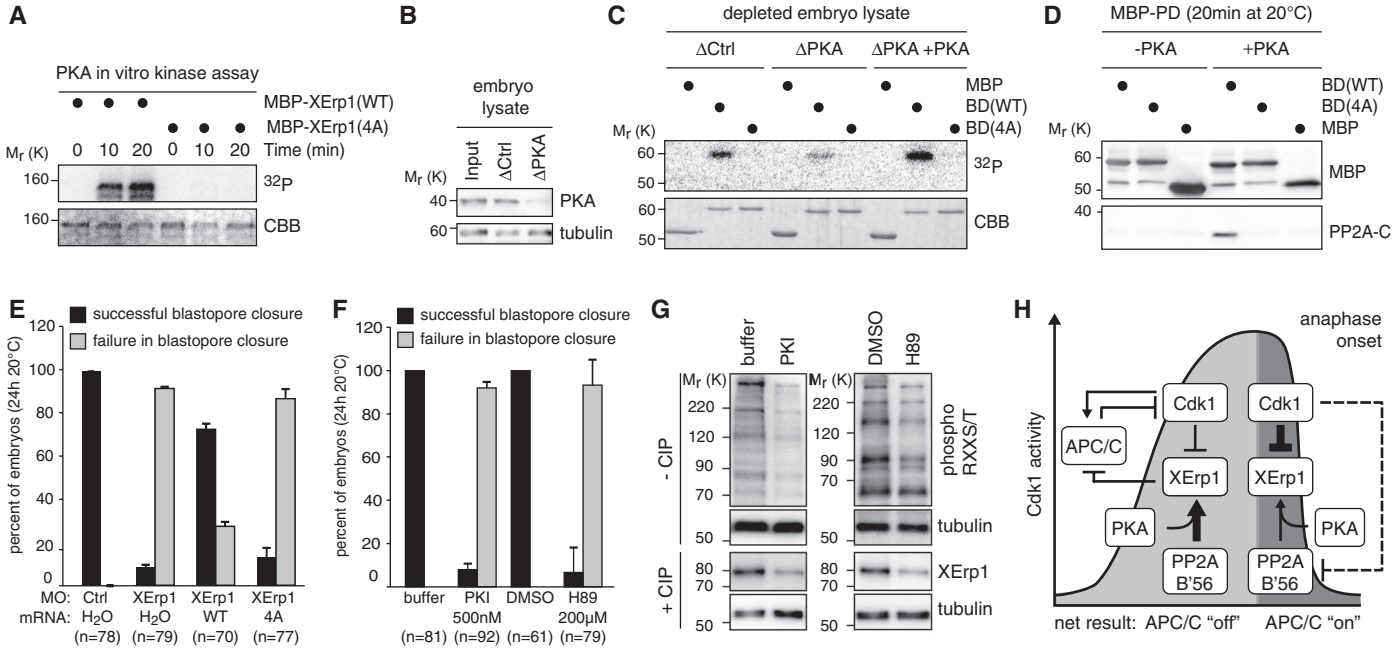


**Fig. 4.** PKA phosphorylates XErp1 at sites critical for PP2A B′56-recruitment. (**A**) In vitro PKA phosphorylation assay using [γ-$^{32}$P]ATP and MBP-tagged full-length WT or PKA phosphomutant (4A) XErp1. γ-$^{32}$P incorporation was analyzed by autoradiography. (**B**) Embryo lysate depleted of PKA (ΔPKA) or treated with control antibodies (ΔCtrl) were immunoblotted for PKA and tubulin. (**C**) Embryo lysates from (B) were supplemented with [γ-$^{32}$P]ATP and phosphorylation of MBP-$XErp1^{BD}$ was analyzed by autoradiography. Recombinant PKA was added to ΔPKA lysate. (**D**) MBP-$XErp1^{BD}$ was phosphorylated by PKA in vitro and incubated for 20 min in embryo extract. After repurification of MBP-$XErp1^{BD}$, the associated PP2A catalytic subunit (PP2A-C) was analyzed by immunoblot. (**E**) One-cell embryos were injected with XErp1-MO or control MO and $H_2O$ or mRNA encoding WT or PKA phosphomutant (4A) XErp1; at 24 hpf, the indicated phenotypes were quantified. Images and immunoblots are shown in fig. S4, B and C. (**F**) One-cell embryos were incubated with H89 or injected with PKI to inhibit PKA; at 24 hpf, the indicated phenotypes were quantified. Images are shown in fig. S4H. (**G**) Embryos were treated as in (F); samples were taken at 6 hpf, CIP-treated as indicated, and immunoblotted for XErp1 and the phosphorylated PKA consensus motif (RXXpS/pT, where X stands for any amino acid and pS/pT for phosphorylated serine or threonine) to monitor PKA activity. (**H**) Model of APC/C regulation in early mitotic divisions.

antagonist PP2A-B55δ via the Gwl-Ensa–Arpp-19 pathway (*21*–*23*). Perhaps Cdk1 itself could inactivate PP2A-B′56 once it reaches maximal activity in metaphase. By identifying XErp1 as a mitotic APC/C inhibitor, our studies provide a framework for understanding how different regulatory modules composed of phosphorylations of Cdc20, APC/C, XErp1, and possibly PP2A-B′56 are interconnected to create oscillatory Cdk1 activity driving cell cycle progression.


**References and Notes**

1. T. Duncan, T. T. Su, *Curr. Biol.* **14**, R305 (2004).
2. R. S. Hartley, R. E. Rempel, J. L. Maller, *Dev. Biol.* **173**, 408 (1996).
3. J. L. Maller *et al.*, Cell cycle transitions in early *Xenopus* development. *Novartis Found. Symp.* **237**, 58 (2001).
4. J. E. Ferrell Jr., M. Wu, J. C. Gerhart, G. S. Martin, *Mol. Cell. Biol.* **11**, 1965 (1991).
5. P. Clute, Y. Masui, *Dev. Growth Differ.* **34**, 27 (1992).
6. K. Ohsumi, A. Koyanagi, T. M. Yamamoto, T. Gotoh, T. Kishimoto, *Proc. Natl. Acad. Sci. U.S.A.* **101**, 12531 (2004).
7. A. Schmidt *et al.*, *Genes Dev.* **19**, 502 (2005).
8. D. Inoue, M. Ohe, Y. Kanemori, T. Nobui, N. Sagata, *Nature* **446**, 1100 (2007).
9. J. Liu, B. Grimison, A. L. Lewellyn, J. L. Maller, *J. Biol. Chem.* **281**, 34736 (2006).
10. J. Liu, J. L. Maller, *Curr. Biol.* **15**, 1458 (2005).
11. T. Nishiyama, K. Ohsumi, T. Kishimoto, *Nature* **446**, 1096 (2007).
12. N. R. Rauh, A. Schmidt, J. Bormann, E. A. Nigg, T. U. Mayer, *Nature* **437**, 1048 (2005).
13. See supplementary materials on *Science* Online.
14. J. Q. Wu *et al.*, *Proc. Natl. Acad. Sci. U.S.A.* **104**, 16564 (2007).
15. M. Isoda *et al.*, *Dev. Cell* **21**, 506 (2011).
16. Q. Wu *et al.*, *Curr. Biol.* **17**, 213 (2007).
17. N. Sagata, N. Watanabe, G. F. Vande Woude, Y. Ikawa, *Nature* **342**, 512 (1989).
18. C. M. Smith, E. Radzio-Andzelm, P. Madhusudan, P. Akamine, S. S. Taylor, *Prog. Biophys. Mol. Biol.* **71**, 313 (1999).
19. C. D. Ashby, D. A. Walsh, *J. Biol. Chem.* **248**, 1255 (1973).
20. T. Chijiwa *et al.*, *J. Biol. Chem.* **265**, 5267 (1990).
21. A. Gharbi-Ayachi *et al.*, *Science* **330**, 1673 (2010).
22. S. Mochida, S. L. Maslen, M. Skehel, T. Hunt, *Science* **330**, 1670 (2010).
23. J. Yu, Y. Zhao, Z. Li, S. Galas, M. L. Goldberg, *Mol. Cell* **22**, 83 (2006).



**Acknowledgments:** We thank D. Bertinetti, A. Bürkle, J. Gannon, T. Hunt, F. W. Herberg, T. Lorca, S. Mochida, and N. Sagata for reagents; the team of D. Schopper and G. Mende for excellent animal care; and the Mayer group and B. Novak for discussions. The authors declare no competing financial interests. Supported by the Doc-fForte program of the Austrian Academy of Science and by the Collaborative Research Center 969 of the German Research Foundation (DFG).


**Supplementary Materials**

www.sciencemag.org/cgi/content/full/science.1228394/DC1
Materials and Methods
Figs. S1 to S5
Movie S1
References (*24*–*27*)


3 August 2012; accepted 4 September 2012
Published online 27 September 2012;
10.1126/science.1228394


# Maturation-Dependent HIV-1 Surface Protein Redistribution Revealed by Fluorescence Nanoscopy


**Jakub Chojnacki,[1] Thorsten Staudt,[2] Bärbel Glass,[1] Pit Bingen,[2] Johann Engelhardt,[2] Maria Anders,[1] Jale Schneider,[2] Barbara Müller,[1] Stefan W. Hell,[2,3] Hans-Georg Kräusslich[1]***



**Human immunodeficiency virus type 1 (HIV-1) buds from the cell as an immature particle requiring subsequent proteolysis of the main structural polyprotein Gag for morphological maturation and infectivity. Visualization of the viral envelope (Env) glycoprotein distribution on the surface of individual HIV-1 particles with stimulated emission depletion (STED) superresolution fluorescence microscopy revealed maturation-induced clustering of Env proteins that depended on the Gag-interacting Env tail. Correlation of Env surface clustering with the viral entry efficiency revealed coupling between the viral interior and exterior: Rearrangements of the inner protein lattice facilitated the alteration of the virus surface in preparation for productive entry. We propose that Gag proteolysis-dependent clustering of the sparse Env trimers on the viral surface may be an essential aspect of HIV-1 maturation.**


The lipid envelope of human immunodeficiency virus type 1 (HIV-1) carries trimers of dimers of the viral envelope (Env) surface glycoprotein gp120 and the transmembrane protein gp41 (Fig. 1). Env proteins mediate virus binding and fusion with the target cell membrane and are essential for infectivity. Env incorporation into the virus particle is thought to occur through interaction of the gp41 C-terminal tail with the viral structural polyprotein Gag (*1*–*3*). Biochemical and cryo-electron microscopy (cryo-EM) studies revealed the presence of only 7 to 14 Env trimers per virus particle (*4*, *5*), whereas related lentiviruses and other enveloped viruses generally have a much higher surface density of viral entry proteins (*6*–*8*). Concomitant with budding, the immature hexameric Gag lattice underneath the viral membrane is dissolved into its constituent domains via HIV-1 protease (PR)–mediated cleavage. This results in formation of the mature infectious HIV-1 structure with its characteristic cone-shaped capsid (Fig. 1). Proteolysis and morphological maturation activate viral replication enzymes and render the metastable capsid shell ready for uncoating, thereby converting the virus from an assembly to an infection mode (*9*).

Immature or partially matured HIV-1 particles display reduced entry efficiency without apparent differences in Env protein structure or composition (*10*, *11*). This effect could be caused by the stiffness of the immature Gag lattice underneath the viral membrane restricting membrane fusion (*12*) or by alterations in Env lateral mobility that may prevent clustering of sparsely distributed Env trimers. Superresolution fluorescence microscopy provides an opportunity to analyze subviral structures on a statistically significant number of particles. Here, we used stimulated emission depletion (STED) microscopy (*13*) to investigate the distribution of Env molecules on the surface of individual HIV-1 particles.

Env was immunolabeled with the human monoclonal antibodies 2G12 (*14*) or b12 (*15*), which recognize the gp120 domain. Antibody-induced clustering was avoided by using purified Fab fragments (fig. S1). To identify the position of individual HIV-1 particles in the image, we used the viral accessory protein Vpr tagged with enhanced green fluorescent protein (eGFP) (*16*) as a "counterstain" reference. Visualization of HIV-1 in the confocal mode of our STED microscopy setup showed blurred spots in the eGFP (green) channel (Fig. 1A). An overlay with a confocal channel mapping the Atto 565–labeled 2G12 Fab immunocomplexes (red) displayed colocalization for ~90% of the eGFP signals, without disclosing any subviral details (Fig. 1A). Visualization of the same area with the Atto 565 signal recorded in the STED mode, resulting in about five times higher resolution (40 nm; fig. S2), revealed distinct, small, punctuate signals colocalizing with eGFP-labeled particles (Fig. 1B). A similar staining pattern was observed when Env was detected with b12 Fab (fig. S3). Fab-derived signals were not detected upon immunostaining of particles lacking Env (Fig. 1C and fig. S3B), demonstrating the specificity of staining. STED analysis revealed differences between the Env distributions on mature and immature particles. Whereas most mature particles displayed a single Env signal or focus (Fig. 1B), the majority of immature particles were found to exhibit two or more Env foci (Fig. 1D


[1]Department of Infectious Diseases, Virology, Heidelberg University, Im Neuenheimer Feld 324, 69120 Heidelberg, Germany. [2]Optical Nanoscopy Division, German Cancer Research Center (DKFZ), Im Neuenheimer Feld 280, 69120 Heidelberg, Germany, and BIOQUANT, Im Neuenheimer Feld 267, 69120 Heidelberg, Germany. [3]Department of NanoBiophotonics, Max Planck Institute for Biophysical Chemistry, Am Fassberg 11, 37077 Göttingen, Germany.

*To whom correspondence should be addressed. E-mail: hans-georg.kraeusslich@med.uni-heidelberg.de

and fig. S3). The distance between Env foci on individual particles did not exceed 150 nm, consistent with the reported average particle diameter of HIV-1 (*17*).

To ensure that the detection of multiple Env foci did not result from particle aggregation unrecognizable in the diffraction-limited confocal mode, we visualized the eGFP.Vpr signal of adhered particles using STED microscopy (fig. S4): 97.2% of mature and 97.6% of immature particles represented individual particles, consistent with previous observations based on diffusion velocity measurements (*18*). We used STED microscopy to determine whether the higher number of Env foci on immature particles indicated differences in Env distribution or simply a higher number of Env molecules by comparing the signal of virus-associated Env molecules with the signal from defined references. Reference samples included Atto 565–labeled secondary Fab fragments (Fig. 2A, black bars), as well as monomeric (light gray bars) or trimeric (dark gray bars) recombinant HIV-1 Env proteins bound to 2G12 Fab and Atto 565–labeled secondary Fab. Side-by-side comparison of Env fluorescence signals on HIV-1 particles with those of reference samples yielded an average of seven and eight Env trimers on mature and immature HIV-1, respectively (Fig. 2B), consistent with published reports (*4*, *5*). These results were supported by quantitative immunoblotting of bulk preparations of mature and immature particles, which showed no significant difference in their respective Env content (Fig. 2D and fig. S5). Finally, we analyzed the relative amount of Fab fragments bound to HIV-1 in solution by immunoblot analysis of particle-Fab complexes. Mature and immature particles featured comparable amounts of bound Fab (Fig. 2E). Thus, the observed differences in STED signal distribution were not caused by differences in Env content or Fab accessibility.

To quantify the observed difference between mature and immature HIV-1 particles, we manually classified the Env signals associated with individual eGFP-labeled particles into three distribution patterns: (i) single focus, (ii) two foci, and (iii) more than two foci (Fig. 3A and fig. S6). These patterns were indistinguishable by confocal microscopy (Fig. 3A, right column). Whereas single Env foci were found in ~70% of the mature particles, they were observed in less than 30% of their immature counterparts (Fig. 3B and table S1). The same difference was seen when Env was expressed from a different plasmid than the remaining HIV-1 proteins. This so-called pseudotyping led to an increase in Env incorporation, but yielded a similar Env surface distribution with ~70% of mature particles and less than 30% of immature particles exhibiting a single focus (Fig. 3C and table S1). Env signal intensities for virus particles displaying different numbers of foci were not significantly different, confirming that multifocal Env distribution patterns did not arise from an increased number of Env molecules on the particle surface (Fig. 2C).

Next, we extended the Env distribution analysis to HIV-1 variants displaying partial maturation defects due to mutation of specific Gag cleavage sites (fig. S7A). This included a variant with a processing defect between the matrix (MA) and capsid (CA) domains of Gag (MA-CA) and one in which all Gag cleavage sites except for the one between MA and CA were blocked (CA-p6). The covalent linkage of MA with the assembled CA domain in the MA-CA variant has been shown to retain the hexameric immature lattice and should keep the MA layer in the same position as in the immature particle. Conversely, the processed MA is released from the underlying lattice in the CA-p6 variant and should be free to move laterally (*19*). The expected Gag processing patterns were confirmed by immunoblotting of purified particles (fig. S7C). Analysis of Env distribution on the viral surface showed that the MA-CA variant resembled the immature phenotype, with ~35% of particles exhibiting a single Env focus, whereas the CA-p6 variant displayed an intermediate phenotype more similar to mature HIV-1 (Fig. 3B and table S1). Thus, Env surface distribution of HIV-1 correlates with the processing of the MA domain of Gag, which lines the inner face of the viral membrane.

The dependence of HIV-1 Env surface distribution on MA processing suggested a role for the unusually long (151 amino acids) Env C-terminal tail (CT) that interacts with the underlying MA layer (*1*–*3*, *20*). Deletion of Env CT and the consequent loss of Env interaction with the underlying Gag lattice may render Env distribution independent of the HIV-1 maturation status. We tested this hypothesis by comparing Env distribution patterns on mature and immature HIV-1 pseudotyped either with full-length Env or an Env CT-deleted variant [Env(ΔCT); fig. S7B]. Env(ΔCT) exhibited an immature-like Env distribution pattern independent of the maturation status of the virus. A single Env cluster was observed in less than 30% of particles for both immature and mature Env(ΔCT) particles, and these numbers were indistinguishable from those obtained for immature HIV-1 with wild-type (wt) Env (Fig. 3C, fig. S8, and table S1). These results suggest that the Env CT is actively involved in Env clustering. Moreover, the observed maturation-dependent formation of a single Env cluster may require both disassembly of the underlying rigid Gag lattice and CT-dependent Env interactions. This conclusion is supported by a previous report showing that the HIV-1 Env CT has the potential for self-association (*21*), which may be the driving force for the observed clustering.

To determine whether clustering of the sparse Env trimers on the HIV-1 surface is relevant for virus entry, we analyzed the infectivity and entry competence of mature HIV-1 particles, carrying either wild-type or C-terminally truncated Env. In

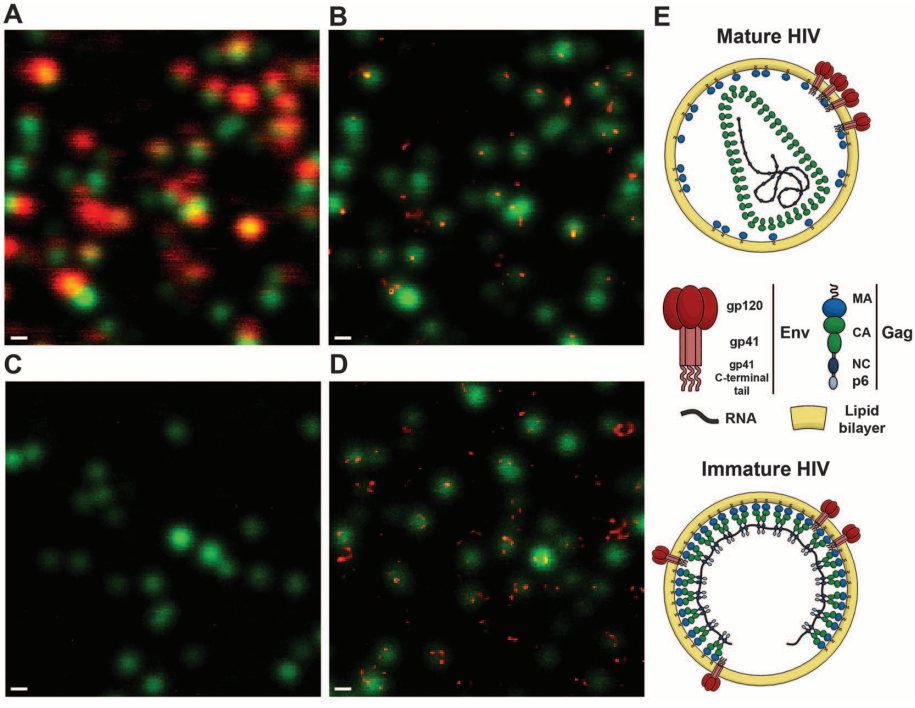


**Fig. 1.** HIV-1 Env distribution visualized by STED microscopy. Purified HIV-1 particles, containing eGFP.Vpr (green), were stained for Env (orange). Images were acquired using the STED setup with the eGFP.Vpr signal recorded in the standard confocal mode to define the localization of particles. Scale bars: 200 nm. (**A**) Env signal of mature particles acquired in the confocal microscope mode. (**B**) The same field of view as in (A), with the Env signal acquired in STED mode. (**C**) Control Env(-) particles with the Env signal acquired in STED mode. (**D**) Env signal of immature particles acquired in STED mode. (**E**) Schematic illustration of the mature and immature HIV particle structures.

agreement with published reports (*3*, *22*), deletion of the C-terminal tail led to a highly significant drop in HIV-1 infectivity. This was observed in a single-round assay (Fig. 4A) and in an end-point titration assay (integrating multiple rounds of infection; Fig. 4B) in lymphocytic cell lines. To extend this analysis to immature particles, we performed entry assays, in which cytosolic delivery of HIV-1 contents after fusion is measured by activity of a virus-incorporated reporter protein (*23*). These experiments were performed with primary human lymphocytes, which are natural target cells of HIV-1. Consistent with the reduced infectivity (Fig. 4, A and B), truncation of the Env C-terminal tail also led to a significant decrease of fusion competence of mature HIV-1 (Fig. 4C). The entry competence was even lower for immature HIV-1 carrying wild-type Env, as observed previously (*10*), but truncation of the C-terminal tail partially rescued entry in this case (Fig. 4C). Thus, entry efficiency generally correlated with the observed Env clustering with the exception of immature HIV-1 with Env(ΔCT). Env CT deletion partially restored entry competence in this case, but did not affect Env clustering on free virus particles.

This phenotype could be explained by a delayed Env clustering upon engagement of the cellular receptor, which would be blocked by the immature Gag lattice in the presence of Env CT. We tested this hypothesis directly by dual-color STED microscopy of HIV-1 particles attached to T cells, recording both the viral glycoprotein and the cellular receptor CD4 with nanoscale resolution. The cell-attached viral particles identified by their GFP signal were almost always associated with CD4 patches on the cell surface. Analysis of more than 60 individual HIV-1 particles per variant revealed a clear polarization of Env foci toward the CD4 patch, suggesting direct receptor engagement (Fig. 4, D to I, and fig. S9). The Env distribution patterns of cell-bound mature and immature particles carrying Env(wt) closely resembled the distributions observed for the respective cell-free viruses (Fig. 4, D, E, and I, and fig. S10). By contrast, virus particles carrying Env(ΔCT) displayed a shift from the predominantly multifocal distribution observed in free particles to a high degree of single foci for CD4-engaged particles (Fig. 4, F, G, and I, and fig. S10). This difference was observed for mature and immature particles carrying Env(ΔCT), indicating that Env clustering can be induced by contact with the receptor, provided that the Env CT is deleted.

On the basis of these results, we propose that Env clustering into a single focus is important for efficient HIV-1 entry. The entry competence of HIV-1 directly correlated with its capacity to form Env clusters, and truncation of the Env C-terminal tail rescued both clustering and cytosolic entry of immature viruses in primary lymphocytes. An involvement of Env clusters in the fusion event has been previously proposed on the basis of structures observed at contact sites between particles and T cells by electron tomography (*24*). Env clustering may be particularly important for HIV-1 because of the low number of Env trimers in the viral membrane.



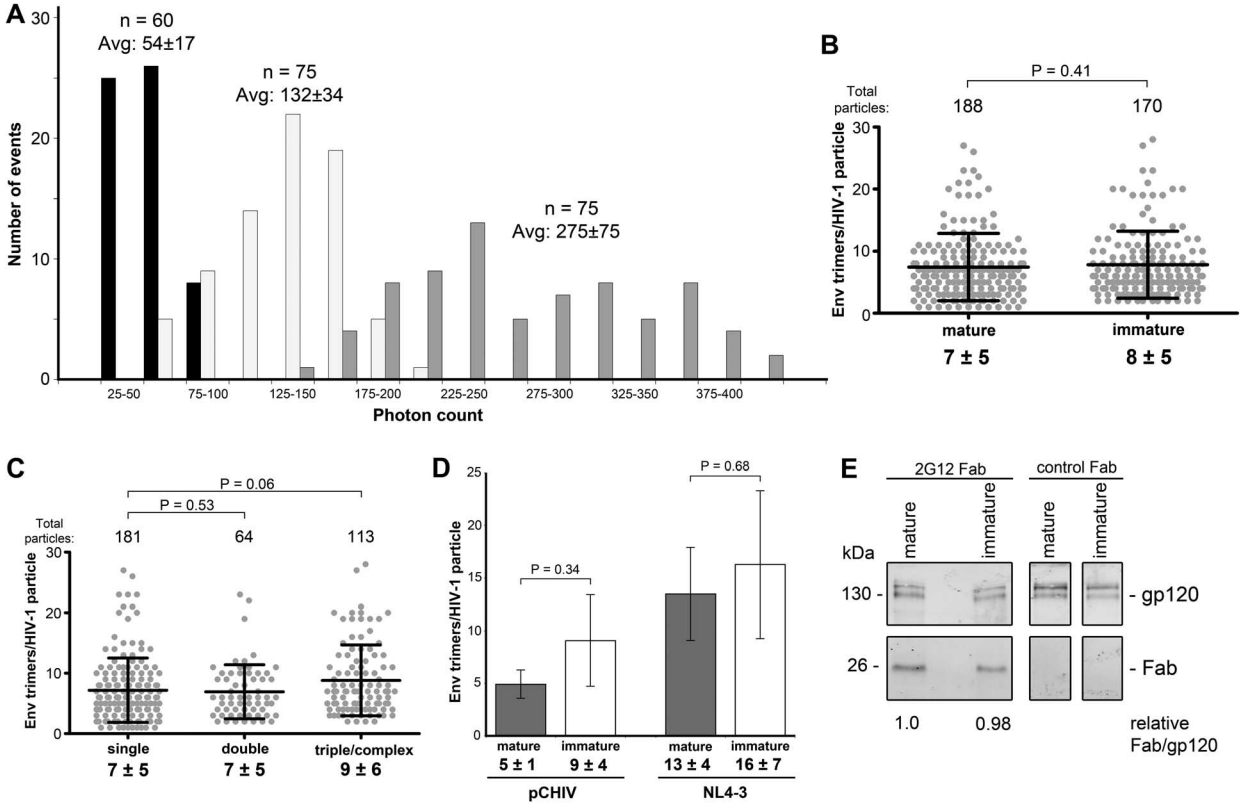


**Fig. 2.** Quantitation of Env trimers on mature and immature HIV-1. (**A**) Fluorescence intensity distribution of reference samples acquired by STED microscopy. Fab fragments were labeled with Atto 565. Black bars: anti-human Fab; light gray bars: recombinant monomeric Env stained with primary and secondary Fab; dark gray bars: recombinant trimeric Env stained with primary and secondary Fab. (**B**) The number of Env trimers on individual mature and immature HIV-1 particles was estimated from the average fluorescence intensity of the recombinant trimeric Env reference sample analyzed in parallel. Mean ± SD values are shown with Wilcoxon rank-sum test for significance. (**C**) Env trimer incorporation classified according to Env distribution class and shown for the combined data of mature and immature HIV-1. Mean ± SD values are shown with Wilcoxon rank-sum test for significance. (**D**) Amounts of gp120 and CA or Gag in purified virus preparations from cells transfected with pCHIV or pNL4-3, respectively, were determined by quantitative immunoblotting. The number of Env trimers per particle was calculated by assuming an average of 2400 CA or Gag molecules per particle (*26*). Mean ± SD values are shown with Wilcoxon rank-sum test for significance ($n$ = 4 experiments). (**E**) A representative immunoblot showing Fab binding to mature and immature HIV-1, respectively. Purified particles were incubated with 2G12 or control Fab fragments and analyzed for Fab binding by quantitative immunoblotting. The ratio of gp120 to Fab in mature particles was set to 1.

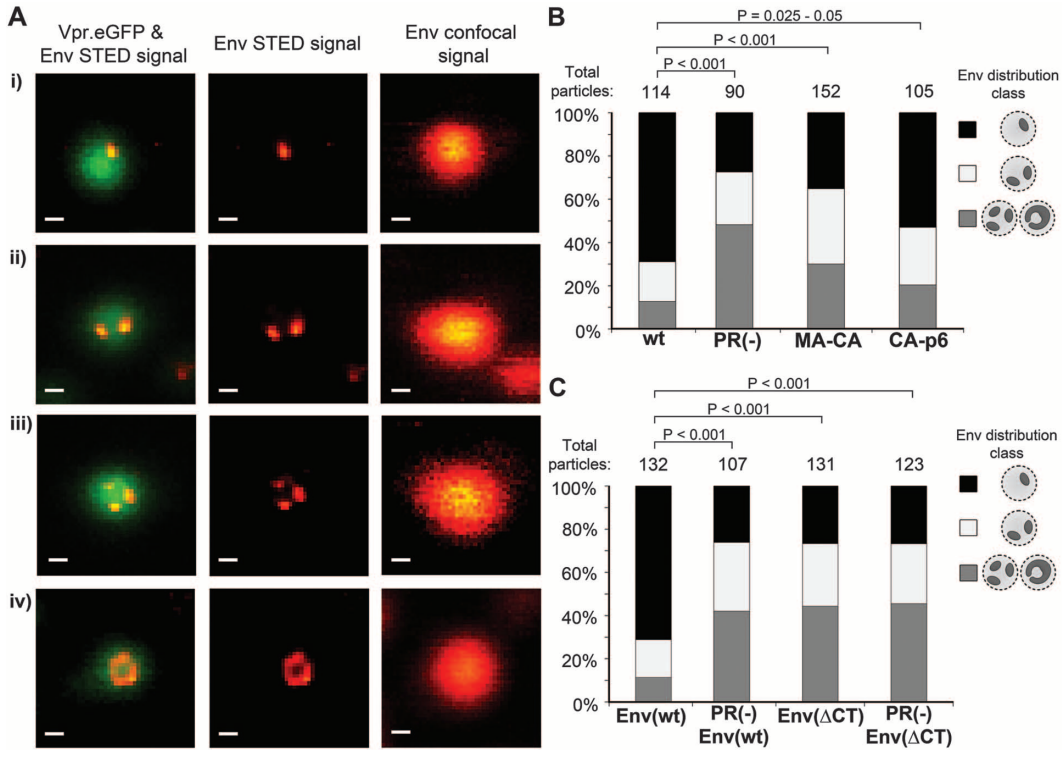


**Fig. 3.** HIV-1 Env distribution patterns depending on Gag maturation state and the presence of Env CT. (**A**) Representative images of eGFP.Vpr (green) containing HIV-1 particles stained for Env (orange), displaying different Env distribution classes: (i) single Env focus, (ii) two Env foci, (iii, iv) three or more Env foci. Scale bars: 100 nm. (**B** and **C**) Env distribution in different HIV-1 variants. Particles identified by eGFP.Vpr staining were classified into three Env distribution classes as exemplified in (A): single Env focus (black bars), two Env foci (light gray bars), three or more Env foci (dark gray bars). Data represent the mean of three independent blind counts by three different investigators with significance assessed by $\chi^2$ test for independence against a wild-type Env distribution at two degrees of freedom. (B) Mature (wt) particles compared to immature (PR-) particles or variants with mutations at distinct PR cleavage sites as described in the text. All derivatives carry Env(wt). (C) Comparison of mature and immature (PR-) particles pseudotyped with Env(wt) or Env(ΔCT), respectively.

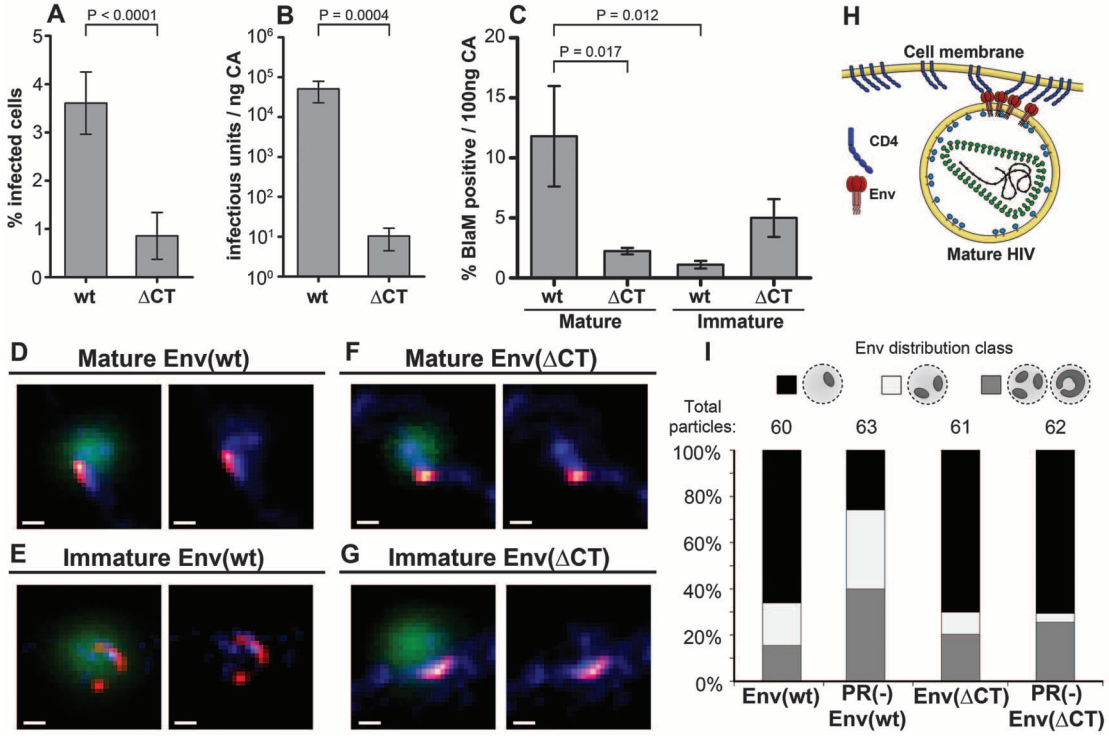


**Fig. 4.** Phenotype of HIV-1 variants and Env distribution of cell-attached virus particles. (**A**) Single-round virus infectivity. SupT1R5 cells were infected with equal amounts of HIV-1 carrying Env(wt) or Env(ΔCT). HIV-1–positive cells were quantitated by flow cytometry. Mean ± SD values from three independent experiments are shown with unpaired *t* test for significance. (**B**) HIV-1 infectious titers determined by endpoint titration on C8166 cells. Mean ± SD values from three independent experiments are shown with unpaired *t* test for significance. (**C**) Cell entry efficiency. Equal amounts of mature or immature reporter particles carrying the indicated Env variants were used to infect primary lymphocytes. Intracellular reporter-mediated cleavage of the fluorescent substrate was measured by flow cytometry. Mean ± SD values from three experiments using cells from three different donors are shown with unpaired *t* test for significance. (**D** to **G**) Env distribution of cell-attached HIV-1. Particles containing eGFP.Vpr (green) were pre-incubated with 2G12 Fab and allowed to attach to SupT1R5 cells followed by immunostaining for Env (orange) and cell surface CD4 (blue). Individual cell-attached particles were localized with the eGFP.Vpr signal in the confocal mode and Env/CD4 signals were analyzed by a dual-color STED microscopy. Panels display representative images of the respective cell-attached particles with eGFP/Env/CD4 signal overlay (left) or Env/CD4 signal overlay (right). Scale bars: 100 nm. (**H**) Schematic illustration of a cell-attached mature HIV particle. (**I**) Env distribution patterns of cell-attached mature and immature (PR-) particles pseudotyped with Env(wt) or Env(ΔCT) were classified as described in the legend to Fig. 3, B and C.

The strength of the phenotype may thus be influenced by the relative incorporation of Env variants. This view is consistent with the finding that the Env(ΔCT) variant shows a cell-type–dependent infectivity defect (*3*, *22*), which correlates with Env incorporation and can be rescued by a mutation that increases this incorporation (*25*).

We suggest that Env trimers are initially recruited to viral budding sites in a random distribution, yielding a multifocal appearance. Their lateral movement is restricted by the underlying rigid Gag lattice interacting with the Env CT and preventing formation of a single Env cluster in the immature virus. Proteolytic maturation, specifically the separation of MA from CA, overcomes this restriction, leading to coalescence into a single Env focus, driven by intermolecular Env CT interactions. This rearrangement polarizes the virus particle with subsequent attachment of the Env cluster to a CD4 patch on the target cell surface, thus initiating virus entry. Whereas Env trimers with truncated CT are mobile irrespective of Gag maturation, they lack the propensity to cluster. Clustering of Env trimers is partially rescued upon engagement of the cellular receptor provided that individual trimers are free to move within the viral membrane. Conversion of the inner core is thereby coupled to surface alterations in a mechanism of "inside-out signaling," ensuring that only particles whose interior has switched to the entry mode are fully competent for membrane fusion.

### References and Notes


1. P. Cosson, *EMBO J.* **15**, 5783 (1996).
2. E. O. Freed, M. A. Martin, *J. Virol.* **70**, 341 (1996).
3. T. Murakami, E. O. Freed, *Proc. Natl. Acad. Sci. U.S.A.* **97**, 343 (2000).
4. E. Chertova *et al.*, *J. Virol.* **76**, 5315 (2002).
5. P. Zhu *et al.*, *Proc. Natl. Acad. Sci. U.S.A.* **100**, 15812 (2003).
6. R. H. Cheng *et al.*, *Cell* **80**, 621 (1995).
7. A. Harris *et al.*, *Proc. Natl. Acad. Sci. U.S.A.* **103**, 19123 (2006).
8. P. Zhu *et al.*, *Nature* **441**, 847 (2006).
9. A. Helenius, *Cell* **69**, 577 (1992).
10. T. Murakami, S. Ablan, E. O. Freed, Y. Tanaka, *J. Virol.* **78**, 1026 (2004).
11. D. J. Wyma *et al.*, *J. Virol.* **78**, 3429 (2004).
12. N. Kol *et al.*, *Biophys. J.* **92**, 1777 (2007).
13. S. W. Hell, J. Wichmann, *Opt. Lett.* **19**, 780 (1994).
14. A. Trkola *et al.*, *J. Virol.* **70**, 1100 (1996).
15. P. Roben *et al.*, *J. Virol.* **68**, 4821 (1994).
16. D. McDonald *et al.*, *J. Cell Biol.* **159**, 441 (2002).
17. J. A. Briggs, T. Wilk, R. Welker, H. G. Kräusslich, S. D. Fuller, *EMBO J.* **22**, 1707 (2003).
18. T. Endress *et al.*, *Eur. Biophys. J.* **37**, 1291 (2008).
19. A. de Marco *et al.*, *PLoS Pathog.* **6**, e1001215 (2010).
20. M. J. Forster, B. Mulloy, M. V. Nermut, *J. Mol. Biol.* **298**, 841 (2000).
21. S. F. Lee *et al.*, *J. Biol. Chem.* **275**, 15809 (2000).
22. T. Wilk, T. Pfeiffer, V. Bosch, *Virology* **189**, 167 (1992).
23. M. Cavrois, C. De Noronha, W. C. Greene, *Nat. Biotechnol.* **20**, 1151 (2002).
24. R. Sougrat *et al.*, *PLoS Pathog.* **3**, e63 (2007).
25. D. Holtkotte, T. Pfeiffer, T. Pisch, V. Bosch, *AIDS Res. Hum. Retroviruses* **22**, 57 (2006).
26. L. A. Carlson *et al.*, *Cell Host Microbe* **4**, 592 (2008).


**Acknowledgments:** We are grateful to J. Mak (Burnet Institute, Melbourne) for purified recombinant HIV-1 Gag and to P. Guardado-Calves (Institut Pasteur, Paris) for monomeric and trimeric Env gp140. We thank L. Castillo for purified recombinant HIV-1 CA, V. Bosch (DKFZ Heidelberg) for HIV-1 gp120 and CD4 antisera as well as HIV-1 Env expression plasmids, R. Doms (University of Pennsylvania) for SupT1R5 cells, C. Aiken (Vanderbilt University Medical Center) for infectious HIV-1 variant plasmids, and T. Hope (Northwestern University Chicago) for the eGFP.Vpr construct. H.-G.K. is an investigator of the Excellence Cluster CellNetworks funded by the German Research Foundation (DFG). S.W.H. holds a patent on STED microscopy in several European countries and the United States, which has been licensed to Leica, a microscope manufacturer.

### Supplementary Materials

www.sciencemag.org/cgi/content/full/338/6106/524/DC1
Materials and Methods
Figs. S1 to S10
Table S1
References (*27*–*33*)

20 June 2012; accepted 6 September 2012
10.1126/science.1226359

# In Vivo Architecture and Action of Bacterial Structural Maintenance of Chromosome Proteins

**Anjana Badrinarayanan,[1]*† Rodrigo Reyes-Lamothe,[1]*‡ Stephan Uphoff,[2] Mark C. Leake,[2]§ David J. Sherratt[1]§**

**SMC (structural maintenance of chromosome) proteins act ubiquitously in chromosome processing. In *Escherichia coli,* the SMC complex MukBEF plays roles in chromosome segregation and organization. We used single-molecule millisecond multicolor fluorescence microscopy of live bacteria to reveal that a dimer of dimeric fluorescent MukBEF molecules acts as the minimal functional unit. On average, 8 to 10 of these complexes accumulated as "spots" in one to three discrete chromosome-associated regions of the cell, where they formed higher-order structures. Functional MukBEF within spots exchanged with freely diffusing complexes at a rate of one complex about every 50 seconds in reactions requiring adenosine triphosphate (ATP) hydrolysis. Thus, by functioning in pairs, MukBEF complexes may undergo multiple cycles of ATP hydrolysis without being released from DNA, analogous to the behavior of well-characterized molecular motors.**

SMC (structural maintenance of chromosome) complexes share conserved architectures and function in chromosome maintenance in all domains of life, although the molecular mechanism by which they act in vivo is unknown (*1*–*3*). In eukaryotes, SMC heterodimers associate with a range of accessory proteins, acting in chromosome organization, sister chromosome cohesion, and other chromosome biology functions, whereas in bacteria an SMC homodimer and associated accessory proteins act in chromosome maintenance (*1*). In *Escherichia coli* and some other γ proteobacteria, a distant SMC relative, MukB with accessory proteins MukE and MukF, replaces the typical SMC complex but has similar functions (*4*, *5*). Bacterial *smc* null mutants are frequently temperature sensitive, produce anucleate cells, and show disturbed chromosome organization at permissive temperature, indicating roles in SMC-mediated chromosome segregation and/or compaction (*1*, *6*, *7*). In *E. coli* undergoing nonoverlapping replication cycles, MukBEF accumulates as "spots" at about one to three discrete chromosome locations, typically at mid-cell and/or quarter-cell, in the same regions as replication origins (*6*). Structural and biochemical MukBEF fragment studies report two subunit arrangements, 2:4:2 or 2:2:1, for MukB:E:F, dependent on whether adenosine triphosphate (ATP) is absent or bound, respectively (*8*) (fig. S1A). Here, our aim was to understand the molecular architecture of active SMC complexes in vivo, as well as the transformations undergone during ATP binding and hydrolysis, as complexes associate with, and dissociate from, the chromosome.

*E. coli* cells, in which endogenous MukBEF genes were replaced by functional yellow fluorescent protein (YPet) fusions, were analyzed by slimfield microscopy, a strategy used previously for studying replisomes (*9*) (Fig. 1A, figs. S1 and S2, and tables S1 to S3). Analysis of the numbers of MukB, E, or F molecules

[1]Department of Biochemistry, University of Oxford, UK. [2]Department of Physics, University of Oxford, UK.

*These authors contributed equally to this work.
†Present address: Department of Biology, Massachusetts Institute of Technology, Cambridge, MA 02139, USA.
‡Present address: Department of Biology, McGill University, Montreal, Quebec H3G 0B1, Canada.
§To whom correspondence should be addressed. E-mail: m.leake1@physics.ox.ac.uk (M.C.L.); david.sherratt@bioch.ox.ac.uk (D.J.S.)

in individual fluorescent spots showed broad stoichiometry distributions, even between spots in the same cell, with mean values 36 ± 3, 36 ± 4, and 19 ± 1 molecules (±SEM) for MukB, E, and F, respectively (*9*, *10*) (Fig. 1B and C). Fourier analysis showed periodicities in stoichiometry of 4:4:2 molecules, respectively, for MukB:E:F (Fig. 1C, insets). Spots were elongated parallel to the cell's long axis (Fig. 1D), suggesting that MukBEF complexes spanned several tens of nm, with a decrease of ~20% in measured spot width with increasing stoichiometry across the range measured, consistent with increasing compaction of MukBEF structures as more molecules are added (fig. S3 and table S4).

Higher-resolution data were obtained using live-cell PALM (photoactivated localization microscopy) (*11*) with functional photoactivatable red fluorescent protein (PAmCherry) fusions to MukBEF. Rapidly diffusing and relatively immobile populations forming about one to three immobile elongated spots per cell were observed, as in slimfield images (Fig. 1E), the latter resolvable into subclusters containing closely associated individual PAmCherry molecules in a diameter of less than 40 nm (figs. S4 and S5).

Slimfield analysis of diffusing cellular YPet fluorescence (*9*) (fig. S6) indicated ~300 to 400 molecules per cell for MukB and E, and ~200 molecules per cell for MukF (table S5), in broad agreement with ensemble western estimates (*12*), implying that only ~20% of cellular MukBEF is integrated into spot complexes. PALM single-particle tracking gave similar apparent diffusion coefficients for diffusing MukB, E, and F, despite large differences in individual molecular weights, compatible with their

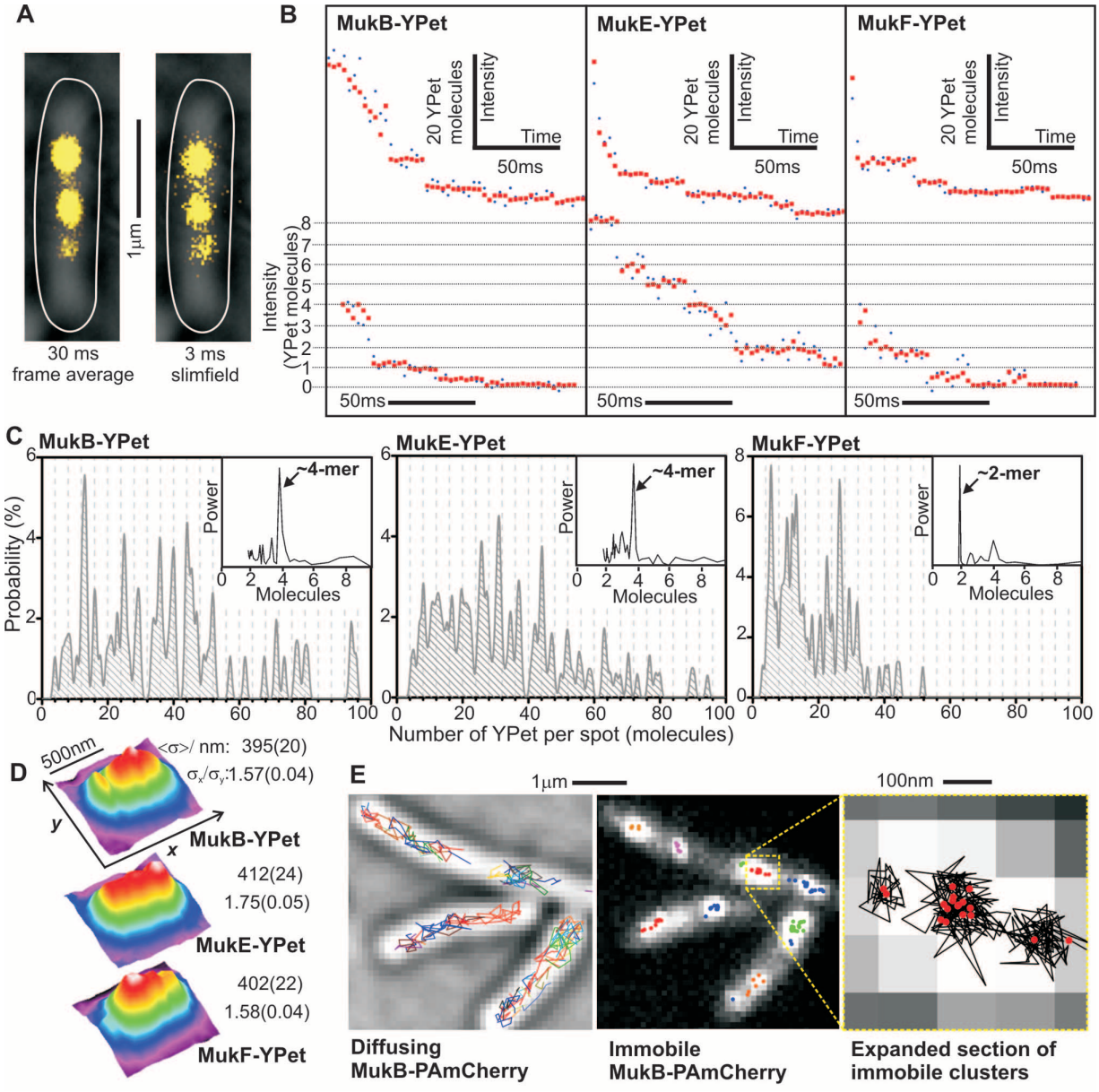


**Fig. 1.** MukBEF imaging. (**A**) Representative frame-average and slimfield MukB-YPet cell images (yellow), brightfield and cell outline overlaid (white). (**B**) Photobleaching of MukBEF-YPet spots, high (upper row) and low stoichiometry data (expanded sections, lower row), raw (blue) and filtered (red). (**C**) Stoichiometry distributions; $N$ = 51 to 84 cells. Four-molecule interval grid lines, power spectra (arbitrary units) inset. (**D**) False-color plots for mean two-dimensional spatial distributions for slimfield images with a 3-ms integration time; $N$ = 197 to 237 spots. Estimates for full width at half maximum σ and $\sigma_x/\sigma_y$ for Gaussian fits parallel to $x$ and $y$ axes (SD error). (**E**) Live-cell PALM, diffusing (gray brightfield, tracks colored) and immobile MukB-PAmCherry (different clusters colored), expanded indicating tracks (black) and clusters (red).

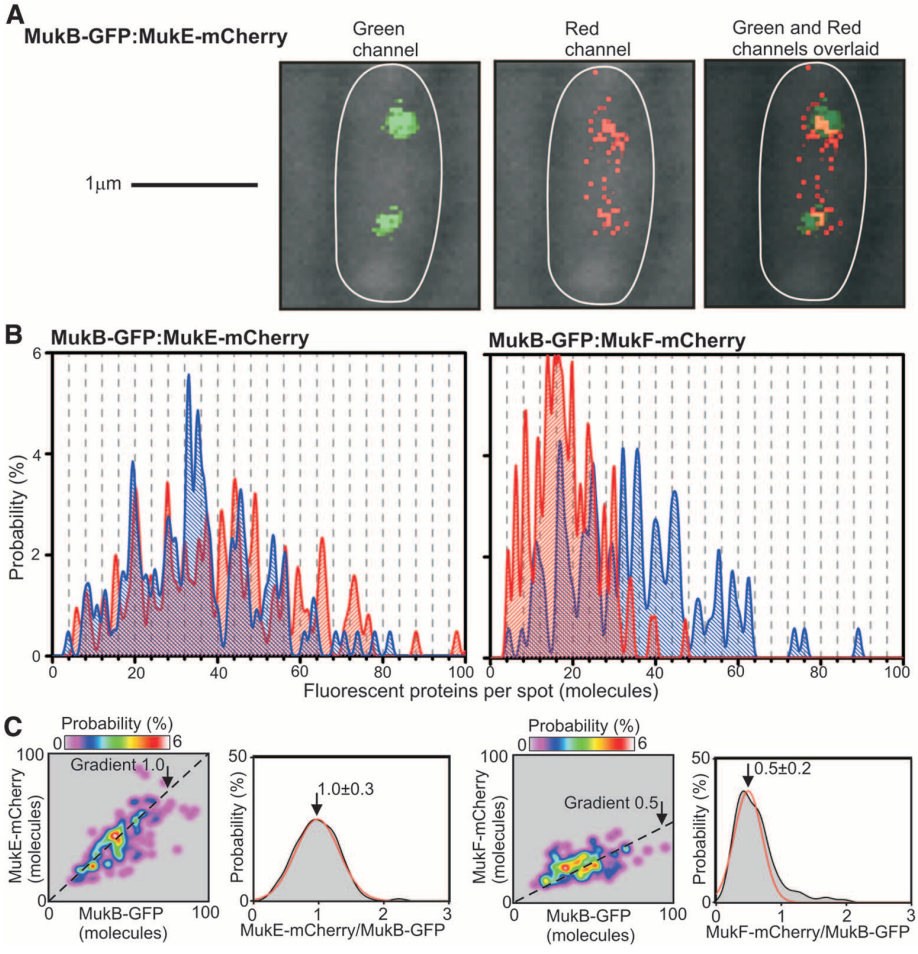


**Fig. 2.** Dual-color single-molecule millisecond imaging. (**A**) Brightfield (gray) and 3-ms fluorescence green (left panel) and red (middle panel) channels, overlaid (right panel) for dual-label strain. (**B**) Unbiased kernel density stoichiometry estimation on mCherry (red) and GFP (blue) components for two dual-label strains, 4-molecule spaced grid lines. (**C**) Stoichiometry of mCherry versus GFP component for each spot; dotted line gradients of 1.0 and 0.5; distribution of ratio of stoichiometry for mCherry and GFP components (gray) with Gaussian fit (red); mean ± SD indicated.

being components of the same large complexes (fig. S5).

We confirmed the stoichiometry periodicity of 4:4:2 for MukB:E:F by measuring simultaneously the intensities of mCherry and green fluorescent protein (GFP) fusions to pairs of MukB, E, and F in the same spots (Fig. 2, figs. S1 and S7, and table S6). A plot of the spot-by-spot stoichiometry gave mean ratio values of 1.0 ± 0.3 (±SD) and 0.5 ± 0.2 for relative content of MukE to MukB and of MukF to MukB, respectively. Thus, the localized MukBEF spots contain ~8 to 10 dimers of dimer 4:4:2 complexes as minimal functional units.

A 2:2:1 MukB:E:F ratio defines an ATP-bound state (*8*), resulting from displacement of one MukF and two MukE from a 2:4:2 putative ATP-free form. Given that MukF forms stable homodimers (*8*, *13*), MukF displacement may allow recruitment of a second 2:2:1 complex through MukF-mediated dimerization (*8*, *12*, *14*), generating the observed 4:4:2 periodicity. Indeed, ATP binding and MukB head engagement were essential for localized spot formation, because they were present in cells of a $MukB_{EQ}$ mutant that binds ATP but is hydrolysis-impaired (*8*, *15*, *16*), but not in cells carrying either nucleotide-binding ($MukB_{DA}$) or engagement-deficient ($MukB_{SR}$) mutations (*17*, *18*) (fig. S8). The relative stoichiometries of $MukB_{EQ}$:E:F in localized spots were similar to wild type, consistent with both being ATP-bound, as was the total number of $MukB_{EQ}EF$ complexes per spot (fig. S9), and the cellular content of diffusing molecules (tables S4 and S5). Because $MukB_{EQ}EF$ cells are $Muk^{-}$, MukBEF complexes must hydrolyze ATP to be functional.

To investigate whether conformational changes during ATP hydrolysis are linked to MukBEF turnover, we compared fluorescence recovery after photobleaching (FRAP) on two $MukB_{EQ}EF$ strains with wild-type counterparts (Fig. 3A and fig. S10). Detection sensitivity was increased using longer cephalexin-treated cells in which the photoactive to bleached MukBEF-YPet content was higher; recovery up to 60% of prebleach levels over several minutes was observed (Fig. 3B). In comparison, steady-state cells gave up to 30% recovery from prebleach levels (fig. S10). Reaction-diffusion modeling indicated dwell times for single MukBEF 4:4:2 complexes of ~50 s, independent of cephalexin treatment, with no dependence on prebleach intensity. Localized spots outside the original bleach zone indicated fluorescence loss in photobleaching (FLIP) over a similar time scale, converging to similar steady-state intensities. Quantifying postbleach fluorescence for all localized spots indicated ~4-molecule periodicity for MukB and MukE, and ~2-molecule periodicity for MukF (fig. S11), consistent with integer units of 4:4:2 complexes turning over. In contrast to wild-type MukBEF, $MukB_{EQ}EF$ spots showed no recovery in fluorescence after photobleaching, showing that ATP hydrolysis promoted MukBEF dissociation from DNA (Fig. 3C and fig. S10).

High-speed imaging allowed us to compare dim spots of rapidly diffusing wild-type MukBEF complexes with those carrying either ATP-binding or ATP-hydrolysis mutations. Fluorescence was converted to stoichiometries using single-molecule YPet intensity (fig. S12). Wild-type and hydrolysis mutants contained mixed populations of MukBEF complexes, with ~30% in the 4:4:2 and ~70% in the 2:4:2 state, whereas complexes of the ATP-binding mutant were exclusively in the dimeric 2:4:2 state.

Although ATP hydrolysis is essential for the activity of SMC complexes, its mechanistic importance has been unclear. Our data indicate that the minimal functional MukBEF complex acting at discrete chromosome positions is an ATP-bound dimer of MukB dimers, with ATP binding and head engagement being necessary for stable chromosome association and ATP hydrolysis required to release complexes from chromosomes. The observation

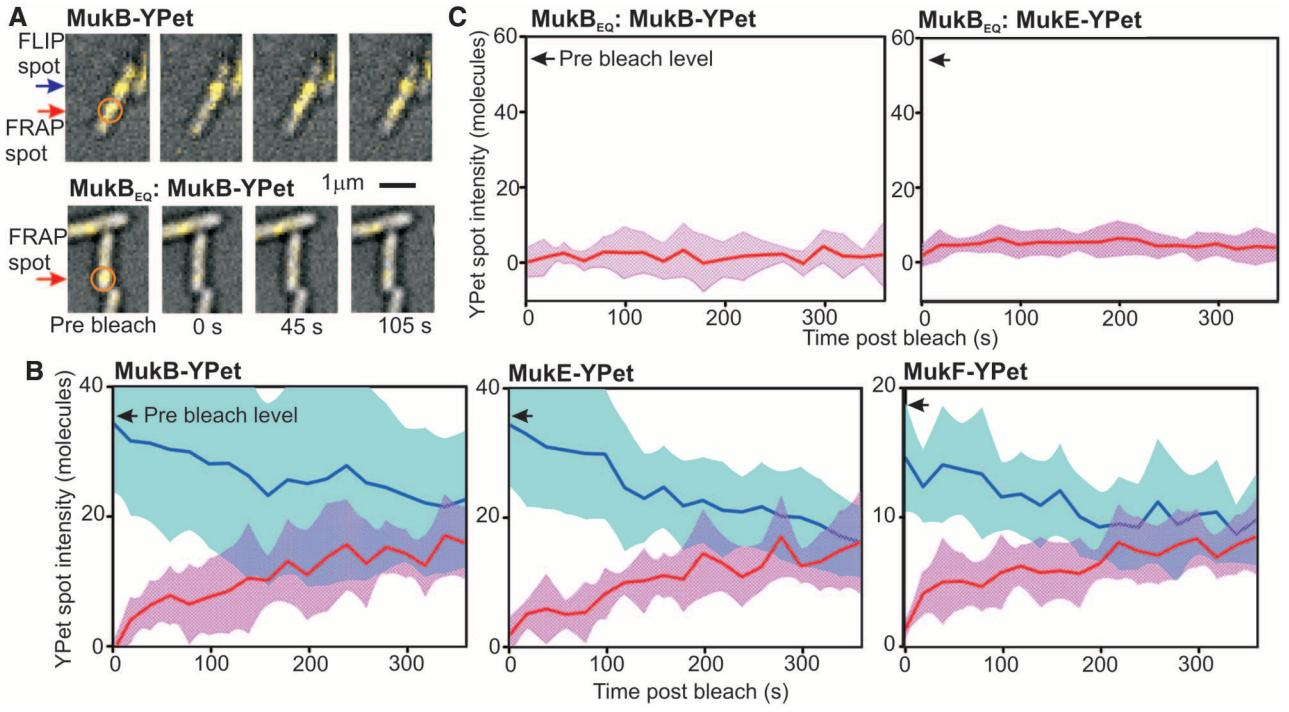


**Fig. 3.** Turnover of MukBEF complexes. (**A**) FRAP of MukB-YPet (upper panel) and ATP hydrolysis mutant MukB$_{EQ}$-YPet (lower panel), laser focus (orange circle), and FRAP (red arrow) and FLIP (blue arrow) indicated; steady-state cells. (**B** and **C**) Mean FRAP (red) and FLIP (blue) traces for cephalexin-elongated cells. SD errorbounds (shaded); prebleach levels shown (arrows); $N$ = 10 to 14 traces.

that turnover of MukBEF complexes from chromosomes is slower than predicted from in vitro adenosine triphosphatase (ATPase) levels (*8*, *19*) (fig. S1F) supports a model where ATP hydrolysis within each ATPase head pair is independent, with all four ATP molecules in the two closed dimer of dimer heads needing to be hydrolyzed almost simultaneously to completely release a single DNA-bound complex. A multimeric form of MukBEF would therefore allow release of one DNA segment and capture of a new segment without releasing the complex from the chromosome, a process akin to a rock climber making trial grabs to reach a hand hold, and one which could lead to ordered MukBEF movement within a chromosome, perhaps leading to DNA remodeling (fig. S1F). This is analogous to the processive "walking" of the molecular motors kinesin and dynein along microtubules (*20*). The functional advantage of dimeric SMC complex oligomerization may be exploited by other SMC complexes, irrespective of the mechanism of multimerization. Like MukBEF, bacterial SMC-ScpAB forms relatively immobile complexes that accumulate at a few chromosome positions. *Bacillus subtilis* SMC-ScpAB can form multimeric complexes in vitro, with SMC and ScpB forming homodimers and ScpA forming monomers or dimers (*15*, *21*). Eukaryote SMC complexes also share similar characteristics to MukBEF in maintaining chromosomes, accumulating at discrete chromosome loci (*22*, *23*), and turning over in seconds, as well as having the same distinctive architecture (*24*, *25*). Although they capture DNA topologically in apparent heterodimeric complexes (*26*), higher-order complexes might form and exploit the type of rock-climbing mechanism described here.

### References and Notes


1. S. Gruber, *Mol. Microbiol.* **81**, 855 (2011).
2. K. Nasmyth, C. H. Haering, *Annu. Rev. Biochem.* **74**, 595 (2005).
3. A. J. Wood, A. F. Severson, B. J. Meyer, *Nat. Rev. Genet.* **11**, 391 (2010).
4. H. Niki *et al.*, *EMBO J.* **11**, 5101 (1992).
5. K. Yamanaka, T. Ogura, H. Niki, S. Hiraga, *Mol. Gen. Genet.* **250**, 241 (1996).
6. O. Danilova, R. Reyes-Lamothe, M. Pinskaya, D. Sherratt, C. Possoz, *Mol. Microbiol.* **65**, 1485 (2007).
7. S. Hiraga *et al.*, *Res. Microbiol.* **142**, 189 (1991).
8. J. S. Woo *et al.*, *Cell* **136**, 85 (2009).
9. R. Reyes-Lamothe, D. J. Sherratt, M. C. Leake, *Science* **328**, 498 (2010).
10. M. C. Leake *et al.*, *Nature* **443**, 355 (2006).
11. B. Huang, M. Bates, X. Zhuang, *Annu. Rev. Biochem.* **78**, 993 (2009).
12. Z. M. Petrushenko, C. H. Lai, V. V. Rybenkov, *J. Biol. Chem.* **281**, 34208 (2006).
13. R. Fennell-Fezzie, S. D. Gradia, D. Akey, J. M. Berger, *EMBO J.* **24**, 1921 (2005).
14. M. Gloyd, R. Ghirlando, A. Guarné, *J. Mol. Biol.* **412**, 578 (2011).
15. M. Hirano, T. Hirano, *EMBO J.* **23**, 2664 (2004).
16. B. Hu *et al.*, *Curr. Biol.* **21**, 12 (2011).
17. P. Arumugam *et al.*, *Curr. Biol.* **13**, 1941 (2003).
18. S. Weitzer, C. Lehane, F. Uhlmann, *Curr. Biol.* **13**, 1930 (2003).
19. N. Chen *et al.*, *J. Bacteriol.* **190**, 3731 (2008).
20. C. Kural *et al.*, *Science* **308**, 1469 (2005).
21. J. Mascarenhas *et al.*, *BMC Cell Biol.* **6**, 28 (2005).
22. C. D'Ambrosio, G. Kelly, K. Shirahige, F. Uhlmann, *Curr. Biol.* **18**, 1084 (2008).
23. M. T. Ocampo-Hafalla, F. Uhlmann, *J. Cell Sci.* **124**, 685 (2011).
24. D. Gerlich, T. Hirota, B. Koch, J. M. Peters, J. Ellenberg, *Curr. Biol.* **16**, 333 (2006).
25. R. A. Oliveira, S. Heidmann, C. E. Sunkel, *Chromosoma* **116**, 259 (2007).
26. C. H. Haering, A. M. Farcas, P. Arumugam, J. Metson, K. Nasmyth, *Nature* **454**, 297 (2008).



**Acknowledgments:** R.R.-L. held the Todd-Bird Junior Research Fellowship of New College (Oxford University). S.U. was supported by a Mathworks scholarship. M.C.L. was supported by a Royal Society University Research Fellowship. We thank R. Oliveira for assistance with FRAP experiments and A. Kapanidis for discussions and provision of the PALM equipment. The experimental work was funded by an Engineering and Physical Sciences Research Council grant to M.C.L. (EP/G061009) and by a Wellcome Trust program grant to D.J.S. (WT083469MA). All data are presented in the supplementary materials, and bacterial strains are available on request. The authors declare that they have no competing financial interests. The project was conceived by all authors, each of whom contributed to writing the manuscript. A.B., R.R.-L., and S.U. performed the experiments, M.C.L. developed the millisecond microscopy and biophysical/analytical methods, and S.U. implemented live-cell PALM. M.C.L., A.B., and S.U. did the analysis. D.J.S. and M.C.L. contributed equally.


### Supplementary Materials

www.sciencemag.org/cgi/content/full/338/6106/528/DC1
Materials and Methods
Figs. S1 to S11
Tables S1 to S6
References (*27*–*46*)


9 July 2012; accepted 4 September 2012
10.1126/science.1227126

# Regulatory T Cells Increase the Avidity of Primary CD8$^+$ T Cell Responses and Promote Memory

Luigia Pace,[1] Andy Tempez,[1]* Catharina Arnold-Schrauf,[2]* Fabrice Lemaitre,[3] Philippe Bousso,[3] Luc Fetler,[4]† Tim Sparwasser,[2]† Sebastian Amigorena[1]‡

Although regulatory T cells ($T_{regs}$) are known to suppress self-reactive autoimmune responses, their role during T cell responses to nonself antigens is not well understood. We show that $T_{regs}$ play a critical role during the priming of immune responses in mice. $T_{reg}$ depletion induced the activation and expansion of a population of low-avidity CD8$^+$ T cells because of overproduction of CCL-3/4/5 chemokines, which stabilized the interactions between antigen-presenting dendritic cells and low-avidity T cells. In the absence of $T_{regs}$, the avidity of the primary immune response was impaired, which resulted in reduced memory to *Listeria monocytogenes*. These results suggest that $T_{regs}$ are important regulators of the homeostasis of CD8$^+$ T cell priming and play a critical role in the induction of high-avidity primary responses and effective memory.

In the absence of Foxp3$^+$ regulatory T cells ($T_{regs}$), multiple organ autoimmune pathologies arise, which lead to death in both humans and mice (*1*). $T_{regs}$ suppress autoreactive T cells through multiple effector mechanisms, acting both during priming in lymph nodes and during the effector phases of immune and inflammatory responses (*1*–*5*). It is intriguing that, in healthy individuals, $T_{reg}$-mediated suppression does not compromise T cell responses to infectious, nonself antigens. Previous reports propose that $T_{regs}$ not only inhibit immune responses to nonself antigens but also may contribute to clearance of viral or parasitic infections (*6*, *7*). How $T_{regs}$ contribute to the priming of T lymphocytes to nonself antigens remains unclear.

To investigate the role of $T_{regs}$ in CD8$^+$ T cell responses to nonself antigens, we used mice expressing the human diphtheria toxin receptor under the control of the Foxp3 promoter (DEREG mice). After two diphtheria toxin (DT) injections (*8*), we confirmed $T_{reg}$ depletion and the absence of any detectable polyclonal T cell activation or changes in dendritic cell (DC) number and activation (*9*).

We first analyzed the response to the H-Y male-specific histocompatibility antigen Uty in female mice. We immunized $T_{reg}$-depleted or control female mice with male splenocytes and measured the response against a peptide derived from the Uty antigen by using D$^b$-Uty multimers. Immunization of control females induced a uniform population of CD8$^+$ T cells strongly labeled by the multimer (Fig. 1A). Depletion of $T_{regs}$ during priming (subgroup G1, received DT on days –1, 0, 5, and 6) (fig. S1A) resulted in the expansion in all mice analyzed ($n = 20$) of a distinct population of CD8$^+$ T cells that bound small amounts of multimers, accompanied by an increase in the total numbers of multimer-positive cells (Fig. 1, A to C). The expression of CD8 was not modified (fig. S1B). In some $T_{reg}$-depleted mice, the high multimer–binding CD8$^+$ T cell population disappeared, most likely because of competition or differences in the T cell receptor (TCR) repertoires. The intensity of multimer binding reflects the affinity of the TCR for major histocompatibility complex (MHC)–peptide complexes (*10*–*15*). The ratio between the mean fluorescent intensity (MFI) for multimer to the MFI for TCR expression (relative affinity) was decreased in the absence of $T_{regs}$, as compared with control littermates (Fig. 1D and fig. S1C). A better estimate of the avidity of the polyclonal response can be obtained using a multimer dilution assay (*12*, *15*, *16*), where the avidity of the response is estimated using the half

[1]INSERM U932, Immunity and Cancer, Institut Curie, F-75248 Paris Cedex 05, France. [2]Institute of Infection Immunology, Centre for Experimental and Clinical Infection Research, TWINCORE, D-30625 Hannover, Germany. [3]INSERM U668, Department of Immunology, Institut Pasteur, F-75015 Paris, France. [4]CNRS UMR 168, Laboratoire de Physico-Chimie Curie, Institut Curie, F-75248 Paris Cedex 05, France.

*These authors contributed equally to this work.
†These authors contributed equally to this work.
‡To whom correspondence should be addressed. E-mail: sebastian.amigorena@curie.fr

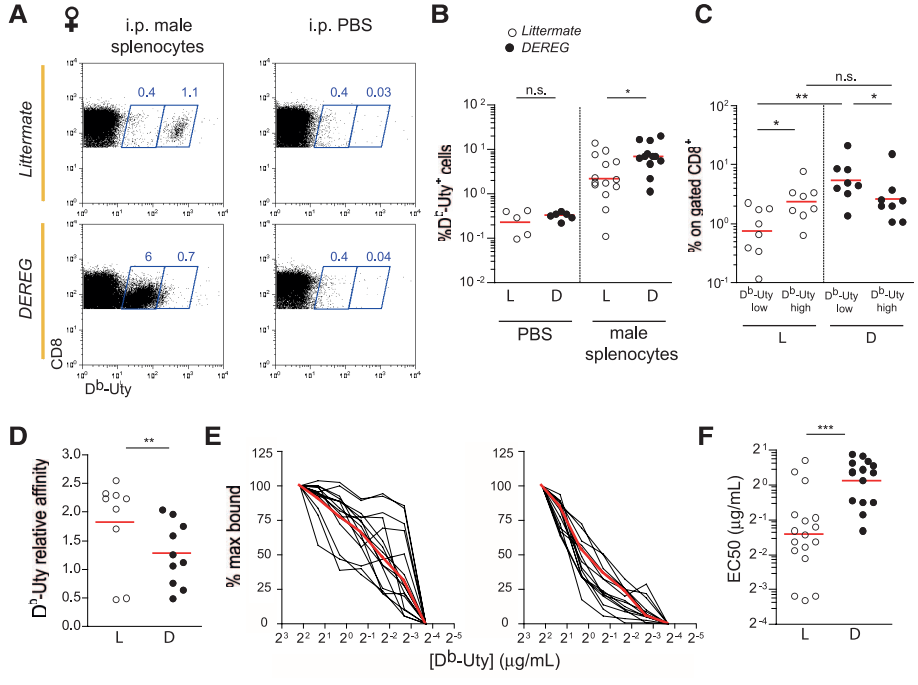


**Fig. 1.** $T_{reg}$ depletion impairs the affinity of H-Y–specific CD8$^+$ T cell responses during naive T cell priming. Flow cytometric analysis of Uty-specific CD8$^+$ T cells in the spleen of female littermates and DEREG mice immunized with $5 \times 10^6$ male splenocytes intraperitoneally (i.p.) that received DT injections on days –1, 0, 5, and 6. Primary CD8$^+$ T cell responses were measured by D$^b$-Uty–multimer staining 12 days after immunization. (**A**) Representative CD8$^+$-gated plots are shown. (**B**) Frequency of D$^b$-Uty multimer–positive among CD8$^+$ T cells in the spleen. L: littermate; D: DEREG; PBS, phosphate-buffered saline. (**C**) The numbers of high-avidity and low-avidity antigen-specific cells were determined by D$^b$-Uty–multimer staining. (**D**) The relative affinity (multimer/TCR MFI ratio) of D$^b$-Uty–specific CD8$^+$ T cells. (**E**) Direct ex vivo multimer-dilution assay. The percentage of D$^b$-Uty multimer–positive cells are normalized to the number of D$^b$-Uty multimer–positive cells at the highest multimer concentration; individual mice (black line) and the mean value for each group (red line) are represented. (**F**) For each mouse, the data obtained in (E) were analyzed to fit to sigmoid dose-response curves and the $EC_{50}$ value was calculated. Results from at least three independent experiments are shown. *$P < 0.05$; **$P < 0.01$; ***$P < 0.001$; n.s., not significant.

maximum response concentration ($EC_{50}$). The $D^b$-Uty multimer dilution assay showed a clear decrease in the avidity of the Uty-specific $CD8^+$ cells upon depletion of $T_{regs}$ (Fig. 1, E and F, and fig. S1D).

To investigate whether the impact of $T_{regs}$ on $CD8^+$ T cell avidity operates during the early phases of T cell activation (i.e., priming) or later during T cell expansion, we delayed the depletion of $T_{regs}$ (G2: DT on days 3, 4, 9, 10; G3: DT on days 5, 6, and 11) (fig. S1A). Delayed $T_{reg}$ depletion still caused an increase in the percentage of $D^b$-$Uty^+$ T cells, indicating that, in all cases, $T_{regs}$ limit T cell expansion (fig. S2A). Decreased T cell avidity, by contrast, was only observed when the depletion of $T_{regs}$ was performed during priming (fig. S2, B to D). We conclude that the presence of $T_{regs}$ during T cell priming to a nonself antigen increases the affinity of the $CD8^+$ T cell response, most likely by inhibiting the priming of T cells bearing low-avidity antigen-specific TCRs.

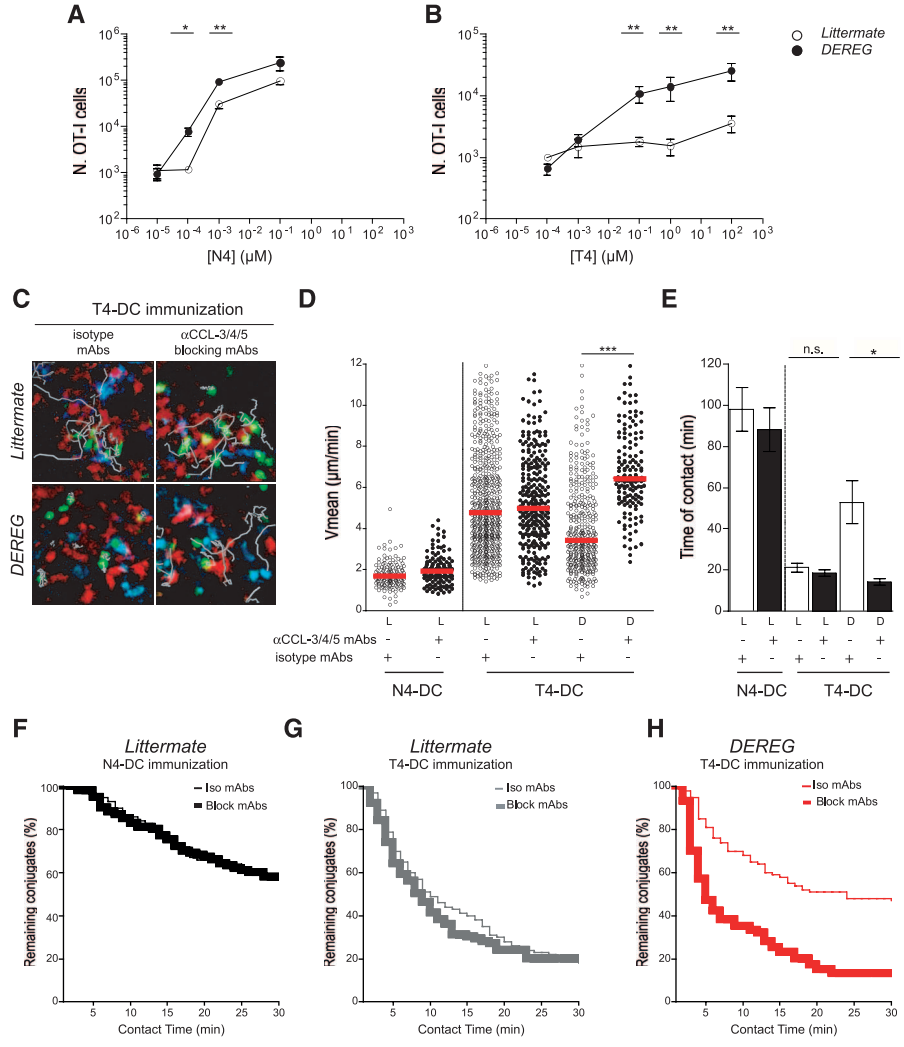


**Fig. 2.** $T_{reg}$ suppression inhibits T cell responses to low-affinity ligands by destabilizing T cell–DC interactions. (**A** and **B**) DEREG (black) or control (white) littermate mice were DT-injected and immunized by foot pad (f.p.) injection with mature DCs loaded with the indicated concentrations of the native N4 or the alternate peptide ligand T4. Eighteen hours later, mice were injected intravenously (i.v.) with $10^5$ naïve CD45.1 OT-I cells. OT-I cell numbers from the harvested dpLNs 5 days after the immunization are reported. (**C** to **H**) TPLSM analysis of OT-I cell priming in DT-treated littermate and DEREG mice. DsRed+ DCs loaded or not with 1 μM of N4 or T4 peptides and unpulsed $CFP^+$ DCs were coinjected in the f.p. of DT-treated littermate or DEREG mice in the presence of monoclonal antibodies (mAbs) that block CCL-3/4/5 or the isotype-matched control antibodies. Twenty hours later, $GFP^+$ OT-I cells were adoptively transferred. Before in vivo imaging, mice received the L-selectin–specific antibody to block lymphocyte homing, and dpLNs were imaged 2 to 6 hours after OT-I cell transfer. (C) Representative TPLSM images are shown. White lines represent migratory paths of OT-I cells. (D) T cell mean velocities are represented; the red line indicates the median value. (E) Average contact duration. (F to H) The percentage of remaining conjugates for interactions between $GFP^+$ OT-I cells and DsRed+ DCs are shown. Data are representative of at least three independent experiments. Error bars represent means ± SEM. $^*P < 0.05$; $^{**}P < 0.01$; $^{***}P < 0.001$; n.s., not significant.

To generalize this observation to other antigens, we next analyzed a $CD8^+$ T cell response to the OVA peptide 257–264 (SIINFEKL, N4) after immunization with peptide-loaded lipopolysaccharide (LPS)–treated DCs and obtained similar results (fig. S3, A to D). In spite of the increase in total $K^b$-N4 multimer–positive cells after priming in $T_{reg}$-depleted mice (fig. S3B), the number or relative affinity of antigen-specific $CD8^+$ memory T cells after challenge (which is increased compared with the avidity of the primary cells) was not enhanced in DEREG mice deprived of $T_{regs}$ during priming (fig. S3, B and D). Indeed, the ratio between the mean number of memory and primary multimer–positive cells was decreased upon $T_{reg}$ depletion during priming (fig. S3C), which indicated that the numerous low-avidity OVA-specific T cells that proliferate in the absence of $T_{regs}$ do not give rise to long-lived memory cells.

Because $T_{reg}$ depletion can perturb the environment, which could indirectly affect T cell priming, we decided to test if injection of isolated antigen-specific $T_{regs}$ would increase the avidity of a polyclonal T cell response. We isolated Dby-specific, $Foxp3^-$, enhanced green fluorescent protein–negative ($EGFP^-$) T helper cells ($T_H$) or $Foxp3^+$ $EGFP^+$ $T_{regs}$ from Foxp3-EGFP $CD4^+$ TCR-transgenic Marilyn mice. We injected these cells into wild-type hosts previously immunized with (N4 + Dby)-loaded DCs. The total numbers of $K^b$-$N4^+$ $CD8^+$ T cells were decreased when the mice were injected with Marilyn $T_{regs}$ (fig. S3, E and F). Moreover, the presence of Marilyn $T_{regs}$ reduced the number of low multimer–binding T cells, as compared with Marilyn $T_H$ cells, which resulted in an increase in the relative affinity of the response (fig. S3, E, G, and H). We concluded that the adoptive transfer of antigen-specific $T_{regs}$ preferentially inhibits low-avidity as opposed to high-avidity $CD8^+$ T cells, thereby increasing the overall avidity of the T cell response.

To directly test whether $T_{regs}$ preferentially inhibit the priming of low-avidity $CD8^+$ T cells, we used two altered peptide ligands that are recognized with different affinities by the OT-I TCR [OT-I is a $CD8^+$, TCR-transgenic line specific for the H-$2K^b$-SIINFEKL (N4, OVA peptide)]. $K^b$-N4 complexes bind the OT-I TCR with high affinity. SIITFEKL (T4) binds $K^b$ with an affinity similar to that for N4, but the $K^b$-T4 complexes are recognized by the OT-I TCR with an affinity lower than $K^b$-N4 complexes by a factor of 70.7 (*16*–*18*). We first verified that the numbers of $K^b$-N4 and $K^b$-T4 complexes present on the DC surface were similar (fig. S4, A and B). Immunization with N4-loaded DCs (N4-DCs) induced effective OT-I expansion both in the presence and absence of $T_{regs}$, although $T_{reg}$ depletion increased the expansion at low peptide concentrations (Fig. 2A and fig. S4, C and D). T4-loaded DCs, as shown previously (*18*), induced very low expansion of OT-I cells in the presence of $T_{regs}$, even at high peptide concentrations (Fig. 2B and fig. S4, C and D). In $T_{reg}$-depleted mice, by contrast, T4-DCs induced effective expansion of OT-I cells over a wide range

of peptide concentrations (Fig. 2B). Similar results were obtained when we assayed OT-I activation using CD69 expression (fig. S5A), which suggests that $T_{regs}$ inhibit some early steps of T cell priming by low-affinity peptides.

To test if $T_{regs}$ suppress priming by low-affinity peptide by acting directly on $CD8^+$ T cells, we next reconstituted the inhibition in vitro. $T_{regs}$, but not $CD4^+$ $T_H$ cells, inhibited the activation of OT-I cells by N4-DCs only at low peptide concentration (fig. S5B). In the case of T4-loaded DCs, the inhibition by $T_{regs}$ was more potent and was observed at both high and low peptide concentrations (fig. S5C). These results suggest that the expansion of low-avidity polyclonal T cells observed in DEREG mice is due to the release of the suppression by $T_{regs}$ of low-avidity T cell clones.

$T_{regs}$ were previously shown to regulate DC–T cell interactions during priming (*3*, *5*) and to suppress the production by DCs of CCL-3/4 (*19*, *20*), a family of chemokines involved in the control of the dynamics of T cell priming (*21*–*23*), as well as in the stability and signaling at DC–T cell synapse (*24*, *25*). We therefore hypothesized that $T_{regs}$ destabilize low-avidity DC–T cell interactions more efficiently than high-avidity interactions through the regulation of chemokine production.

To investigate this possibility, we first analyzed the production of CCL-3/4/5 during T cell priming in vivo by DCs loaded with N4 or T4 peptides, in the presence or absence of $T_{regs}$ (fig. S6, A to C). In littermates, unloaded LPS-treated DCs induced the production of all three chemokines in draining popliteal lymph nodes (dpLNs). Loading of the DCs with T4 hardly modified chemokine production, whereas loading with N4 increased the production of CCL-3/4 (fig. S6, A and B). $T_{reg}$ depletion did not modify the expression of activation markers by the adoptively transferred DCs (fig. S5, D to H). By contrast, it increased CCL-3/4 production in mice injected with unloaded or T4-loaded DCs but not with N4-DCs (most likely because the production of these chemokines was already very high).

We therefore investigated the effects of $T_{reg}$ depletion and the eventual role of these chemokines on DC–T cell interactions induced by high- or low-affinity peptides using intravital dynamic two-photon laser scanning microscopy (TPLSM). Littermates or DEREG mice treated with DT were adoptively transferred with a 1:1 mix of DsRed fluorescent protein (DsRed)–expressing DCs pulsed with either N4 or T4 and unloaded control cyan fluorescent protein–positive ($CFP^+$) DCs (as a control T cell–DC contacts). $GFP^+$ OT-I T cells were then adoptively transferred to the mice. The possible involvement of CCL-3/4/5 was addressed by using a previously described mix of blocking antibodies (*21*, *23*).

The injection of blocking antibodies had no major effect on DC and OT-I recruitment to the dpLNs, as compared with the effects on control mice (fig. S7, A and B). In these mice, N4-DCs caused a marked arrest of OT-I cells and long-lasting DC–T cell contacts, as compared with T4-DCs (movies S2 and S4 and Fig. 2, C to H), which confirmed that high-affinity peptides induce longer-lasting DC–T cell contacts with naïve T cells than do low-affinity peptides (*16*, *26*). Depletion of $T_{regs}$ did not affect the arrests and long-lasting DC–T cell contacts observed with N4-DCs (fig. S7C). By contrast, the intermediate OT-I mean velocity (Vmean) observed in mice injected with T4-DCs was reduced upon depletion of $T_{regs}$ (Fig. 2, C and D, G, and H; movies S4 and S6), whereas the average contact duration of the individual contacts was increased (Fig. 2, E to H) (*27*). Therefore, the low-affinity T4 peptide mediates relatively stable DC–OT-I interaction only in the absence of $T_{regs}$, consistent with the observation that it only induces expansion after $T_{reg}$ depletion.

Treatment of the mice with CCL-3/4/5–blocking antibodies had no major effect on OT-I

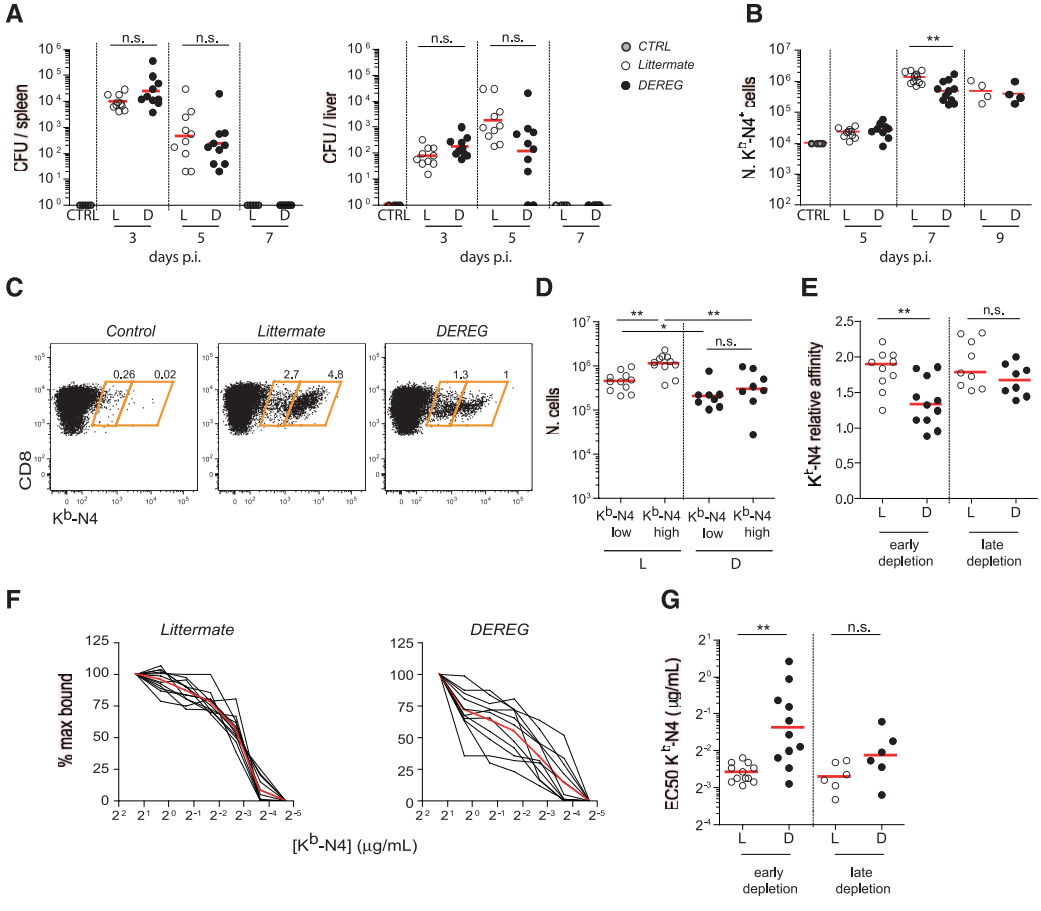


**Fig. 3.** $T_{regs}$ promote high-avidity $CD8^+$ T cell primary immune responses to rLM-OVA infection. DT-treated DEREG and littermate mice were injected i.v. with $5 \times 10^3$ rLM-OVA. (**A**) At days 3, 5, and 7 after infection (p.i.), the number of live bacteria per spleen (left) and liver (right) was determined as CFU, colony-forming units. (**B**) Primary $CD8^+$ T cell responses were measured after the infection by $K^b$-N4–multimer staining. The number of $CD8^+$ $K^b$-$N4^+$ cells is reported. (**C**) $CD8^+$-gated flow cytometry plots from samples collected day 7 after infection are shown. (**D**) The numbers of high-avidity and low-avidity antigen-specific cells were determined by $K^b$-N4 multimer staining. (**E**) Relative affinity for $K^b$-$N4^+$ cells was determined after early (DT days −1, 0) or late depletion (DT days 3 to 4). (**F**) Ex vivo multimer-dilution assay at day 7 after rLM-OVA infection. The graph shows the percentage of $K^b$-N4 multimer–positive on gated $CD8^+$ T cells, normalized to the number of $K^b$-N4 multimer–positive cells at the highest multimer concentration. Individual mice (black line) and the mean values (red line) are represented. (**G**) For each individual mouse, the data obtained in (F) were analyzed to fit to sigmoid dose-response curves and the $EC_{50}$ value was calculated. $T_{regs}$ were depleted at days −1 and 0 (early depletion) or at days 3 and 4 postinfection (late depletion). Data are representative of three independent experiments. Error bars represent means ± SEM. N.s., not significant. $^*P < 0.05$; $^{**}P < 0.01$; n.s., not significant.

displacement or contact durations in the case of N4-DCs (movie S1 and Fig. 2, D to F). In mice injected with T4-DCs, by contrast, the blocking antibodies reversed the effects of $T_{reg}$ depletion, both in terms of reduction of the Vmean and of the duration of the individual contacts (Fig. 2, D to E, G, and H; movies S3 and S5). The lack of effect of the chemokine antibodies in mice injected with N4-DCs could be because of the higher levels of chemokine production observed in these mice (fig. S6, A to C), or stable N4-DC–T cell conjugates may become chemokine-independent. These results suggest that the stable interactions of T cells with DCs bearing low-affinity peptides that occur in the absence of $T_{regs}$ require CCL-3/4/5. We propose that by limiting the production of CCL-3/4/5, $T_{regs}$ normally inhibit stable interactions between DCs and low-avidity T cells, thereby limiting their priming.

To investigate the role of $T_{regs}$ during $CD8^+$ T cell responses to a microbe-associated nonself antigen, we infected DT-treated DEREG mice or littermates with *Listeria monocytogenes* (LM) expressing recombinant OVA (rLM-OVA) (*28*). $T_{reg}$ depletion affected neither the proportion of myeloid cells (fig. S8, A to F) nor the bacterial burden at days 3 and 5 postinfection, or the capacity of the mice to clear the infection (Fig. 3A) [clearance of the primary LM infection is known to be mainly mediated by innate immunity (*29*)]. $T_{reg}$ depletion caused a reduction in the total numbers of $K^b$-N4 multimer–positive T cells at day 7 (peak of the response, Fig. 3B). In the presence of $T_{regs}$, rLM-OVA infection induced primarily a population of high multimer–binding T cells (Fig. 3C). Upon $T_{reg}$ depletion, the proportion of low multimer–binding cells increased (Fig. 3, C and D, and fig. S9, A to D). These cells were antigen-specific, as they did not bind a control $K^b$-SSIEFARL multimer (fig. S9A). Although the total numbers of both high and low multimer–binding cells decreased slightly in $T_{reg}$-depleted mice, the decrease was significantly greater for the high multimer–binding cells (Fig. 3D). This decrease could be because of overstimulation of high-avidity T cells (which may impair T cell activation (*30*)] or to competition of the OVA-specific cells with the very numerous T cells that respond to other LM antigens in the absence of $T_{regs}$ (fig. S10, A and B).

As expected from the changes in the proportions of high and low multimer–binding cells, $T_{reg}$ depletion induced a decrease in the relative affinity of the OVA-specific–responding T cells (Fig. 3E and fig. S9, C and D). Decreased multimer labeling was not due to lower levels of CD8 expression (fig. S9B). Decrease in the avidity of the OVA-specific $CD8^+$ T cell response upon depletion of $T_{regs}$ was also evident in the multimer dilution assay (Fig. 3, F and G). Interferon-γ (IFN-γ) production by $CD8^+$ T cells was shown previously to correlate with the avidity of LM-specific immune responses (*10*). Both the number of OVA-specific IFN-γ–producing $CD8^+$ T cells and the amount of IFN-γ per cell (MFI) were lower when the infection took place in the absence of $T_{regs}$ (fig. S11, A to C). When $T_{reg}$ depletion was delayed to days 3 to 4 after infection, the relative affinity and the $EC_{50}$ of multimer binding assay (Fig. 3, E and G), as well as the numbers of $K^b$-$N4^+$ multimer$^+$ and IFN-$\gamma^+$ cells, were all unaffected, whereas the MFI of the IFN-γ labeling was slightly increased (fig. S12, A to C).

To investigate the mechanisms involved in the beneficial effects of $T_{regs}$ during priming to LM antigens, we harvested the spleens of mice infected in the presence or absence of $T_{regs}$ and analyzed different inflammatory mediators. No major effects were seen on the secretion of CXCL1 and CXCL10) (fig. S13, A and B). By contrast, the production of CCL-2/3/4 was increased upon $T_{reg}$ depletion in vivo (fig. S13, C to E). Furthermore, upon ex vivo restimulation with heat-killed (HK)-rLM-OVA, the splenocytes isolated from infected mice showed substantially enhanced secretion of CCL-3/4/5 when the infection in vivo took place in the absence of $T_{regs}$ (fig. S14). These findings indicate that, as shown previously by others (*19*, *20*), $T_{regs}$ inhibit in vivo the production of CCL-2/3/4/5.

Because our previous results implicate CCL-3/4/5 in the control of the priming of low-avidity T cells, we decided to explore the possible involvement of the overproduction of these chemokines in the detrimental effects of $T_{reg}$ depletion on T cell priming during LM infection. To do so, we injected a mix of blocking antibodies to CCL-3/4/5 after $T_{reg}$ depletion and infection with rLM-OVA (*21*, *23*). In both isotype control and blocking antibody–treated mice, the bacteria were undetectable in the spleen at day 7. By contrast, only injection of the blocking antibodies reversed the effects of $T_{reg}$ deprivation on the proportion of low- and high multimer–binding cells

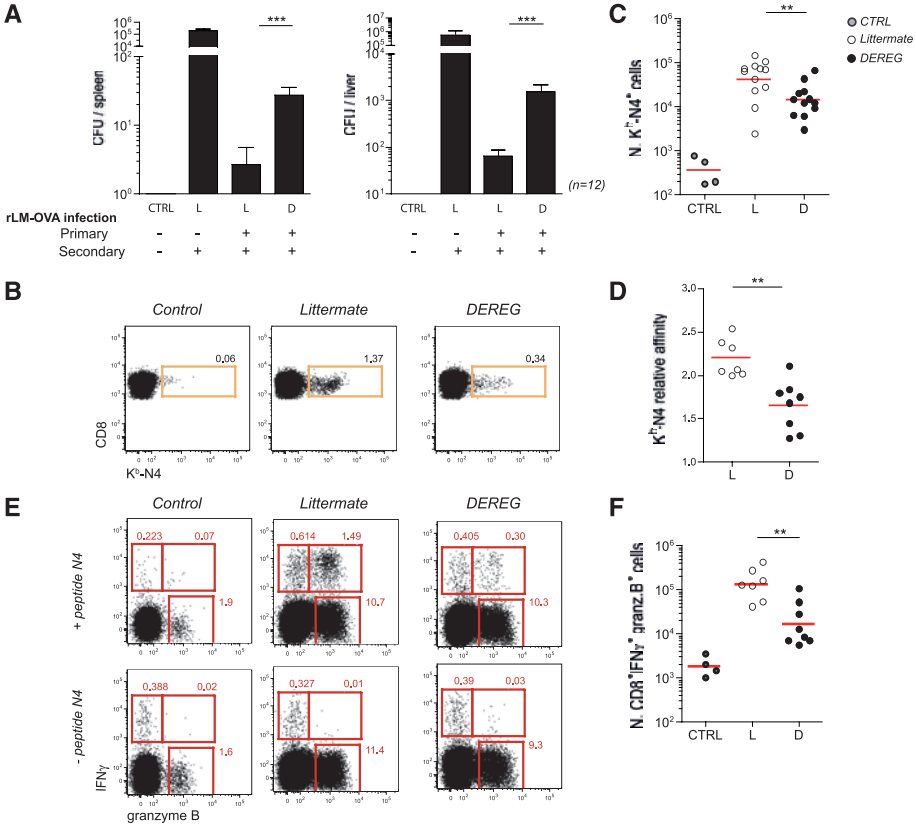


**Fig. 4.** During T cell priming, $T_{regs}$ are required to generate a protective immune response after secondary rLM-OVA challenge. Littermates and DEREG mice were treated with DT and infected with rLM-OVA, and tested for memory protection 50 days later. For memory T cell generation, naïve and 50-days postinfection mice were given $5 \times 10^3$ and $2 \times 10^5$ rLM-OVA, respectively. (**A**) The number of live bacteria per spleen (left) and liver (right) was determined 3 days after secondary challenge. As control, C57BL/6 mice that had not received primary infection were similarly infected. In 10 of 12 spleens from littermate mice, the bacteria were undetectable. (**B** to **F**) $K^b$-$N4^+$ multimer and intracellular IFN-γ and granzyme B staining were done to determine the percentage of antigen-specific cells in $CD8^+$ T cell population. (B) $CD8^+$-gated flow cytometry plots are shown (samples were collected 3 days after challenge). (C) The number of $K^b$-$N4^+$ cells is shown. Individual mice are represented, control uninfected (gray), littermate (white), and DEREG (black). Results from three independent experiments are shown. (D) Relative affinity for $K^b$-$N4^+$ cells was determined. (E and F) After ex vivo N4 restimulation, IFN-γ and granzyme B staining was done to determine the number of $CD8^+$ antigen-specific cells. (E) $CD8^+$-gated flow cytometry plots are shown. (F) The number of IFN-$\gamma^+$ granzyme $B^+$ $CD8^+$ cells is shown. Data are representative of three independent experiments. Error bars represent means ± SEM. $^{**}P < 0.01$; $^{***}P < 0.001$.

and of the relative affinity of the responding OVA-specific T cells (fig. S15, A and B). These results suggest that CCL-3/4/5 production in the absence of $T_{regs}$ is required for the observed reduction in avidity of the OVA-specific $CD8^+$ T cells after LM infection.

We next investigated the functional relevance of the presence of $T_{regs}$ during the primary infection by rLM-OVA. Because the avidity of primary responses was suggested to influence memory responses (*12*, *15*), we investigated the memory responses generated after LM infection in $T_{reg}$-deprived mice. Littermates and DEREG mice treated with DT were primed with rLM-OVA and tested for memory responses by re-infecting the mice with rLM-OVA 50 days later. After secondary infection, 10 to 25 times more bacterial burden was detected in both spleen and liver when $T_{regs}$ had been depleted before the primary infection (Fig. 4A). Consistent with this result, both the number of memory $K^b$-N4 multimer–positive T cells (Fig. 4, B and C) and their relative affinity (Fig. 4D) were reduced. After ex vivo restimulation, we found reduced numbers of IFN-γ–granzyme B double-positive memory $CD8^+$ cells (Fig. 4, E and F). Therefore, the presence of $T_{regs}$ during the primary rLM-OVA infection is required for the establishment of fully effective high-avidity $CD8^+$ T cell memory responses.

We propose that the absence of $T_{regs}$ reduces the "fitness" of primary $CD8^+$ T cell responses, causing the overproliferation of low-avidity T cells, and may impair the activation of high-avidity T cells, although this remains to be explored. The inhibition of low-avidity T cell clones by $T_{regs}$ could also help explain why $T_{regs}$ fully control T cell reactivity to self-antigens [which are generally of low avidity because of negative selection (*10*)], while sparing T cell responses to nonself antigens (which target a nonnegatively selected repertoire that includes high-avidity T cells). These results unravel an unexpected function for $T_{regs}$ during $CD8^+$ T cell priming and should inform $T_{reg}$ manipulation for the design of long-term vaccination.

### References and Notes


1. K. Wing, S. Sakaguchi, *Nat. Immunol.* **11**, 7 (2010).
2. M. Feuerer, Y. Shen, D. R. Littman, C. Benoist, D. Mathis, *Immunity* **31**, 654 (2009).
3. Q. Tang *et al.*, *Nat. Immunol.* **7**, 83 (2006).
4. D. R. Littman, A. Y. Rudensky, *Cell* **140**, 845 (2010).
5. C. E. Tadokoro *et al.*, *J. Exp. Med.* **203**, 505 (2006).
6. Y. Belkaid, C. A. Piccirillo, S. Mendez, E. M. Shevach, D. L. Sacks, *Nature* **420**, 502 (2002).
7. J. M. Lund, L. Hsing, T. T. Pham, A. Y. Rudensky, *Science* **320**, 1220 (2008).
8. K. Lahl *et al.*, *J. Exp. Med.* **204**, 57 (2007).
9. A. Boissonnas *et al.*, *Immunity* **32**, 266 (2010).
10. D. Zehn, M. J. Bevan, *Immunity* **25**, 261 (2006).
11. E. S. Huseby *et al.*, *Cell* **122**, 247 (2005).
12. D. H. Busch, E. G. Pamer, *J. Exp. Med.* **189**, 701 (1999).
13. C. Bouneaud, P. Kourilsky, P. Bousso, *Immunity* **13**, 829 (2000).
14. M. M. Davis, J. D. Altman, E. W. Newell, *Nat. Rev. Immunol.* **11**, 551 (2011).
15. P. A. Savage, J. J. Boniface, M. M. Davis, *Immunity* **10**, 485 (1999).
16. H. D. Moreau *et al.*, *Immunity* **37**, 351 (2012).
17. S. C. Jameson, M. J. Bevan, *Eur. J. Immunol.* **22**, 2663 (1992).
18. D. Zehn, S. Y. Lee, M. J. Bevan, *Nature* **458**, 211 (2009).
19. S. Morlacchi *et al.*, *J. Immunol.* **186**, 6807 (2011).
20. V. Dal Secco *et al.*, *PLoS ONE* **4**, e7696 (2009).
21. F. Castellino *et al.*, *Nature* **440**, 890 (2006).
22. S. Hugues *et al.*, *Nat. Immunol.* **8**, 921 (2007).
23. H. D. Hickman *et al.*, *J. Exp. Med.* **208**, 2511 (2011).
24. B. Molon *et al.*, *Nat. Immunol.* **6**, 465 (2005).
25. R. L. Contento *et al.*, *Proc. Natl. Acad. Sci. U.S.A.* **105**, 10101 (2008).
26. R. A. Gottschalk *et al.*, *Proc. Natl. Acad. Sci. U.S.A.* **109**, 881 (2012).
27. J. B. Beltman, S. E. Henrickson, U. H. von Andrian, R. J. de Boer, A. F. Marée, *J. Immunol. Methods* **347**, 54 (2009).
28. K. E. Foulds *et al.*, *J. Immunol.* **168**, 1528 (2002).
29. E. G. Pamer, *Nat. Rev. Immunol.* **4**, 812 (2004).
30. A. M. Kalergis *et al.*, *Nat. Immunol.* **2**, 229 (2001).


**Acknowledgments:** We thank all the U932 and TWINCORE Sparwasser members; D. Raulet, A. Dielmann, P. Paul-Gilloteaux, O. Lantz, and M. Albert; the Nikon Imaging Center and flow cytometry platform; and the animal facilities of Institut Curie and TWINCORE for help with the experiments and helpful discussions. rLM-OVA was kindly provided by H. Shen. This work was supported by funding from the Institut Curie; Institut National de la Santé et de la Recherche Médicale; Centre National de la Recherche Scientifique; La Ligue Contre le Cancer; Association de Recherche Contre le Cancer (ARC); EC grant ENCITE, Health-F5-2008-201842, SFB 900. L.P. has been supported by ARC, A.T. was a fellow of Ministère de l'Education et de la Recherche. C.A.-S. was supported by the Boehringer Ingelheim Fonds, Foundation for Basic Research in Medicine. The authors have no conflicting financial interests. The data are tabulated in the main paper and in the supplementary materials.

### Supplementary Materials

www.sciencemag.org/cgi/content/full/338/6106/532/DC1
Materials and Methods
Figs. S1 to S15
References (*31*–*35*)
Movies S1 to S6

6 July 2012; accepted 10 September 2012
10.1126/science.1227049



# Elfn1 Regulates Target-Specific Release Probability at CA1-Interneuron Synapses

**Emily L. Sylwestrak[1,2,3] and Anirvan Ghosh[1,2]***

**Although synaptic transmission may be unidirectional, the establishment of synaptic connections with specific properties can involve bidirectional signaling. Pyramidal neurons in the hippocampus form functionally distinct synapses onto two types of interneurons. Excitatory synapses onto oriens–lacunosum moleculare (O-LM) interneurons are facilitating and have a low release probability, whereas synapses onto parvalbumin interneurons are depressing and have a high release probability. Here, we show that the extracellular leucine-rich repeat fibronectin containing 1 (Elfn1) protein is selectively expressed by O-LM interneurons and regulates presynaptic release probability to direct the formation of highly facilitating pyramidal-O-LM synapses. Thus, postsynaptic expression of Elfn1 in O-LM interneurons regulates presynaptic release probability, which confers target-specific synaptic properties to pyramidal cell axons.**

Regulated control of synaptic transmission is essential to the gating of information flow through neuronal circuits. The efficacy of synaptic transmission depends on the probability that an action potential will elicit vesicle release (*1*). Different synapses on a single axon can have different release properties depending on the identity of the postsynaptic partner, suggesting that cell type–specific signals from the postsynaptic neuron define this property (*2*, *3*). The importance of target-specific synaptic release properties is exemplified by CA1 pyramidal cell axons, which make synapses on different classes of inhibitory interneurons (Fig. 1A). CA1 pyramidal cell synapses onto parvalbumin (PV)– and somatostatin (Sst)–containing interneurons have different release probabilities (*4*–*6*). High release probability at pyramidal-PV cell synapses results in initially strong but rapidly depressing excitatory synaptic currents. (*4*). In contrast, pyramidal-Sst cell synapses have much lower release probability and are strongly facilitating (*5*, *7*). The presynaptic pyramidal neurons must therefore receive target-derived information from the postsynaptic cells to assemble synapses with distinct properties. Although these properties are critical for regulating the dynamics of hippocampal circuits, the transsynaptic signals that assemble pyramidal cell terminals with differing release probability are unknown.

To identify cues on the postsynaptic cell that might direct the development of cell type-

[1]Neurobiology Section, Division of Biological Sciences, University of California, San Diego, La Jolla, CA 92093–0366, USA. [2]CNS Discovery, F. Hoffmann La Roche, 4070 Basel, Switzerland. [3]Biozentrum of the University of Basel, 4056 Basel, Switzerland.

*To whom correspondence should be addressed. E-mail: anirvan.ghosh@roche.com

specific synapses, we used mRNA expression data from the Allen Brain Atlas to identify genes expressed in distinct hippocampal interneuron subpopulations (*8*). Comparison of expression patterns of candidate genes with those of Sst and PV revealed similar expression patterns between the leucine-rich repeat (LRR) protein Elfn1 and a group of Sst-expressing cells, oriens–lacunosum moleculare (O-LM) cells (Fig. 1B). LRR proteins have been shown to function as transsynaptic regulators (*9*, *10*), suggesting that Elfn1 may function as a signal on Sst-positive O-LM interneurons to specify synaptic properties.

To determine whether individual cells coexpress Elfn1 and somatostatin, we combined in situ hybridization (ISH) for Elfn1 mRNA with immunohistochemical (IHC) detection for interneuron cell type. We crossed mice with a Cre-conditional tdTomato reporter with mice expressing Cre recombinase under Sst or PV promoters, Sst::tdTomato and PV::tdTomato, respectively (Fig. 1C) (*11*–*13*). In CA1 and the hilus, 75% of Sst interneurons contained Elfn1 mRNA. However, horizontally oriented cells adjacent to the alveus, putative O-LM cells, showed 95% colabeling of Sst and Elfn1 (Fig. 1D). In contrast, PV-containing cells comprised only 5% of all Elfn1-expressing cells (fig. S1). These data show that Elfn1 is selectively expressed in perialvear Sst-positive interneurons.

To assess the cellular distribution of Elfn1 protein, we cultured primary hippocampal neurons and immunostained them with cell-type markers and a pan-Elfn antibody (figs. S2 and S3). We found strong dendritic staining in somatostatin interneurons (fig. S3). Because these neurons do not express Elfn2 (fig. S2), we concluded that Elfn1 is localized to the dendrites of Sst+ interneurons. Similar to the in situ expression, 69% of Sst cells in culture expressed Elfn1 protein (Table 1 and fig. S3). O-LM cells are a subset of these Sst-containing cells and can be identified by their strong expression of metabotropic glutamate receptor 1α (mGluR1α). Accordingly, 88% of mGluR1α-expressing cells contained Elfn1 (Table 1). In hippocampal slices, Elfn1 immunoreactivity was enriched in the outer oriens next to the alveus, where O-LM cells lie, consistent with enrichment of Elfn1 in O-LM cell dendrites (fig. S3). Elfn1 was found in discrete punta along these dendrites, and colocalized with glutamatergic, but not γ-aminobutyric acid–mediated, synaptic markers (Fig. 1E). Taken together, these data indicate that Elfn1 is localized to excitatory synapses onto Sst-containing O-LM interneurons.

To determine whether Elfn1 was necessary for short-term facilitation at synapses between pyramidal and O-LM cells, we examined the functional consequence of knocking down Elfn1 in vivo. We used Sst::tdTomato mice to identify Sst-containing interneurons for electrophysiological recording (fig. S4). To knock down Elfn1 in vivo, we generated a lentiviral construct containing green fluorescent protein (GFP) and a short hairpin RNA (shRNA) targeting Elfn1 (Fig. 2A). We injected lentivirus into the CA1 region of hippocampus at postnatal day 6 (P6) and recorded from perialvear Sst interneurons at P13 to P16. O-LM interneurons receive synapses from pyramidal cell axon collaterals as they exit CA1 in the alveus, where they can be selectively stimulated (*7*) (Fig. 2B). Control GFP-infected neurons showed a strong facilitation to alvear stimulation (Fig. 2C). In marked contrast, short-term facilitation was substantially reduced in neurons expressing the Elfn1 shRNA (Fig. 2C). The deficit in short-term facilitation was seen across several different interstimulus intervals, suggesting that Elfn1 regulates short-term facilitation across a range of physiologically relevant input frequencies (Fig. 2D). When the viral injection was performed earlier (at P1), the effect of Elfn1 knockdown was even stronger, suggesting that the presence of Elfn1 is particularly important when these synapses are established (Fig. 2C). Elfn1 knockdown did not affect the short-term plasticity of disynaptic inhibition onto O-LM cells (Fig. 2E). Thus, Elfn1 selectively regulates the magnitude of synaptic facilitation at pyramidal-O-LM synapses.

Facilitating synapses have low release probabilities. Their release depends on accumulation of calcium through several action potentials (*14*–*16*). If the reduced facilitation mediated by Elfn1 shRNA is due to increased release probability,

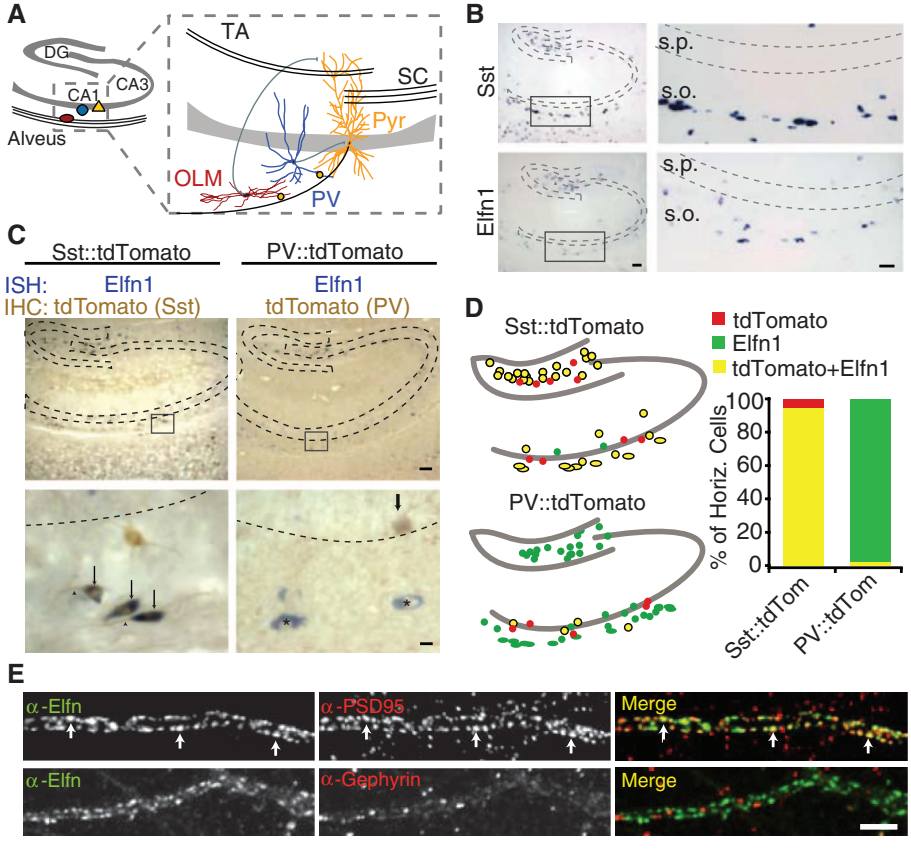


**Fig. 1.** Elfn1 is expressed in hippocampal O-LM interneurons. (**A**) CA1 axons contact PV cells and O-LM cells, which provide feedback inhibition. DG, dentate gyrus; Pyr, pyramidal cell. (**B**) ISH for Elfn1 and somatostatin at P14, both showing expression in the stratum oriens and hilus of the hippocampus. s.p., stratum pyramidale; s.o., stratum oriens. Scale bars indicate 25 (left) or 10 (right) μm. (**C**) ISH (blue) for Elfn1 and immunostaining (brown) for tdTomato in transgenic mouse lines in which tdTomato is expressed in Sst or PV interneurons. Elfn1 expression is highest near the alveus in somata (arrows) and proximal dendrites (arrowheads) of Sst-tdTomato neurons. Elfn1-expressing cells show little colocalization in tdTomato-PV mice (asterisks). Scale bars indicate 25 or 2.5 μm. (**D**) Quantification of the percent of horizontal cells in each mouse line that contain Elfn1, tdTomato, or both. Sst:tdTomato, $n$ = 145 cells, PV::tdTomato, $n$ = 157 cells. (**E**) Dendrites of neurons from dissociated hippocampal cultures stained for Elfn1 and PSD95 or gephyrin. Scale bar, 5 μm.

**Table 1.** Elfn1 expression by cell type.

| Cell type | % of Elfn+ cells with marker | % of each cell type with Elfn |
|---|---|---|
| GAD | 97 | 18 |
| CamKII | 0 | 0 |
| Sst | 96 | 69 |
| PV | 4 | 3 |
| mGluR1α | 97 | 88 |

evoked transmission onto Elfn1 shRNA–expressing neurons should be increased compared with control neurons. To test this prediction, we compared pyramidal cell inputs onto neighboring infected and uninfected neurons (*17*). We found that cells infected with the control lentivirus did not differ from uninfected neighbors in the strength of their pyramidal cell input, whereas shElfn1-infected neurons showed an increase in the evoked response when compared with simultaneously recorded neighboring cells (Fig. 3, A and B). Although this is consistent with an effect of Elfn1 on release probability, it could also reflect a role of Elfn1 on the postsynaptic response to glutamate. However, we found no effect of Elfn1 knockdown on AMPA/*N*-methyl-D-aspartate (NMDA) ratio, decay kinetics of the AMPA receptor (AMPAR)– and NMDA receptor (NMDAR)–mediated components, miniature excitatory postsynaptic current (mEPSC) amplitude, or rectification (fig. S5). Together these observations suggest that Elfn1 does not exert a significant effect on postsynaptic properties.

We also examined whether Elfn1 has synaptogenic properties, because other LRR proteins have been shown to regulate synaptic density or synaptic differentiation (*18*–*20*). We found that Elfn1 does not regulate synapse number in vitro (fig. S6). In addition, Elfn1 expressed in heterologous cells did not induce hemisynapse formation in contacting axons, unlike other LRR-containing proteins (LRRTMs, NGLs, and TrkC) (*18*, *20*, *21*) (fig. S7). These observations suggest that Elfn1 exerts a selective effect synaptic transmission. The robust effect on short-term facilitation at CA1-O-LM synapses, while leaving other synaptic parameters unaffected, strongly suggests that Elfn1 acts in a target-selective manner to control presynaptic release at pyramidal-O-LM synapses.

To further verify that Elfn1 knockdown regulates release probability at pyramidal-O-LM synapses, we recorded from control and Elfn1 shRNA–expressing O-LM interneurons while repeatedly stimulating the alveus in the presence of the irreversible, use-dependent NMDAR antagonist MK801. Because MK801 blocks open NMDARs, synapses that have a higher probability of release will release glutamate more often, and NMDARs at those synapses will be blocked more quickly (*22*). Neurons expressing Elfn1 shRNA showed a much faster block of NMDA EPSCs compared with control infected neurons (Fig. 3, C and D), indicating that Elfn1 knockdown increases release probability, producing a larger evoked response and reduced short-term facilitation.

Both O-LM and PV cells provide feedback inhibition to CA1 pyramidal cells. O-LM cells target distal pyramidal cell dendrites, whereas PV cells target pyramidal cell somata. Strongly facilitating inputs engage O-LM cells most effectively after repetitive pyramidal cell activity, producing delayed but persistent inhibi-

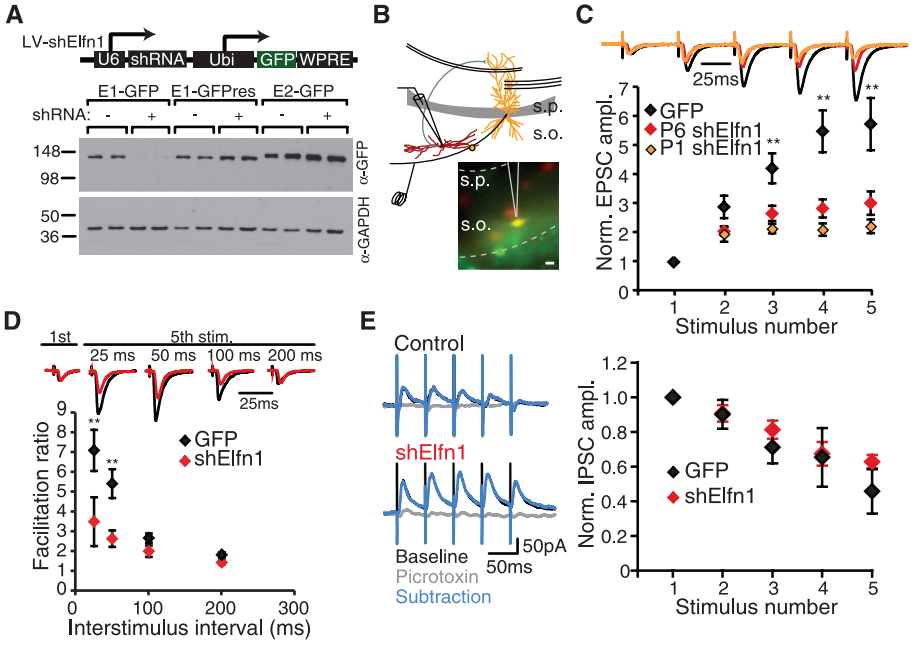


**Fig. 2.** Elfn1 knockdown reduces short-term facilitation at CA1-O-LM synapses. (**A**) Western blot from human embryonic kidney (HEK) cells expressing Elfn1-GFP cotransfected with Elfn1 shRNA, blotted for GFP and glyceraldehyde-3-phosphate dehydrogenase (GAPDH). Knockdown is rescued by a point mutation in the target sequence of the Elfn1-GFP cDNA (E1-GFPres). (**B**) Recording configuration and epifluorescence images of tdTomato and GFP in stratum oriens. Scale bar, 20 μm. (**C**) (Top) Average postsynaptic response of control and shElfn1-expressing cells to five stimuli to the alveus at 20 Hz, normalized to the amplitude of the first EPSC. Black, GFP; red, shElfn1 at P6; orange, shElfn1 at P1. (Bottom) Population data for EPSC amplitude normalized to first EPSC. GFP, $n = 13$; P6 shElfn1, $n = 20$; P1 shElfn1, $n = 7$. (**D**) (Top) Example cells comparing first to fifth EPSC at different interstimulus intervals. (Bottom) Population data for facilitation ratio, calculated as the amplitude ratio of the fifth EPSC to the first EPSC. GFP, $n = 12$; shElfn1, $n = 8$. $^{**}P < 0.01$, analysis of variance (ANOVA) with Tukey's honestly significant difference (HSD). (**E**) (Left) Example recordings of inhibitory synaptic responses in control and shElfn1-expressing cells to a 20-Hz stimulus before and after picrotoxin application. (Right) Average inhibitory postsynaptic current (IPSC) amplitude, normalized to the first IPSC amplitude. GFP, $n = 7$; shElfn1, $n = 5$. Error bars in all figures indicate SEM.

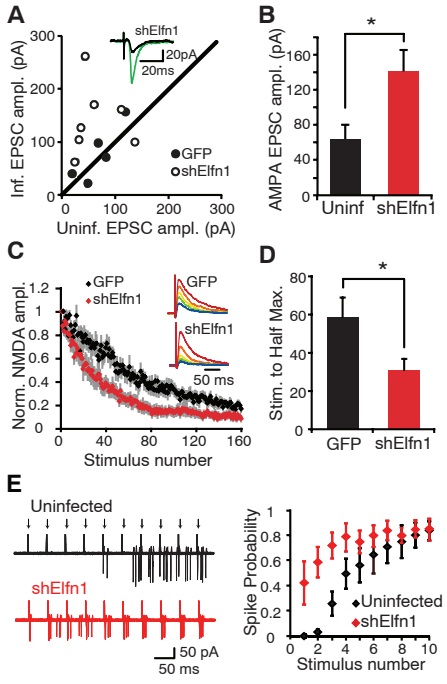


**Fig. 3.** Postsynaptic Elfn1 regulates release probability at CA1-O-LM synapses. (**A**) Evoked EPSC amplitude recorded from neighboring O-LM interneurons, one uninfected and one infected with a lentivirus expressing GFP or GFP plus shElfn1. Each point represents one pair of simultaneously recorded neurons. Solid circle, GFP control; open circle, shElfn1. (Inset) Example traces of evoked EPSC amplitude from uninfected (black) and infected (green) neurons. (**B**) Average EPSC amplitude of data in (A). $n = 7$ pairs. $P < 0.05$, paired $t$ test. (**C**) Kinetics of NMDA block in control and shElfn1-expressing neurons. NMDA EPSC is recorded at a holding potential of +40 mV in DNQX, and the alveus is stimulated in the presence of MK801 (40 μM) at 0.2 Hz. Peak NMDA-mediated current is normalized to the initial peak NMDA EPSC amplitude. (**D**) Average time to half maximum NMDA EPSC amplitude. GFP, $n = 8$; shElfn1, $n = 10$. $P < 0.05$, $t$ test. (**E**) Cell-attached, simultaneous recording from neighboring uninfected and shElfn1-infected O-LM cells. Ten stimuli are delivered to the alveus (arrows) at 20 Hz. (Left) Overlayed traces of subsequent sweeps to show spiking distribution. (Right) Spiking probability is plotted as a function of stimulus number. $n = 5$ pairs.

tion to distal pyramidal cell dendrites. Strong but rapidly depressing inputs to PV cells result in fast but transient inhibition to the soma (*7*). This arrangement channels inhibition to different somatodendritic compartments at distinct times relative to pyramidal cell spiking. To determine whether Elfn1 regulates the recruitment of O-LM neurons in response to pyramidal cell spiking, we performed simultaneous cell-attached recordings from neighboring uninfected and shElfn1-infected O-LM neurons. As previously demonstrated (*7*), uninfected O-LM neurons require repetitive stimulation of pyramidal cell axons to reach spike threshold (Fig. 3E). In contrast, shElfn1-infected neurons showed a significant increase in spike probability at early stimuli in the train (Fig. 3E), as predicted by larger underlying EPSC amplitudes. Thus, by regulating short-term facilitation, Elfn1 influences the temporal dynamics of O-LM recruitment in response to pyramidal cell activity.

Next, we investigated whether Elfn1 expression in target cells was sufficient to alter functional properties of CA1 outputs. Pyramidal cells form depressing synapses onto PV interneurons. To determine whether we could convert depressing pyramidal-PV synapses into facilitating synapses, we overexpressed Elfn1-GFP in CA1 by using lentiviral-mediated infection in PV::tdTomato mice and recorded at pyramidal-PV synapses. Elfn1 overexpression converted pyramidal-PV synapses into moderately facilitating synapses (Fig. 4A), indicating that postsynaptic Elfn1 can instruct the output properties of CA1 pyramidal cell axons.

Last, we examined whether Elfn1 regulates short-term facilitation by engaging one of the pathways that has been implicated in controlling release probability. Short-term facilitation at synapses onto other types of Sst interneurons has been shown to arise from the activation of presynaptic glutamate receptors, which produces direct depolarization and calcium influx into the presynaptic terminal. At Schaffer-collateral synapses, presynaptic GluR5- and GluR6-containing kainate receptors underlie target-specific facilitation at terminals on another group of Sst interneurons in the stratum radiatum (*23*, *24*). In cortex, presynaptic NMDARs have recently been shown to control release probability at pyramidal-Sst interneuron synapses (*25*). To investigate whether similar mechanisms regulate release at pyramidal-O-LM synapses, we used a pharmacological approach to examine the contribution of these presynaptic receptors. We found that blocking presynaptic GluR5-containing kainate receptors and presynaptic NMDARs had no effect on facilitation (fig. S8). However, the GluR-6–specific kainate receptor antagonist NS102 significantly reduced facilitation, suggesting that these kainate receptors contribute to setting release probability at pyramidal-O-LM synapses (Fig. 4B).

To determine whether Elfn1 acts by engaging a kainate receptor–mediated mechanism, we examined the effect of NS102 on synaptic transmission onto cells expressing shElfn1. The effect of NS102 was attenuated when recording from Elfn1 knockdown neurons, suggesting that the kainate-mediated component of facilitation is sensitive to postsynaptic Elfn1 levels (Fig. 4B). The mechanism by which Elfn1 signals to the presynaptic terminal is unclear and could include a direct presynaptic interaction, an additional postsynaptic cofactor that bridges the synapse, or a diffusible signal. Our data and previous studies (*26*) have shown that initial release probability is low at pyramidal-O-LM synapses, which cannot be explained by glutamate-induced activation of kainate receptors (Fig. 3, A and B). Although additional mechanisms may keep initial release probability lower at pyramidal-O-LM synapses (*14*, *23*), our data suggest that kainate receptors contribute to the large increase in release probability that occurs during repetitive activation of pyramidal cells and that Elfn1 acts by engaging a GluR6-dependent mechanism to regulate facilitation.

Our observations indicate that postsynaptic Elfn1 regulates target-specific presynaptic properties, namely the differential release probability at CA1-O-LM versus CA1-PV synapses (Fig. 4C). This influences the timing of recruitment of inhibitory neuron subtypes. O-LM neurons target distal CA1 pyramidal cell dendrites, whereas PV neurons target pyramidal cell somata, so the differential recruitment of these interneuron types dictates when inhibition is channeled to distinct somatodendritic compartments to regulate hippocampal output. The activity of O-LM and PV interneurons is synchronized to theta rhythms (*27*), which are associated with distinct behavioral states, including active exploration and memory formation or retrieval (*28*–*30*). Thus, by regulating the temporal dynamics of interneuron recruitment, Elfn1 could exert substantial effect on hippocampus-dependent behavior. Although we have emphasized Elfn1 function in the hippocampus, Elfn1 is expressed in other interneuron populations that receive facilitating synapses, such as somatostatin cells of the neocortex and hilar perforant path-associated (HIPP) cells of the dentate gyrus. Elfn1 may therefore broadly regulate circuit dynamics in the central nervous system and consequently exert considerable influence on cortical output and cognitive function.

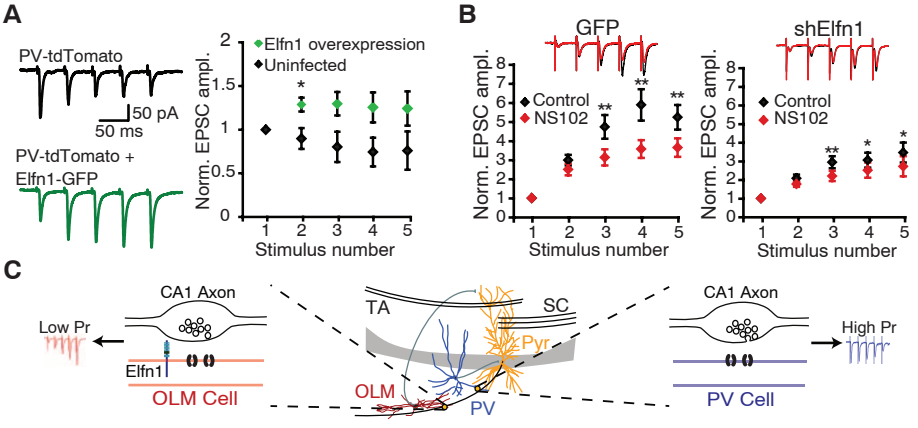


**Fig. 4.** Elfn1 is sufficient to modulate CA1 outputs. (**A**) Lentivirus overexpressing Elfn1-GFP is injected into P5 PV::tdTomato mouse pups. Stratum pyramidale or stratum oriens PV neurons in the infected area are targeted for recording. (Left) Response of control and shElfn1-expressing PV neurons to five stimuli delivered to the alveus at 20 Hz. (Right) Quantification of short-term plasticity in Elfn1 overexpressing PV cells. *$P < 0.05$ by Mann-Whitney U test. (**B**) (Right) Example recording and quantification of evoked EPSC in GFP-infected Sst neurons before and after application of the GluR6-selective kainate receptor antagonist, NS102 (20 μM). (Left) Average postsynaptic response of GFP-infected Sst interneurons before and after NS102, $n = 8$. (Right) Average postsynaptic response of shElfn1-infected Sst interneurons before and after NS102, $n = 14$. *$P < 0.05$; **$P < 0.01$ by ANOVA with Tukey's post-hoc test. (**C**) Model of Elfn1 function at the synapse. In CA1, Elfn1 is selectively localized to excitatory synapses onto O-LM interneurons. Elfn1 signals transsynaptically to contacting CA1 axons to reduce probability of release and create a facilitating synapse.

### References and Notes


1. H. L. Atwood, S. Karunanithi, *Nat. Rev. Neurosci.* **3**, 497 (2002).
2. H. J. Koester, D. Johnston, *Science* **308**, 863 (2005); 10.1126/science.1100815.
3. A. Reyes *et al.*, *Nat. Neurosci.* **1**, 279 (1998).
4. A. B. Ali, J. Deuchars, H. Pawelzik, A. M. Thomson, *J. Physiol.* **507**, 201 (1998).
5. A. B. Ali, A. M. Thomson, *J. Physiol.* **507**, 185 (1998).
6. J.-C. Lacaille, A. L. Mueller, D. D. Kunkel, P. A. Schwartzkroin, *J. Neurosci.* **7**, 1979 (1987).
7. F. Pouille, M. Scanziani, *Nature* **429**, 717 (2004).
8. E. S. Lein *et al.*, *Nature* **445**, 168 (2007).
9. J. Dolan *et al.*, *BMC Genomics* **8**, 320 (2007).
10. J. de Wit, W. Hong, L. Luo, A. Ghosh, *Annu. Rev. Cell Dev. Biol.* **27**, 697 (2011).
11. S. Hippenmeyer *et al.*, *PLoS Biol.* **3**, e159 (2005).
12. L. Madisen *et al.*, *Nat. Neurosci.* **13**, 133 (2010).
13. H. Taniguchi *et al.*, *Neuron* **71**, 995 (2011).
14. A. A. Biró, N. B. Holderith, Z. Nusser, *J. Neurosci.* **25**, 223 (2005).
15. H. Kamiya, R. S. Zucker, *Nature* **371**, 603 (1994).
16. B. Katz, R. Miledi, *J. Physiol.* **195**, 481 (1968).

17. J. J. Zhu, J. A. Esteban, Y. Hayashi, R. Malinow, *Nat. Neurosci.* **3**, 1098 (2000).
18. S. Kim *et al.*, *Nat. Neurosci.* **9**, 1294 (2006).
19. J. Ko *et al.*, *Neuron* **50**, 233 (2006).
20. M. W. Linhoff *et al.*, *Neuron* **61**, 734 (2009).
21. H. Takahashi *et al.*, *Neuron* **69**, 287 (2011).
22. C. Rosenmund, J. D. Clements, G. L. Westbrook, *Science* **262**, 754 (1993).
23. H. Y. Sun, L. E. Dobrunz, *J. Neurosci.* **26**, 10796 (2006).
24. H. Y. Sun, A. F. Bartley, L. E. Dobrunz, *J. Neurophysiol.* **101**, 1043 (2009).
25. K. A. Buchanan *et al.*, *Neuron* **75**, 451 (2012).
26. H. Y. Sun, S. A. Lyons, L. E. Dobrunz, *J. Physiol.* **568**, 815 (2005).
27. T. Klausberger *et al.*, *Nature* **421**, 844 (2003).
28. G. Buzsáki, *Neuroscience* **31**, 551 (1989).
29. J. Larson, D. Wong, G. Lynch, *Brain Res.* **368**, 347 (1986).
30. C. H. Vanderwolf, *Electroencephalogr. Clin. Neurophysiol.* **26**, 407 (1969).

**Acknowledgments:** We thank M. Scanziani, P. Scheiffele, and members of the Ghosh lab for suggestions and comments on the manuscript; J. de Wit for generating the Elfn1-GFP construct; and M. Macias, C. Sanchez, and E. Kang for help with virus and protein production. This work was supported by NIH grant R01NS067216 and the Gatsby Charitable Foundation.

**Supplementary Materials**
www.sciencemag.org/cgi/content/full/science.1222482/DC1
Materials and Methods
Supplementary Text
Figs. S1 to S8
References (*31*–*34*)

27 March 2012; accepted 11 September 2012
Published online 4 October 2012;
10.1126/science.1222482

# Oxytocin/Vasopressin-Related Peptides Have an Ancient Role in Reproductive Behavior

**Jennifer L. Garrison, Evan Z. Macosko, Samantha Bernstein, Navin Pokala, Dirk R. Albrecht, Cornelia I. Bargmann**

Many biological functions are conserved, but the extent to which conservation applies to integrative behaviors is unknown. Vasopressin and oxytocin neuropeptides are strongly implicated in mammalian reproductive and social behaviors, yet rodent loss-of-function mutants have relatively subtle behavioral defects. Here we identify an oxytocin/vasopressin-like signaling system in *Caenorhabditis elegans*, consisting of a peptide and two receptors that are expressed in sexually dimorphic patterns. Males lacking the peptide or its receptors perform poorly in reproductive behaviors, including mate search, mate recognition, and mating, but other sensorimotor behaviors are intact. Quantitative analysis indicates that mating motor patterns are fragmented and inefficient in mutants, suggesting that oxytocin/vasopressin peptides increase the coherence of mating behaviors. These results indicate that conserved molecules coordinate diverse behavioral motifs in reproductive behavior.

Animal behaviors such as mating, feeding, or foraging typically involve combinations of simpler actions and motor patterns that develop over different time scales. In the case of reproductive behavior, neuropeptide signaling through oxytocin and vasopressin peptides may provide a global organizing role. The mammalian hypothalamic neuropeptide oxytocin, released during birth, stimulates maternal behaviors as well as uterine contractions and lactation, and the related peptide vasopressin is linked to male-typical behaviors in rodents and fish, in addition to its role in fluid homeostasis (*1*). Similarly, administration of the oxytocin/vasopressin-related peptide conopressin to leeches stimulates reproductive behaviors and mating-related neuronal activity (*2*). A more general role for oxytocin in social behaviors is suggested by the social amnesia of oxytocin mutant mice (*3*) and by altered social decision-making in humans after oxytocin administration (*4*). However, mammalian oxytocin and vasopressin mutants have subtle behavioral defects relative to the potency of the administered peptides (*5*). To define the role of these neuropeptides in endogenous reproductive behaviors, we here address their function through genetic analysis of an oxytocin/vasopressin-related neuropeptide in the nematode *Caenorhabditis elegans*.

Through homology searches, we identified a gene in *C. elegans* with similarity to mammalian vasopressin and oxytocin (*ntc-1*; Fig. 1, A and B, and fig. S1). To determine whether this gene generates an authentic neuropeptide, we isolated total neuropeptides from wild-type animals and characterized them by tandem mass

Howard Hughes Medical Institute, Lulu and Anthony Wang Laboratory of Neural Circuits and Behavior, The Rockefeller University, New York, NY 10065, USA.

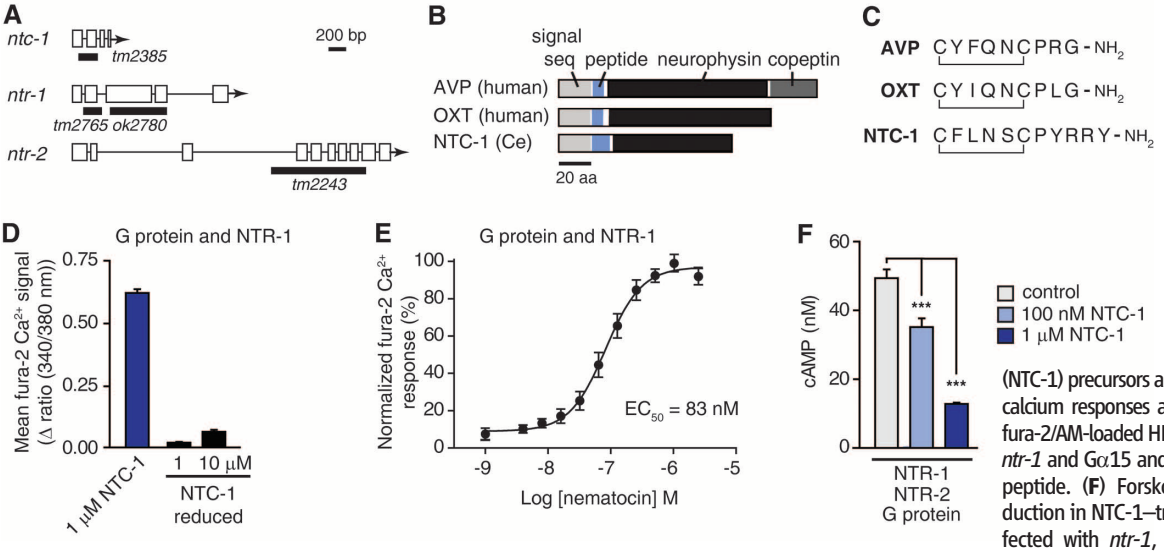


**Fig. 1.** *ntc-1* encodes an oxytocin/vasopressin-related peptide that signals through receptors encoded by *ntr-1* and *ntr-2*. (**A**) Gene models with deletions in mutant alleles indicated by horizontal black bars (www.wormbase.org). (**B** and **C**) Domain structure and amino acid sequence of vasopressin (AVP), oxytocin (OXT), and nematocin (NTC-1) precursors and peptides. (**D** and **E**) Mean calcium responses and dose-response curves of fura-2/AM-loaded HEK293T cells transfected with *ntr-1* and Gα15 and exposed to synthetic NTC-1 peptide. (**F**) Forskolin-stimulated cAMP production in NTC-1–treated HEK293T cells transfected with *ntr-1*, *ntr-2*, and Gα15. ***$P <$ 0.0001. Error bars in all figures indicate SEM.

spectrometry (*6*), identifying a peptide matching the mass predicted for an 11–amino acid cyclized peptide with an amidated C terminus (Fig. 1C and fig. S2). Fragmentation of this peptide by liquid chromatography–tandem mass spectrometry confirmed the existence of a *C. elegans* neuropeptide, nematocin. The *C. elegans* genome also predicts two genes encoding G protein–coupled receptors related to vertebrate oxytocin and vasopressin receptors, the nematocin receptor (*ntr*) genes (Fig. 1A and figs. S3 and S4). To determine whether these encode nematocin receptors, we expressed *ntr-1* and *ntr-2* cDNAs in HEK293T cells with the promiscuous G protein Gα15 and administered a synthetic cyclized peptide corresponding to nematocin. Cells transfected with *ntr-1* responded to nematocin with calcium transients and a nanomolar median effective concentration ($EC_{50}$) (Fig. 1, D and E, and fig. S1). Cells transfected with *ntr-2* did not mobilize calcium in response to nematocin, but cells cotransfected with both receptors responded to nematocin with decreases in intracellular cyclic adenosine monophosphate (cAMP), suggesting coupling to a signaling pathway that antagonizes adenylyl cyclase (Fig. 1F and fig. S1) (*7*). Although heterologous expression may not capture all native functions, these results suggest that NTR-1 and NTR-2 can contribute

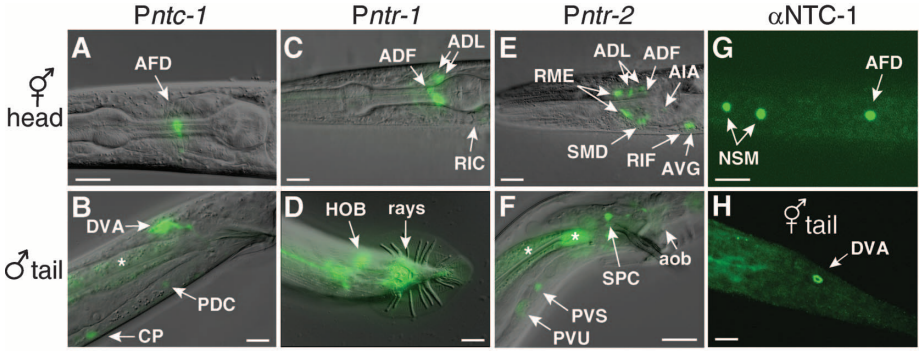


**Fig. 2.** *ntc-1*, *ntr-1*, and *ntr-2* expression patterns. P, gene promoter fragment used. The upper panels show expression in adult hermaphrodite heads; the lower panels show male [(B), (D), and (F)] and hermaphrodite (H) tails. (**A** to **F**) Expression of *ntc-1*, *ntr-1*, and *ntr-2* reporter genes (table S1). (**G** and **H**) Immunostaining of AFD, NSM, and DVA neurons with antisera to nematocin. White arrows indicate expression in specified neurons. Asterisks mark autofluorescence; scale bars represent 10 μm.

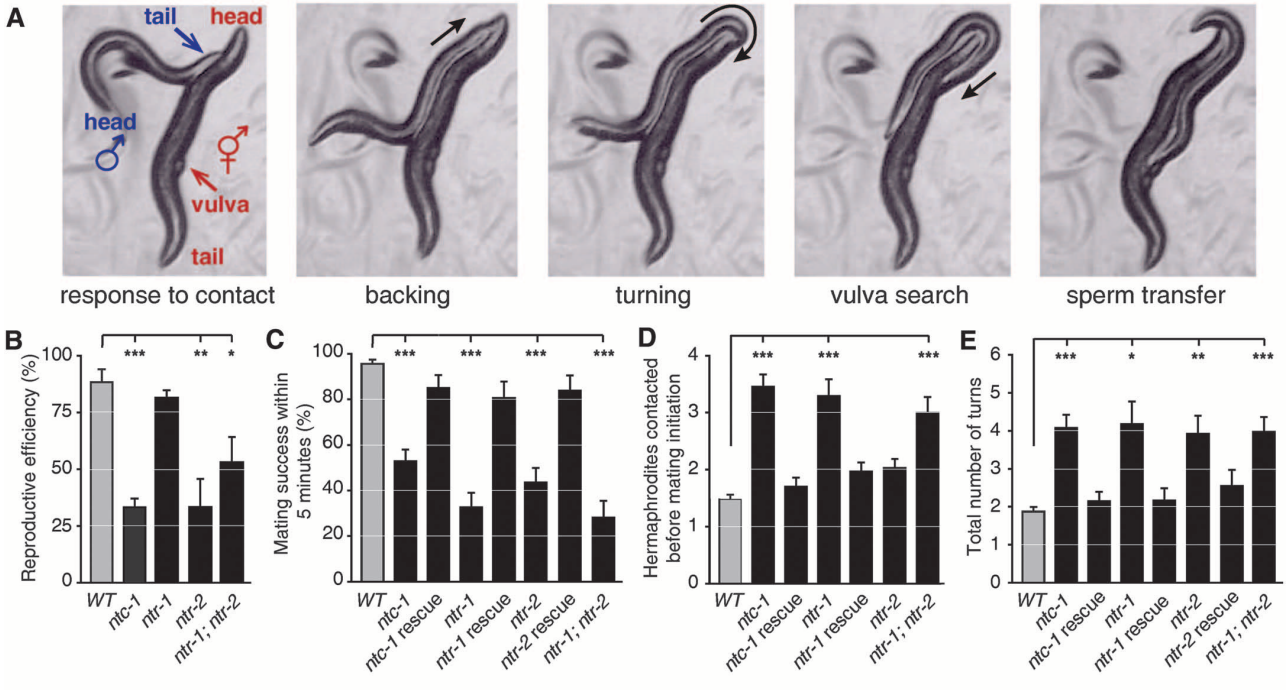


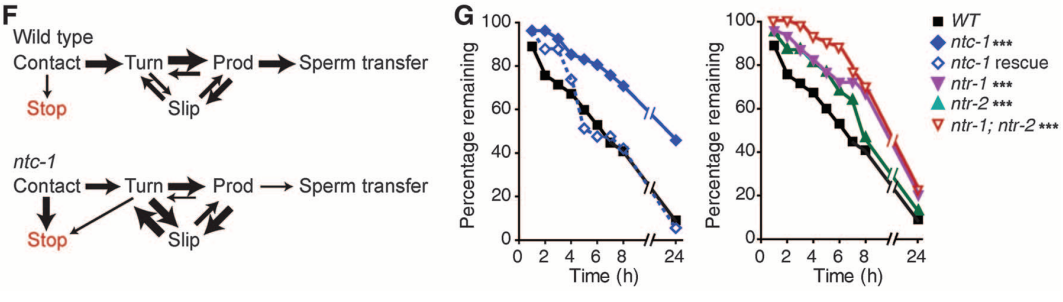


**Fig. 3.** Nematocin-deficient males exhibit mating defects. (**A**) Steps in male mating behavior. The black arrow notes the direction of male movement. (**B**) Reproductive efficiencies of wild-type (WT, gray bars) and mutant males (black bars) in long-term single-pair mating crosses (no. of cross-progeny/no. of total progeny). (**C**) Percentage of males that successfully transferred sperm within 5 min of first tail contact with a hermaphrodite. (**D**) Mean number of hermaphrodites that a male's tail contacted before he initiated mating. (**E**) Mean total number of turns a male executed around the hermaphrodite's body before locating the vulva. (**F**) Summary of the behavioral transitions in ethograms of male mating behavior (figs. S8 and S9); the arrow width indicates the probability of behavioral transitions. (**G**) Male mate search behavior, measured as the rate at which a single male leaves food in the absence of hermaphrodites (*15*). *$P < 0.01$, **$P < 0.001$, ***$P < 0.0001$.

to nematocin-mediated signaling alone (NTR-1) or as heterodimers (NTR-1/NTR-2).

The expression of nematocin and *ntr* genes was examined by conventional and fosmid-recombineered green fluorescent protein (GFP) reporter genes and additionally with antisera generated against synthetic nematocin (Fig. 2, A to H; figs. S5 and S6; and table S1). *C. elegans* has two sexes, self-fertilizing hermaphrodites that can also mate as females, and cross-fertilizing males (*8*). Both sexes expressed nematocin in the AFD thermosensory neurons, which mediate thermotaxis (*9*), and in the DVA mechanosensory neuron, which regulates locomotion and posture (*10*); and males expressed nematocin in male-specific CP motor neurons that control turning behavior during mating (*11*) (Fig. 2, A and B, and G and H). Both sexes expressed *ntr* receptor reporter genes in partly overlapping sets of head and tail neurons, and males additionally expressed them in male-specific neurons and muscles implicated in mating (Fig. 2, C to F; fig. S6; and table S1): *ntr-1* in hook and tail sensory neurons [HOB, which senses the vulva; and rays 1, 5, 7, and 9, which sense hermaphrodite contact (*12*)] and in spicule protractor muscles, which act during sperm transfer (*13*); and *ntr-2* in the male-specific SPC sensory-motor tail neurons that induce spicule penetration and muscle contraction for sperm transfer (*13*, *14*) and in the male-specific oblique muscles that promote prolonged vulval contact (*14*). The reporter genes rescued all behavioral phenotypes described below, indicating that they are expressed in functionally relevant sites (Fig. 3).

Null mutants for nematocin and the two *ntr* genes were viable and fertile as hermaphrodites, with normal locomotion speed, egg-laying behavior, and numbers of progeny (fig. S7). The males were also viable, but they had reduced mating success: When single males were housed with single mating partners, the number of progeny per male was reduced 2.5-fold in nematocin or *ntr-2* mutants as compared to wild-type males (Fig. 3B). We characterized the male mating defect by quantitative analysis of mating encounters between individual virgin males and hermaphrodite mating partners in a 5-min viewing period, and found that nematocin mutant males were inefficient at multiple mating stages. When placed in a small arena with food and mating partners, a wild-type male typically attempted to mate with the first hermaphrodite that his tail touched, located her vulva after he made one or two turns around her body, and successfully transferred sperm within 5 min (Fig. 3A and C to E, and fig. S8). Nematocin mutant males attempted to mate only after numerous hermaphrodite contacts (Fig. 3D), made more turns around the hermaphrodite before locating the vulva (Fig. 3E), and had difficulty executing turns, maintaining vulval contact, and transferring sperm within the assay period (Fig. 3C and fig. S8). Ethograms showed fragmentation of the mating sequence and repetition of early mating steps in nematocin mutant males (Fig. 3F and fig. S9). All defects were rescued by transgenes that spanned the nematocin gene (Fig. 3, B to E, and fig. S8).

Null mutations in the receptor genes disrupted partly overlapping aspects of the mating response. *ntr-1* was required for the initial response to hermaphrodite contact (Fig. 3D), matching *ntr-1* expression in male ray neurons that mediate this behavior (*12*). This defect was partially rescued by *ntr-1* expression in a subset of ray neurons (fig. S10). *ntr-2* had a substantial effect on overall reproductive efficiency (Fig. 3B). Both receptors were required for correct execution of turns and mating success (Fig. 3, C and E).

*C. elegans* males have a long-term mate search behavior in which they leave a bacterial food source that lacks hermaphrodite mating partners (*15*). Nematocin mutant males and *ntr* mutant males were partly deficient in male-typical leaving behavior, suggesting a defect in mate search (Fig. 3G). This behavioral change was not due to a general locomotion or sensory defect, because nematocin mutants had normal locomotion parameters on and off of food and normal responses to aversive stimuli, touch, and drugs (figs. S11 and S12).

The broad actions of nematocin on male mating behaviors could result from humoral secretion that activates many targets, precise release at specific neuronal sites, or a mixture of the two. To identify relevant sites of nematocin action without risking misexpression, we focused on rescue with the endogenous nematocin promoter, manipulating its precise expression pattern through Cre-mediated recombination (Fig. 4A). Cre-mediated recombination in all *ntc*-expressing cells caused defects in all male mating behaviors (fig. S13), whereas specific Cre-mediated recombination in the DVA mechanosensory neuron led to defects in initial contact response and vulva location efficiency, but did not affect turning behaviors (Fig. 4, C to F). Laser ablation of the DVA neuron caused the same defect in the hermaphrodite contact response as the DVA nematocin knockout (Fig. 4B). DVA ablation also generated striking male-specific defects in locomotion speed and posture that were not observed in nematocin mutants (fig. S14). DVA has only mild effects on hermaphrodite loco-

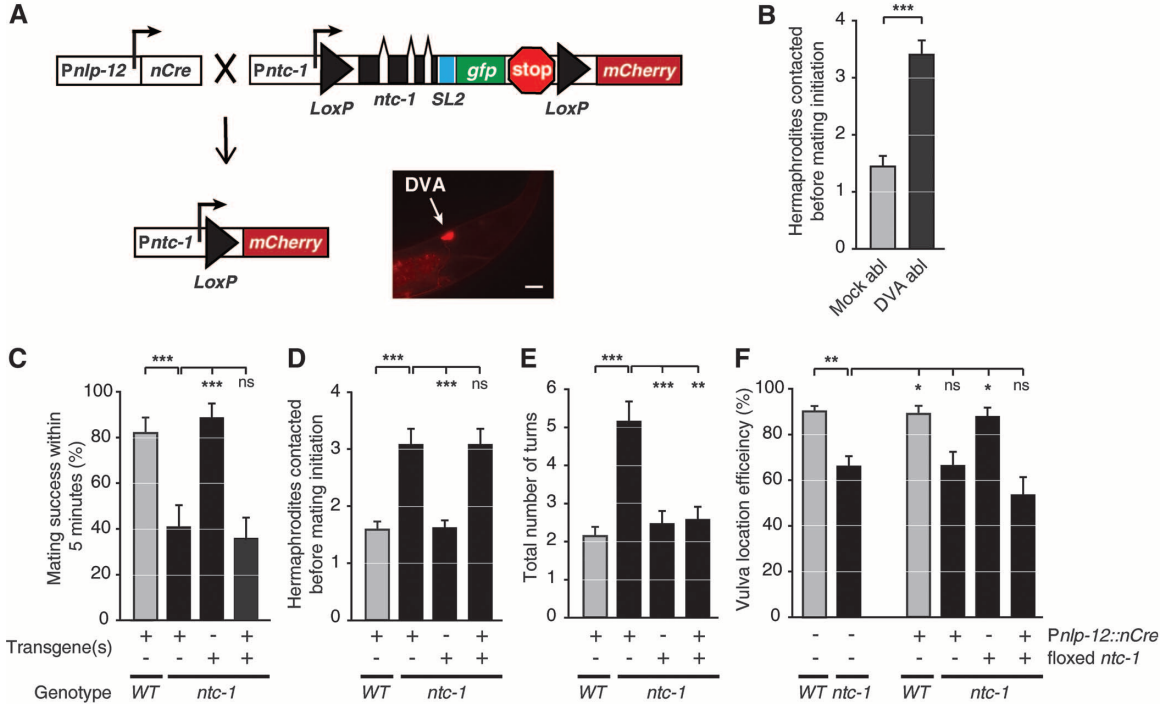


**Fig. 4.** Selective inactivation of *ntc-1* in DVA affects individual steps of male mating behavior. (**A**) Cre/Lox strategy to selectively inactivate *ntc-1* in DVA. (Inset) Tail of larval stage 4 male expressing mCherry and not GFP in DVA, indicating successful DVA-specific recombination. Scale bar, 10 μm. (**B** to **F**) Behavioral phenotypes of males with *ntc-1* inactivated in DVA [(C) to (F)] or after DVA laser ablation (B). (C) to (E) Behaviors as in Fig. 3. (F) Vulva location ability of males (percentage of positive vulva detections/total vulva encounters). *$P < 0.01$, **$P < 0.001$, ***$P < 0.0001$.

motion and is not obviously sexually dimorphic, so its strong male-specific effects on movement were unexpected.

These results indicate that nematocin provides a neuromodulatory input to organize diverse aspects of male mating, increasing the effectiveness by which distributed circuits generate coherent behaviors. DVA is directly proprioceptive (*10*) and also receives synaptic input from the male sensory ray neurons and mechanosensory neurons (*16*); its ability to release nematocin that activates NTR-1 on ray neurons may provide a feedback signal at the onset of mating. The DVA neuron produces additional transmitters and performs other functions, and nematocin is released from additional sources, so the functions of mating neurons and peptides are partly orthogonal (*7*, *12*, *13*). We suggest that nematocin and its receptors prime neurons in a variety of local circuits to generate a neuroethological "appetitive" function in mating. This insight refines the likely functions of oxytocin/vasopressin-related neuropeptides and suggests that they have ancient roles in reproductive behaviors that are conserved in bilaterian vertebrates, lophotrochozoa, and nematodes. The apparent conservation of oxytocin/vasopressin peptides in reproductive behavior stands in contrast with the diversity of mechanisms for sex determination, sex chromosomes, and dosage compensation (*17*).

### References and Notes


1. Z. R. Donaldson, L. J. Young, *Science* **322**, 900 (2008).
2. D. A. Wagenaar, M. S. Hamilton, T. Huang, W. B. Kristan, K. A. French, *Curr. Biol.* **20**, 487 (2010).
3. J. T. Winslow, T. R. Insel, *Neuropeptides* **36**, 221 (2002).
4. M. Kosfeld, M. Heinrichs, P. J. Zak, U. Fischbacher, E. Fehr, *Nature* **435**, 673 (2005).
5. I. D. Neumann, A. H. Veenema, D. I. Beiderbeck, *Front. Behav. Neurosci.* **4**, 12 (2010).
6. Materials and methods are available as supplementary materials on *Science* Online.
7. K. Kim *et al.*, *Science* **326**, 994 (2009).
8. J. Hodgkin, *Annu. Rev. Genet.* **21**, 133 (1987).
9. I. Mori, Y. Ohshima, *Nature* **376**, 344 (1995).
10. W. Li, Z. Feng, P. W. Sternberg, X. Z. Xu, *Nature* **440**, 684 (2006).
11. C. M. Loer, C. J. Kenyon, *J. Neurosci.* **13**, 5407 (1993).
12. K. S. Liu, P. W. Sternberg, *Neuron* **14**, 79 (1995).
13. L. R. Garcia, P. Mehta, P. W. Sternberg, *Cell* **107**, 777 (2001).
14. Y. Liu *et al.*, *PLoS Genet.* **7**, e1001326 (2011).
15. J. Lipton, G. Kleemann, R. Ghosh, R. Lints, S. W. Emmons, *J. Neurosci.* **24**, 7427 (2004).
16. T. A. Jarrell *et al.*, *Science* **337**, 437 (2012).
17. H. Ellegren, *Nat. Rev. Genet.* **12**, 157 (2011).



**Acknowledgments:** Strains bearing *ntc-1, ntr-1,* and *ntr-2* mutations are available through the *C. elegans* National BioResource Project (NBRP), subject to a materials transfer agreement. Sequence accession numbers are as follows: NM_001038459.1 (*ntc-1*), NM_060792 (*ntr-1*), NM_078076 (*ntr-2*). We thank S. Emmons for sharing the male wiring diagram before publication; D. Anderson, S. Emmons, S. Flavell, A. Gordus, W. Kristan, T. Maniar, P. McGrath, L. Vosshall, and Y. Xu for discussions; S. Chalasani for plasmids; S. Mitani and the National Bioresource Project for *ntc-1, ntr-1,* and *ntr-2* mutants; and the Rockefeller Proteomics Facility, the Rockefeller Bioimaging Facility, and the Rockefeller High Throughput Screening Facility for technical support. This work was supported by a grant from the G. Harold and Leila Y. Mathers Foundation, by Harvey Karp and Helen Hay Whitney Fellowships to J.L.G., by NIH grant K99GM092859 to J.L.G., and by NIH grant GM07739 to E.Z.M. C.I.B. is an Investigator of the Howard Hughes Medical Institute.


### Supplementary Materials

www.sciencemag.org/cgi/content/full/338/6106/540/DC1
Materials and Methods
Figs. S1 to S14
Table S1
References (*18*–*36*)


18 June 2012; accepted 9 August 2012
10.1126/science.1226201


# Vasopressin/Oxytocin-Related Signaling Regulates Gustatory Associative Learning in *C. elegans*


**Isabel Beets,[1] Tom Janssen,[1] Ellen Meelkop,[1]* Liesbet Temmerman,[1] Nick Suetens,[1] Suzanne Rademakers,[2] Gert Jansen,[2] Liliane Schoofs[1]†**



**Vasopressin- and oxytocin-related neuropeptides are key regulators of animal physiology, including water balance and reproduction. Although these neuropeptides also modulate social behavior and cognition in mammals, the mechanism for influencing behavioral plasticity and the evolutionary origin of these effects are not well understood. Here, we present a functional vasopressin- and oxytocin-like signaling system in the nematode *Caenorhabditis elegans*. Through activation of its receptor NTR-1, a vasopressin/oxytocin-related neuropeptide, designated nematocin, facilitates the experience-driven modulation of salt chemotaxis, a type of gustatory associative learning in *C. elegans*. Our study suggests that vasopressin and oxytocin neuropeptides have ancient roles in modulating sensory processing in neural circuits that underlie behavioral plasticity.**


The neurohypophyseal peptides vasopressin (VP) and oxytocin (OT) are related key hormones that regulate mammalian physiology (*1*–*3*). Their gene origin dates back at least 700 million years as indicated by the presence of structurally related peptides in some invertebrate phyla (*4*, *5*). Peripheral effects of VP/OT-related peptides, primarily on water homeostasis and reproduction, are equally conserved (*5*, *6*). Mammalian VP and OT peptides can act as central nervous system mediators of social behaviors, including parental care, pair bonding, social cognition, and aggression (*7*, *8*). They also modulate vertebrate cognition in a nonsocial context, although mechanistic complexities confound a clear understanding of these effects (*9*). Here, we identify and study a VP/OT-related system in the genetically tractable model *Caenorhabditis elegans*, which displays a high level of behavioral plasticity despite its relatively simple nervous system (*10*).

Through in silico data mining of the *C. elegans* genome, we characterized 91 presumptive neuropeptide heterotrimeric guanine nucleotide–binding protein (G protein)–coupled receptor (GPCR) genes (*11*). Protein sequences of two orphan rhodopsin class GPCR genes, which we named nematocin receptors *ntr-1* (T07D10.2) and *ntr-2* (F14F4.1), clustered in the VP and OT receptor clade (fig. S1 and table S1). Sequence alignment with insect, mollusk, and mammalian VP/OT receptors revealed the presence of specific amino acid residues important for VP/OT peptide binding (fig. S2 and table S1).

To determine the cognate ligand of NTR-1 and NTR-2, we cloned and transiently expressed each receptor in Chinese hamster ovary (CHO) cells stably overexpressing apo-aequorin and the promiscuous $G\alpha_{16}$ subunit (*12*). We challenged these cells with a synthetic library of 262 known and predicted *C. elegans* peptides. NTR-1–expressing cells responded dose-dependently with a nanomolar half maximal effective concentration ($EC_{50}$) to a single peptide CFLNSCPYRRYamide (*13*), henceforward named nematocin (Fig. 1A). Several amino acid residues of nematocin match the neurohypophyseal peptide motif, supporting that it belongs to the VP/OT peptide family (table S2). Structural conservation is also evident at the level of its preproprotein (Fig. 1B, fig. S3, and table S3) encoded by the nematocin precursor gene *ntc-1* (F39C12.4). Similar to the architecture of VP/OT-related precursors, NTC-1 comprises a cysteine-rich neurophysin domain located immediately downstream of the mature peptide. Insect and octopus VP/OT-related peptides and a predicted, truncated form of nematocin, CFLNSCPY (*13*), were unable to activate NTR-1 (Fig. 1A and fig. S4), indicating the importance of the C-terminal nematocin residues for receptor activation. NTR-2 did not respond to nematocin or affect the dose-dependent activation of NTR-1 (fig. S5). We conclude that the VP/OT-related


[1]Department of Biology, Functional Genomics and Proteomics Unit, KU Leuven, 3000 Leuven, Belgium. [2]Department of Cell Biology, Erasmus MC, 3000 CA Rotterdam, Netherlands.

*Present address: Queensland Brain Institute, The University of Queensland, Brisbane, Australia.

†To whom correspondence should be addressed. E-mail: liliane.schoofs@bio.kuleuven.be

nematocin peptide is the likely cognate ligand of the *C. elegans* NTR-1 receptor.

We investigated intracellular signaling of NTR-1 by measuring the calcium and cyclic adenosine monophosphate (cAMP) responses in NTR-1–expressing cells that lacked $G\alpha_{16}$ or co-expressed the cAMP response element (CRE)–luciferase reporter. Both second messenger levels increased upon nematocin administration (fig. S6), indicating that the NTR-1 receptor can signal through both calcium and cAMP messengers, similar to its mammalian VP and OT receptor counterparts (*14*).

To explore the cells and tissues involved in nematocin signaling, we observed full-length green fluorescent protein (GFP)–tagged NTR-1 receptor

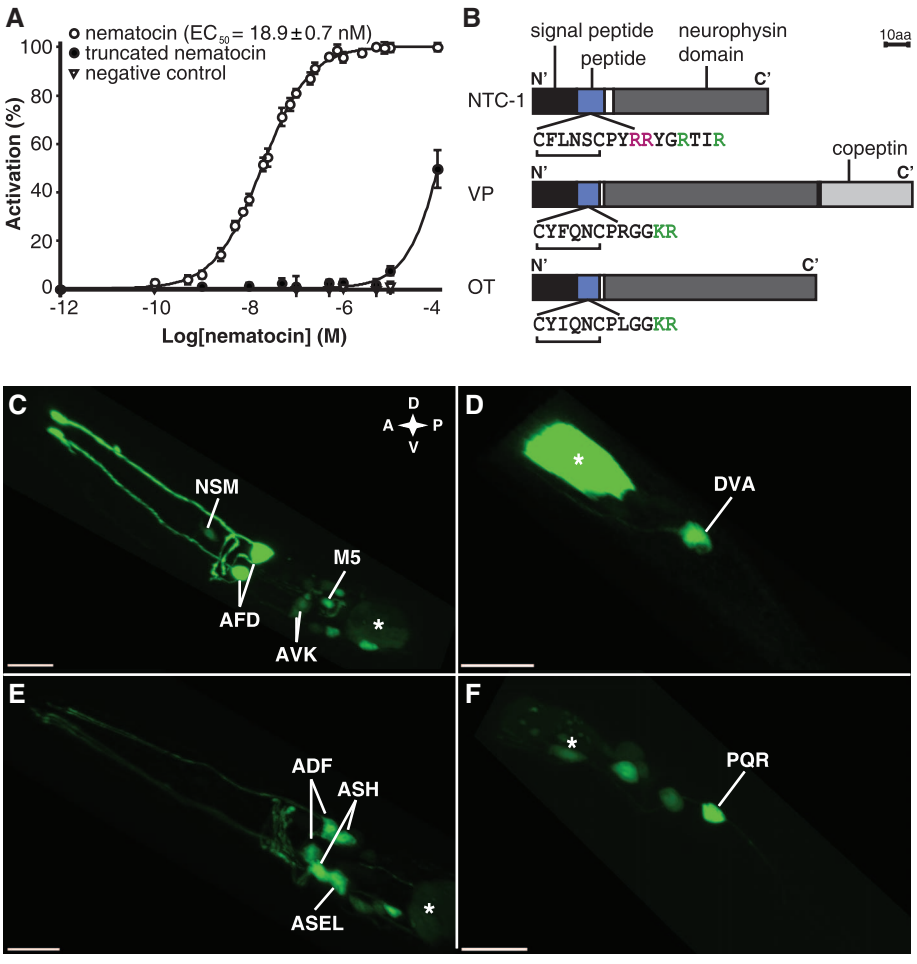


**Fig. 1.** *ntc-1* encodes a VP/OT-related peptide, nematocin, that signals through the NTR-1 receptor. (**A**) Dose-response curves for calcium responses evoked by nematocin (CFLNSCPYRRYamide) and its C-terminally truncated variant CFLNSCPY (*13*) in CHO cells either expressing NTR-1 or transfected with an empty vector (negative control). Each point (±SEM) represents the average of two independent experiments performed in triplicate. Dose-response data are shown as relative (%) to the highest value (100% activation) after normalization to the maximum calcium response. (**B**) Domain structures of NTC-1 and human VP and OT (*13*). Predicted proprotein convertase sites are in purple and green; N′, amino terminus; C′, C terminus. (**C** and **D**) Expression of *ntc-1::gfp* reporter transgene. (**E** and **F**) Expression of *ntr-1::gfp* transgene. (C to F) Left and right panels are labeled confocal Z-stack projections of the head and tail region (L1 wild-type hermaphrodite), respectively. Asterisks mark fluorescence in the intestine, resulting from the co-injection marker P*elt-2::mCherry*. Scale bars represent 10 μm. A, anterior; P, posterior; D, dorsal; V, ventral.

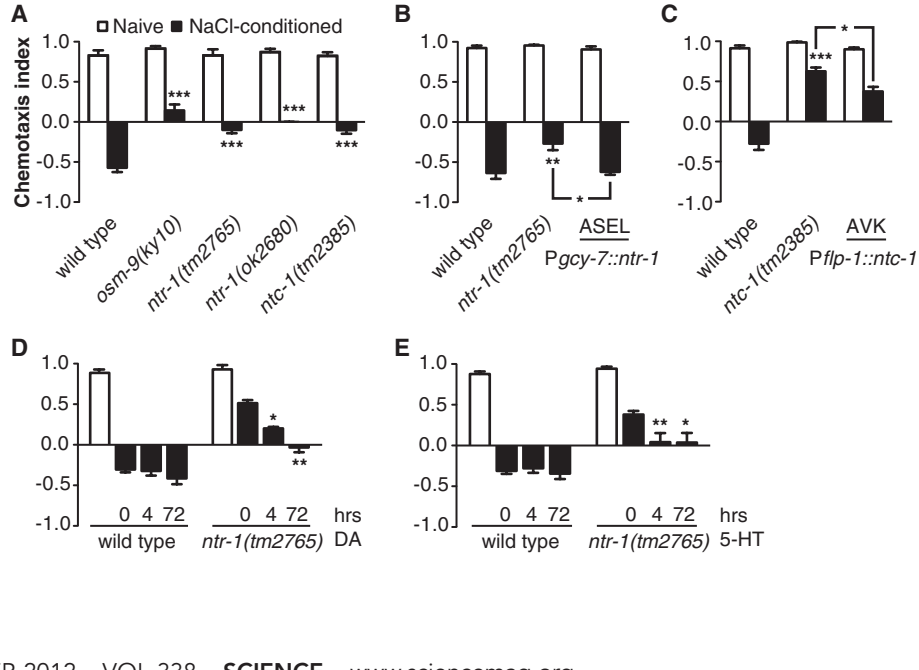


**Fig. 2.** Nematocin signaling regulates gustatory plasticity. (**A**) Gustatory plasticity of *ntr-1* and *ntc-1* mutants. The mean chemotaxis index toward 25 mM NaCl of animals preexposed in buffer with (conditioned) or without (naive) NaCl is plotted. *osm-9* mutants were used as positive control. (**B** and **C**) *ntr-1* or *ntc-1* were expressed by cell-specific promoters in the *ntr-1(tm2765)* or *ntc-1(tm2385)* background, respectively, and gustatory plasticity of transgenic animals was tested. (**D** and **E**) Responses of wild-type and *ntr-1(tm2765)* animals after 4 or 72 hours of culture on plates containing 2 mM dopamine (DA) or serotonin (5-HT). Open and solid bars represent naive and NaCl-conditioned behaviors, respectively. For (A) to (C), responses were compared to wild type (unless indicated otherwise) by one-way analysis of variance (ANOVA) and Tukey post-hoc comparison. For (D) and (E), statistical significance scores refer to the relative change in mutant behavior compared with wild-type changes upon dopamine or serotonin exposure and were based on coefficients of a fitted linear model. *$P < 0.05$, **$P < 0.01$, ***$P < 0.001$; error bars indicate SEM ($n \geq 4$ assays).

and NTC-1 precursor proteins in transgenic *C. elegans*. We found that *ntc-1* is expressed in thermosensory AFD neurons, neurosecretory NSM cells, AVK interneurons, the pharyngeal neuron M5, and the mechanosensory DVA neuron (Fig. 1, C and D). The *ntr-1* gene is strongly expressed in the left ASE (ASEL) gustatory neuron, the chemosensory neuron pairs ASH and ADF, and most likely the PQR tail neuron (Fig. 1, E and F; complete *ntc-1*, *ntr-1*, and *ntr-2* expression patterns are reported in fig. S7 and movies S1 to S3). These expression patterns suggest a role for nematocin signaling in modulating sensory neural circuits.

Because the *ntr-1*–expressing ASEL, ADF, and ASH neurons perform critical functions in chemotaxis of *C. elegans* toward water-soluble (gustatory) cues (*15*, *16*), we studied the salt chemotaxis behavior of mutants defective in nematocin signaling. Null mutants for nematocin or its receptor showed wild-type attraction to low NaCl concentrations and avoidance of high osmotic strength (fig. S8). Hence, defects in the nematocin signaling pathway do not compromise the normal detection of NaCl and subsequent attractive or aversive responses.

Next, we investigated whether nematocin plays a more subtle role in sensory processing and focused on gustatory plasticity, which implies a change in salt chemotaxis behavior on the basis of prior experience (*17*, *18*). We subjected mutants lacking nematocin or its receptor to this associative learning paradigm by using a short-term gustatory plasticity assay. Chemotaxis toward the attractant NaCl was compared between naive worms and animals that were shortly (15 min) preexposed to the attractant in the absence of food (an aversive stimulus) (fig. S9). Although preexposed wild-type worms showed reduced attraction to or even avoidance of NaCl, this aversive response was significantly reduced in *ntc-1* and *ntr-1* mutants (Fig. 2A). These results suggest that defects in the nematocin signaling cascade disrupt gustatory associative learning. To dissect part of the cellular circuit behind this effect, we generated transgenic lines expressing *ntr-1* or *ntc-1* under promoters specific to selected target cells. Cell-specific expression of *ntr-1* in the gustatory ASEL neuron and of the nematocin precursor *ntc-1* in AVK neurons rescued the plasticity defect of *ntr-1* and *ntc-1* mutants, respectively (Fig. 2, B and C, and fig. S10). Our findings imply that nematocin, originating at least partly from the AVK interneurons, facilitates gustatory associative learning through NTR-1–mediated signaling in the ASEL sensory neuron, which has previously been found essential for salt-attractive behaviors and gustatory plasticity (*19*). Null mutants for *ntr-2* showed wild-type gustatory plasticity, whereas the plasticity defects of *ntr-1; ntr-2* double mutants resembled that of the *ntr-1* single mutant (fig. S11B).

Starvation prior to the learning assay is known to enhance gustatory plasticity of wild-type worms, resulting in stronger aversive responses (*18*). Starved nematocin signaling mutants, however, showed wild-type gustatory plasticity (fig. S11), indicating that starvation triggers a nematocin-independent mechanism to induce NaCl avoidance after preexposure.

Previous work revealed that G protein as well as calcium signaling, via the Gγ subunit GPC-1 and the TRPV channel OSM-9, among others, regulate gustatory plasticity (*19*). We generated double mutants for *ntr-1* and *ntc-1* with the *gpc-1* or *osm-9* genes. Their plasticity resembled that of single mutants (fig. S12, A and B), indicating that nematocin functions in the same genetic pathway. We then investigated whether nematocin interacts with dopamine and/or serotonin neurotransmitters, which play important roles in associative learning in mammals and *C. elegans* (*18*, *20*, *21*). Nematocin signaling mutants also lacking serotonin or dopamine biosynthesis because of mutations in the *tph-1* or *cat-2* genes (*18*), respectively, showed no additive gustatory plasticity defects (fig. S12, C and D). Considering the severe plasticity defect of the *cat-2* single mutant, the behaviors of double mutants carrying the *cat-2* loss-of-function allele were deemed less conclusive (fig. S12D). On the basis of our finding that nematocin acts in the same genetic pathway as *tph-1* and probably also *cat-2*, we tested whether exogenous serotonin or dopamine could restore gustatory plasticity of *ntr-1* mutants. Short- (4 hours) or long (72 hours)–term exposure to these neurotransmitters partially restored gustatory plasticity of mutants lacking the NTR-1 receptor (Fig. 2, D and E), whereas naive responses of mutants and the behaviors of wild-type animals were unaffected (fig. S13). These results suggest that nematocin receptor signaling interacts with serotonergic and dopaminergic neurotransmission in gustatory plasticity.

The ability of animals to monitor environmental cues and adapt their behavior accordingly is crucial for their survival. We have shown that in *C. elegans*, VP/OT-related signaling is critical for gustatory associative learning, in line with the emergence of VP and OT as key regulators of mammalian cognition and behavior (*8*, *22*). Our results indicate that VP and OT neuropeptides have ancient roles in modulating sensory processing in central neural circuits underlying behavioral plasticity. Hence, this neuropeptide signaling system likely arose when animals became mobile and started to make experience-based decisions, which happened before the divergence of protostomes and deuterostomes more than 700 million years ago.

### References and Notes


1. M. S. Soloff, M. Alexandrova, M. J. Fernstrom, *Science* **204**, 1313 (1979).
2. W. Rosenthal *et al.*, *Nature* **359**, 233 (1992).
3. M. Schumacher, H. Coirini, D. W. Pfaff, B. S. McEwen, *Science* **250**, 691 (1990).
4. E. Stafflinger *et al.*, *Proc. Natl. Acad. Sci. U.S.A.* **105**, 3262 (2008).
5. R. E. van Kesteren *et al.*, *Neuron* **15**, 897 (1995).
6. M. J. Aikins *et al.*, *Insect Biochem. Mol. Biol.* **38**, 740 (2008).
7. L. J. Young, Z. Wang, *Nat. Neurosci.* **7**, 1048 (2004).
8. A. Meyer-Lindenberg, G. Domes, P. Kirsch, M. Heinrichs, *Nat. Rev. Neurosci.* **12**, 524 (2011).
9. D. de Wied, M. Diamant, M. Fodor, *Front. Neuroendocrinol.* **14**, 251 (1993).
10. E. L. Ardiel, C. H. Rankin, *Learn. Mem.* **17**, 191 (2010).
11. T. Janssen, M. Lindemans, E. Meelkop, L. Temmerman, L. Schoofs, *Ann. N. Y. Acad. Sci.* **1200**, 1 (2010).
12. Materials and methods are available as supplementary materials on *Science* Online.
13. Single-letter abbreviations for the amino acid residues are as follows: C, Cys; F, Phe; G, Gly; I, Ile; K, Lys; L, Leu; N, Asn; P, Pro; Q, Gln; R, Arg; S, Ser; T, Thr; and Y, Tyr.
14. H. Orcel *et al.*, *Mol. Pharmacol.* **75**, 637 (2009).
15. C. I. Bargmann, H. R. Horvitz, *Neuron* **7**, 729 (1991).
16. J. G. Culotti, R. L. Russell, *Genetics* **90**, 243 (1978).
17. G. Jansen, D. Weinkove, R. H. Plasterk, *EMBO J.* **21**, 986 (2002).
18. R. K. Hukema, S. Rademakers, G. Jansen, *Learn. Mem.* **15**, 829 (2008).
19. R. K. Hukema, S. Rademakers, M. P. Dekkers, J. Burghoorn, G. Jansen, *EMBO J.* **25**, 312 (2006).
20. P. Redgrave, K. Gurney, *Nat. Rev. Neurosci.* **7**, 967 (2006).
21. A. Izquierdo *et al.*, *Behav. Brain Res.* **233**, 494 (2012).
22. C. McCall, T. Singer, *Nat. Neurosci.* **15**, 681 (2012).



**Acknowledgments:** We thank the *Caenorhabditis* Genetics Center, S. Mitani, C. Bargmann, and M. Alkema for strains and reagents; L. Vanden Bosch, M. Vanhove, and W. De Haes for technical assistance. I.B., T.J., and L.T. benefit from the Fund for Scientific Research-Flanders (FWO) and E.M. from the KU Leuven Faculty Research Fund. This work was supported by the KU Leuven concerted research grant GOA/11/002 and FWO grants G.0767.09 and G.0601.11. GenBank accession numbers of *ntc-1*, *ntr-1*, and *ntr-2* sequences are JQ277480, JQ277731, and JQ277479. Strains carrying the *tm2385*, *tm2765*, and *tm2243* alleles are available through the *C. elegans* National BioResource Project (NBRP), subject to a materials transfer agreement.


### Supplementary Materials

www.sciencemag.org/cgi/content/full/338/6106/543/DC1
Materials and Methods
Figs. S1 to S13
Tables S1 to S3
References (*23*–*66*)
Movies S1 to S3


2 July 2012; accepted 21 August 2012
10.1126/science.1226860


# *Science* Careers Advertising

For full advertising details, go to ScienceCareers.org and click For Employers, or call one of our representatives.

**Tracy Holmes**
Worldwide Associate Director
*Science* Careers
Phone: +44 (0) 1223 326525

THE AMERICAS

E-mail: advertise@sciencecareers.org
Fax: 202-289-6742

**Tina Burks**
East Coast/West Coast/South America
Phone: 202-326-6577

**Allyson Rosen**
Midwest/Canada/Corporate
Phone: 202-326-6578

**Marci Gallun**
Sales Administrator
Phone: 202-326-6582

**Online Job Posting Questions**
Phone: 202-312-6375

EUROPE & REST OF WORLD

E-mail: ads@science-int.co.uk
Fax: +44 (0) 1223 326532

**Lucy Nelson**
Phone: +44 (0)1223 326527

**Kelly Grace**
Phone: +44 (0) 1223 326528

JAPAN

**Yuri Kobayashi**
Phone: +81-50-3696-5100
E-mail: ykobayas@aaas.org

CHINA & TAIWAN

**Ruolei Wu**
Phone: +86-1367-1015-294
E-mail: rwu@aaas.org



Science Careers
From the journal *Science* AAAS

## UC DAVIS

**Assistant Professor in Plant Sciences**
**Crop Ecology/Agroecology**
**Department of Plant Sciences**

**RESPONSIBILITIES:** The successful candidate's research will focus on agricultural systems and how management practices affect the use and quality of natural resources. Possible topics might include cropping systems analysis and research to attain sustainable production of irrigated annual and perennial crops (e.g.: resource cycling (nutrients, carbon, water), energy flows, climate change, agrobiodiversity, agroecosytem services. Creativity in collaborative research using field station and farm locations is expected. The appointee will collaborate with other scientists at UC Davis including staff and faculty affiliates of the Agricultural Sustainability Institute, Cooperative Extension specialists, advisors and researchers from other universities and agencies to address important agricultural/environmental issues in California. Interest in international agriculture is desirable. Teaching is assigned by the department chair and will include responsibilities in the Sustainable Agriculture and Food Systems undergraduate major and include courses in sustainable agriculture systems, agroecosystem management and crop ecology. Graduate teaching will involve teaching activity in the Horticulture and Agronomy and/or Ecology Graduate Groups. Creative approaches to teaching will be encouraged, including experiential and problem-based learning. Advising and mentoring of undergraduate and graduate students is expected. The position is an academic year (9 month) tenure-track position. This **Assistant Professor** position will include and appointment in the **Agricultural Experiment Station**. Faculty members who hold an Agricultural Experiment Station appointment have a responsibility to conduct research and outreach relevant to the mission of the California Agricultural Experiment Station. The successful candidate will be expected to participate in departmental, college, and campus committees and with state, regional and national organizations as appropriate.

**QUALIFICATIONS:** Candidates must have a strong and well-documented background in agroecology, crop ecology agroecosystem management, agronomy or related fields and a Ph.D. or equivalent degree in an appropriate discipline.
**SALARY:** Commensurate with qualifications and experience.
**TO APPLY:** Candidates should begin the application process by registering online at **http://recruitments.plantsciences.ucdavis.edu/**

For technical or administrative questions regarding the application process please email Melanie Greenleaf at **mjgreenleaf@ucdavis.edu**. Review of the applications for all positions will begin **January 1, 2013**. The position will remain open until filled.

*UC Davis is an Affirmative Action/Equal Employment Opportunity Employer and is dedicated to recruiting a diverse faculty community. We welcome all qualified applicants to apply, including women, minorities, veterans, and individuals with disabilities.*

## KU THE UNIVERSITY OF KANSAS

**Bioinformatics/Computational Biology**

The Center for Bioinformatics (Bioinformatics Program) and the Department of Molecular Biosciences invite applications for an assistant professor tenure-track faculty position to begin as early as August 18, 2013. The interdisciplinary Center for Bioinformatics (**www.bioinformatics.ku.edu**) complements existing strengths in the Department of Molecular Biosciences (**www.molecularbiosciences.ku.edu**), including structural biology, computational chemistry, proteomics, and developmental/molecular genetics, as well as strengths in drug design and information technology in the Schools of Pharmacy and Engineering. The Center fosters international activities in Bioinformatics and combines outstanding research and a Ph.D. program.

**Required Qualifications:** Ph.D. and postdoctoral experience in a discipline related to Bioinformatics is expected by the start date of the appointment; potential for excellence in research in Bioinformatics; commitment to teaching life sciences courses; and strong record of research accomplishments in at least one of the following areas: modeling of macromolecular structure and interactions, modeling of protein networks, genomics, and systems biology.

For the full position announcement and to apply online, go to: **http://employment.ku.edu** and search by key words "Bioinformatics/Computational Biology". Submit a CV, letter of application, statement of past and future research, statement of teaching interests and philosophy, and a list of at least three references who may be contacted via telephone or e-mail. Initial review of applications begins November 19, 2012 and will continue as long as needed to identify a qualified pool. Direct inquiries to Dr. Ilya Vakser (**vakser@ku.edu**).

The University of Kansas is especially interested in hiring faculty members who can contribute to four key campus-wide strategic initiatives: (1) Sustaining the Planet, Powering the World; (2) Promoting Well-Being, Finding Cures; (3) Harnessing Information, Multiplying Knowledge; and (4) Building Communities, Expanding Opportunities. See **www.provost.ku.edu/planning/themes/** for more information.

*Equal Opportunity Employer M/F/D/V.*

Johnson & Johnson

FAMILY OF COMPANIES

# What type of mark will you make?

## Janssen Research & Development

**Janssen Research & Development, LLC, discovers and develops some of the most innovative technology platforms and biologic medicines today. We are a world leader in monoclonal antibody technology and have a strong pipeline of novel antibodies in development.**

**Join our Informatics Group and be part of something revolutionary.**

Imagine working at the cutting edge of quantitative biomedicine to tackle the challenges of drug discovery… surrounded by reminders of the earliest days of American history. Janssen Research & Development is based in Spring House, Pennsylvania, a quiet escape from urban life that had its beginnings in the 1700s. Within our Spring House campus, you will be interacting with a multidisciplinary team of researchers focused on bringing therapies to patients. Looking for more excitement? Philadelphia, New Hope, Princeton, Lancaster, New York City and the New Jersey beaches are an easy, scenic drive away. Can you picture yourself here? Come work with us.

We are looking for experts from around the globe with a driven, passionate, and pioneering spirit to join our team. This is an outstanding opportunity to make a difference in the lives of people living with chronic diseases, and to work in a beautiful setting that is far from ordinary.

**We are currently recruiting outstanding scientific leaders with experience and expertise for the following roles:**

- **Head, Computational & Systems Biology**
  Requisition# **3489120829**
- **Head, High Performance Computing**
  Requisition# **2671120821**
- **Senior Scientist, Computational & Systems Biology**
  Requisition# **3468120829**
- **Senior Scientist, High Performance Computing**
  Requisition# **2568120816**

**Relocation packages are available.**

BE VITAL

careers.jnj.com

**Help us make history.**

If you need assistance locating these positions on our website, please email JRegan14@ITS.JNJ.com.

The George Washington University
WASHINGTON DC

## Faculty Position in Cardiovascular/Respiratory/ Autonomic Disorders Department of Pharmacology and Physiology School of Medicine and Health Sciences

The Department of Pharmacology and Physiology is accepting applications for a tenure-eligible faculty member at the rank of Assistant, Associate or Full Professor with expertise in the genetic, cellular or molecular characterization of autonomic, cardiovascular and/or respiratory disorders. This individual will participate in medical and graduate education in the Department of Pharmacology and Physiology as well as the Institute for Biomedical Sciences. **Basic Qualifications:** Applicants must have a terminal degree (Ph.D. or M.D.) in an appropriate discipline and substantial accomplishments in biomedical research as demonstrated by a significant number of first and/or senior author publications in outstanding peer-reviewed journals as well as promise or success in obtaining external research support. The successful candidate will participate in collaborative research activities including development of multi-investigator projects for extramural funding. Salary and start up funds will be commensurate with experience.

**To be considered**, please complete an online faculty application at **https://www.gwu.jobs/postings/11698** and submit a complete curriculum vitae and names and contact information for 3 references. Review of applications will begin on **December 1, 2012**, and will continue until the position is filled. Only complete applications will be considered.

*GW is an Equal Opportunity/Affirmative Action Employer.*

JAAS 江苏省农业科学院

## Jiangsu Academy of Agricultural Sciences

### Open position as Deputy Director and Full Professor in the Institute of Agricultural Facility and Equipment

Jiangsu Academy of Agricultural Sciences (JAAS) is a professional agricultural research and extension institution that has been established since 1932. JAAS ranks at the top of provincial agricultural academies in China in terms of the comprehensive strength in agriculture. JAAS's headquarter and main research facilities are located in Nanjing, Jiangsu,China.

Currently, JAAS is seeking a deputy director with the rank of full professor in the area of agricultural facility and equipment researches. Applicant should have a commitment to scientific excellence and the enthusiasm, energy, and innovative thinking necessary to lead a dynamic institute with a broad and diverse portfolio. Applicant must possess a faculty position already beyond the assistant professor level in a university or the equivalent position in a research institution. In addition, the candidate should demonstrate excellent records of research accomplishment and has a command of bilingual language for English and Chinese, both in spoken and written.

Successful applicant will be offered a competitive package, including sufficient laboratory space, startup funding, relocation fee and competitive salary commensurate with experience, in addition to a housing allowance, and other employee benefits. Applicant can go to **www.jaas.ac.cn** for application details.

In addition, more information for other regular faculty positions from JAAS relevant to a variety of disciplines in agriculture is also available at **www.jaas.ac.cn**.

**Contact information**
E-mail: **rsc-gbk@jaas.ac.cn**; Tel: **086-25-84390037**

THE UNIVERSITY OF HONG KONG
香 港 大 學

Founded in 1911, The University of Hong Kong is committed to the highest international standards of excellence in teaching and research, and has been at the international forefront of academic scholarship for many years. The University has a comprehensive range of study programmes and research disciplines spread across 10 faculties and about 100 sub-divisions of studies and learning. There are over 23,400 undergraduate and postgraduate students coming from 50 countries, and more than 1,800 members of academic and academic-related staff, many of whom are internationally renowned.

## Tenure-Track Professor in the Department of Physics (Ref.: 201200995)

Applications are invited for a tenure-track appointment as Professor in the Department of Physics, from as soon as possible. The post will initially be made on a three-year term basis, with the possibility of renewal subject to mutual agreement. Tenure may be offered to qualified candidates.

The position will be in any field of Physics. Existing research activities in the Department include astrophysics, condensed matter physics, high energy physics, and materials science. Candidates with excellent qualifications and commitment to high-quality research and excellence in teaching are encouraged to apply. The appointee is expected to provide academic leadership in research and teaching.

A globally competitive remuneration package commensurate with the appointee's qualifications and experience will be offered. The appointment will attract a contract-end gratuity and University contribution to a retirement benefits scheme, totalling up to 15% of basic salary, as well as housing benefits, leave, and medical benefits. At current rates, salaries tax does not exceed 15% of gross income.

For enquiries about the existing research activities and the specific job requirements, please write to Professor F.C. Zhang, Head, Department of Physics (e-mail: physhead@hku.hk). Interested applicants should submit a completed application form, together with a full C.V., a detailed publication list, a research plan, and a statement on teaching philosophy to scphy@hku.hk. Please indicate clearly "Ref.: 201200995 (Tenure-Track Professor in Department of Physics)" in the subject of the email.

Application forms (341/1111) can be obtained at http://www.hku.hk/apptunit/form-ext.doc. Further particulars can be obtained at http://jobs.hku.hk/. **Closes December 8, 2012.** The University thanks applicants for their interest, but advises that only shortlisted applicants will be notified of the application result.

**The University is an equal opportunity employer and is committed to a No-Smoking Policy**

Western University of Health Sciences
*The discipline of learning. The art of caring.*
www.westernu.edu

## Faculty Positions in Microbiology/Virology and other disciplines available for 2013

The College of Osteopathic Medicine of the Pacific – Northwest (COMP-Northwest) inaugurated its first class of physicians-in-training in Lebanon, Oregon in Fall, 2011. As the newest expansion of Western University of Health Sciences in Pomona, California, we have established a thriving center for medical education and human health care in Oregon.

A major responsibility of the Department of Basic Medical Sciences is to provide preclinical education for the first and second-year students in COMP. Our current initiative is to add instructional and research strength within the discipline of Microbiology/Virology. This is a 12-month, tenure-track appointment at the Assistant/Associate/ or full Professor rank depending upon qualifications. Successful candidates will join a large intercampus faculty in the department of Basic Medical Sciences and be located either at the COMP-Pomona campus, California, or at the new campus in Lebanon. Applicants must have a Ph.D. in Microbiology or related fields and at least two years of postdoctoral experience. Similar positions in biochemistry and pharmacology are also available at both campuses. Preference is given to effective educators with a record of excellence in teaching, significant scholarly activity and strong potential for independent grant-supported research. Submit a current curriculum vitae and a cover letter describing your teaching experience, research activity and goals. Please include contact information for at least three references. These positions will remain open until filled.

Nissar A. Darmani, PhD
Associate Dean for Basic Sciences and Research
Department of Basic Medical Sciences
College of Osteopathic Medicine of the Pacific
Western University of Health Sciences
309 E. Second Street, Pomona, CA 91766-1854
Email Address: ndarmani@westernu.edu

Western University of Health Sciences is an equal opportunity employer.

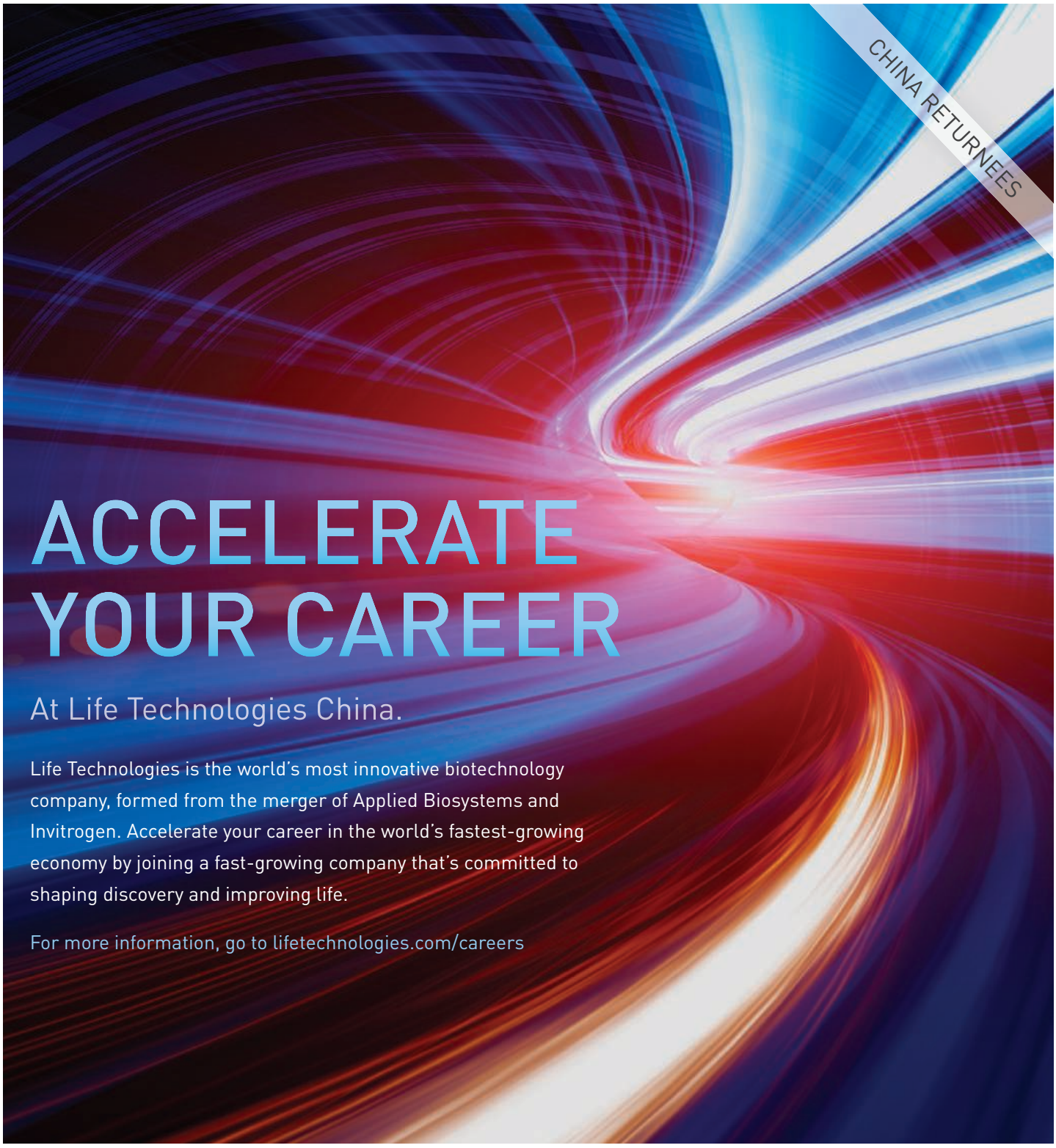


We want to hear from you. Email us at **cn.recruit@lifetech.com**

life technologies™



Invitrogen™ Applied Biosystems® Gibco® Molecular Probes® Novex® TaqMan® Ambion® Ion Torrent™

University of Massachusetts
UMASS Medical School

## Tenure-Track Faculty Position

### Department of Microbiology and Physiological Systems

The Department of Microbiology and Physiological Systems at the University of Massachusetts Medical School (http://www.umassmed.edu/) invites applications for a tenure-track faculty position at the rank of Assistant Professor. Depending on qualifications, candidates may be proposed for a more senior appointment at the rank of Associate or Full Professor. The Department is seeking candidates who can build on its core strengths in host-pathogen interactions, immunology, virology, and cellular physiology. We are particularly interested in candidates with cross-disciplinary approaches to problems in bacterial or viral infection including, but not limited to: integrative/systems biological approaches to infection; analysis of complex microbial communities and their impact on host responses; molecular mechanisms of pathogenesis; cell biology of infection; and host defenses and adaptation to infection. Candidates will be expected to develop and maintain an innovative, externally funded research program. We offer generous support and a highly collaborative environment with opportunities for both basic and translational research. The position will be highly competitive with regard to start-up funds and salary.

**Applicants should submit a cover letter explaining their interest in the Department, a curriculum vitae that includes honors and publications, and a succinct research plan to https://academicjobsonline.org/ajo/jobs/2054. To expedite the review process, applicants should invite three individuals who are familiar with their work and potential for success to upload recommendation letters at the same web address. Review of applications will begin immediately and continue until the position is filled.**

*As an equal opportunity and affirmative action employer, UMMS recognizes the power of a diverse community and encourages applications from individuals with varied experiences, perspectives and backgrounds.*

National Taiwan University

## National Taiwan University Presidential Search

National Taiwan University (NTU) is a full-fledged comprehensive university with outstanding achievements. As the current presidency ends in June, 2013, Presidential Search Committee now invites nominations and applications for the position of President.

President candidates should meet the following requirements: Academician at Academia Sinica, or professor, or professional with prior teaching and academic research experience equivalent to that required of a professor, and at least three years of experience, accumulative, as a director in schools, government agencies, or in other state-owned or private business entities. The ideal President should be a leader of integrity with excellent academic achievement and administrative skills in education. The new leader should also be able to administer matters impartially and beyond the interests of any political groups.

For those who would like to nominate a candidate, please fill in all required forms and send it to the address below via registered mail or express mail delivered **before 5pm on December 3, 2012**. Application dossier will not be returned.

**NTU Presidential Search Committee**
**No.1, Sec. 4, Roosevelt Road**
**Taipei**
**Taiwan 10617**

If you have any inquiries, please call **(886)-2-33662035**, or fax **(886)-2-23629997**. The nomination form can be downloaded from the NTU Website: **http://www.ntu.edu.tw/president/eng.html**

MUSC
MEDICAL UNIVERSITY of SOUTH CAROLINA

## Recruiting Senior Faculty with Research Interests in Lipid Signaling and Metabolic Pathways

The Department of Biochemistry & Molecular Biology and the Hollings Cancer Center at the Medical University of South Carolina (MUSC) are pleased to announce openings for senior level faculty with research experience in cancer lipid signaling and/or metabolism, including various aspects of cancer biology and/or therapeutics, such as regulation of PI/PI3K signaling, RNA transcription/translation, lipid-protein interaction, and/or anti-cancer drug function. State-of-the-art laboratories, outstanding resources and research support are available. Endowed chair positions are available for qualified candidates. We are seeking outstanding basic and/or clinical scientists who would complement and expand existing programs at MUSC.

Candidates should have a national reputation, outstanding track record, and solid record of collaborative and peer-reviewed funded research. The Hollings Cancer Center is a National Cancer Institute Designated Center, and with its state-of-the-art research and shared resource facilities, including an outstanding Lipidomics Core, it has a strong culture of promoting basic and translational research.

Located on the Atlantic coast in South Carolina, Charleston boasts one of the nation's most historic downtown areas, beaches and year-round outdoor life, as well as international cultural events such as the Spoleto Festival USA and outstanding cuisine.

Interested researchers should submit a CV, summary of research interests, and contact information for three references online at website: **www.jobs.musc.edu/applicants/Central?quickFind=189086**.

**Philip H. Howe, Ph.D.**
**Professor & Chair**
**Biochemistry & Molecular Biology**
**Associate Director of Basic Sciences**

**Besim Ogretmen, Ph.D.**
**Professor**
**Biochemistry & Molecular Biology**
**Program Leader**

**Hollings Cancer Center**
**Medical University of South Carolina**
**PO Box 25063**
**Charleston, SC 29425**
**campbetb@musc.edu**

*MUSC is an Equal Opportunity Employer, promoting workplace diversity.*

NANYANG TECHNOLOGICAL UNIVERSITY

## RISE TO THE OPPORTUNITY

with one of the world's fastest-rising universities. **NTU.**

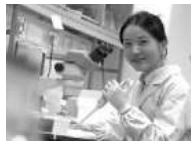

### Faculty Positions at School of Chemical and Biomedical Engineering (SCBE)

Nanyang Technological University (NTU) in Singapore is ranked 47th in the 2012 QS World University Rankings and is the fastest-rising university in the world's top 50.

SCBE at NTU invites applications for Assistant, Associate or Full Professors. For more information, visit www.scbe.ntu.edu.sg/About_Us/Pages/Open_Positions.aspx

**Research Areas**

**Chemical and Biomolecular Engineering Division**
- Process systems engineering
- Product and process design
- Pharmaceutical engineering
- Food engineering
- Separation technology

**Bioengineering Division**
- Cardiovascular biomechanics
- Bioinstrumentation
- Biosignal processing and imaging
- Biofluid
- Neuro bioengineering
- Nature inspired bioengineering

**Application Details**

Guidelines: www.ntu.edu.sg/ohr/Career/SubmitApplications/Pages/Faculty.aspx

Email: scbe_recruit@ntu.edu.sg

**www.ntu.edu.sg**

## AAAS is here –
### promoting universal science literacy.

In 1985, AAAS founded Project 2061 with the goal of helping all Americans become literate in science, mathematics, and technology. With its landmark publications *Science for All Americans* and *Benchmarks for Science Literacy*, Project 2061 set out recommendations for what all students should know and be able to do in science, mathematics, and technology by the time they graduate from high school. Today, many of the state standards in the United States have drawn their content from Project 2061.

Every day Project 2061 staff use their expertise as teachers, researchers, and scientists to evaluate textbooks and assessments, create conceptual strand maps for educators, produce groundbreaking research and innovative books, CD-ROMs, and professional development workshops for educators, all in the service of achieving our goal of universal science literacy.

As a AAAS member, your dues help support Project 2061 as it works to improve science education. If you are not yet a member, join us. Together we can make a difference.

To learn more, visit
aaas.org/plusyou/project2061

AAAS + U = Δ

BINGHAMTON UNIVERSITY
STATE UNIVERSITY OF NEW YORK

## FACULTY POSITIONS IN BIOCHEMISTRY AND EVOLUTIONARY GENETICS

The Department of Biological Sciences at Binghamton University invites applications for tenure-track faculty positions in Biochemistry and Evolutionary Genetics at the assistant professor level. See **http://binghamton.interviewexchange.com** for more information about these positions and how to apply.

*Binghamton University, one of the four doctoral-granting university centers of the State University of New York, is an Affirmative Action, Equal Opportunity Employer, and it encourages applications from women and minorities.*

UNIVERSITY OF CALIFORNIA
UCMERCED

## Two Assistant Professorships in Biostatistics and Biochemistry/ Molecular Biology

The Molecular Cell Biology group at the University of California, Merced, seeks applicants for two tenure-track assistant professor positions in the areas of Biostatistics and Biochemistry/ Molecular Biology. Candidates are expected to have an excellent publication record and to teach biology effectively at both undergraduate and graduate levels. The successful candidate in Biostatistics will be expected to cultivate collaborative research relationships with faculty in biology, health sciences, and may also collaborate with applied mathematics. For the Biochemistry or Molecular Biology position, candidates with expertise in protein biochemistry, structural biology, enzymology, molecular biology, biochemical or biophysical techniques, metabolomics, or proteomics are preferred. Current strengths of the Molecular Cell Biology group include cancer, diabetes, neurobiology, inflammation, infectious disease, and mechanisms of cell fate decisions. For more information on the two positions go to the following links:

**http://jobs.ucmerced.edu/n/academic/position.jsf?positionId=4252**
**http://jobs.ucmerced.edu/n/academic/position.jsf?positionId=4259**

Applications will be considered until **December 10, 2012**.

*UC Merced is an AA/EOP Employer.*

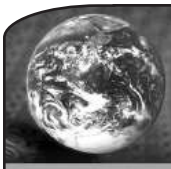


**AAAS is here** – helping scientists achieve career success.

Every month, over 400,000 students and scientists visit ScienceCareers.org in search of the information, advice, and opportunities they need to take the next step in their careers.

A complete career resource, free to the public, *Science* Careers offers a suite of tools and services developed specifically for scientists. With hundreds of career development articles, webinars and downloadable booklets filled with practical advice, a community forum providing answers to career questions, and thousands of job listings in academia, government, and industry, *Science* Careers has helped countless individuals prepare themselves for successful careers.

As a AAAS member, your dues help AAAS make this service freely available to the scientific community. If you're not a member, join us. Together we can make a difference.

To learn more, visit **aaas.org/plusyou/sciencecareers**

AAAS + U = Δ

## POSITIONS OPEN

Massachusetts Institute of Technology

### FACULTY POSITIONS in Mechanical Engineering Massachusetts Institute of Technology

The Department of Mechanical Engineering at the Massachusetts Institute of Technology seeks outstanding candidates for tenure-track faculty positions in the following fields to begin July 1, 2013 or thereafter: Bioengineering; Thermal Sciences and Engineering; Instrumentation and Robotics.

A detailed description for each position is provided at **website: http://search-meche.mit.edu**. Applicants should hold an earned Ph.D. in mechanical engineering or a relevant field by the start of employment. Faculty duties include teaching at the graduate and undergraduate levels, research, and supervision of student research.

We seek candidates who will provide inspiration and leadership in research and actively contribute to core mechanical engineering undergraduate, and graduate level teaching. New faculty hires are expected to have a research focus in one of the disciplinary fields listed above. Applicants must have demonstrated: (1) outstanding research strength; (2) a strong disciplinary background; (3) strong experimental and/or theoretical skills; and (4) the potential to work across disciplinary boundaries. Appointment would be at the **ASSISTANT** or untenured **ASSOCIATE PROFESSOR** level. In exceptional cases, a senior faculty appointment may be possible.

Applicants should send curriculum vitae, a research statement, a teaching statement, and copies of not more than three publications. They should also arrange for four individuals to submit letters of recommendation on their behalf. This information must be entered electronically at the following **website: http://search-meche.mit.edu**. Full consideration will be given to applications submitted by December 31, 2012.

*MIT is an Equal Opportunity/Affirmative Action Employer. Women and underrepresented minorities are especially encouraged to apply.*

### FACULTY AND RESEARCHER OPENING at Hunan University

The State Key Laboratory for Chemo/Biosensing and Chemometrics, College of Biology and College of Chemistry and Chemical Engineering at Hunan University will recruit multiple faculty members and research scientists to expand its effort in biology, molecular sciences and biomedical sciences and engineering. We welcome applicants in the following four widely defined areas: chemical biology, Life sciences (plant molecular biology and plant biotechnology), biomedical engineering, and molecular medicine. Applicants should have a Ph.D. or M.D. in related areas such as biology, medicine, biomedical engineering, and chemistry, etc. Applicants at all academic levels are welcome to apply with the following materials: curriculum vitae, research and teaching statements and the names of five referees. These materials can be sent to **e-mail: hudabiology@gmail.com** for candidates for faculty positions, and to **e-mail: hudaresearcher@gmail.com** for research scientists, postdoctors, and graduate students. For faculty candidates, competitive salary, and startup package will be offered based on qualification. Review of applications will begin on November 15, 2012, and continue until the positions are filled. Hunan University is a 985 Project University with intensive and expanding research programs in biology, chemistry, and biomedical sciences and engineering.

**RESEARCH ASSOCIATE**, Department of Pharmacology, School of Medicine, experience required. Send resume to: **V. Tripodo, Administrator, Case Western Reserve University, SOM, Department of Pharmacology, 10900 Euclid Avenue, Wood, Room 321, Cleveland, OH 44106-4965**. Must reference **job code 100212**.

## POSITIONS OPEN

Smithsonian

### RESEARCH ZOOLOGIST Department of Invertebrate Zoology National Museum of Natural History Smithsonian Institution

The Smithsonian's National Museum of Natural History seeks a zoologist to conduct an integrative, specimen- or collection-based research program in invertebrate evolution and biodiversity (exclusive of hexapods, myriapods, and arachnids). The successful candidate is expected to develop an internationally recognized research program that makes important contributions to understanding invertebrate evolution and biodiversity through synthetic research involving phylogenetics, genetics, anatomy, development, genomics, biogeography, conservation, informatics, or related fields. Frequent publication of highly regarded papers in competitive, peer-reviewed journals, curation of collections in specialty area, service to the scientific community in leadership capacities, acquisition of external funding, engagement in outreach activities, and mentorship of students are expected. Fit with existing strengths of the department's collections and staff is desirable but not essential.

Full-time four-year term appointment with full Government benefits to be filled at the GS-12 level; *U.S. citizenship required.* The museum's authorized salary range for this position at this time is $74,872 - $79,864 per annum. For complete requirements and application procedures, go to **websites: http://www.sihr.si.edu** or **http://www.usajobs.gov** and refer to **Announcement 13A-JW-297914-DEU-NMNH**. The announcement opens October 22, 2012. Applications must be received online by December 3, 2012 and must reference the announcement number. All applicants will be notified by e-mail when their application is received. *The Smithsonian Institution is an Equal Opportunity Employer.*

### ASSOCIATE PROFESSOR Geographic Information Science Center of Excellence South Dakota State University

The Geographic Information Science Center of Excellence (GIScCE) seeks a person with research experience and teaching interests focused on remote sensing science and applications that enable understanding of the rates, causes, and consequences of land cover land use change. This 12-month position is funded by state funds and carries a workload of 80% research, 10% teaching, and 10% service. Responsibilities include securing externally funded research grants, recruiting and mentoring doctoral students and postdoctoral researchers, and delivering one graduate course per year. Minimum qualifications include an earned Ph.D. degree in an appropriate field with a background in remote sensing; minimum of five years' experience conducting externally funded research; scholarly activity, including collaborative research and peer-reviewed publications as first author; and a demonstrated ability to communicate effectively. A diverse portfolio of sponsored research, demonstrated excellence in mentoring students, demonstrated leadership in professional service are desired qualifications. For questions on the position, contact the search committee chair, **Dr. David Roy** electronically at **e-mail: david.roy@sdstate.edu**. Application deadline is December 21, 2012. To view a full position description and to apply, visit **website: https://yourfuture.sdbor.edu/applicants/Central?quickFind=56621** and click on "apply for this posting." For questions on the electronic employment process, contact South Dakota State University (SDSU) Human Resources at **telephone: 605-688-4128**. *SDSU is an Affirmative Action/Equal Employment Opportunity Employer.*

## POSITIONS OPEN

Northern Michigan University

### NEUROSCIENTIST Northern Michigan University

Applications are invited for a tenure-earning faculty position at the **ASSISTANT PROFESSOR** level beginning August 2013. The position will be posted until December 3, 2012. Submit application materials to **website: https://employme.nmu.edu**, where a description and requirements are posted. *Northern Michigan University is an Equal Opportunity/Affirmative Action Employer and is strongly committed to increasing the diversity of its faculty.*

### TENURE-TRACK FACULTY POSITION Neuroscience California State Polytechnic University, Pomona

The Biological Sciences Department at California State Polytechnic University, Pomona (Cal Poly Pomona) invites applications for a tenure-track, **ASSISTANT PROFESSOR** position in neuroscience, beginning September 2013. The area of specialty is open. Candidates who use molecular, optical, electrophysiological, and/or neuroinformatic techniques to address modern questions in neuroscience are encouraged to apply. A Ph.D. in neuroscience or related field is required. Postdoctoral experience and previous teaching experience are preferred. The successful candidate will have the potential for excellence in undergraduate teaching, and for developing an externally funded research program that will involve undergraduate and Master's students. Teaching responsibilities will include a neuroscience course and specialty courses in the candidate's area of expertise, and may also involve participation in introductory biology and other courses. Cal Poly Pomona is a comprehensive Master's university with a diverse student body. The successful candidate will have demonstrated an ability to be responsive to the educational equity goals of the university and its increasing ethnic diversity and international character. Applicants should forward: (1) a cover letter that briefly describes the candidate's training, experience, and teaching and research interests; (2) curriculum vitae; (3) statement of teaching philosophy; (4) proposed plan of research; (5) a maximum of five representative publication reprints; and (6) the names and contact information of five references to: **Chair, Neuroscience Search Committee, Biological Sciences Department, California State Polytechnic University, 3801 West Temple Avenue, Pomona, CA 91768**. Electronic submission of application materials as a single PDF is preferred (**e-mail: neurosci_search@csupomona.edu**). Review of applications begins on December 3, 2012. Official transcripts and three letters of reference will be required of all finalists. For further information, visit the Department **website: http://www.csupomona.edu/~biology**.

*California State Polytechnic University, Pomona is an Equal Opportunity/Affirmative Action Employer.*

### ASSISTANT PROFESSOR Marine Biological Modeling

The Department of Biological Sciences at California State University, Long Beach (CSULB) invites applications for a tenure-track Assistant Professor position starting August 19, 2013. We seek broadly trained applicants who address fundamental research questions in marine biology using mathematical modeling of physiological, biophysical, or ecological processes. In addition to developing an externally funded research program involving undergraduate and M.S. students, the successful candidate will teach at the undergraduate and graduate levels. Applicants must have a Ph.D. and postdoctoral experience. For further information, please see the position description at **website: http://www.csulb.edu/divisions/aa/personnel/jobs/posting/1072/index.html**. Screening of applications will begin December 12, 2012. *CSULB is an Equal Opportunity Employer.*

Washington University in St. Louis

## Tenure Track Faculty Positions in Neurobiology

The Department of Anatomy and Neurobiology at Washington University School of Medicine is undergoing a major expansion and is recruiting outstanding scientists interested in developing independent research programs in neural development, synapse physiology, neural circuitry underlying behavior, or developmental disorders of cognition. We seek investigators for Assistant Professor positions using innovative cellular, molecular, genetic or epigenetic approaches.

Candidates should email a single pdf file containing: cover letter, curriculum vitae and summary of research accomplishments and plans to **neurosearch@pcg.wustl.edu** before **December 1, 2012**. Address materials to:

**Dr. Paul Taghert, Search Committee Chair**
**Department of Anatomy & Neurobiology**
**Washington University School of Medicine**
**660 South Euclid Avenue, Campus Box 8108**
**Saint Louis, MO 63110**

Candidates should also arrange to have three letters of recommendation (as pdf files) sent to the committee (**neurosearch@pcg.wustl.edu**) before **December 1, 2012**.

*Washington University is an Equal Opportunity Employer. AA/EOE M/F/D/V.*

UCLA

## Chief of the Division of Rheumatology at the David Geffen School of Medicine at UCLA

The Department of Medicine of the University of California at Los Angeles is seeking an exceptional leader with the expertise and skills needed to be the Chief of Rheumatology at UCLA. We are seeking a world class scientist that will continue the distinguished research that has been the hallmark of the Division over many decades. The Division includes 31 faculty members and an ACGME accredited fellowship training program consisting of 8 fellowship positions.

Individuals interested in this position should have a national/international reputation in the field of academic Rheumatology. The candidates must have a strong background in basic research in Rheumatology-related research themes with emphasis on novel approaches, a track record of extramural research funding, and publications consistent with this position. The selected individual will facilitate and coordinate all Rheumatology clinical and research activities of the Division. The candidate should have a willingness to foster collaborative interactions between clinical and laboratory scientists, and a strong interest in mentoring of junior faculty/fellows. A tenured faculty appointment at a rank commensurate with experience will be considered.

This position will control substantial resources from the Department of Medicine, and commands a competitive salary enhanced by an attractive benefits package, including medical malpractice coverage and a collegial work environment. Candidates should email their curriculum vitae, a letter with a statement of career goals, and the names of three references to the Chair of the Search Committee:

**Charalabos Pothoulakis, M.D.**
**Professor of Medicine**
**David Geffen School of Medicine at UCLA**
**c/o Juan Vaquerano, Administrator**
**e-mail: jvaquerano@mednet.ucla.edu**

*The David Geffen School of Medicine at UCLA is an Affirmative Action/ Equal Opportunity Employer. Women and Minorities are encouraged to apply.*

UAMS
UNIVERSITY OF ARKANSAS FOR MEDICAL SCIENCES

## ASSISTANT AND ASSOCIATE PROFESSOR Faculty Positions in Cancer Biology

The College of Medicine at the University of Arkansas for Medical Sciences is seeking applications for two tenure track faculty members at the level of Assistant Professor or Associate Professor in the Department of Biochemistry and Molecular Biology (**http://www.uams.edu/biochem/**). The department is seeking highly qualified biochemists/molecular biologists who will participate in the campus-wide effort to establish cross-discipline research programs in cancer biology, broadly defined. Areas of interest include but are not limited to the application of nanotechnology to treatment or diagnosis of cancer, signal transduction, the DNA damage response, and epigenetic mechanisms in cancer. The positions offer competitive salary (state supported), benefits, start up packages and outstanding new research space in the 300,000 sq. ft. expansion to the Winthrop P. Rockefeller Cancer Institute (**http://cancer.uams.edu/**).

Candidates must possess a PhD and/or MD degree. Successful candidates will be expected to have or develop an internationally leading research program and contribute to teaching medical and graduate students. Little Rock is a small city (area population of 600,000) with many cultural amenities, a very affordable cost of living, a temperate climate, and beautiful natural surroundings.

Consideration of candidates will begin immediately and will continue until the positions are filled. Applicants should submit curriculum vitae, a brief statement of proposed research, and arrange for three reference letters to be sent to (electronic submission preferred): **Biochemistry Search Committee, Department of Biochemistry and Molecular Biology, University of Arkansas for Medical Sciences, 4301 W. Markham St., Little Rock, AR 72205. E-mail: Biochemsearch@uams.edu**.

*University of Arkansas for Medical Sciences is an Equal Opportunity/ Affirmative Action Employer.*

# ANNOUNCEMENTS

**ESPCA/São Paulo School of Advanced Science**

## Advances in Molecular Structuring of Food Materials

**Faculty of Animal Science and Food Engineering, University of São Paulo, BRAZIL - April 1st to 5th, 2013**

**Food Science and Engineering** are increasingly interested in the food/ consumer relationship in terms of new food roles such as the **"delight" or "satisfaction"** that food provides. All of these are a consequence of a combination of chemical, biochemical, microbiological and structural factors inherent to food, either raw or processed. Several leading academics from Brazil and abroad will promote an advanced discussion of those topics.

**100 grants covering the cost of travelling, accommodation and subsistence** from 31MAR to 06APR, sponsored by FAPESP, are available for 60 selected post-graduate students from outside Brazil and 40 from Brazilian post-graduate programmes.
Additional participants will be accepted among post-graduate students from nearby post-graduate programmes, young-Doctors (PhD completed up to four years) and academics from any Brazilian university.

**Deadline for application and registration:**
**November 01, 2012 (23h59 Brasilia time)**

**Information:**
**http://spsas.vitis.uspnet.usp.br/molecularstructuringfood/**

**E-mail: structfood@gmail.com**

FAPESP

FZEA USP

## POSITIONS OPEN

### FACULTY POSITION in Bacterial Pathogenesis University of Minnesota

The Department of Microbiology at the University of Minnesota Medical School, in conjunction with the Corridors of Discovery initiative in Infectious Diseases, invites applications for a faculty position to be filled at the tenure-track **ASSISTANT PROFESSOR** level.

We seek an outstanding scientist who will establish a competitive research program in bacterial pathogenesis (broadly defined, but focused on prokaryotes: including bacterial physiology, microbiome studies, genetics, genomics, and pathogen-immune system interactions). This position is part of the University's commitment to the study of infectious diseases, which includes a major capital investment in a new Microbiology Research Facility. This building will be the latest addition to the Biomedical Discovery District and research home to departmental faculty. The University of Minnesota offers exceptional startup support, a dynamic intellectual environment, and outstanding research and core facilities. The department and affiliated units at the University have broad research strengths in microbiology and immunology, including microbial pathogenesis, microbial physiology, immunity and host defense, genetics, genomics, virology, mycology, environmental microbiology, and biotechnology. Additional information about the Department of Microbiology, affiliated institutes and centers, and the graduate training program, can be found on the department **website: http://www.microbiology.med.umn.edu**.

Minimum qualifications: Ph.D., M.D., or equivalent in a relevant field of study, plus applicable postdoctoral or faculty experience. To apply, please upload a curriculum vitae and concise summary of current and planned research in response to **requisition number 172214** at **website: http://employment.umn.edu**. Please also arrange to have three letters of recommendation sent to **e-mail: microbiology@umn.edu** or to: **Sandra K. Armstrong, Ph.D., Search Committee Chair, Department of Microbiology, University of Minnesota, MMC 196, 420 Delaware Street S.E., Minneapolis, MN 55455**.

*The University of Minnesota shall provide equal access to and opportunity in its programs, facilities, and employment without regard to race, color, creed, religion, national origin, gender, age, marital status, disability, public assistance status, veteran status, sexual orientation, gender identity, or gender expression.*

### FACULTY POSITIONS in Molecular & Cell Biology

The Department of Anatomy in the Howard University College of Medicine is seeking applicants for two tenure-track faculty positions at any level to start in the first half of 2013. Applicants must possess a Ph.D. and have postdoctoral experience. Within the context of molecular and cell biology, the candidate may be involved in neuroscience, developmental, genomic, or other innovative molecular and cell biology research. Highest priority will be given to candidates with a strong history of scholarly activity with either an established research program or the potential to develop an externally funded research program. The College of Medicine is currently expanding its basic science faculty and offers a competitive startup package. The preferred teaching competency of the applicant is in histology and cell biology. There are abundant opportunities for collaborations within the College of Medicine and at nearby institutions (NIH, FDA, USDA). Applicants should electronically send either a Word (.doc) or a PDF file that includes a comprehensive curriculum vitae, research interests and goals, and a minimum of three references (name, institutional address, telephone number, and e-mail address) to: **Dr. Raymond L. Bernor, Professor, Chair of Search Committee, College of Medicine, Department of Anatomy, Howard University, 520 W Street N.W., Washington D.C. 20059** (**e-mail: rbernor@howard.edu**). *Howard University is an Affirmative Action/Equal Opportunity Employer.*

University of Vermont Department of Animal Science seeks a tenure-track **ASSISTANT PROFESSOR** in Animal Health. Evaluation of applicants begins December 15, 2012. For full position description, see **website: http://www.uvmjobs.com**. *The University of Vermont is an Affirmative Action/Equal Opportunity Institution.*

### HARVARD UNIVERSITY

The Department of Psychology anticipates hiring a **SENIOR LECTURER** to begin July 1, 2013.

The appointee will be expected to teach four courses per academic year including undergraduate and graduate courses in statistics, research design, and data analysis. In addition to expertise in standard multivariate techniques of data analysis, working knowledge of simulation techniques and potentially techniques including graph theory and Bayesian analysis would be desirable. The appointee may also be asked to serve on undergraduate senior thesis committees, dissertation committees and other departmental committees.

This appointment requires a Ph.D. and candidates will ordinarily have held a faculty position at a research university or a selective undergraduate institution. Candidates can submit application materials online at **website: https://academicpositions.harvard.edu/postings/4305**. Questions regarding this position at Harvard may be sent to **e-mail: jenniferwalker@fas.harvard.edu**. The closing date for applying is December 1, 2012.

This appointment is renewable every five years based on performance and curricular needs. *Harvard is an Affirmative Action/Equal Opportunity Employer and welcomes applications from women and members of minority groups.*

### ASSISTANT PROFESSOR in Biochemistry

Georgetown University wishes to recruit a tenure-track Assistant Professor in Biochemistry to begin fall 2013, who will be housed in Regents Hall, a newly opened, state-of-the-art science center. Research areas in biochemistry as broadly defined will be considered that complement those of existing faculty in the Department. Research interests related to sustainability and energy or xenobiotics and the environment are especially welcome. Candidates must have a Ph.D. degree in chemistry or a closely related field and postdoctoral training or equivalent is desirable. Development of an internationally recognized, externally funded research program and teaching at the undergraduate and graduate levels, particularly biochemistry sequences, are expected. Please send curriculum vitae, description of research plans, statement of teaching philosophy as one document in PDF format, and arrange for three letters of recommendation to be sent to **e-mail; chemsearch@georgetown.edu**. For full consideration, complete applications should arrive before December 15, 2012. *Georgetown University is an Equal Opportunity/Affirmative Action Employer fully dedicated to achieving a diverse faculty and staff; applications from qualified women and minority candidates are encouraged.*

### POSTDOCTORAL POSITION in Brain Targeting/Cancer Immunology

A position (two years) is available immediately in the laboratory of **Ulrich Bickel,** M.D., Department of Pharmaceutical Sciences, Texas Tech University Health Sciences Center at Amarillo. Our group focuses on blood-barrier transport mechanisms and drug delivery. The successful applicant will work on an innovative new project exploring the targeting of breast cancer metastases in brain using a novel type of monoclonal antibody (*J. Cell Physiol.* **225:**664-672; *J. Immunol.* **186:**3265-3276) funded by the DoD Breast Cancer Research Program. Candidates with background in pharmacology/pharmaceutical sciences or related areas and with hands-on experience in pharmacokinetic studies in rodents, cell culture, and histological techniques, including (confocal) fluorescence microscopy are preferred. For more information about this position and to apply, visit our **website: http://jobs.texastech.edu**. *Equal Opportunity Employer/Affirmative Action/ADA.*

### TENURE OR TENURE-TRACK FACULTY POSITION in Systems Biology University of California, Irvine

The University of California, Irvine (UCI) is continuing its recruiting initiative in Systems Biology.

One position is available this year, for which candidates will be considered from all areas of Systems Biology, including modeling, mathematical and computational biology, biological networks, regulatory dynamics and control, spatial dynamics and morphogenesis, and synthetic biology. Applications are being solicited at the **ASSISTANT PROFESSOR** level, and appointment can be made in any of several departments, including Developmental and Cell Biology, Molecular Biology and Biochemistry, Ecology and Evolutionary Biology, Biomedical Engineering, Mathematics, Physics and Astronomy, Computer Science, and Statistics. We highly value candidates with strong backgrounds in modeling and/or computation. Applications at the **ASSOCIATE** and **FULL PROFESSOR** level will also be considered, with appointment being subject to the availability of funds.

The successful applicant is expected to conduct a strong research program and to contribute to the teaching of undergraduate and graduate students. Systems Biology research and training at UCI is fostered by several interdisciplinary research units, an NIGMS National Center for Systems Biology, and Ph.D. training programs in Bioinformatics, and Mathematical and Computational Biology (for more information, see **website: http://ccbs.uci.edu**). Applicants should submit a letter of application, curriculum vitae, bibliography, three letters of reference, and statements of research and teaching interests using the online recruitment system (see instructions at **websites: http://ccbs.uci.edu** or **https://recruit.ap.uci.edu**, under "Institutes and Centers"). To receive full consideration, material should be received by December 3, 2012.

*The University of California, Irvine is an Equal Opportunity Employer committed to excellence through diversity, and strongly encourages applications from all qualified applicants, including women and minorities. UCI is responsive to the needs of dual career couples, is dedicated to work-life balance through an array of family-friendly policies, and is the recipient of an NSF ADVANCE Award for gender equity.*

### ASSISTANT PROFESSOR of Biology (Microbiology and Immunology)

The Department of Biology at Wheaton College (IL) seeks candidates for a full-time, tenure-track position at the Assistant Professor level to begin August 2013. A Ph.D. in microbiology, immunology, or closely related field is required. Postdoctoral experience and experience in bioinformatics are preferred. The ideal candidate will be committed to teaching, maintaining active research in collaboration with students, and mentoring students in spiritual and personal growth.

Review of applications will begin December 15, 2012, and continue until the position is filled. Interested persons should send curriculum vitae, a description of the applicant's teaching philosophy, research interests, and a cover letter that addresses his/her mission fit with Wheaton College, to: **Dr. Jennifer Busch, Chair, Department of Biology, Wheaton College, 501 College Ave, Wheaton, IL 60187**, or to **e-mail: jennifer.busch@wheaton.edu**. Application materials will be sent to eligible candidates.

*Wheaton College is an evangelical Protestant Christian liberal arts college whose faculty and staff affirm a Statement of Faith and adhere to lifestyle expectations of the Wheaton College Community Covenant. The College complies with federal and state guidelines for nondiscrimination in employment. Women and minority candidates are encouraged to apply.*

**Nontraditional Careers:** Opportunities Away From the Bench

Webinar

Want to learn more about exciting and rewarding careers outside of academic/industrial research? View a roundtable discussion that looks at the various career options open to scientists and strategies you can use to pursue a nonresearch career.

**Now Available On Demand**
**www.sciencecareers.org/webinar**

Produced by the *Science*/AAAS Business Office.

Science Careers
From the journal *Science* AAAS

## POSITIONS OPEN

### GENOMICS/BIOINFORMATICS

The Department of Biology and Biochemistry at the University of Houston (UH) invites applications for a faculty position at any level from individuals using genomic, bioinformatic, or computational approaches to investigate fundamental problems in eukaryotic cell or molecular biology. Areas of interest include, but are not limited to, neuroscience and behavior, developmental biology, metabolic regulation, or regulation of gene expression at the transcriptional or posttranscriptional levels. Individuals using in vivo model systems are especially encouraged to apply. The department and university offer a scientifically diverse and highly collaborative environment. The successful applicant will be expected to develop and maintain a competitively funded research program and participate in graduate and undergraduate teaching. Qualifications include an earned Doctorate and an established record of research as demonstrated by publications and strong potential for continued external funding. Candidates should submit a PDF that includes a cover letter, a personal statement, curriculum vitae, and names and contact information of at least three references to **e-mail: genomics@nsm.uh.edu**. Consideration of applications will begin immediately and will continue until the position is filled. *The University of Houston is an Equal Opportunity/Affirmative Action Employer. Minorities, women, veterans, and persons with disabilities are encouraged to apply.*

### FACULTY POSITION in Synthetic Biology

The Division of Biochemistry in the Department of Biology and Biochemistry at the University of Houston (UH) invites applications for a faculty position in Synthetic Biology. Researchers in this area may be crating designer molecules, novel metabolic and molecular networks, developing artificial cells and organisms, and carrying out quantitative modeling all leading to biotechnology or biomedical breakthroughs. Preference will be given to a scientist whose interests take advantage of existing strengths at UH. The University of Houston has outstanding facilities in DNA sequencing, proteomics, structural biology, single-molecule studies, and computational modeling. Applicants should have a Ph.D. in a related field, an outstanding record of research, and a strong commitment to education. The position can be filled at any rank. Please submit a curriculum vitae and an outline of future research interest to **e-mail: synbiosrch@nsm.uh.edu**. Please also arrange for three letters of recommendation to be electronically sent to **e-mail: synbiosrch@nsm.uh.edu**. Consideration of applications will begin immediately and will continue until the position is filled. *The University of Houston is an Affirmative Action/Equal Opportunity Employer. Minorities, women, veterans, and person with disabilities are encouraged to apply.*

### TENURE-TRACK ASSISTANT PROFESSORS in Ecology and Animal Physiology

The Department of Biology, University of Wisconsin-Stevens Point, offers two tenure-track, nine-month faculty positions (Assistant Professor), beginning August 2013.

Ecology—Teaching includes general ecology, plant or community ecology, and introductory biology.

Animal Physiology—Teaching includes animal physiology to biology and natural resource majors, a senior seminar, and an upper level course in specialty.

Research involving undergraduates, service, and student advising are expected. Broad training in biology and Ph.D. with emphasis in specialty is required. Teaching and research experience are required. *We seek applicants from underrepresented groups.* Applications should include a cover letter, curriculum vitae, statements of teaching philosophy and research interests, three letters of recommendation, undergraduate and graduate transcripts. Send application materials to: **Dr. Christopher Yahnke, Chair; Biology Department, University of Wisconsin-Stevens Point, Stevens Point, WI 54481**. Review begins 3 December 2012. For more information, **telephone: 715-346-2455, fax: 715-346-3624, e-mail: cyahnke@uwsp.edu**.

*Affirmative Action/Equal Opportunity Employer.*

## POSITIONS OPEN

University of California, Merced School of Engineering: Bioengineering Tenured/tenure-track faculty. **ASSISTANT/ASSOCIATE/FULL PROFESSOR**. Unique opportunity for one individual to join faculty in the School of Engineering at the new University of California campus. Research focus for this position is physiological modeling. However, excellent applicants in other bioengineering research areas will also be considered.

To apply or for more information, please visit our **website: http://jobs.ucmerced.edu/n/academic/position.jsf?positionId=4264**. *Affirmative Action/Equal Opportunity Employer.*

University of California, Merced School of Engineering: Bioengineering **ASSISTANT/ASSOCIATE/FULL PROFESSOR**.

Unique opportunity for one individual to join faculty in the School of Engineering at the new University of California campus. Research focus is in the area of Recombinant Biosensors. However, excellent applicants in other research areas as genetic engineering, protein engineering, or biosensor nanotechnology will also be considered.

To apply or for more information, please visit our **website: http://jobs.ucmerced.edu/n/academic/position.jsf?positionId=4266**. *Affirmative Action/Equal Opportunity Employer.*

### PHYSIOLOGIST
**Concordia College, Moorhead, MN**

A full-time tenure-track position at the **ASSISTANT PROFESSOR** level to teach introductory Cell Biology and upper-level Human Anatomy and Physiology beginning in August of 2013. Commitments to excellent teaching, supervising undergraduate research, and the educational mission of a liberal arts Lutheran college are expected. Online application process at **website: http://www.cord.edu/Offices/hr1.php**. Application review will begin December 3 and continue until position is filled. *Concordia College is an Equal Opportunity Employer seeking a diverse faculty.*

Find your future here.

Science Careers
From the journal *Science* AAAS

www.ScienceCareers.org

## MARKETPLACE

Affymetrix®
Revolutionize life

# The Definitive Evolution of **Genotyping**

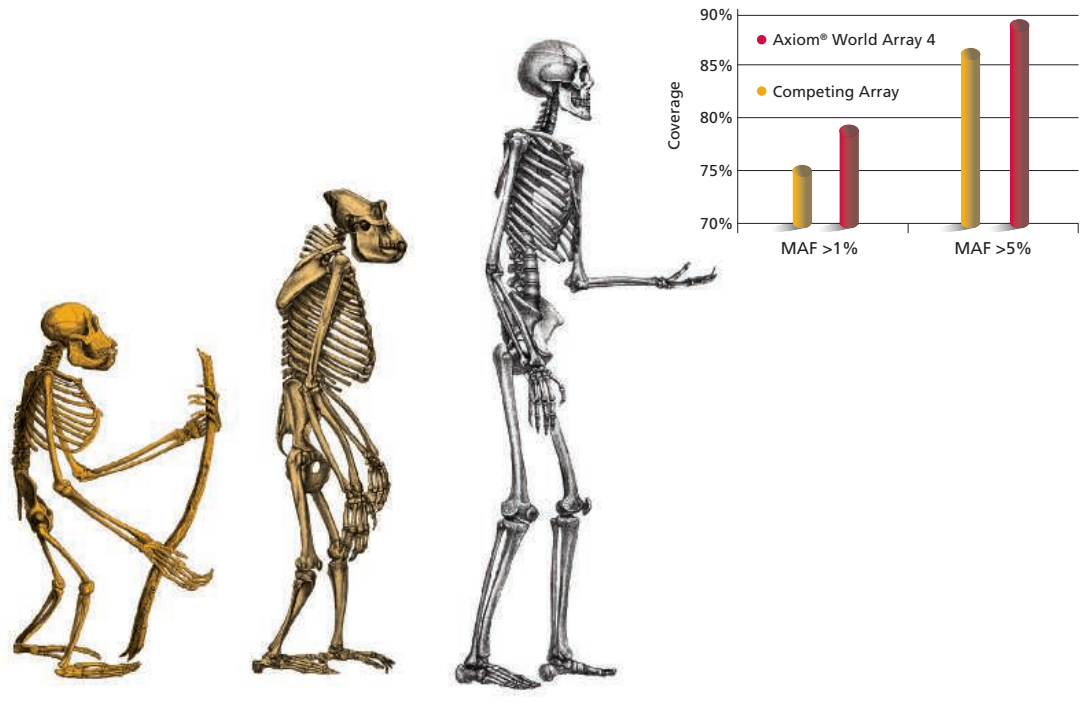


**Axiom® Genotyping Solution. Survival of the fittest.**
Axiom Genotyping Solution is the most powerful genotyping workflow delivering superior coverage of populations, disease genes, and rare variants at an affordable price.

- **Unique GWAS, replication, and fine-mapping content on one array**
- **Unrivaled coverage of the exome, disease genes, and functional regions**
- **Cost-effective custom array design with 100% SNP conversion**

Axiom Genotyping Solution adapts to the needs of your research—coverage and flexibility like never before. Contact your Affymetrix representative today or come see us at booth #918/920 at ASHG 2012.

**Join our luncheon seminars:**

**Wednesday, Nov. 7, 12:45 – 2:15 PM**
**Room 302, Esplanade Level (South),**
**Moscone Center**
Population-optimized strategies and genotyping solutions for expanding our understanding of the genetic variations in complex diseases

**Thursday, Nov. 8, 12:45 – 2:15 PM**
**Room 307, Esplanade Level (South),**
**Moscone Center**
Next-generation cytogenetics solution for constitutional and cancer research applications

**Visit www.affymetrix.com/ashg to register for these seminars.**

Box lunch will be provided. First come, first served.

# MILLIONS OF STUDENTS AND RESEARCHERS USE ENDNOTE TO MANAGE THEIR REFERENCES AND CREATE BIBLIOGRAPHIES. WHY NOT YOU?

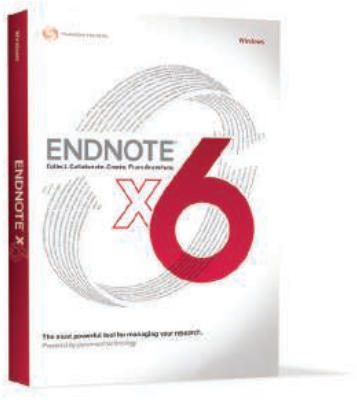


INTRODUCING

## ENDNOTE® X6

**Collect. Collaborate. Create. From Anywhere.**

**With *EndNote*, you can:**

- Access your references from anywhere and manage your *EndNote* library from multiple computers with *EndNoteSync*.
- Search hundreds of online resources to collect references and PDFs
- Format references for any project with patented *Cite While You Write*® technology
- Use the new PubMed direct export format to import records in fewer steps
- Create and share custom groups, smart groups, or combined groups
- Enjoy a FREE 2-year subscription to *EndNote Web* with advanced features
- And so much more!

1-800-722-1227 • rs.sales@thomson.com

**endnote.com**



THOMSON REUTERS™

Thermo SCIENTIFIC

# Quantify, verify,

In science there are always essential steps in any workflow. Accurate measurements of DNA, RNA and protein samples are critical for confidence in qPCR, sequencing, microarrays or bioproduction, but there's a better alternative to the time and complexity of conventional methods. Using minimal sample (0.5 – 2.0 µL), **Thermo Scientific NanoDrop** instruments make concentration and purity analysis so incredibly easy, and so much faster, you won't notice this step on the way to your ultimate discovery.

# simplify

• Realize the difference.
Try any NanoDrop instrument for FREE.
www.thermoscientific.com/nanodrop

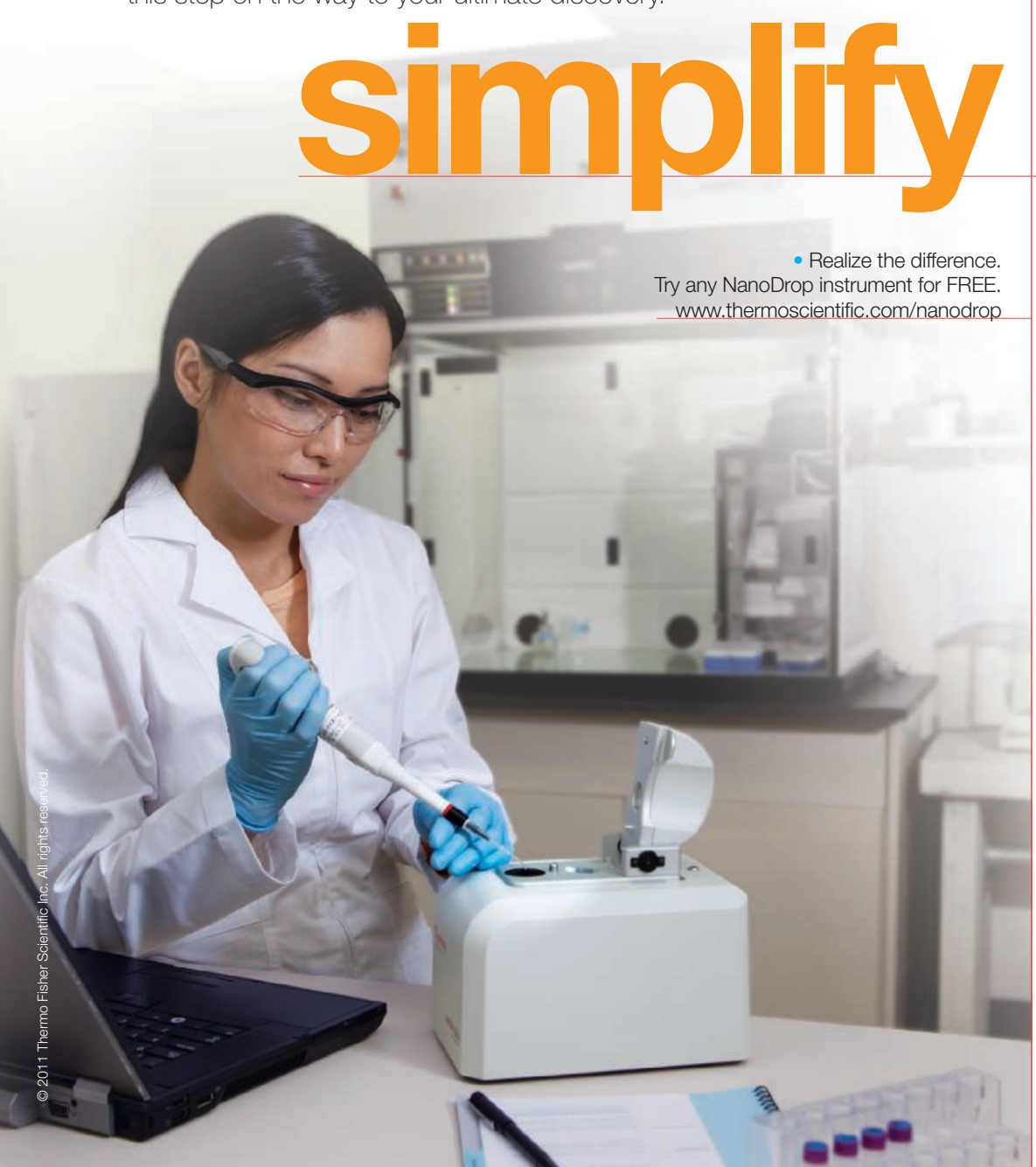


**NanoDrop™ Lite**
Basic microvolume measurements

**NanoDrop™ 2000C**
Full-spectrum microvolume and cuvette measurements in a single instrument

**NanoDrop™ 2000**
Full-spectrum microvolume measurements

**NanoDrop 8000**
Higher throughput, full-spectrum microvolume measurements

**NanoDrop 3300**
Full-spectrum microvolume fluorescence measurements


MiSeq. Next-generation sequencing for all you seek.

You want amazing accuracy and performance on your benchtop. Illumina delivers—yet again. The MiSeq Personal Sequencer is the only fully integrated, truly end-to-end benchtop solution around. It's just one more example of why Illumina solutions generate a remarkable 90% of all the world's sequencing data. Discover what's possible.

*www.illumina.com/iseek*

illumina®

# Improve your NGS performance

## On any sequencing platform

### Speed up and simplify your workflow with new preanalytic solutions for NGS

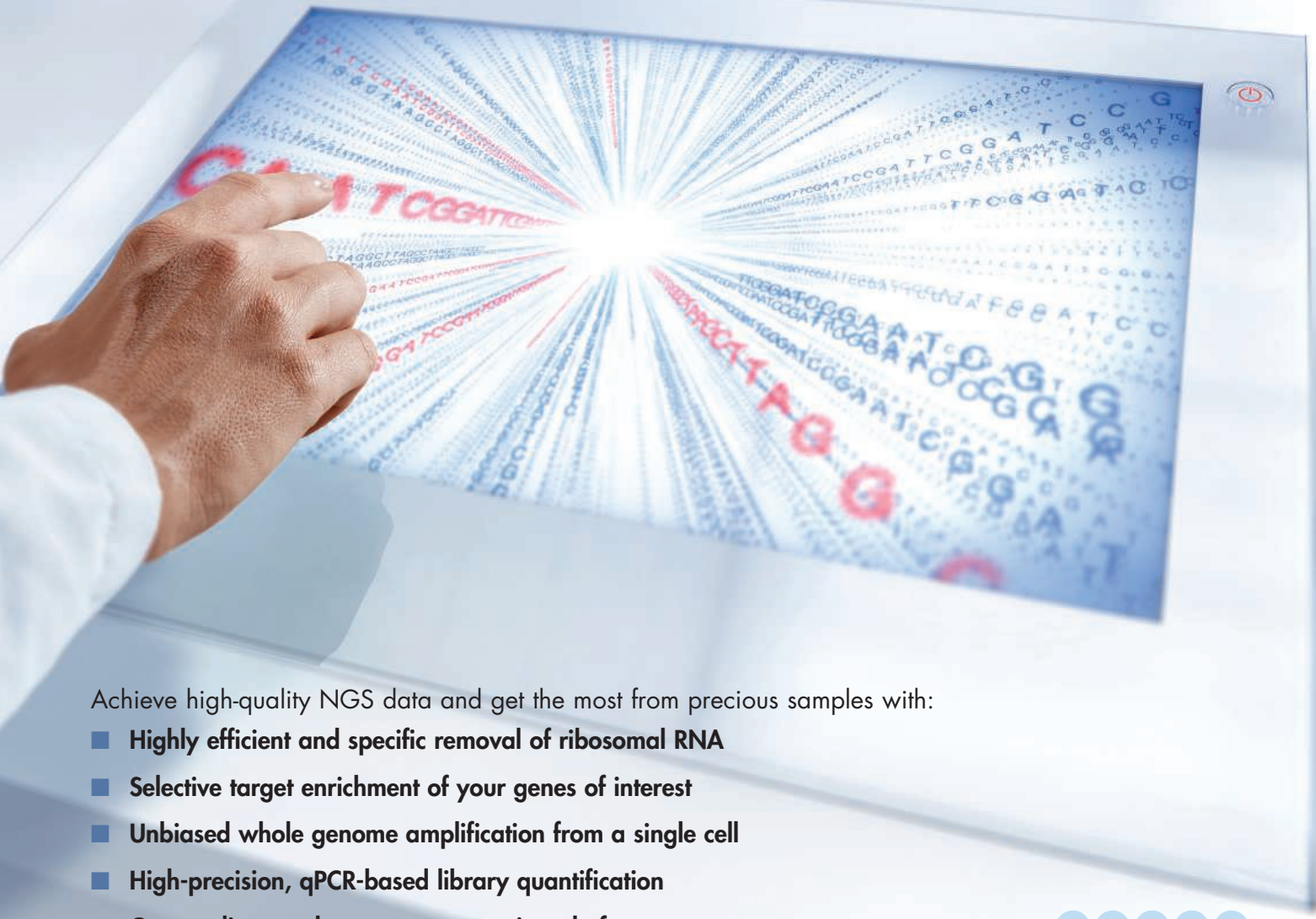

Achieve high-quality NGS data and get the most from precious samples with:

- **Highly efficient and specific removal of ribosomal RNA**
- **Selective target enrichment of your genes of interest**
- **Unbiased whole genome amplification from a single cell**
- **High-precision, qPCR-based library quantification**
- **Outstanding results on any sequencing platform**

Visit www.qiagen.com/goto/NGS and keep up-to-date on our expanding portfolio of new and innovative technologies for next-generation sequencing.



NGS1012S1WW

QIAGEN®

Sample & Assay Technologies

# Transcriptome Analysis


## Is true "single-cell" RNA-seq feasible?

**Find out at www.clontech.com/rnaseq-single**

**or call 1.800.662.2566**

Clontech

Clontech Laboratories, Inc.
A Takara Bio Company

United States/Canada: +1.800.662.2566 • Asia Pacific: +1.650.919.7300 • Europe: +33.(0)1.3904.6880 • Japan: +81.(0)77.543.724

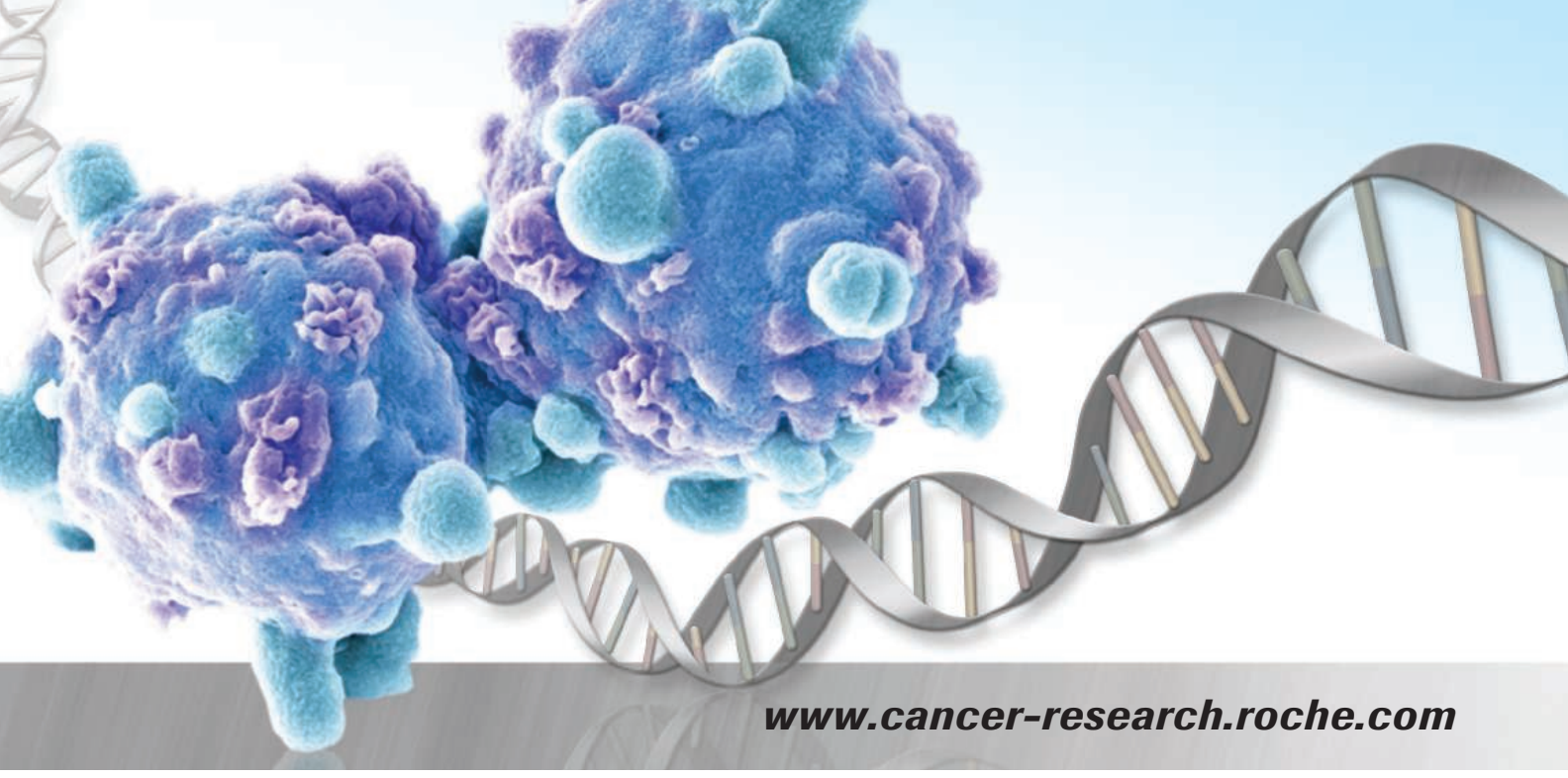


# Choose a Trusted, Experienced Partner

## *To Help You Advance Your Cancer Research Faster*

**Quantify Gene Expression**

**Analyze DNA Methylation**

**Detect and Characterize Genomic Variations**

**Research Proliferation, Apoptosis, and Cytotoxicity**

**Continuously Monitor Cell Invasion and Migration**

**Study the Role of Proteins in Cancer**

Hoping to advance your cancer research more quickly? Start by combining **Roche Applied Science**'s world-class reagents and instruments to rapidly, accurately study cancer at the level of the gene, transcript, protein, and cell.

As part of the world's leading supplier of oncology treatments (Roche Pharmaceuticals/Genentech) and tissue-based diagnostics, Roche Applied Science is uniquely qualified to be your primary partner in cancer research, offering:

- **Performance you can trust, plus innovation:** Combine time-tested reagents with novel instrumentation that enables you to study cancer in new ways.
- **Flexible, efficient solutions that help you make more from less:** Obtain more results faster in many applications.
- **Our commitment to you:** Confidently rely on our dedicated service professionals, on-site reagent stocking, customized research solutions, and much more.

**Let Roche help you reveal the cellular and molecular mechanisms of cancer. Learn more by visiting *www.cancer-research.roche.com***

Roche Diagnostics Corporation
Roche Applied Science
Indianapolis, Indiana

**For life science research only.**
**Not for use in diagnostic procedures.**

GE Healthcare
Life Sciences

# >32

## Believe the unbelievable

The new Cytell™ Image Cytometer. With three clicks, more than 32 cellular measurements can be captured in under 2.5 minutes.

The next generation in image cytometry is here.
Experience more. **www.gelifesciences.com/cytell**



imagination at work

Produced by the *Science*/AAAS Custom Publishing Office

## LIFE SCIENCE TECHNOLOGIES

Genomics

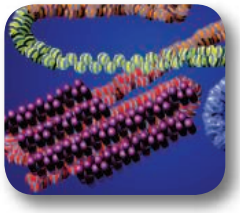

# Epigenomics:

## The New Technologies of Chromatin Analysis

### In This Issue

Multicellular organisms are essentially clonal. Every cell possesses the same DNA as every other. So what distinguishes a liver cell from a neuron? Epigenetics, that constellation of noncoding RNAs, protein-DNA interactions, and molecular modifications that govern which genes are expressed and which stay silent. Epigenetic mechanisms influence processes from stem cell differentiation to cancer, and researchers are keen to understand how these events differ at the genomic scale—the so-called epigenome. The problem is daunting, but the research community is resourceful. The epigenome has never seemed closer.

**See full story on page 546.**

### Upcoming Features

Tissue Engineering: 3-D/Scaffolding—December 7
The Connectome—January 18, 2013
Genomics—February 15, 2013

eppendorf

**Eppendorf Xplorer® plus**
**With additional functions**

# Simply Better Pipetting!

**Eppendorf Xplorer® and Eppendorf Xplorer® plus—the electronic pipettes**

People who give 100 % every day deserve the best equipment.

The electronic pipettes Eppendorf Xplorer and Xplorer plus were specially designed for high professional standards to provide optimal support for you in your work.

> Intuitive handling: Selection dial and multi-function rocker
> Optimal ergonomics: Eppendorf PhysioCare Concept®
> High reproducibility: Spring loaded tip cone and individual adjustment
> NEW: Eppendorf Xplorer plus!

www.eppendorf.com/xplorer

Genomics

# Epigenomics:

## The New Technologies of Chromatin Analysis

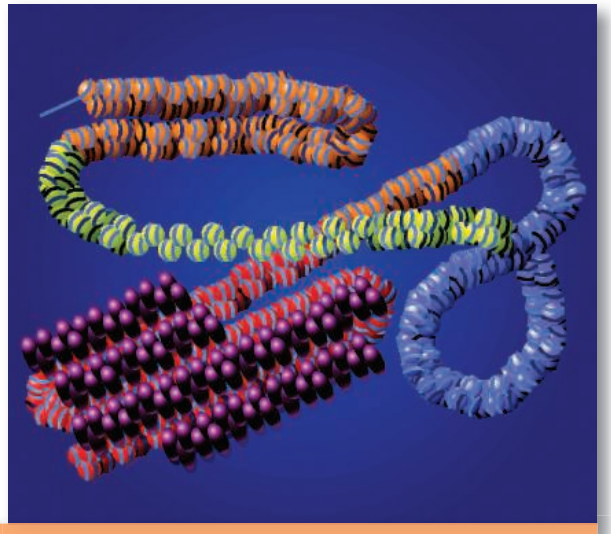

Multicellular organisms are essentially clonal. Every cell possesses the same DNA as every other. So what distinguishes a liver cell from a neuron? Epigenetics, that constellation of noncoding RNAs, protein-DNA interactions, and molecular modifications that govern which genes are expressed and which stay silent. Epigenetic mechanisms influence processes from stem cell differentiation to cancer, and researchers are keen to understand how these events differ at the genomic scale—the so-called epigenome. The problem is daunting, but the research community is resourceful. The epigenome has never seemed closer.
**By Jeffrey M. Perkel**

"We've got the technology, we've got the need, people are starting to do this, the lack of reference sets and new technologies are holding the field back. That was why [epigenomics] was identified as a good investment."

In early 2008, the **U.S. National Institutes of Health (NIH)** announced that it was earmarking $190 million over five years to study the problem of epigenomics. The effort, part of the NIH Roadmap Initiative, had several overarching goals, including creating a series of epigenomic reference maps for normal human cells and tissues and developing novel technologies to aid in that process.

According to James Anderson, director of the Division of Program Coordination, Planning, and Strategic Initiatives, the unit within the NIH's Office of the Director that oversees the Common Fund (and hence, the Roadmap Initiative), epigenomics was a natural fit for the Roadmap, which is a cross-NIH funding mechanism that essentially concerns itself with grand challenges in the biological sciences.

Previously, he explains, researchers were attacking the epigenome piecemeal, but nobody could put it all together. After consulting with experts, NIH realized the field was fundamentally stymied by the lack of one essential resource: a reference dataset, an epigenomic metric against which other datasets might be measured. Without such a reference, a complete cataloging of all epigenetic marks and how they vary across development and disease could not possibly be completed. Yet at the same time, new technologies had been developed that for the first time meant the problem was not actually intractable, simply vast.

NIH decided to pull the trigger. "It all came together," Anderson says. "We've got the technology, we've got the need, people are starting to do this, the lack of reference sets and new technologies are holding the field back. That was why [epigenomics] was identified as a good investment."

Today, that labor is beginning to bear fruit. The NIH Common Fund, along with individual institutes and centers, has awarded 68 grants under the Epigenomics Program, which according to Anderson have yielded some 52 reference epigenomes—maps of DNA methylation and histone modifications across multiple cell types. (Those datasets join the fruits of an earlier, parallel effort, the National Human Genome Research Institute-funded ENCODE project (Encyclopedia of DNA Elements), which in September 2012 released 30 papers mapping not just DNA methylation and histone modifications, but also transcription-factor binding sites, higher-order chromatin structure, transcribed regions, and more across the human genome in nearly 150 cell lines; both those and the NIH Roadmap Epigenome Project datasets are freely accessible online.) But perhaps just as importantly, they have led to a slew of new epigenetic and epigenomic technologies that are providing researchers the tools to gain an increasingly clearer picture of what is really going on in cells at the genomic level.

Indeed, says Anderson, that's really the point of spending all these millions. "Our intent is not to finish the epigenome. It is to transform individual investigators' ability to do their work."

### ATTACKING THE METHYLOME

One researcher supported under the Epigenomics Program is Bing Ren, a member of the **Ludwig Institute for Cancer Research** in San Diego. Ren is principal investigator (PI) of a grant to establish one of four epigenome mapping centers charged with compiling the critical epigenomic maps. His center focuses on embryonic stem cells. The **San Diego Epigenome Center** has been awarded $15.7 million since 2008, which it has used to map both DNA methylation and some 20 histone modifications in both human embryonic stem cells (hESCs) and four hESC-derived cell types.

The significance of the Epigenome Project "is equivalent to sequencing the human genome," Ren says. "When you have the human genome, then you have a blueprint to understand human development. But without a detailed understanding of the epigenome we can't read that blueprint."

### UPCOMING FEATURES

**Tissue Engineering: 3-D/Scaffolding—December 7**

**The Connectome—January 18, 2013**

**Genomics—February 15, 2013**

The San Diego Epigenome Center builds its maps with the two key technologies of epigenomics: chromatin immunoprecipitation (ChIP)-Seq, which uses next generation DNA sequencing technology to identify the location of specific histone modifications across the genome, and MethylC-Seq, a genome-wide method for determining the position of 5-methylcytosine modifications.

MethylC-Seq is basically an optimized version of bisulfite sequencing for today's blazing-fast next-gen DNA sequencers. The problem it solves is this: Standard DNA sequencing methods cannot distinguish cytosine from 5-methylcytosine (5-mC). But if the DNA is first treated with sodium bisulfite they can, because bisulfite converts unmodified cytosines to uracil, which appears in DNA sequencer reads as thymine (T). By comparing bisulfite-treated samples against an untreated control, researchers can determine which bases were methylated and which were not.

Researchers have been using bisulfite conversion to interrogate methylation at the nucleotide level for decades, and in 2008 Joseph Ecker's team at the Salk Institute in San Diego (Ecker is also an investigator in the San Diego Epigenome Center) updated the method for the **Illumina** Genome Analyzer. That's MethylC-Seq. But in 2009 a new wrinkle appeared. That year, teams led independently by Nathaniel Heintz at the Rockefeller University in New York and Anjana Rao at Harvard Medical School reported that mammalian DNA contains a previously undiscovered methylated base, 5-hydroxymethylcytosine (5-hmC).

Bisulfite sequencing, as it turns out, cannot distinguish between 5-mC and 5-hmC, meaning that at least some sites reported as containing the former, may in fact contain the latter.

"What it means to the scientific community is that whatever information we had before is not true, because we don't know what percentage of the apparent 5-methycytosines are actually 5-hydroxymethylcytosine," says Sriharsa Pradhan, head of the RNA Biology division at **New England Biolabs,** which sells restriction enzyme-based kits to distinguish between the two bases.

This year, researchers finally developed strategies to circumvent this problem. The first, developed by a team in Cambridge, UK, and called oxidative bisulfite sequencing (oxBS-Seq), uses an oxidizing reagent (potassium perruthenate) to oxidize 5-hmC residues to 5-formylcytosine (5-fC), which reads as T after bisulfite conversion.

The second method, developed in a collaboration between Ren's lab, Chuan He at the University of Chicago, and Peng Jin at Emory University, uses an enzyme to selectively protect 5-hmC residues. Called Tet-assisted bisulfite sequencing (TAB-Seq, commercialized by a Chicago-area firm named **WiseGene**), this method uses a ten-eleven translocation (Tet)-family oxidase enzyme to convert 5-mC to 5-carboxylcytosine (5-caC), which also reads as T after bisulfite treatment. (The Tet enzyme progressively oxidizes 5-mC to 5-hmC, and then to 5-fC, and finally to 5-caC.)

First though, TAB-Seq uses β-glucosyltransferase to couple a glucose moiety to 5-hmC, protecting it from Tet. Thus, the only residues that should appear as cytosines during sequencing should be 5-hmC. Comparison with standard bisulfite-converted and sequenced DNA should reveal the balance of 5-mCs. (New England Biolabs' EpiMark 5-hmC and 5-mC Analysis Kit is based on a similar principle; it uses β-glucosyltransferase to render a sequence resistant to a restriction enzyme.)

Ren and He's team used TAB-Seq to decipher the methylome of human embryonic stem cells, identifying some 691,000 5-hmC sites. Based on the distribution of that epigenetic mark, Ren says, it appears that 5-hmC plays a role in regulating transcriptional enhancers. "This type of element has a high abundance of hydroxymethylcytosine," he says, "and a correspondingly lower level of methylcytosine in the same sequence."

Bisulfite sequencing, as it turns out, cannot distinguish between 5-mC and 5-hmC.

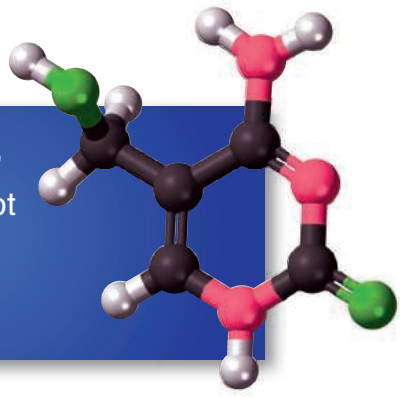

New England Biolabs is working on an alternative method to interrogate 5-hmC directly. The company recently described the enzymatic properties of the PvuRts1I family of proteins, which binds 5-hmC (or its glucosylated form, 5-(β-glucosyloxymethyl)cytosine) and cleaves 9 to 13 bases on either side, releasing a 24-base fragment with the modified base in the center. These fragments can then be sequenced directly, an approach the company calls "ABASeq," ("like the musical group, but only one B," Pradhan quips) in honor of AbaS1, the PvuRTS1I family member used in the assay.

"You don't need a bisulfite conversion; you don't need any kind of Tet-based approach or oxidation-based approach," Pradhan says. "Your sequence output is just going to align with the genome sequence." According to Pradhan, the team has already used this approach to map 5-hmC residues in a mouse embryonic stem cell line, though those data are not yet published.

## CATALOGING HISTONE MODIFICATIONS

Another recipient of NIH Epigenome Project funding is Brian Strahl, associate professor of biochemistry and biophysics at the **University of North Carolina (UNC) School of Medicine.** With UNC colleague Xian Chen, Strahl submitted an application focusing on the discovery of novel epigenetic marks.

"One of the questions we wanted to address is whether there were novel sites of histone modification that had gone undetected," Strahl explains. "This is relevant because to really understand epigenomics, or even epigenetics, you need to know first what are all the modifications on histones to begin with."

Put another way, you cannot map modifications you don't know exist. Those can be of two types: known modifications in novel locations, and novel modification types.

To find both types, many researchers turn to mass spectrometry. Strahl and Chen, for instance, have used top-down proteomics analyses on a **Bruker Daltonics** 12-Tesla Fourier transform ion cyclotron resonance (FT-ICR) mass spectrometer to show that histone H2B lysine 37 in *Saccharomyces cerevisiae* contains a previously unknown modification.

"One of the peaks that came out … was, as far as we can tell, dimethylated on one particular lysine that had not been reported elsewhere," Strahl says. "Unfortunately, we couldn't link any particular biology to it; it's just too new." continued>

## Genomics

That's not to say the modification isn't important, he says. "If the cell cares that much to burn so many ATPs to get a particular modification on a residue, it's got to be there for a reason," he says.

Researchers are also discovering entirely novel modifications. One team that has made several such discoveries is led by Yingming Zhao, a professor in the **Ben May Department for Cancer Research at the University of Chicago** and another Epigenome Project grant recipient.

Using high-resolution mass spectrometry, Zhao has discovered several new posttranslational modifications on histone proteins, including lysine propionylation and butyrylation in 2007, lysine crotonylation in 2011, and earlier this year, lysine succinylation and malonylation.

Zhao's discovery of lysine crotonylation is actually a case study in why researchers should always verify what the computer tells them. In this case, that due diligence yielded a high-profile paper in *Cell.*

At the time, Zhao's lab had already discovered lysine butyrylation. Now, using a high-end **Thermo Scientific** LTQ Orbitrap Velos system, they were trying to map sites of that modification. Normally in this type of study, researchers rely on computers to chew through the data and map observed ion masses against possible modifications. It's simply too laborious to do it manually. But computers can make mistakes, so Zhao's team double-checks the computer's math.

When they checked the spectral assignments in this case, they noticed that some didn't quite match up—they were off by 2 daltons (Da). Looking more closely, they were able to narrow down the modification's molecular formula to $C_4H_5O$, a crotonyl group.

Using a homemade "pan-crotonyl" antibody, Zhao's team used ChIP-Seq to tackle the mark's distribution throughout the genome, and found that it is associated with transcriptional start sites, enhancers, and active genes, and also "plays a role in the reprogramming of gene expression in postmeiotic male germ cells," he says.

### OF READERS AND DOWNSIZING

Of course, a histone modification is just that: a modification. It's like a genomic street sign, and signs don't exist in a vacuum. There must also be proteins that add and remove those signs, and "reader" proteins that interpret what they mean.

To find those readers, researchers like C. David Allis, head of the Laboratory of Chromatin Biology and Epigenetics at **Rockefeller University,** sift through protein extracts, looking for activities that can recognize, add, or remove a given modification. The key, says Allis: "Fractionate, fractionate, fractionate." Using that strategy, Allis says his team has begun to home in on what they believe are a family of enzymes that can add a crotonyl group to histones—that is, histone crotonylases.

The results are not yet published, so Allis is fairly tight-lipped. But he did reveal that "it has a functional sort of twist to it, some personality … that looks very exciting and different from what has been well-accepted for acetyl-lysine."

Or Gozani, associate professor of biology at **Stanford University,** another Epigenome Project grant winner, uses an alternate strategy for reader identification, probing microarrays of modified histone peptides with purified candidate reader proteins. Currently, Gozani's arrays contain about 100 peptides, and in one recent study his team, in collaboration with Dinshaw Patel at Memorial Sloan-Kettering Cancer Center in New York, used them to determine that a protein associated with DNA replication called ORC1 binds specifically to dimethylated lysine-20 on histone H4.

"There's a lot of room left to discover new readers," Gozani says.

And there are a lot of new methods in the epigenomics application space to study them. But that doesn't mean the field has achieved technological maturity, says Kenneth Zaret, codirector of the epigenetics program at the **University of Pennsylvania School of Medicine.** "Base technologies" like ChIP-Seq work best with immortalized cell lines that can provide the hundreds of thousands or even millions of cells required to make that technique work; when sample size is limited, during stem cell development or embryogenesis, for instance, these techniques are harder to pull off. What is needed, Zaret says, is a way to apply epigenomics approaches to smaller cell populations.

Already, he and others are making headway. **Cornell University** Professor Paul Soloway, with colleague Harold Craighead, has developed a nanofluid approach called SCAN (single chromatin analysis at the nanoscale) to monitor groups of modifications simultaneously on anywhere from one to 10 nucleosomes—asking, for instance, whether a single nucleosome contains both H3K27-trimethyl and methylated DNA.

Zaret is using fluorescence-activated cell sorting to isolate discrete cell populations, which he then analyzes using a modified ChIP protocol. Applying that approach to nine transcriptionally silent genes in a few thousand mouse stem cell progenitors, Zaret's team discovered distinct "prepatterns" that appear to position different sets of genes in different ways. Now the team is scaling this approach up to the genomic level.

Look for these data and more from the NIH Roadmap Epigenome Project in the months and years ahead. In the meantime, those hoping to mine the epigenome datasets can do so today at the Project's official data-coordination website, www.genboree.org/epigenomeatlas.

*Jeffrey M. Perkel is a freelance science writer based in Pocatello, Idaho.*

DOI: 10.1126/science.opms.p1200069

### FEATURED PARTICIPANTS

**Ben May Department for Cancer Research, University of Chicago**
benmay.uchicago.edu

**Bruker Daltonics**
www.bdal.com

**Cornell University**
www.cornell.edu

**Illumina**
www.illumina.com

**Ludwig Institute for Cancer Research, UCSD**
www.ludwigsd.org

**New England Biolabs**
www.neb.com

**NIH Common Fund Office of Strategic Coordination Epigenomics Program**
commonfund.nih.gov/epigenomics

**The Rockefeller University**
www.rockefeller.edu

**San Diego Epigenome Center**
epigenome.ucsd.edu

**Stanford University**
www.stanford.edu

**Thermo Fisher Scientific**
www.thermoscientific.com

**University of North Carolina at Chapel Hill School of Medicine**
www.med.unc.edu

**University of Pennsylvania Perelman School of Medicine**
www.med.upenn.edu

**WiseGene**
www.wisegeneusa.com

# New Products: Genomics

## DNA METHYLATION KIT

The new EZ DNA Methylation-Lightning Kit is for complete bisulfite conversion of DNA prior to methylation analysis by polymerase chain reaction (PCR), MSP, array, or next-gen sequencing. The ready-to-use liquid format Lightning Conversion Reagent is added directly to a DNA sample (as low as 100 pg) for conversion in about an hour. High yield, converted DNA can be eluted into minimal volumes using Zymo's unique spin columns, 96-well spin plates or—a first of its kind—magnetic bead format. This new format enables bisulfite treatment of DNA to be used in conjunction with automated platforms (e.g., Tecan - Freedom EVO) for high throughput processing applications. The EZ DNA Methylation-Lightning Kit is designed to simplify DNA methylation analysis and epigenetic research.

**Zymo Research Corporation**

**For info: 888-882-9682 | www.zymoresearch.com**


## METHYLATED DNA LIBRARY PREP

The NEXTflex Methyl-Seq 1 Kit is designed to enrich and prepare single, paired-end, and multiplexed methylated DNA libraries for sequencing using Illumina MiSeq, GAIIx, and HiSeq platforms while allowing for the multiplexing of up to 96 samples facilitating a methylome-level assessment of genomic DNA. NEXTflex Methyl-Seq Kit utilizes versatile MeDIP or MeCAP protocols for detection of methylated DNA allowing the user to easily assess the methylation state of the genome, quantify absolute DNA methylation levels, and identify differentially methylated regions. The NEXTflex Methyl-Seq 1 Kit includes "Enhanced Adapter Ligation Technology" resulting in library preps with a larger number of unique sequencing reads. This specially designed NEXTflex ligation enzymatic mix allows users to perform ligations with longer adapters and better ligation efficiencies. This kit also uses a completely gel-free protocol making the workflow compatible with liquid handler automation.

**Bioo Scientific**

**For info: 888-208-2246 | www.biooscientific.com**

## SINGLE-STRANDED DNA QUANTITATION SYSTEM

The QuantiFluor ssDNA System is designed for highly sensitive quantitation of single-stranded DNA (ssDNA). The QuantiFluor ssDNA dye enables quantitation of small amounts (as little as 200 pg per well) of ssDNA in solution, saving your valuable sample for downstream assays. For low-concentration samples, the new system delivers sensitivity several thousandfold greater than absorbance at 260 nm and has a higher dynamic range. The QuantiFluor ssDNA System includes all the required reagents to deliver consistent ssDNA quantitation results. It is easy to set up on microplate or single-tube fluorometers and is available as an integrated solution with instrument pairing. Detecting and quantitating ssDNA is important for a variety of molecular biology research applications. These include studying ssDNA viruses, quantitating short synthetic ssDNA probes for site-directed mutagenesis, analyzing first-strand complementary DNAs (cDNAs), and quantitating bisulfate-treated DNA to study DNA methylation.

**Promega**

**For info: 608-274-4330 | www.promega.com/qfss**

## DNA SAMPLE PREPARATION

PureGenome kits and reagents are designed for rapid and efficient next generation sequencing (NGS) sample preparation. With these reagent sets, library preparation has been streamlined to two steps in under two hours, followed by a short enrichment step, thus alleviating a typical bottleneck in the sequencing process. PureGenome library preparation is a simple, two-step process followed by amplification using EMD Millipore's ultrahigh fidelity KOD Hot Start DNA Polymerase Mastermix. This unique polymerase amplifies DNA with high processivity in highly thymine-adenine (TA)- or guanine-cytosine (GC)-rich regions. The combined efficiency of library construction and accuracy of amplification enables maximum library yields from lower input DNA with minimal bias. The PureGenome NGS library preparation reagents are validated for Illumina platform-compatible NGS libraries; however, end users have the flexibility to optimize for other platforms.

**EMD Millipore**

**For info: 800-645-5476 | www.emdmillipore.com/ngs**

## WHOLE GENOME AMPLIFICATION KITS

The new illustra Ready-To-Go GenomiPhi kits provide researchers with a predispensed, room temperature stable formulation for whole genome amplification, enabling a simplified workflow for obtaining large amounts of high-quality DNA from small genomic DNA samples. The new kits also deliver improved yields over the current GenomiPhi kits. Previous GenomiPhi kits contain liquid enzyme formulations that require storage at -80°C degrees. The new kits incorporate Ready-To-Go stabilization technology which delivers single-dose reaction mixes in a solid format that can be stored for months at the bench without the need for refrigeration. The new illustra Ready-To-Go GenomiPhi kits are available in two formats: Ready-To-Go GenomiPhi V3, which improves upon the current GenomiPhi V2 kit with more than double the previous DNA yield, and Ready-To-Go GenomiPhi HY, which is specifically developed for high yield requirements, achieving 40 to 60 µg DNA yield from just 10 ng of starting DNA.

**GE Healthcare**

**For info: 800-526-3593 | www.gelifesciences.com/RTG-Genomiphi**

Electronically submit your new product description or product literature information! Go to **www.sciencemag.org/products/newproducts.dtl** for more information.

Newly offered instrumentation, apparatus, and laboratory materials of interest to researchers in all disciplines in academic, industrial, and governmental organizations are featured in this space. Emphasis is given to purpose, chief characteristics, and availability of products and materials. Endorsement by *Science* or AAAS of any products or materials mentioned is not implied. Additional information may be obtained from the manufacturer or supplier.

# *INTRODUCING* MERCK'S NEW POSTDOCTORAL RESEARCH FELLOW PROGRAM

Join the Merck Networks for immediate news and recruitment alerts:

merck careers

merckcareers1

merckcareers1

merck

Scan this code with your smartphone to explore our mobile career site.

Bringing important medicines and vaccines to people around the world through innovative science is what we do. At Merck, we strive to improve human life, achieve scientific excellence, operate with the highest standards of integrity, expand access to our products and employ a diverse workforce that values collaboration.

## Developing Talent, Harnessing Innovation, Building for the Future

Merck Research Laboratories is proud to announce the launch of a new Postdoctoral Research Fellow Program that will build on our legacy of scientific excellence and innovation.

If you join us, you'll be a part of a team of motivated scientists working to discover and develop medicines and vaccines that help meet the world's unmet medical needs. You will work alongside outstanding researchers and collaborators as part of Merck's industry-leading research and development organization. Our postdocs will:

- Work in unique laboratory environments with top capabilities, equipment, expertise and knowledge
- Obtain experience in drug discovery and development
- Generate innovative science resulting in high-quality external publications
- Participate in seminars, lectures and meetings, and have the opportunity to interact with the local scientific community
- Be positioned for choice careers in pharma, biotechnology, or academia

As a postdoc, you will receive a competitive salary and access to the full benefits programs offered by Merck.

At Merck, our passion is improving health. This is what keeps us at the forefront of scientific discovery and innovation. We invite you to apply.

**To learn more about the MRL Postdoctoral Research Fellow Program, or to apply for a position, visit www.merck.com/careers/postdoc today, or scan the QR code for more information.**

Postdoctoral Research Fellow Program

MERCK
*Be well*

NEW ENGLAND BioLabs® Inc.
enabling technologies in the life sciences

# Stick together.

## New DNA Ligases and Ligase Master Mixes

New England Biolabs offers the most extensive selection of high-quality and performance-optimized DNA ligases and ligase master mixes to streamline your cloning experiments.

Our expanded portfolio now includes:

- Blunt/TA Ligase Master Mix, optimized for blunt-end and single-base overhang substrates
- Instant Sticky-end Ligase Master Mix, uniquely formulated for the rapid ligation of sticky-end substrates
- T7 DNA Ligase, specific for sticky ends
- ElectroLigase,™ directly compatible with electroporation

Stick together with DNA Ligases and Ligase Master Mixes from NEB.

To request a FREE SAMPLE of our new DNA Ligase Master Mixes, visit **NEBStickTogether.com**

Blunt/TA Ligase Master Mix outperforms the competition

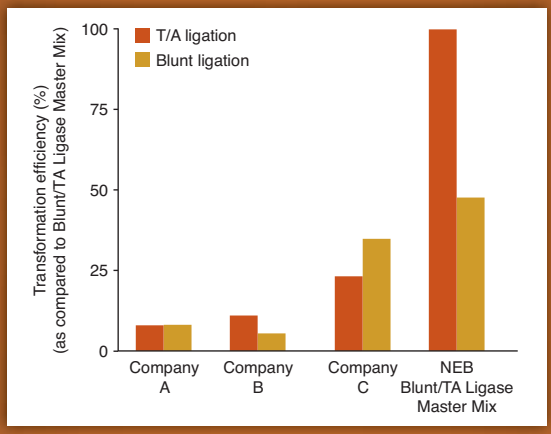


*Duplicate ligation reactions of blunt or T/A vector/insert pairs were set up according to the master mix vendors' suggestions. Equal amounts of ligated DNA were used to transform NEB 10-beta Competent E. coli (NEB #C3019) and triplicate plating was performed. Transformation results were averaged and graphed as a percentage of the highest performing reaction, T/A ligation using the Blunt/TA Ligase Master Mix.*